GULLY EROSION AND HEADCUT ADVANCE

By

KERRY MARK ROBINSON

Bachelor of Science
Oklahoma State University
Stillwater, Oklahoma
1975

Master of Science
Oklahoma State University
Stillwater, Oklahoma
1981

Submitted to the Faculty of the
Graduate College of the
Oklahoma State University
in partial fulfillment of
the requirements for
the Degree of
DOCTOR OF PHILOSOPHY
May, 1996

GULLY EROSION AND HEADCUT ADVANCE

Thesis Approved:

Thesis Adviser

Dean of the Graduate College

ACKNOWLEDGMENTS

This work was supported by funds provided by the U. S. Department of Agriculture, Agricultural Research Service (ARS). The support provided at all levels of ARS is genuinely appreciated. The Biosystems Engineering Department, headed by Dr. Bill Barfield, was also supportive and sincerely interested in this work.

I am indebted to my major adviser, Dr. Charles E. Rice, for his patience and guidance. His encouragement and constant support made this work possible. I am also grateful for the professional advice and support of my committee members, Dr. Ronald L. Elliott, Dr. Donald R. Snethen, and Dr. Daniel E. Storm.

I appreciate the invaluable assistance provided by Dr. Gregory J. Hanson, Mr. Kevin R. Cook, and Mr. Bobby J. Sappington of the USDA Hydraulics Unit. Their efforts helped make this work possible.

Finally, I would like to thank my wife, Jennifer, for being supportive while enduring many sacrifices. To her and to all those that knew I would finish, I dedicate this work.

PREFACE

The research reported herein is presented as a collection of five professional papers. An introduction (Chapter 1) precedes these articles and provides a problem statement and research objectives. Each article (Chapters 2, 3, 4, 5, and 6) has its own abstract, introduction, literature review, experimental equipment, results, and references section. Chapter 7 summarizes the information and provides recommendations for future research. Supporting information is attached in the appendices. The citations for each article are:

Chapter 2: Robinson, K. M. 1992. Predicting stress and pressure at an overfall. *Transactions of the ASAE* 35(2):561-569.

Chapter 3: Robinson, K. M. and G. J. Hanson, 1995. Large-scale headcut erosion testing. *Transactions of the ASAE* 38(2):429-434.

Chapter 4: Robinson, K. M. and G. J. Hanson, 1994. Influence of a sand layer on headcut advance. *Proceedings of the ASCE National Conference on Hydraulic Engineering*, Buffalo, New York.

Chapter 5: Robinson, K. M. and G. J. Hanson, 1996. Gully headcut advance. *Transactions of the ASAE* 39(1):33-38.

Chapter 6: Robinson, K. M. and G. J. Hanson, 1996. Influence of backwater on headcut advance. *Proceedings of the ASCE North American Water and Environment Congress*, Anaheim, California.

TABLE OF CONTENTS

LIST OF TABLES

Table **Page**

LIST OF FIGURES

CHAPTER 1

INTRODUCTION

PROBLEM STATEMENT

Earth emergency spillways serve an important function by conveying excess storm runoff safely around an impoundment structure. These auxiliary spillways typically transfer floodwater from an elevation near the top of a dam to an elevation at or near a base stream elevation. Earth spillways are designed to operate infrequently during statistically rare runoff events. The recurrence interval of the design storm is often related to the potential risk of damage should a structure fail. The vast majority of earth spillways perform as designed. In a relatively small number of instances earth spillways experience damage that threatens the integrity of the dams they are designed to protect. Because the failure of a dam can pose a substantial risk to people and property downstream, the criteria used to design earth spillways are subject to examination and improvement.

Earth spillways typically fail by the formation and movement of a gully headcut. This dominant form of damage usually forms as a result of a flow concentration. The flow concentration causes the development of a scour hole that, with time, transitions into a gully headcut. A headcut is typically characterized as having a vertical or near vertical face. Water discharging over the brink of an overfall creates a reverse roller near the base of the overfall. This flow circulation allows erosion at the base of the headcut that contributes to headcut instability. As material is removed by stress detachment and mass failure erosion processes, the headcut advances upstream. A breach occurs when a headcut advances through the crest of a spillway, and the water stored in an impoundment is released downstream.

Little is known about the dominant processes that control the rate of headcut advance. This study examines the attacking hydraulic forces, as well as, the resisting soil forces. These large-scale tests were performed to develop hydraulic and soil forces near magnitudes commonly found in the field. While information is available describing gully growth over time, little information exists concerning the mechanics of gully formation and growth. This work attempts to fill that void. Related areas of study that can potentially benefit from this investigation are field gully growth, rill erosion mechanics, knickpoint migration in streams, and fuseplug design.

OBJECTIVES

The following objectives were identified for this study:

1. Measure the hydraulic shear stress transmitted to the boundary of an overfall, and develop prediction relations for the magnitude, location, and variance of stress and pressure forces at an overfall.

2. Describe the large-scale headcut erosion test facility and present headcut advance test results. The flow conditions were held constant while the soil properties were varied.

3.. Determine the influence of a sand layer at the base of an overfall on the rate of headcut advance.

4. Examine the influence of flow rate and overfall height on the rate of headcut advance by attempting to hold soil properties constant.

5. Determine how the backwater level downstream of the overfall influences the rate of headcut advance.

LIMITATIONS

Research was conducted to represent field conditions as closely as possible. However, limitations were imposed that prevented exact duplication of field conditions. To measure boundary shear stresses with hot-film anemometry, the overfall model was required to have a hydraulically smooth boundary. The model was also constructed as a straight drop rigid boundary model. A gully overfall would not be as smooth as this model, and an erodible boundary would certainly deform in response to an applied stress. These simplifications were necessary to measure the boundary stress in time and space.

Spillways typically convey wide and shallow flows, so a two-dimensional flow approximation appears appropriate. For this research the discharge per unit width is considered to be a reasonable representation of gully flow conditions. A real world gully is very much a three-dimensional process. Lateral inflow along the sides of a gully contributes to gully widening and thus headcut advance. The large-scale study examines headcut advance in two dimensions only. A 1.83-m wide flume was constructed with 2.44-m high sidewalls. These dimensions limit the headcut sizes and the flow rates that can be tested. The concrete flume floor also acts as an inerodible boundary layer.

The research reported herein was conducted on two soil types with the bulk of the work using only one soil. More than 800 m^3 of this soil were used on this project. The development of headcut advance data for more soil types is desirable. The test fill section was constructed by compacting stockpiled soil in layers. While care was exercised in the placement and compaction of each layer, the fill material retained characteristics of the layered construction that were different from insitu soils. That is, the placed fill was not as homogeneous as undisturbed soils.

Other factors such as subsurface seepage may well play a major role in certain gully advance settings. To breach a spillway, however, a headcut must move quickly during a single flood event. Therefore, the time available for changes in the moisture regime of the soil profile is limited. While seepage influences have been intentionally limited in this research, the potential for a dramatic influence on headcut advance is acknowledged.

DISSERTATION FORMAT

The research described in this dissertation is presented as a collection of three journal articles and two proceedings papers (Chapters 2, 3, 4, 5, and 6). Each article contains an abstract, introduction, literature review, experimental equipment, results, and references section. An introduction (Chapter 1) precedes these articles and contains a problem statement and research objectives. Chapter 7 summarizes the information and provides recommendations for future research. Supporting information is attached in the appendices. The formal citations for each professional paper are shown in the preface.

CHAPTER 2

PREDICTING STRESS AND PRESSURE AT AN OVERFALL

ABSTRACT

Hydraulic shear stress and pressure forces have a major influence on the development and movement of a gully headcut or overfall. These forces were measured in a straight drop overfall model, and generalized prediction equations were developed using the dominant hydraulic and geometric parameters. The relatively simple models discussed herein provide a means of predicting the magnitude and variance of stress and pressure on the boundary of an overfall. Reasonable estimates of boundary shear stress allow estimation of headcut movement.

INTRODUCTION

Overfall erosion occurs in rills, field gullies, gullies in earth auxiliary spillways, and retreating knickpoints in major river systems. While the scale of the erosion process varies greatly, the driving hydraulic forces in the erosion process remain much the same. As flowing water encounters an abrupt change in elevation, the resulting plunging action can create a reverse roller that undercuts the upper surface and allows the gully to move upstream. The obvious impact of the overfall process is to increase soil erosion, dissect farmland with retreating gullies, and threaten the safety of hydraulic structures.

The magnitude and variance of hydraulic shear stress and pressure transmitted to the boundary of the overfall are considered major components in the overfall erosion process. The objective of this study was to develop prediction relations for the magnitude, location, and variance of stress and pressure at the overfall. Boundary stress is considered a key component of the headcut advance process. By providing a means of estimating stress, headcut advance can also be estimated.

Certainly, stress and pressure are not the only factors contributing to gully movement. Other erosion processes such as mass wasting, material weathering, and subsurface seepage would be expected, in certain conditions, to significantly contribute to overfall erosion.

The reader is reminded that the results presented herein were developed using a hydraulically smooth model with an impervious boundary. An erodible soil boundary would quickly deform when exposed to high hydraulic stresses. A soil boundary is also pervious which would allow pressure forces to be transmitted into the soil. While a soil boundary may react quite differently with time, the forces transmitted to the overfall boundary at the start of the erosion process are represented by model results.

This research was conducted primarily to model the forces causing gully movement in earth emergency spillways. Spillways typically transmit wide, shallow flows. Therefore, the models use a flow rate per unit width as a discharge variable. Other gully settings may not be best described by use of a unit discharge.

RELATED WORK

A detailed examination of energy loss below a free overfall was conducted by Moore (1943). He found that the energy losses below the fall were appreciable and should be considered in hydraulic design. Using the momentum equation, Moore also developed a relation for the height of standing water underneath the nappe for low tailwaters. In his discussion of Moore's paper, Rouse (1943) derived a relationship for the ultimate vertical thickness of the nappe, which is approached asymptotically as the pressure intensity within the falling nappe approaches atmospheric. In another review of Moore's paper, Bakmeteff and Feodoroff (1943) discussed the differences in behavior of aerated and non-aerated nappes at the overfall. The nappe of a non-aerated overfall is deflected toward the vertical wall when compared with the aerated case. As described herein, an aerated nappe has atmospheric pressure above and below the nappe. The non-aerated nappe has atmospheric pressure above the nappe and subatmospheric pressure below the nappe.

The shear stress and pressure forces produced by planar jets impinging a smooth boundary at normal and oblique angles were examined by Kamoi and Tanaka (1972) and Beltaos (1976). Beltaos and Rajaratnam (1974) also examined impinging circular turbulent jets. All three studies used air as the flow medium by keeping air speeds well inside the incompressible range. Beltaos used dimensional analysis to develop stress and pressure prediction equations for a fully developed jet in the impingement region. These researchers found that the stagnation pressure is located at or just upstream of the point of jet impact with the bed. The maximum shear stress was observed downstream of the maximum pressure location.

Hanson et al. (1990) used hot-film anemometry with water to examine the stress distribution below a submerged circular jet. The mean pressure and shear stress distributions were similar to Beltaos and Rajaratnam's air results.

A model study of the erosive potential of aerated and non-aerated nappes in earth spillways was conducted by May (1989). The unvented or non-aerated nappes were observed to shift the nappe profile closer to the vertical face and increase the rate of headcut advance. May noted that the highest rate of headcutting does not necessarily correspond to the highest discharge.

An analysis of the mechanics of headcut migration in rills was conducted by Stein (1990). A model was developed that related two-dimensional headcut migration to sediment detachment just upstream and downstream of the headcut. If erosion upstream of the headcut dominates, then the overfall gradually decreases and approaches the eroding channel bed. If the downstream erosion dominates, then a headcut with a near vertical face migrates upstream with time.

Robinson (1989a, 1989b) measured the boundary shear stress and pressure forces below a straight drop overfall using hot-film anemometry and pressure transducers. Stress and pressure variations in time and space were recorded over selected ranges of overfall height, flow rate, and basin backwater level. The nappe was intentionally not aerated, to deflect the nappe closer to the overfall and maximize stress on the vertical wall. This data base was used to develop the simplified prediction equations presented in this paper for the maximum time-averaged values of stress and pressure transmitted to the surface of the overfall.

EXPERIMENTAL EQUIPMENT AND PROCEDURE

A straight-drop overfall model constructed entirely of acrylic plastic was used in this study. The smooth-boundary model had a horizontal approach, a vertical overfall, and a horizontal escape slope. The model width was 0.91 m (3 ft), and the vertical overfall heights examined were 76.2, 50.8, and 25.4 cm (30, 20 and 10 in). An overflow tailgate allowed separate adjustment of the tailwater below the overfall (fig. 2.1). Flush-mounted hot-film anemometry probes were calibrated in a pipe loop before and after inserting them into the model for stress measurement. A constant-temperature anemometer was used to measure magnitude and variation of boundary shear stress. A temperature-compensated pressure transducer was connected to 1.6-mm diameter piezometer taps in the model floor and vertical wall to measure pressure magnitude and variance. The pressure transducer was calibrated using a static water column. A thermistor thermometer was used to monitor calibration loop and model temperatures. A digital oscilloscope was used to receive and record the stress, pressure, and temperature signals.

The majority of stress and pressure measurements were taken at 7.62-cm (3-in) intervals along the vertical wall and basin floor. The origin for probe positioning was at the base of the overfall. Flow rates of 0.028, 0.056, 0.085, and 0.113 m^3/s (1, 2, 3, and 4 ft^3/s) were all examined at multiple drop heights. The basin backwater was initially set high to a point where the basin was fully submerged. The backwater was then lowered in 7.62-cm (3-in) intervals until no backwater was imposed. Detailed descriptions of test procedures and equipment are included in Robinson (1989a) for those readers requiring more detail.

Previous analysis of the hot-film probe calibration curves used the relation $\tau = aV^b$ where τ is the shear stress, V is the average sweep voltage, and a and b are fitted coefficients. Calibrations taken before and after each model run were required to display a correlation coefficient greater than or equal to 0.95 or the test was repeated. The present study used a least squares optimization procedure to fit the calibration equation $\tau = aV^b + c$, where V represents individual voltage measurements (approximately 160,000 per run). Fitted coefficients are a, b, and c. This change was made to eliminate non-linear biasing. If the summation of the square of the error was greater than 0.03, the test was not included in the analysis. This more restrictive criteria caused 16 of the 80 model runs to be dropped from the analysis and introduced gaps in the data base.

DISCUSSION / RESULTS

A two-stage approach was used to analyze the data. The first stage involved developing prediction equations for the nappe profile above the backwater pool. Input parameters for this prediction are the approach flow depth, unit discharge, overfall height, and backwater level (fig. 2.2). The approach flow depth (D_a), as described by Rouse (1943), is measured 3.5 D_a upstream of the overfall brink. This approach depth definition consistently treats flows with Froude numbers of unity or larger. The approach depth was determined iteratively from flow depths measured upstream of the overfall. Stage 1 calculations describe the nappe up to the point where the nappe enters the backwater pool. The stage 2 calculations consider the nappe from the point of entry into the backwater pool until it strikes the basin floor. Most of the prediction equations included in this paper use stage 1 parameters. The equations developed herein describe the nappe profile, as well as, the magnitude, location, and variance of the stress and pressure at the overfall. These equations are dimensionless and may be used with any consistent system of units unless otherwise indicated.

Aerated Nappe Profile

Rouse (1943) provides data for the aerated nappe profile over a range of Froude numbers. Using Rouse's data, a fitted equation was developed. The origin for this equation is at the top of the vertical overfall. The horizontal position X and the vertical position Y are each nondimensionalized with the approach flow depth D_a.

$$Y/D_a = K\ F^A\ (X/D_a)^B + C \tag{2.1}$$

where: (F >=1, X >= 0)

$F = V_a^2/(g\ D_a)$

D_a = Approach depth

V_a = Average approach velocity

g = Gravitational acceleration

K = -0.483

A = -0.546

B = 1.600

C = 0.823

The approach velocity (V_a) was determined at the location of the approach flow depth (D_a). The definition for F, taken directly from Rouse (1943), is equivalent to the Froude number squared.

This prediction equation does a good job ($R^2 = 0.98$) of fitting Rouse's data for F<=3.02 (fig. 2.3). Note that the equation predicts a constant nappe width of 0.823 D_a for all values of F at the overfall brink (X=0). Rouse (1943) showed that the brink depth is actually 0.715 D_a at F=1 and increases asymptotically toward unity as F increases. The stress and pressure data base exhibited F values ranging from unity to approximately 2.5. The aerated nappe profile equation is also useful as a framework from which modifications can be made to describe the non-aerated nappe profile.

Non-Aerated Nappe Profile

Predicting the non-aerated nappe profile is more challenging. As illustrated in figures 2.4 and 2.5, the non-aerated profile deflects different amounts as the backwater level is changed. The reader should note that at high and low backwaters, the non-aerated case approaches the aerated case. An examination of the horizontal boundary pressures for both aeration states reveals a backwater-dependent shift. A plot of the location of maximum average boundary pressure versus backwater (fig. 2.6) illustrates that the deflection is a maximum for this flow condition at a 38.1-cm backwater. The location of the maximum average boundary pressure is measured as the horizontal distance downstream from the vertical wall.

The vast majority of nappe profiles were collected in the non-aerated state. A relationship was developed to correct for the non-aerated profile deflection assuming that the non-dimensional fall height $F_h = (H\text{-}Bw)/H$ and the ratio H/D_a govern the profile deflection.

$$C_n = C_1 + C_2\, F_h\, (H/D_a)^{C_3}\, \mathrm{EXP}(C_4\, F_h) \qquad \textbf{(2.2)}$$

where: C_n = Non-aerated overfall correction

H = Overfall height

D_a = Approach depth

$F_h = (H-B_w)/H$

$C_1 = 0.146$

$C_2 = 27.452$

$C_3 = -0.852$

$C_4 = -6.102$

A plot of this function is attached for three H/D_a values (fig. 2.7). Note that the maximum value, and thus the maximum deflection, is predicted at a F_h value of approximately 0.2. Therefore a backwater level of approximately 0.8 H would be expected to produce the greatest nappe deflection.

The non-aerated nappe profile was then predicted using the following equation:

$$Y/D_a = K\ F^{A}\ (X/D_a)^{(B+C_n)} + C \qquad \textbf{(2.3)}$$

$(F >= 1, X >= 0)$

The fitted coefficients K, A, B, and C are the same as for the aerated condition. The origin is located at the top of the vertical overfall. A plot of measured vs. predicted Y/D_a values (fig. 2.8) for the non-aerated profiles suggests a reasonable fit (R^2=0.99). This equation incorporates the change in non-aerated profile deflection associated with a change in backwater.

Derived Parameters

For given values of approach depth, unit discharge, backwater, and overfall height, the predicted nappe profile can be calculated. Figure 2.9 illustrates the stage 2 or derived parameters that can be developed from a predicted nappe profile. The impact angle of the upper nappe surface as it enters the backwater pool (A_n) can be determined by taking the derivative of the profile equation (Eq. 2.3) evaluated at the point of impact with the backwater pool.

$$dY/dX = K\ F^{A}\ (B+C_n)\ (X/D_a)^{(B+C_n)-1} \qquad \textbf{(2.4)}$$

The impact angle can be represented in degrees by taking the arctangent of this entry slope. The predicted point of impact with the horizontal floor (D_s) is determined by assuming the nappe projects to the bed as a tangent (N_l) to the entry angle (fig. 2.9).

If the predicted brink depth is assumed to be the vertical nappe thickness, a lower nappe profile is available as well. The nappe width on entry into the backwater pool (N_w) was determined by iteratively calculating the distance between upper and lower profiles on a line normal to the lower nappe. For a given unit discharge and a calculated nappe width, the average impact velocity (V_n) can be readily determined. The predicted nappe profile is of primary importance in the determination of the stage 2 parameters (N_w, V_n, A_n, N_l, and D_s).

Dimensional Analysis

Due to the sensitivity of the stage 2 parameters to the water surface profile prediction, dimensional analysis was performed on both the stage 1 parameters and the stage 2 parameters. The stage 1 parameters are simpler to apply, so prediction equations that follow use these parameters. Both methods provide reasonable prediction of stress magnitude on the horizontal floor and vertical wall. The location of peak stress and pressure was estimated using only stage 2 parameters.

The prediction equations were developed using non-linear multivariate analysis to determine fitted constants for selected groupings of dimensionless pi terms. The reader should apply judgment and appropriate caution when extrapolating these equations beyond the data base.

Stagnation Pressure

Horizontal Stagnation Pressure Magnitude

The excess or stagnation pressure observed on the horizontal floor was defined as the difference between the maximum and minimum time-averaged pressure along the horizontal boundary for a given flow rate, overfall height, and backwater level. The location of maximum pressure which coincides closely with the nappe impact on the floor is described as the distance downstream of the vertical overfall.

Analysis of the collected data suggests the development of two separate prediction equations based on the basin backwater level. As the nappe enters the backwater pool, the nappe diffuses by increasing in width and decreasing in average velocity. Albertson et al. (1950) found that the jet core velocity equals the entry velocity up to a distance of approximately six times the nappe width downstream of the jet entry point (fig. 2.10). It is reasonable to assume that when the backwater is sufficiently low, the nappe entry velocity is not diffused. Thus nondiffused or low backwater conditions are represented by one equation, while diffused or higher backwater levels are represented by another equation. Dimensional analysis will show that the maximum time-averaged horizontal stagnation pressure can be represented by the pi terms:

$\pi_1 = P_s/D_a$

$\pi_2 = q^2/(g\,D_a^3)$

q = discharge per unit width

$\pi_3 = H/D_a$

$\pi_4 = B_w/D_a$

The prediction equations were developed for plunging nappes ($B_w <= 0.9$ H). The maximum horizontal stagnation pressure (P_s) for high backwater ($N_l/N_w > 6$) can be represented as:

$$\pi_1 = 1.298\ \pi_2^{0.686}\ \pi_3^{1.020}\ \pi_4^{-1.495} \qquad \textbf{(2.5)}$$

(High Backwater)

Comparison of predicted versus measured values yielded an $R^2 = 0.98$ (fig. 2.11). Considering only the low backwater cases ($N_l/N_w <= 6$) where the core velocity of the nappe is not diffused prior to impact with the bed, the horizontal stagnation pressure is represented as follows:

$$\Pi_1 = 0.756\ \Pi_2^{0.434}\ \Pi_3^{0.791}\ \Pi_4^{0.134} \qquad \textbf{(2.6)}$$

(Low Backwater)

Predicted versus measured values also yielded an $R^2 = 0.98$ (fig. 2.12). Use of the stage 2 derived parameters allows a reasonable break between prediction equations at $N_l/N_w = 6$. However, use of stage 1 parameters does not provide as apparent a break between applicable equations. To apply the above equations with stage 1 information, calculate the maximum stagnation pressure using each equation, then use only the smallest predicted value. That is, the minimum of the predicted values from each equation is the appropriate value to use. Figure 2.13 graphically illustrates the transfer between the high and low backwater equations. All of the high and low backwater equations that follow can be applied in this manner.

Horizontal Stagnation Pressure Location

The location of the maximum horizontal stagnation pressure (X_p) may be estimated using the relations:

$$S/N_l = 0.154\ \mathrm{COT}(A_n) \qquad \textbf{(2.7)}$$

where: S = eccentricity, per Schauer and Eustis (1963).

$$X_p = D_s - S - (N_w/2) \tag{2.8}$$

D_s, S, N_l and N_w must all have the same units.

The eccentricity (S) has been physically interpreted as the small distance upstream of the predicted tangential impact with the bed required for streamlines to impact normal to the floor (Beltaos, 1976). A comparison of predicted versus measured maximum pressure location yielded an $R^2 = 0.98$.

Vertical Wall Stagnation Pressure

The stagnation pressure exerted on the vertical face was much smaller than the stagnation pressures observed on the horizontal floor. While pressure fluctuations were measured, the pressure is adequately approximated by hydrostatic conditions. An exception to the hydrostatic condition is at low backwater levels. As noted by Moore (1943), the water level below the nappe is greater than the backwater setting. Moore explained that the standing water behind the fall is due to a change in horizontal momentum as the water strikes the channel floor.

Shear Stress

Horizontal Stress Magnitude

The magnitude of the maximum time-averaged horizontal stress (τ_h) can be represented as:

$\pi_1 \quad = \quad \tau_h/(\gamma\ D_a)$

γ = unit weight of the water

$\pi_2 \quad = \quad q^2/(g\ D_a^3)$

$\pi_3 \quad = \quad H/D_a$

$\pi_4 \quad = \quad B_w/D_a$

Again considering only plunging nappes (B_w <= 0.9 H), the stress prediction equations for high and low backwater cases are:

$$\pi_1 = 0.032\ \pi_2^{0.204}\ \pi_3^{0.852}\ \pi_4^{-1.796} \tag{2.9}$$

Equation 2.9 is for high backwater and equation 2.10 is for low backwater.

$$\pi_1 = 0.011\ \pi_2^{-0.001}\ \pi_3^{0.582}\ \pi_4^{-0.114} \tag{2.10}$$

The π_2 exponent for low backwater cases is very near zero, so this term can be dropped without adversely affecting the predicted value. All terms are included for the sake of consistency. The measured versus predicted stress values for high and low backwater cases are shown as figures 2.14 (R^2 = 0.95) and 2.15 (R^2 = 0.97). The transfer between high and low backwater stress prediction equations can be performed in the same manner as described above for stagnation pressure by using the minimum predicted value (fig. 2.16).

Horizontal Stress Location

The location of the maximum horizontal stress (X_h) can be estimated with the relation:

$$X_h = D_s + 1.417\ D_a \tag{2.11}$$

D_s and D_a must have the same units. That is, the maximum stress is located a small distance downstream of the predicted point of nappe impact with the floor. This location is reasonable recognizing that the flow accelerates downstream away from the point of nappe impact. Comparison of predicted versus measured horizontal stress location yielded an $R^2 = 0.98$.

Vertical Wall Stress Magnitude

The magnitude of the maximum stress on the vertical wall (τ_v) can be represented as:

$$\pi_1 = \tau_v/(\gamma\ D_a)$$

$$\pi_2 = q^2/(g\ D_a^3)$$

$$\pi_3 = H/D_a$$

$$\pi_4 = B_w/D_a$$

$$\pi_5 = X_p/D_a$$

X_p is the location of the maximum pressure on the horizontal floor, and γ is the unit weight of the water.

$$\pi_1 = 0.025\ \pi_2^{-1.295}\ \pi_3^{0.026}\ \pi_4^{0.221}\ \pi_5^{-1.062} \qquad \textbf{(2.12)}$$

No distinction is made between high and low backwaters for the vertical wall stress prediction equation. The last pi term (π_5) recognizes that as the nappe deflects closer to the overfall an attendant increase in wall stress occurs. A plot of predicted versus measured stresses on the vertical wall is attached as figure 2.17 ($R^2 = 0.94$).

Vertical Wall Stress Location

The location of stress on the vertical wall was not reduced to a prediction equation. However, the maximum time-averaged values of stress on the vertical wall were all observed to occur near the base of the overfall. That is, the maximum vertical wall stress may be safely assumed to occur near the base of the overfall.

Variance

While predictions of stress and pressure magnitude are important, knowledge of the variability of these parameters may be equally important. Variance as used herein was calculated using:

$$\text{Variance} = \sum_i (x_i - \bar{x})^2/(n-1)$$

The estimated variance of a random variable (x) is the average squared deviation from the sample mean for a discrete population of size n.

Horizontal Stagnation Pressure Variance

The variance (V_p) associated with the horizontal stagnation pressure prediction is as follows:

$$\pi_1 = V_p/P_s^2$$

$$\pi_2 = q^2/(g\, D_a^3)$$

$$\pi_3 = H/D_a$$

$$\pi_4 = B_w/D_a$$

The horizontal stagnation pressure variance prediction equations for the high and low backwater cases are:

$$\pi_1 = 0.025\, \pi_2^{-0.379}\, \pi_3^{0.691}\, \pi_4^{0.436} \qquad \textbf{(2.13)}$$

Equation 2.13 is for high backwater and equation 2.14 is for low backwater.

$$\pi_1 = 0.012\, \pi_2^{0.032}\, \pi_3^{-1.254}\, \pi_4^{0.496} \qquad \textbf{(2.14)}$$

Predicted versus measured stagnation pressure variance values for high (R^2 = 0.96) and low backwater (R^2 = 0.92) show reasonably good agreement.

Horizontal Stress Variance

The variance of the maximum time-averaged horizontal stress (V_h) can be represented as:

$\pi_1 = V_h/\tau_h^2$

$\pi_2 = q^2/(g\ D_a^3)$

$\pi_3 = H/D_a$

$\pi_4 = B_w/D_a$

The horizontal stress variance prediction equations for high and low backwater cases are:

$$\pi_1 = 0.064\ \pi_2^{-0.669}\ \pi_3^{0.521}\ \pi_4^{0.240} \tag{2.15}$$

Equation 2.15 is for high backwater and equation 2.16 is for low backwater.

$$\pi_1 = 0.393\ \pi_2^{-1.691}\ \pi_3^{-1.396}\ \pi_4^{0.096} \tag{2.16}$$

Predicted versus measured horizontal stress variance values exhibit an R^2 of 0.94 for high backwater and 0.81 for low backwater.

Vertical Stress Variance

The variance of the vertical wall stress (V_v) can be represented as:

$\pi_1 = V_v/\tau_v^2$

$\pi_2 = q^2/(g\ D_a^3)$

$\pi_3 = H/D_a$

$\pi_4 = B_w/D_a$

$\pi_5 = X_p/D_a$

$$\pi_1 = 0.140\ \pi_2^{0.741}\ \pi_3^{-0.313}\ \pi_4^{-0.156}\ \pi_5^{0.777} \qquad \textbf{(2.17)}$$

Measured versus predicted values for vertical wall stress variance exhibit an R^2 of 0.90.

Error

The bulk of the data were measured at 7.62-cm (3-in) intervals along the boundary, and, certainly, error is expected. Nearly all of the predicted horizontal stress data are within ± 5 Pa (0.1 psf) of the measured values. The predicted vertical wall stresses were within ± 2.5 Pa (0.05 psf) of the measured values. The horizontal pressure predictions were nearly all within ± 5 cm (2 in) of the measured values. If, as in the case of variance, a predicted value is used in a subsequent prediction, the error scatter would be expected to increase.

SUMMARY

The stress and pressure forces on the boundary of an overfall are considered key components in the advance rate of a gully headcut. While other failure processes contribute to headcut movement, particularly mass wasting due to headcut instability, the boundary stress is considered to be a "trigger" force that can strongly influence the erosion process. The contribution of pressure fluctuations in the headcut erosion process is not well understood.

Prediction equations are developed to estimate the maximum time-averaged stress and stagnation pressure on the horizontal floor below the overfall. The equations were developed for non-aerated overfalls to examine the worst case stress condition. Nappe profile equations are presented for both aerated and non-aerated cases. At low backwaters, the impacting nappe was not completely diffused, and prediction relations consider both the high and low backwater (diffused and non-diffused) cases. A prediction equation is also provided for the maximum time-averaged stress on the vertical wall. Equations are presented to locate the horizontal position of the maximum time-averaged stress and pressure. The variance of stress and pressure are described by a prediction equation as well. The reader is reminded that a prediction of the maximum time-averaged stress or pressure suggests that the instantaneous value will be greater than the mean 50 % of the time.

The data used to develop these prediction equations were obtained for drop heights of 25.4, 50.8, and 76.2 cm (10, 20, and 30 in) exposed to flow rates of 0.028, 0.056, 0.085, and 0.113 m^3/s (1, 2, 3, and 4 ft^3/s). The 0.91-m (3-ft) wide model results have not been validated at overfall heights and flow rates beyond these limits. Caution is advised if these relations are extrapolated.

The logical extension of this work is to develop a stress detachment model and compare predicted gully advance rates versus field and laboratory data. To be useful for cohesive soils, the model must incorporate a headcut stability or mass wasting component. The thrust of future research will be the development of a gully advance model.

REFERENCES

Albertson, M. L., Y. B. Dai, R. A. Jensen, and Hunter Rouse. 1950. Diffusion of submerged jets. *Transactions of the ASCE* 115:639-697.

Bakmeteff, B. A. and N. V. Feodoroff. 1943. Discussion of: Energy loss at the base of a free overfall by W. L. Moore. *Transactions of the ASCE* 108:1364-1373.

Beltaos, S. 1976. Oblique impingement of plane turbulent jets. *Journal of the Hydraulics Division,* ASCE 102(HY9):1177-1192.

Beltaos, S. and N. Rajaratnam. 1974. Impinging circular turbulent jets. *Journal of the Hydraulics Division,* ASCE 100(HY10):1313-1328.

Hanson, G. J., K. M. Robinson and D. M. Temple. 1990. Pressure and stress distribution due to a submerged impinging jet. In *Proc. 1990 National Conf., Hydraulics Div.,* ASCE, 525-530.

Kamoi, A. and H. Tanaka. 1972. Measurements of wall shear stress, wall pressure and fluctuations in the stagnation region produced by oblique jet impingement. *Fluid Dynamic Measurements*, Conference papers, Leicester University Press 1:217-227.

May, J. H. 1989. Geotechnical aspects of rock erosion in emergency spillway channels; Report 4, Geologic and hydrodynamic controls on the mechanics of knickpoint migration. US Army Corps of Engineers Technical Report REMR-GT-3. Vicksburg, MS.

Moore, W. L. 1943. Energy loss at the base of a free overfall. *Transactions of the ASCE* 108:1343-1360.

Robinson, K. M. 1989a. Stress distribution at an overfall. *Transactions of the ASAE* 32(1):75-80.

Robinson, K. M. 1989b. Hydraulic stresses on an overfall boundary. *Transactions of the ASAE* 32(4):1269-1274.

Rouse, H. 1943. Discussion of: Energy loss at the base of a free overfall by W. L. Moore. *Transactions of the ASCE* 108:1383-1387.

Schauer, J. J. and R. H. Eustis. 1963. The flow development and heat transfer characteristics of plane turbulent impinging jets. Technical Report 3. Dept. of Mechanical Engineering, Stanford Univ., Stanford, CA.

Stein, O. R. 1990. Mechanics of headcut migration in rills. Dissertation for PhD., Colorado State Univ., Fort Collins, CO.

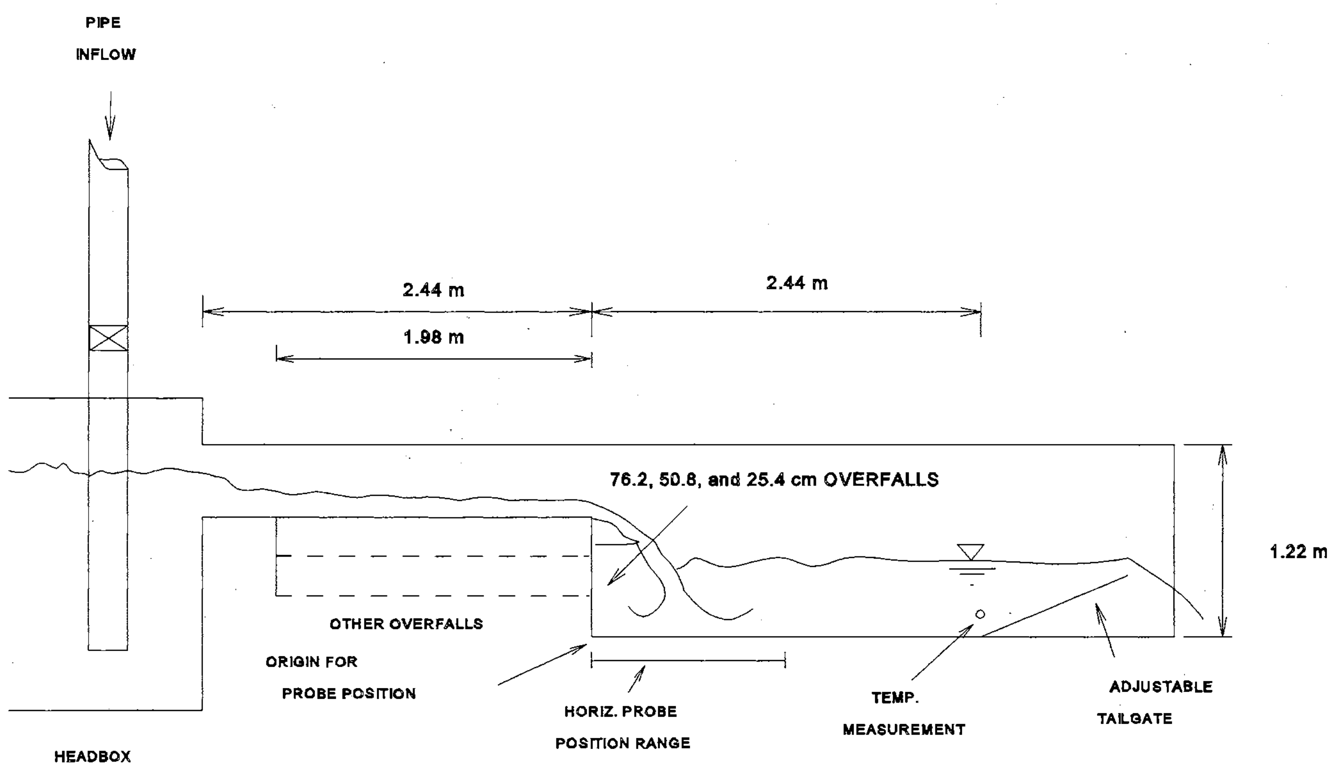

Figure 2.1. Overfall model

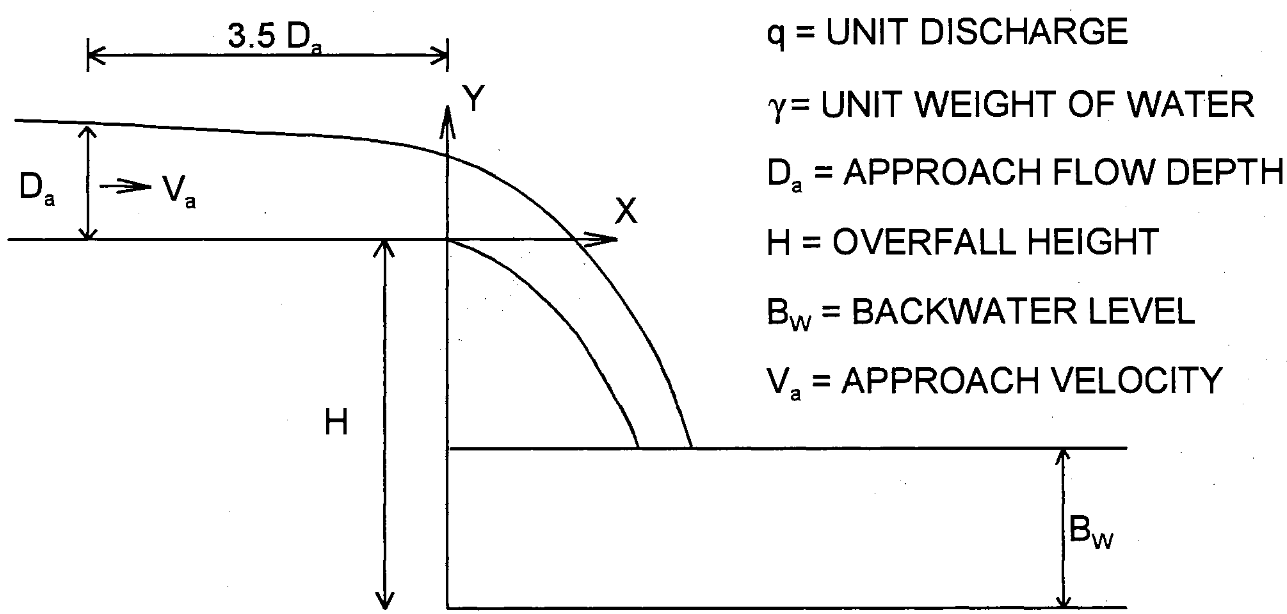

Figure 2.2. Stage 1 parameters

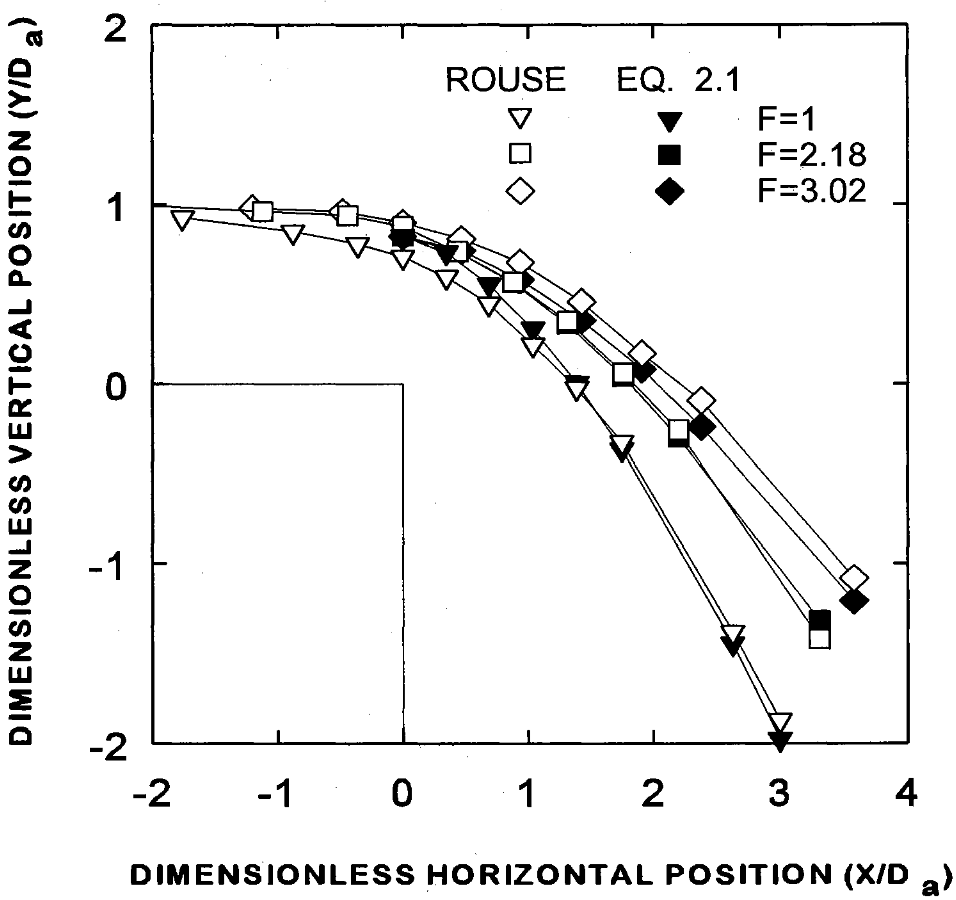

Figure 2.3. Predicted versus measured aerated nappe profiles

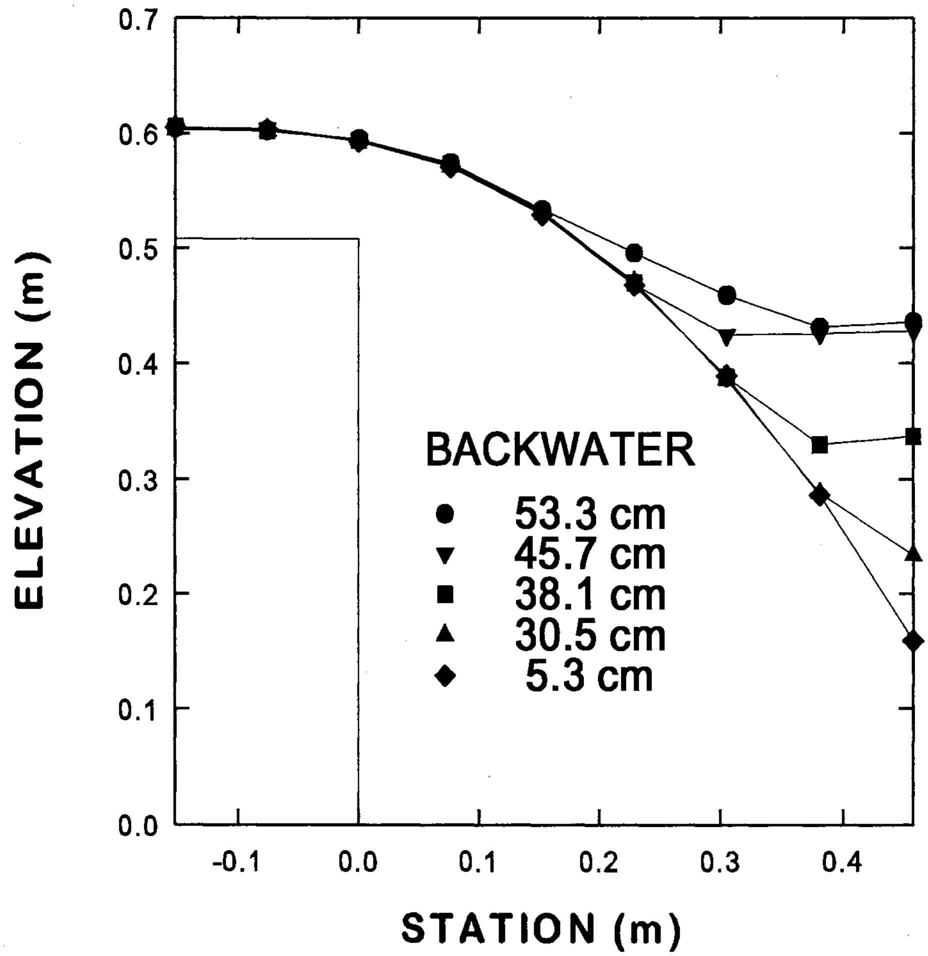

Figure 2.4. Measured aerated nappe profiles for $H = 50.8$ cm and $q = 0.038\ m^2/s$

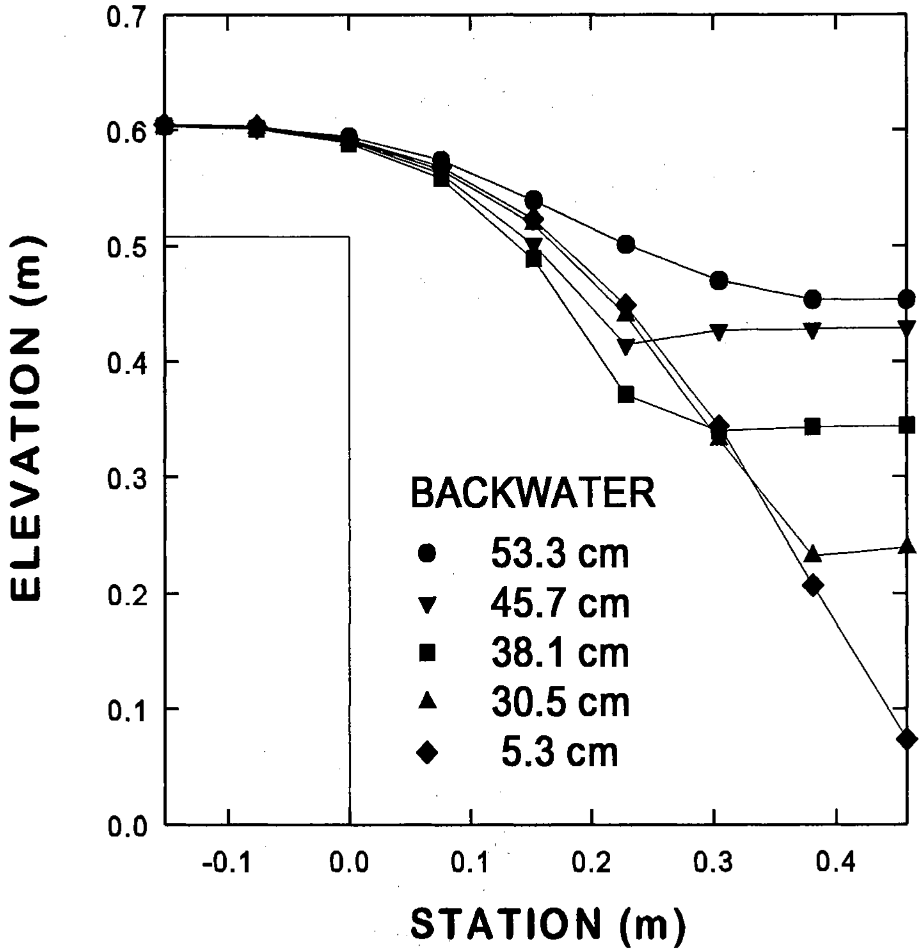

Figure 2.5. Measured non-aerated nappe profiles
for H = 50.8 cm and q = 0.038 m^2/s

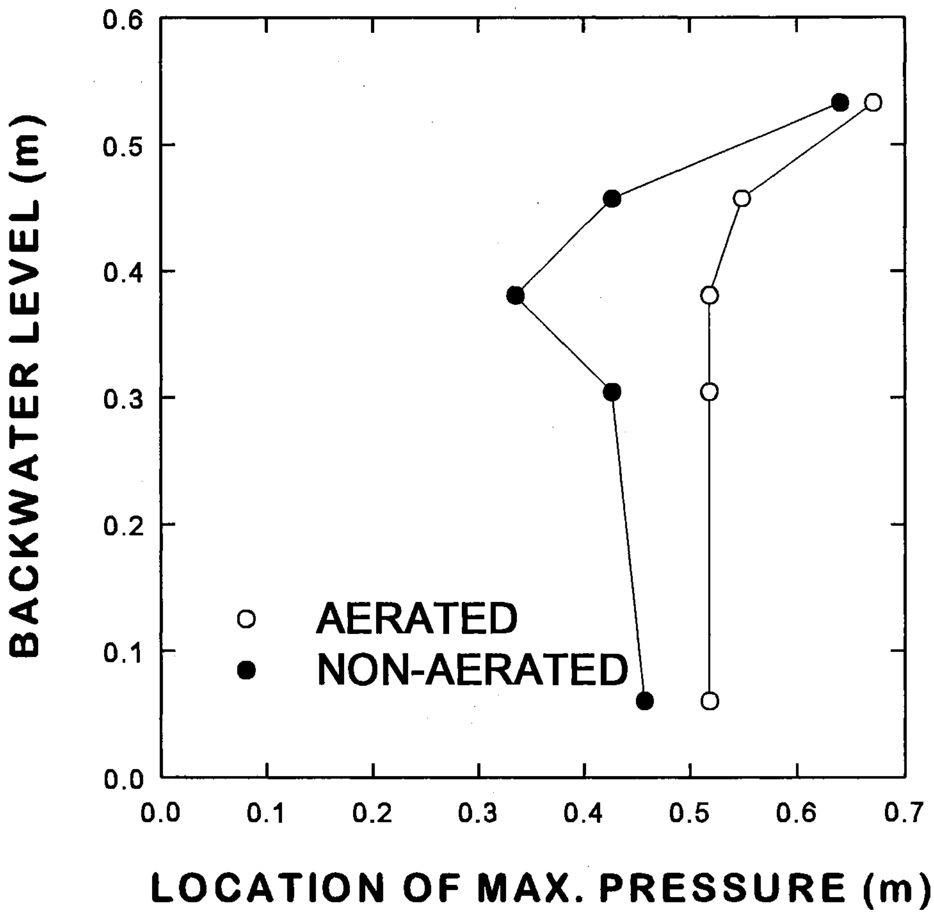

Figure 2.6. Location of maximum horizontal floor pressure for H = 50.8 cm and q = 0.038 m^2/s

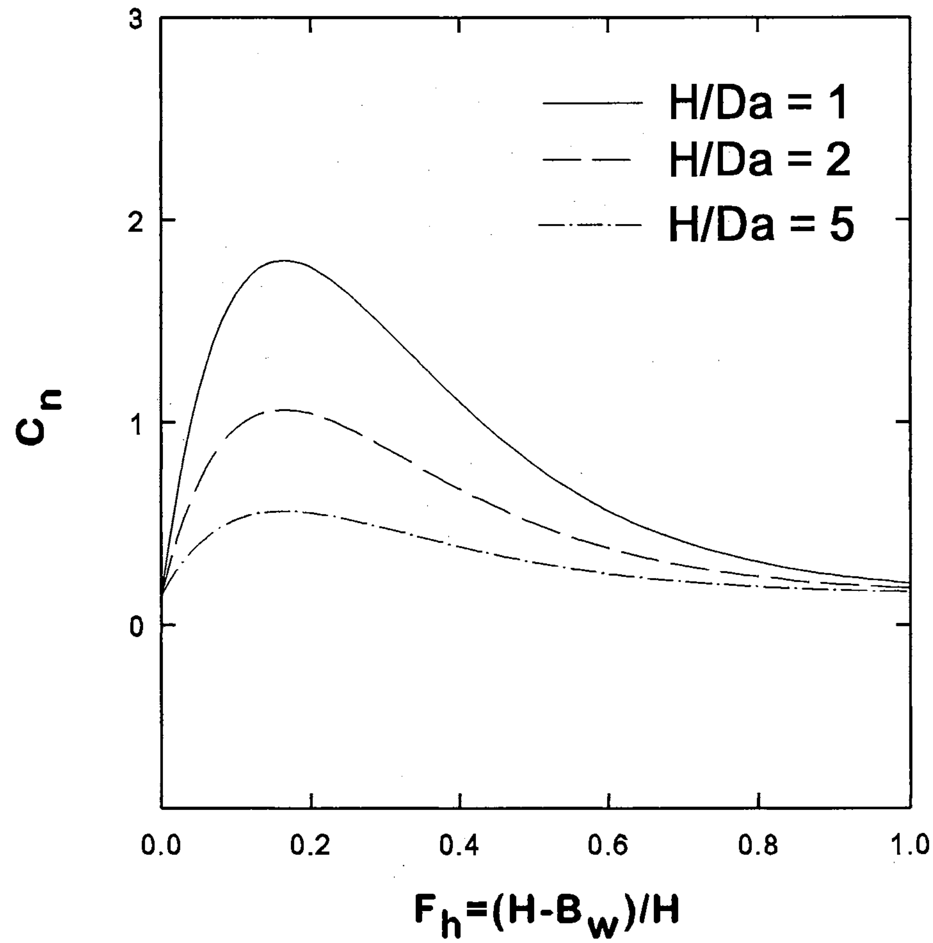

Figure 2.7. Non-aerated nappe profile correction function for three H/D_a values

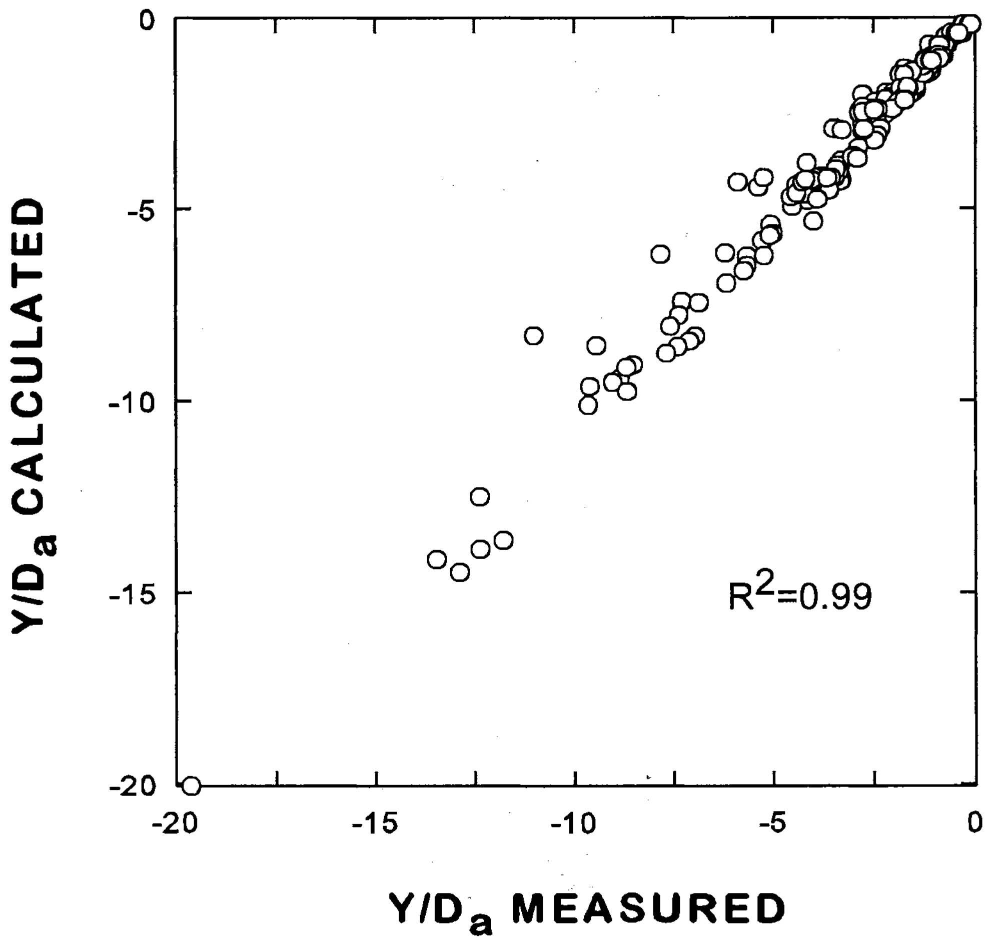

Figure 2.8. Predicted versus measured non-aerated Y/D_a values

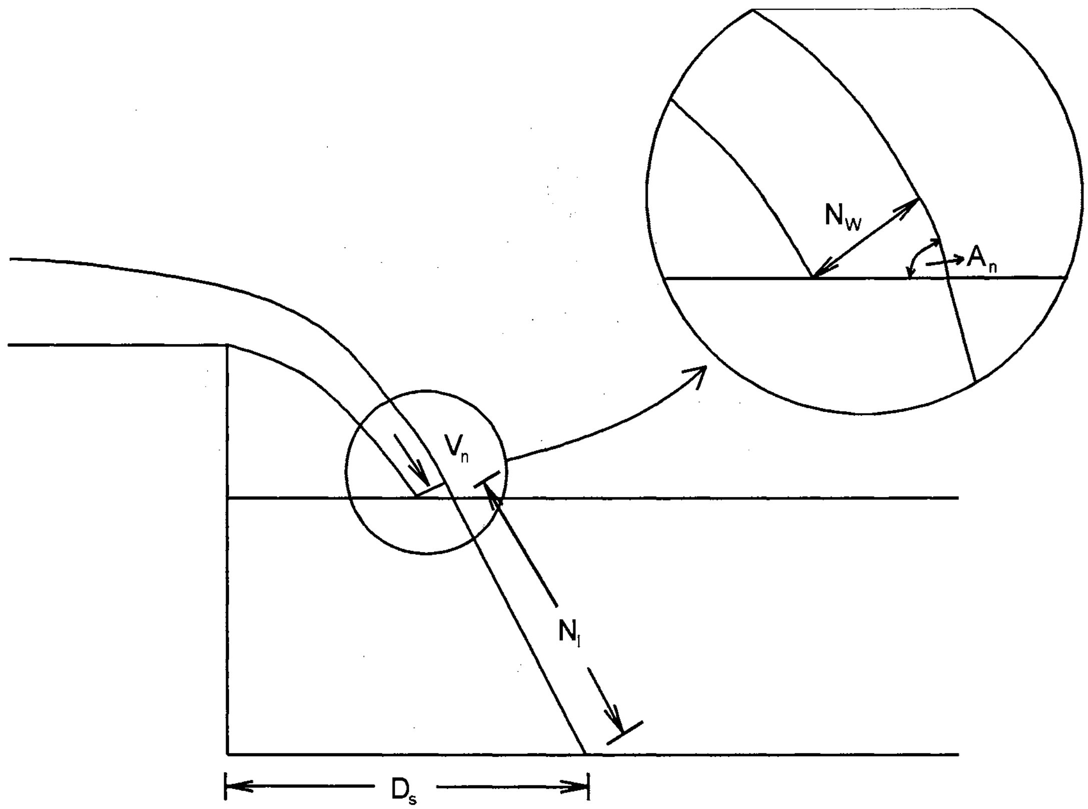

N_W = NAPPE WIDTH

A_n = UPPER NAPPE ENTRY ANGLE

V_n = NAPPE ENTRY VELOCITY

N_l = TANGENTIAL DISTANCE TO BED

D_s = HORIZ. DISTANCE FROM OVERFALL

Figure 2.9. Stage 2 or derived parameters

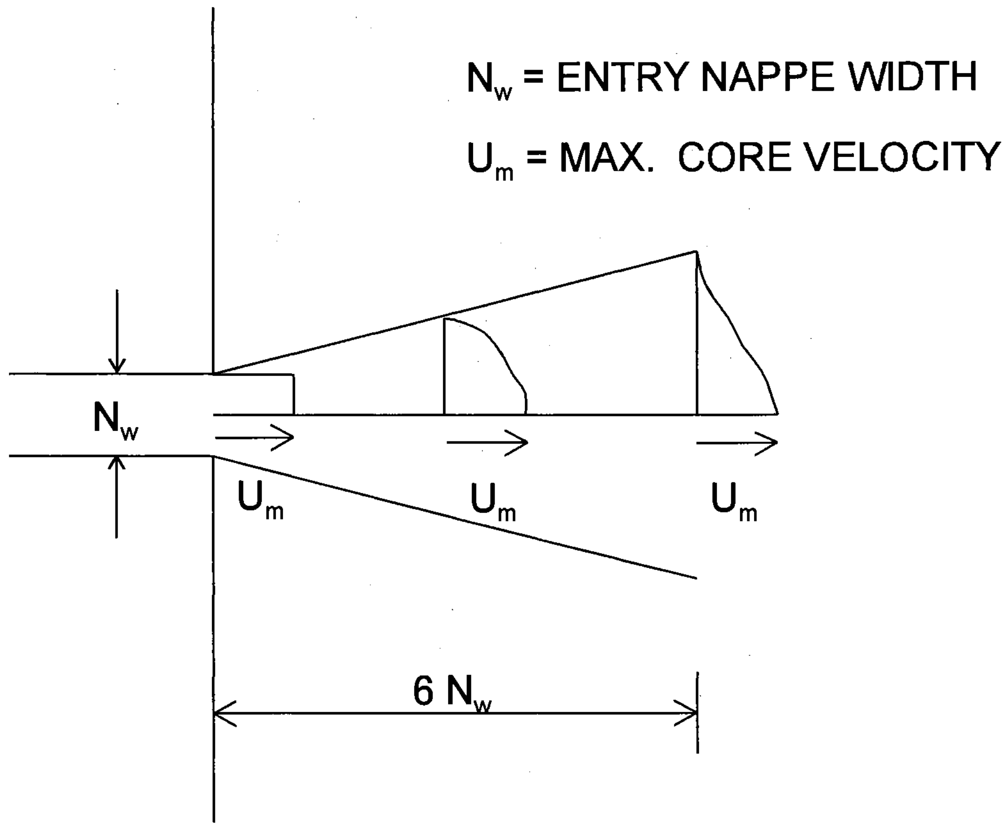

Figure 2.10. Jet diffusion

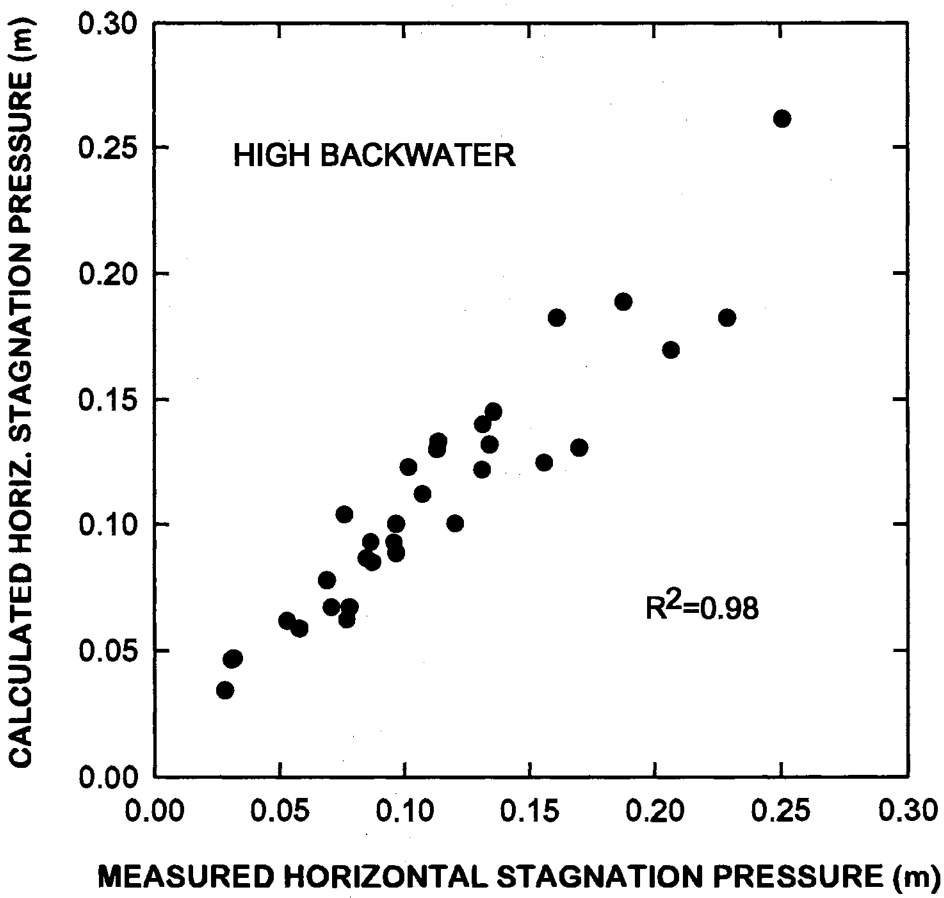

Figure 2.11. Predicted versus measured horizontal stagnation pressure using the high backwater equation

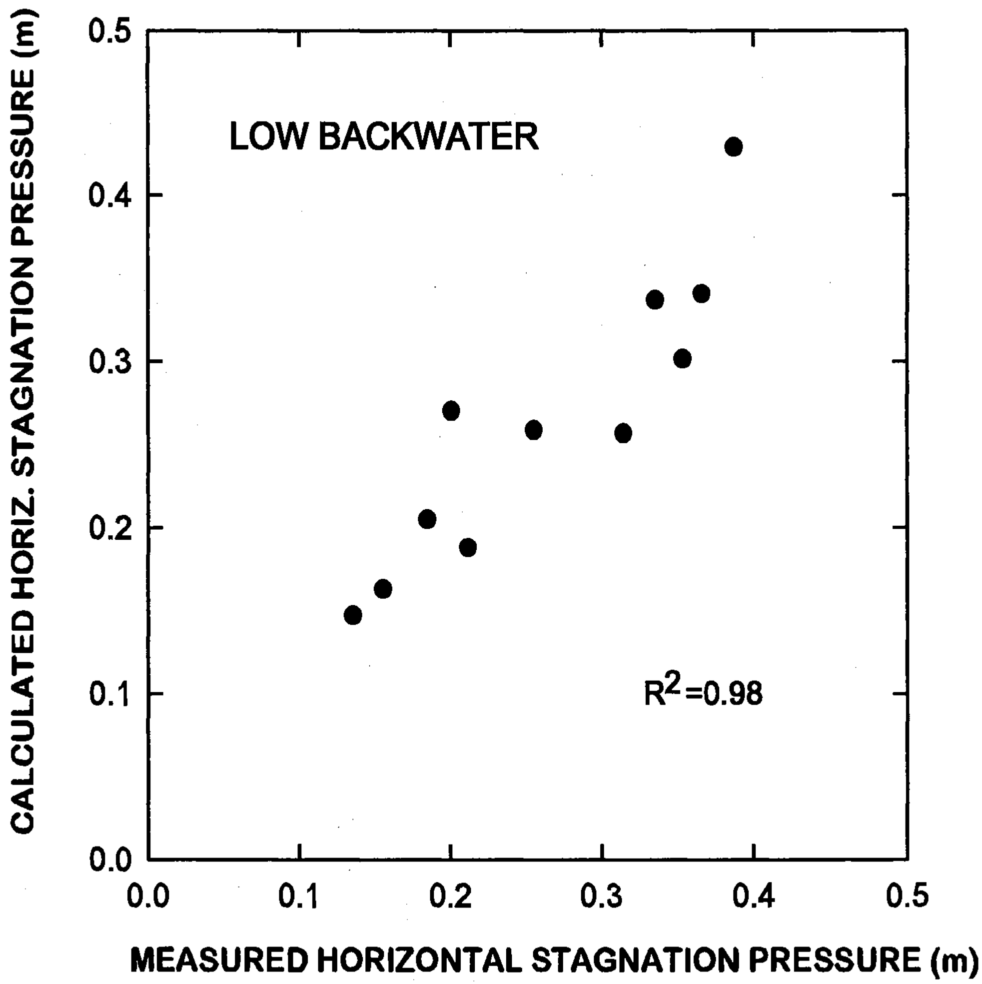

Figure 2.12. Predicted versus measured horizontal stagnation pressure using the low backwater equation

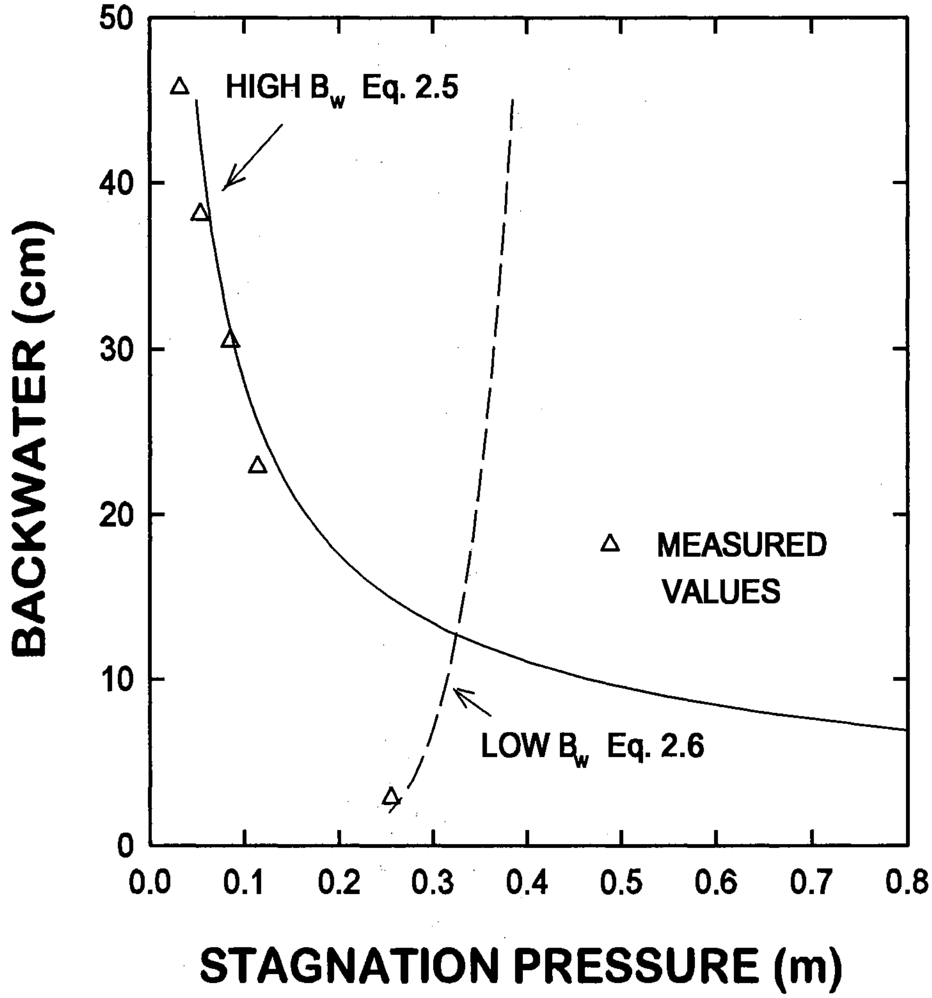

Figure 2.13. Typical plot of horizontal stagnation pressure prediction equations for D_a = 6.4 cm, H = 50.8 cm, and q = 0.062 m^2/s

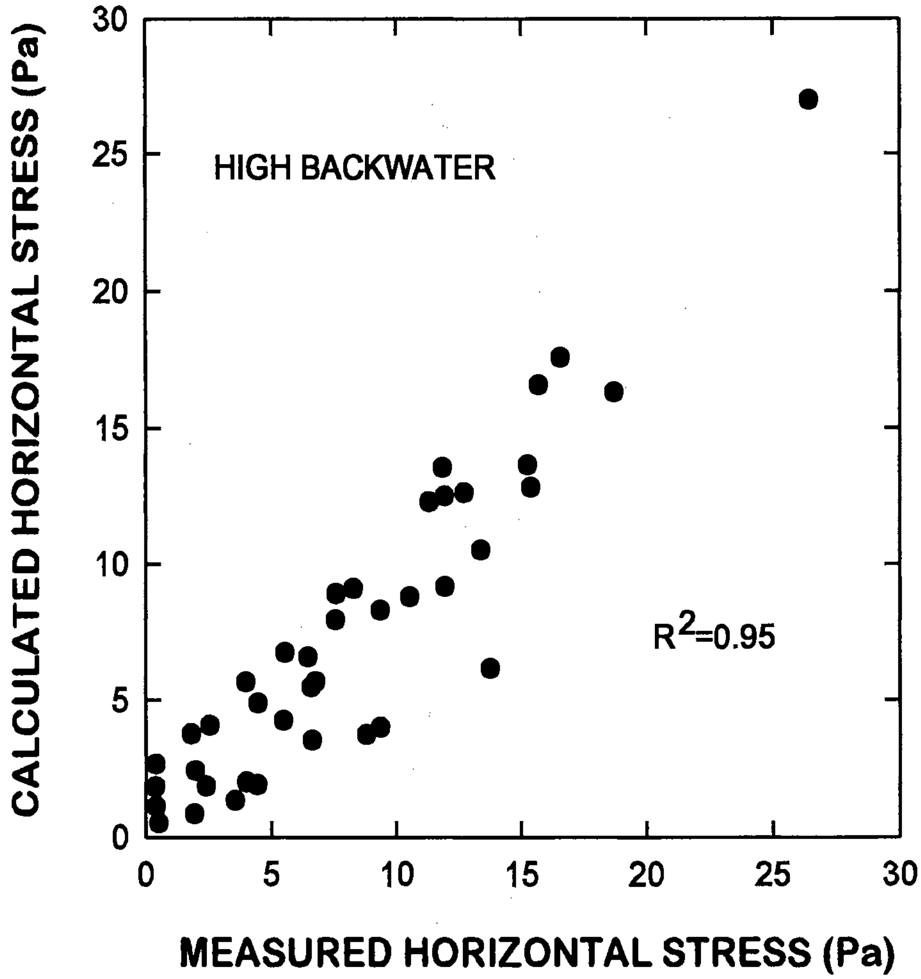

Figure 2.14. Predicted versus measured maximum horizontal stress using the high backwater equation

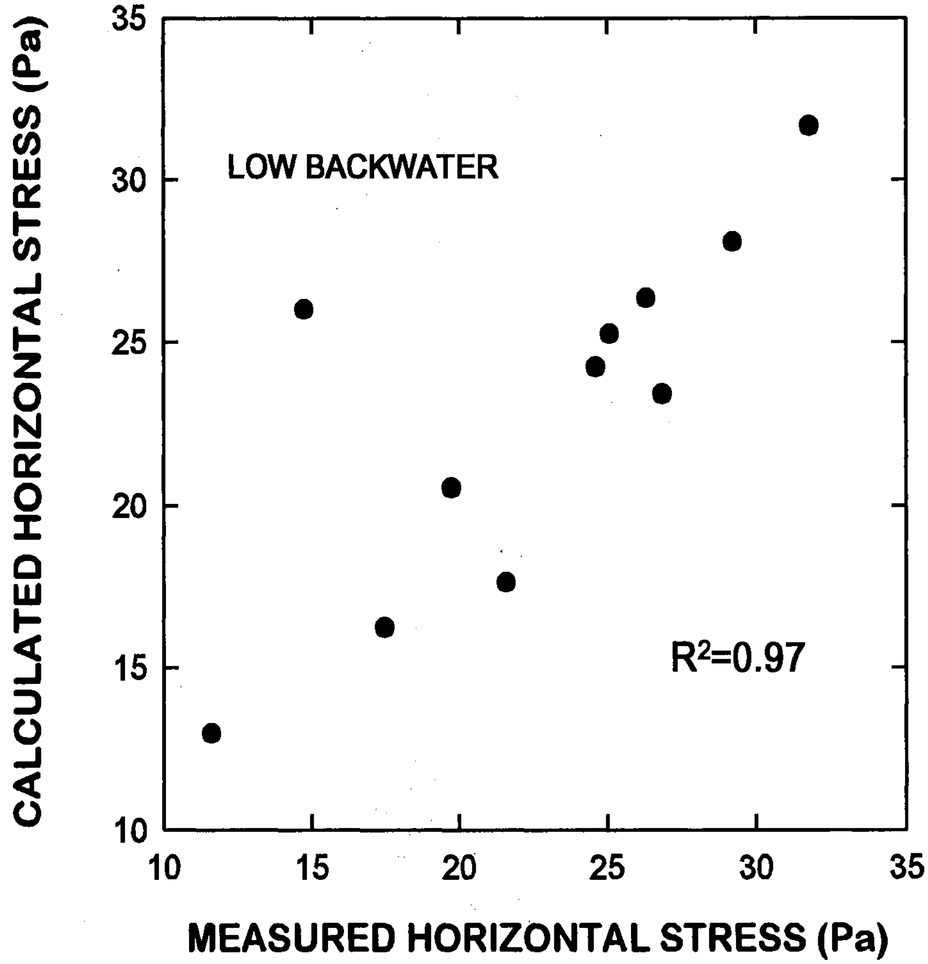

Figure 2.15. Predicted versus measured maximum horizontal stress using the low backwater equation

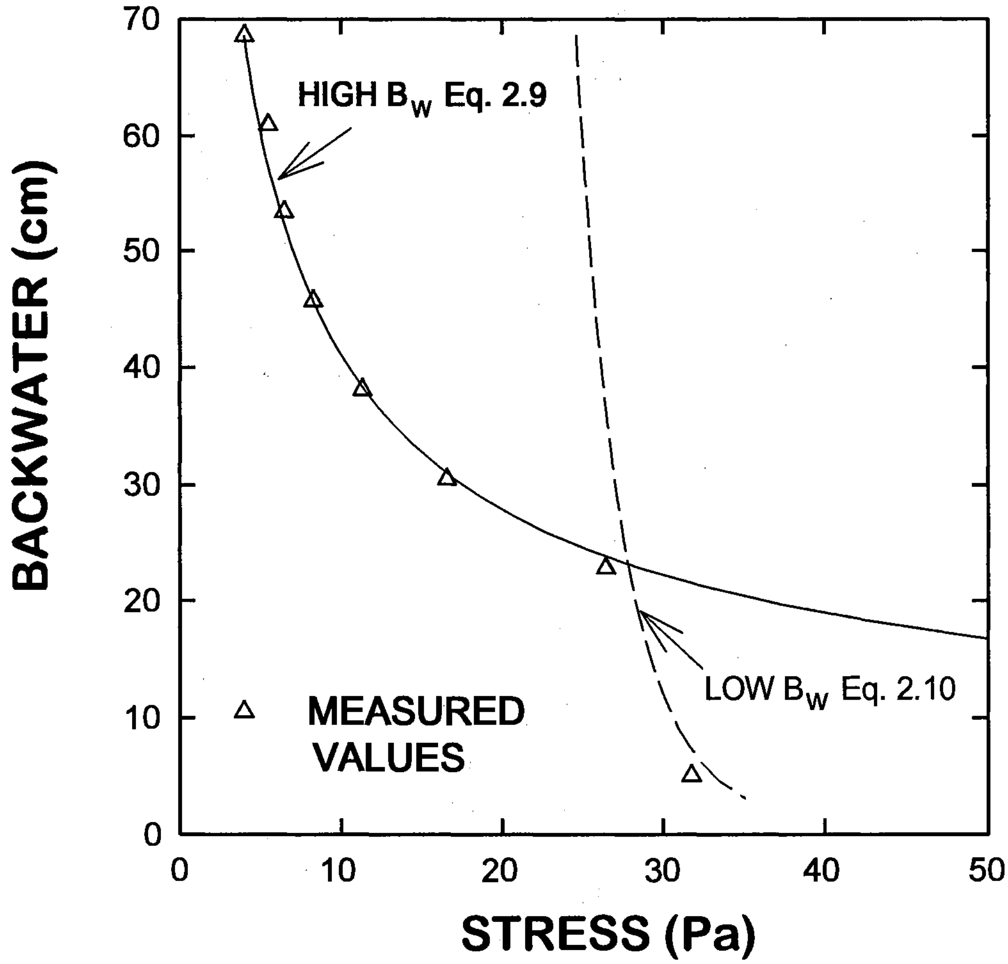

Figure 2.16. Typical plot of horizontal shear stress prediction equations for D_a = 7.8 cm, H = 76.2 cm, and q = 0.099 m^2/s

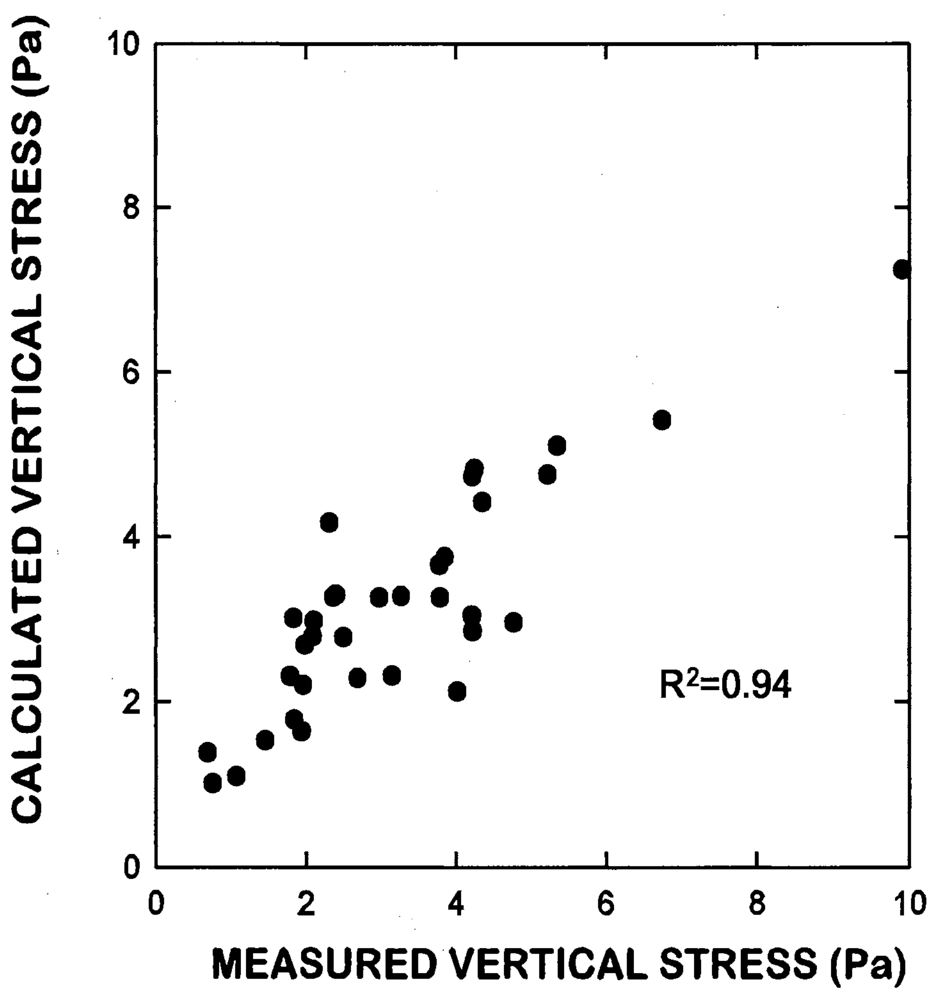

Figure 2.17. Predicted versus measured vertical wall shear stress

CHAPTER 3

LARGE-SCALE HEADCUT EROSION TESTING

ABSTRACT

The development and movement of gully headcuts can cause major damage in earth emergency spillways. A 1.8-m wide and 29-m long flume with 2.4-m high sidewalls was constructed to perform research on headcut advance. Headcut advance tests were conducted holding discharge, overfall height, and backwater level constant while varying soil properties. Two soil types were examined, and the soil properties were altered by compacting the material in the flume at varying moisture and density conditions. The observed headcut advance rates varied by a factor of more than 100 depending on the placement conditions. By placing a sand layer under the upstream half of the fill, the influence of a sand layer on headcut advance was also examined. Headcut advance and failure mechanics were observed and described.

INTRODUCTION

Failure of an earth spillway poses a threat to the people and property downstream of a dam. The formation and movement of a gully headcut are often the dominant form of damage observed in an earth spillway. To evaluate the risk of a spillway failure or dam breach, the rate of headcut advance or gully movement must be predicted. This prediction requires knowledge of the physical processes and erosion mechanics acting at the overfall. A large-scale headcut erosion test facility was constructed to scrutinize these erosion processes and to measure headcut advance rates. The objectives of this paper are to describe the test facility and to present test results. These test results concentrate on material properties and their impact on headcut advance. Headcut advance rates are presented for two soils examined at various moistures and densities. The discharge rate and overfall height were held constant for all tests. The influence of a sand layer on headcut advance was also examined by placing a sand layer under the downstream half of the test fill. The observed erosion processes are also described.

The migration of a gully headcut is very much a three-dimensional process. Lateral inflow along the sides of a gully contributes to gully widening and thus headcut advance. However, this large-scale flume study examines headcut advance in two-dimensions only. Velocity components in the horizontal and vertical directions were considered and lateral inflow velocities were ignored. This simplification was necessary for tests in a narrow flume; however, this simplification appears reasonable considering the wide, shallow flows typically transmitted in a spillway. For this study the headcut movement occurred uniformly across the full width of the flume due to flow over the headcut. The flume floor also acts as an inerodible layer thereby limiting vertical erosion. While an erosion resistant material that limits headcut depth is often observed in the field, the reader is reminded of this limiting condition. It is understood that factors such as subsurface seepage can play a major role in gully headcut advance. To breach a spillway, however, a headcut must move quickly during a single flood flow. Therefore, the time available for changes in the moisture regime of the soil profile is limited.

RELATED WORK

This paper describes research being conducted to better understand headcut movement in earth spillways. Related areas of study such as rill erosion, field gully migration, embankment overtopping, and fuse plug design can potentially benefit from this work. Examples of headcut advance models are those developed by De Ploey (1989), Temple (1992), and Robinson and Hanson (1992). De Ploey (1989) proposed a deterministic model of headcut advance encompassing material properties and fluid dynamics. The material properties were incorporated into an erodibility factor that included the material cohesion, the resistance to penetration, the bulk unit weight, and the field erodibility coefficient. The field erodibility coefficient included the complex interaction of the geometry of the banks and the plunge pool as well as the mechanical and structural properties of the material. De Ploey concluded that future research should focus on the erodibility factor.

Temple (1992) proposed a simplified headcut model of the form:

$$X = Cq^{a}H^{b}$$

The unit discharge (q) in m^2/s and the overfall height (H) in m are used to predict the headcut advance rate (X) in m/h. Exponents a and b are constants expected to be about 1/3 and 1/2, respectively. While a value of the material-dependent coefficient (C) was provided for four specific headcuts, a method of determining C is required for general application of this model. Robinson and Hanson (1992) proposed a more complex computer model that combines a stress prediction model with a mass wasting model. The model incorporates prediction equations for hydraulic shear stress on the boundary of an overfall developed by Robinson (1992). The Culmann method for failure of cohesive soils (Lohnes and Handy, 1968) was used to predict mass wasting events; therefore, the material properties are an important part of this model. This modeling effort attempted to describe overfall erosion mechanics, and the model identified areas where research was needed. The rate of headcut movement was predicted once the necessary input information was determined. An improved understanding is needed for input parameters such as soil erodibility, soil mass properties, tension cracks, and mass failure processes. A better understanding of the hydraulic boundary stresses and the variation of backwater level is also needed. The large-scale headcut advance testing described herein is an effort to acquire that information.

EXPERIMENTAL EQUIPMENT

The headcut advance test facility is composed of three major reinforced concrete structures (fig. 3.1) connected by earthen dikes. A profile of the flowline along the centerline of the test facility is also shown (fig. 3.2). A description of each structure along with their appurtenant structures follows:

Drop Structure

A laboratory supply canal provides open channel flow to the test facility. A 2.4-m wide modified Parshall flume for flow measurement was constructed just upstream of a 2.7-m wide straight drop spillway (Donnelly and Blaisdell, 1965). The drop structure was constructed with a 3.0-m vertical drop to conform with site conditions and to provide subcritical flow to the test flume. A flow control gate was positioned at the downstream end of the flow measurement flume, and a bridge was constructed over the drop structure to improve access to the test area.

Flume

The drop structure and test flume are connected by an earth forebay with a floor elevation 0.6 m below the test flume floor elevation. A 2.4-m long reinforced concrete transition section was constructed at the upstream end of the flume to provide a 0.9-m horizontal and a 0.6-m vertical contraction. The 29-m long horizontal test flume (fig. 3.3) is 1.8 m wide and has 2.4-m tall sidewalls. The flume was constructed with two 1.2-m wide, 2.1-m tall viewing ports in one side. These windows allow a side view of the erosion process as the headcut passes the window. A rail-mounted carriage was placed on top of the flume walls to allow rapid surface measurements. The carriage and rails are not shown in figure 3.3.

Outlet Structure

Downstream of the flume is an earth outlet basin where the majority of sediment is deposited after a test. The outlet basin has a concrete floor slab to allow access for debris removal. An outlet structure, located at the downstream end of the outlet basin, is equipped with a 2.3-m wide overflow tailgate. This winch-operated tailgate allows independent control of the tailwater setting in the flume. Flow exits the outlet basin into a collection channel. The outlet basin is also connected to the supply canal so it can be filled to a desired backwater before beginning a test flow.

Support Facilities

Test flows are provided through five 500-mm diameter siphons, and flows of up to 3.4 m^3/s can be conveyed through the test facility. Redundant flow measurement is provided at the gatehouse with an Ogee-crested weir. The supply canal is equipped with diversion channels and gates that allow flow bypass and control.

EXPERIMENTAL PROCEDURE

Soil Material and Sampling

A red sandy clay soil (CL) and a silty sand (SM) were examined during this study. These two soils were selected primarily since large quantities of these soils could be obtained with uniform soil properties. The red sandy clay soil exhibited a liquid limit of 26 and a plasticity index of 15. Using the Unified Classification System, the red sandy clay (CL) exhibited 25% clay, 40% silt, and

35% sand, and the silty sand (SM) had 13% clay, 30% silt, and 57% sand. The silty sand soil displayed a liquid limit of 16 and a plasticity index of 3. Standard Proctor tests on the CL soil exhibited a maximum dry density of 1.9 Mg/m^3 at an optimum moisture of 12%, while the SM soil exhibited a maximum dry density of 2.2 Mg/m^3 at an optimum moisture of 10.5% (fig. 3.4). Soil strength is an important parameter in headcut advance. Unconfined compressive strength tests were conducted in accordance with ASTM Standard D2166. Figures 3.5 and 3.6 show unconfined compressive strength test results for the CL and SM soil, respectively. These plots suggest that a strong relationship exists between the density and strength for these two soils.

Following placement of the soil in the flume and before testing, samples were taken from the downstream end of the placed soil. Density samples were taken with 76-mm diameter push tubes at 152 mm intervals in the vertical profile. Unconfined compressive strength samples were taken at 305 mm intervals with 51-mm diameter push tubes. Typically, seven density samples and three strength samples were taken for each test.

Fill Preparation

The test flume was filled by placing soil in horizontal loose lift layers of 152 or 203 mm thickness. If necessary, water was added to achieve a desired soil moisture. A tiller was used to mix the soil layer and to reduce aggregate sizes. Depending on the soil stockpile moisture conditions, the wetting and tilling process was repeated several times. A self-propelled vibratory padfoot roller was used to compact each soil layer. The 0.9-m wide roller effectively covered the 1.8-m wide flume with two side-by-side passes. The number of compactor passes for each layer was held constant during fill placement. A hand-held pneumatic compactor was used to compact the soil next to the concrete walls. The compacted soil surface was then tilled to a shallow depth. This scarification process was done to improve bonding with subsequent layers. These fill placement procedures were repeated until the desired fill depth was obtained.

As the soil increased in depth, a ramp was constructed at each end of the fill. This ramp allowed compactor access to the top of the fill. The downstream ramp was removed with a skid-steer loader just before testing. A near vertical overfall or headcut was prepared at the downstream end of the test section. Typically, the fill section was prepared with approximately 0.9 m of additional horizontal length to allow for soil sampling at the downstream end of the test section.

The desired mode of failure of the placed soil was by headcut advance. The potential for stress detachment damage along the horizontal soil surface was recognized, and a surface protection scheme was developed using all-weather carpet strips. The 1.8 m long and 406 mm wide carpet strips were overlapped much like roofing shingles starting at the overfall. The 1.8 m dimension was placed perpendicular to the flow, and the carpet strips were overlapped approximately 200 mm. The carpet pieces were pinned to the soil surface and weighted with steel bars. As the soil material was undercut, the carpet strips could fall away, thereby protecting the surface without influencing headcut advance.

The two viewing ports or windows were constructed with four removable panels in each window. While the channel was being filled, a set of plywood window panels were installed. Just before testing, the plywood panels were replaced with acrylic plastic panels. This procedure reduced scratching of the clear plastic panels. Each panel was constructed with angle iron frames to resist the substantial pressures at the window.

Testing

Each flume test was conducted following a routine sequence of events. The soil sampling was completed, and the headcut was preformed. The headcut or overfall is simply an abrupt change in elevation. The clear window panels were installed, and bed surface measurements were taken. An overflow tailgate setting was made, and the outlet basin was filled to establish the desired test tailwater condition. The tailwater or backwater level is simply the depth of the water downstream of the headcut. The flow control gate was then opened and the forebay was filled. As water filled the entrance section and began to flow over the test fill, the headcut position was monitored with time. Headcut movement was documented with photographs and video. Particular emphasis was placed on the erosion processes acting at the headcut. Water surface profiles were taken at regular time intervals, as were discharge readings at the modified Parshall flume. In most cases the test continued until the headcut breached the horizontal fill section.

RESULTS

A total of 10 headcut advance tests were performed in the flume. The horizontal test sections varied from 6.1 m to 12.2 m in length. Eight tests were conducted with the red sandy clay soil (CL), while the remaining two tests were performed on the silty sand material (SM). Six of the eight tests that used the red sandy clay were prepared with a sand layer of up to 305 mm in thickness under the downstream half of the test fill. This procedure allowed the influence of a sand layer on the advance rate to be examined. These tests were all performed at a flow rate of approximately 1.55 m^3/s and an overfall height of approximately 1.2 m. A low tailwater setting of approximately 0.3 m was used for tests 1 and 2, while a tailwater setting of approximately 1.0 m, as measured at the flume exit, was used for all other tests. The moisture content of the fill was controlled by adding water during fill placement. The density of the fill was varied by changing the loose lift thickness or altering the number of passes with the padfoot roller. Tests 1 and 2 were constructed with 203-mm loose lift layers, and all other tests used a 152-mm loose lift thickness. A vibration load was applied with the compactor for tests 4, 6, 7, and 8. The remaining tests used the same compactor without a vibration load.

Table 3.1 provides a summary of the experimental test conditions. Information about the fill materials, sand layers, tailwater, and overfall or headcut height is summarized. Table 3.2 provides a summary of the test results. The average moisture content, average dry density, and average unconfined compressive strength are presented, as are the observed advance rates. The maximum and minimum values of moisture, density, and strength are also presented to alert the reader of the variation in these test data. The moisture contents for tests 3, 4, and 5 were notably less than the remaining tests using the CL soil. The unconfined compressive strengths also exhibited a wide range in measured values. The headcut position was plotted versus the elapsed time, and the advance rate was determined as the slope of this plot. A plot of headcut movement data for run 1 (fig. 3.7) displays a typically linear advance rate. A linear regression was performed on the advance data, and all tests except test 6 displayed a coefficient of determination (R^2) of 0.92 or larger. Test 6 eroded very slowly with a total measured advance of only 1.2 m after approximately 8 hours of flow. The test 6 advance rate exhibited an R^2 value of 0.81. The linear advance rates observed for all tests suggest that the test fill was placed consistently. That is, the constant rate of headcut advance suggests the density and moisture of the fill was also relatively constant.

A plot of the average density versus the average moisture content (fig. 3.8) illustrates that the moisture ranges examined were above and below the optimum moisture of 12% for the CL soil and above the optimum moisture of 10.5% for the SM soil. The average density ranged from 81 to 94% of the maximum dry density for the CL soil. The average density of the SM soil was 84.5% and 80% of the maximum dry density. A plot of advance rate versus average density (fig. 3.9) illustrates that the advance rate decreases as the density increases. The data show a remarkably consistent trend considering the changes in moisture content. The advance rate plotted versus the average unconfined compressive strength (fig. 3.10) also displays an inverse relationship. These density and strength relationships appear logical.

A 305-mm thick sand layer placed at the bottom of the fill extended 4.6 m horizontally into the 9.2-m long horizontal fill for tests 4, 5, 6, 8, and 9. The influence of the sand layers on headcut advance is illustrated in figure 3.11. The sand layers were composed of a non-plastic SP-SM material for tests 3, 4, and 5 and a SM material with a plasticity index of 3 for tests 6, 8, and 9. Test 3 was not included in figure 3.11 since the sand layer was 152 mm thick. Tests 4 and 5, compacted on the dry side of optimum at moisture contents of 9.2% and 11.6%, achieved dry densities of 1.68 and 1.59 Mg/m^3, respectively. For test 4 the fill underlain by sand eroded at 4.67 m/h, while the fill without a sand layer eroded more rapidly at 5.38 m/h. For this highly erodible soil condition, the sand layer appeared to have little influence on the rate of advance. For test 5 the fill underlain by sand eroded at 9.10 m/h, while the fill without the sand advanced at 6.75 m/h. Tests 6, 8, and 9 were compacted on the wet side of optimum at essentially the same moisture content of over 14%. The average dry densities obtained were 1.79, 1.79, and 1.71 Mg/m^3, respectively. The measured advance rates in fill with sand layers were 1.67, 1.67, and 2.24 m/h, while the fill without the sand layers eroded at rates of 0.15, 0.34, and 0.93 m/h. The sand layers greatly increased the headcut advance rate for tests 6, 8, and 9. When the overlying material was more erosion resistant, the sand layer dramatically increased the headcut movement. As the overlying material becomes more erodible, the influence of the sand layer diminishes.

The headcut erosion processes were carefully observed. The homogeneous fill materials typically failed with a sloping headcut face. The erosion often took place with multiple headcuts operating along placed soil lift boundaries. Exceptions to this description certainly occurred, and vertical headcuts were also observed. The material underlain by sand typically failed by mass wasting with a more vertical headcut face. The supporting sand material was eroded from the base of the overfall, and tension cracks would form in the overlying material immediately before a mass wasting event.

Additional tests are planned in this large-scale flume to broaden the data base, and to improve our understanding of headcut erosion processes.

SUMMARY

The formation and movement of gully headcuts in earth emergency spillways can pose a serious threat to the integrity of floodwater retarding structures. A large-scale flume was constructed to examine headcut advance mechanics. The flume is 1.8 m wide and 29 m long with 2.4-m high sidewalls. The flume is equipped with two viewing ports or windows that allow a side view of erosion at the headcut. A description of the flume and support facilities is presented.

Test results are presented for eight tests on a red sandy clay soil and two tests on a silty sand material. The soil was placed and compacted in horizontal layers at selected values of moisture content and density. All of these tests were performed at a flow rate of approximately 1.55 m^3/s and an overfall height of 1.2 m. Summary tables of test conditions and results are provided. The plots of headcut position versus time displayed typically linear advance rates for all tests. The linear advance rates suggest that the fill sections were consistently placed. That is, the constant rate of headcut advance suggests the density and moisture

in the fill was also relatively constant. The advance rate was found to decrease as the average density and average unconfined compressive strength increased. The soil strength increased as the soil density increased.

The influence of a sand layer on the rate of headcut advance was also examined. The sand did not appear to influence the rate of advance when a highly erodible soil was the overlying material. However, when the overlying material was more erosion resistant, the sand layer dramatically accelerated the headcut advance rate. Homogeneous fill materials typically failed with a sloping headcut. Multiple smaller headcuts would normally erode along the placed soil layers. The fill underlain with sand typically failed by mass wasting with a near vertical overfall. Tension cracks would form and mass failure would occur in the overlying material after the supporting sand was removed.

Additional testing is planned to improve the understanding of headcut advance processes.

REFERENCES

De Ploey, J. 1989. A model for headcut retreat in rills and gullies. CATENA Supplement 14, pp.81-86. Cremlingen, W. Germany.

Donnelly, C. A. and F. W. Blaisdell. 1965. Straight drop spillway stilling basin. *Journal of the Hydraulics Division, Proceedings of the ASCE*, Vol. 91, No. HY3, May, 1965.

Lohnes, R. A. and R. L. Handy. 1968. Slope angles in friable loess. *The Journal of Geology*, Vol. 76, pp. 247-258.

Robinson, K. M. 1992. Predicting stress and pressure at an overfall. *Transactions of the ASAE* 35(2):561-569.

Robinson, K. M., and G. J. Hanson. 1992. A deterministic headcut advance model. ASAE Paper 92-2638, St. Joseph, MI.

Temple, D. M. 1992. Estimating flood damage to vegetated deep soil spillways. *Applied Engineering in Agriculture* 8(2):237-242.

Table 3.1. Experimental conditions

TEST#	1	2	3	4	5	6	7	8	9	10
FILL MATERIAL	CL	CL	CL	CL	CL	CL	SM	CL	CL	SM
TOTAL FILL LENGTH (m)	7.3	7.3	12.2	9.2	9.2	9.2	6.1	9.2	9.2	7.3
LOOSE LIFT THICKNESS (mm)	203	203	152	152	152	152	152	152	152	152
SAND LAYER PRESENT?	NO	NO	YES	YES	YES	YES	NO	YES	YES	NO
SAND LAYER THICKNESS (mm)	--	--	152	305	305	305	--	305	305	--
SAND LAYER LENGTH (m)	--	--	6.1	4.6	4.6	4.6	--	4.6	4.6	--
TAILWATER DEPTH (m)	0.3	0.3	1.0	1.0	1.0	1.0	1.0	1.0	1.0	1.0
OVERFALL HEIGHT (m)	1.2	1.2	1.2	1.2	1.2	1.2	1.2	1.2	1.2	1.2

Table 3.2. Experimental results

	TEST#	1	2	3	4	5	6	7	8	9	10
MOISTURE CONTENT (%)	AVG	13.3	14.0	9.2	9.2	11.6	14.4	12.1	14.4	14.3	12.0
	MAX	15.6	17.2	10.7	10.3	14.7	15.9	13.8	16.4	16.6	13.8
	MIN	8.5	11.5	7.8	6.8	9.0	11.9	11.7	13.1	12.1	11.0
DRY DENSITY (Mg/m^3)	AVG	1.63	1.58	1.54	1.68	1.59	1.79	1.86	1.79	1.71	1.76
	MAX	1.75	1.67	1.76	1.84	1.77	1.81	1.96	1.83	1.82	1.84
	MIN	1.38	1.43	1.35	1.56	1.44	1.76	1.80	1.75	1.55	1.59
UNCONF. COMP. STRENGTH (kPa)	AVG	54.9	35.9	29.5	57.9	21.4	88.8	76.2	82.9	64.5	30.2
	MAX	69.4	37.0	36.8	79.7	23.2	150.4	97.5	116.1	102.9	37.6
	MIN	28.1	34.1	25.3	42.6	18.1	47.7	53.6	57.2	38.6	21.0
ADVANCE RATE (m/h)	WITH SAND	—	—	17.6	4.67	9.10	1.67	—	1.67	2.24	—
	WITHOUT SAND	9.05	10.9	18.6	5.38	6.75	0.15	1.25	0.34	0.93	3.62

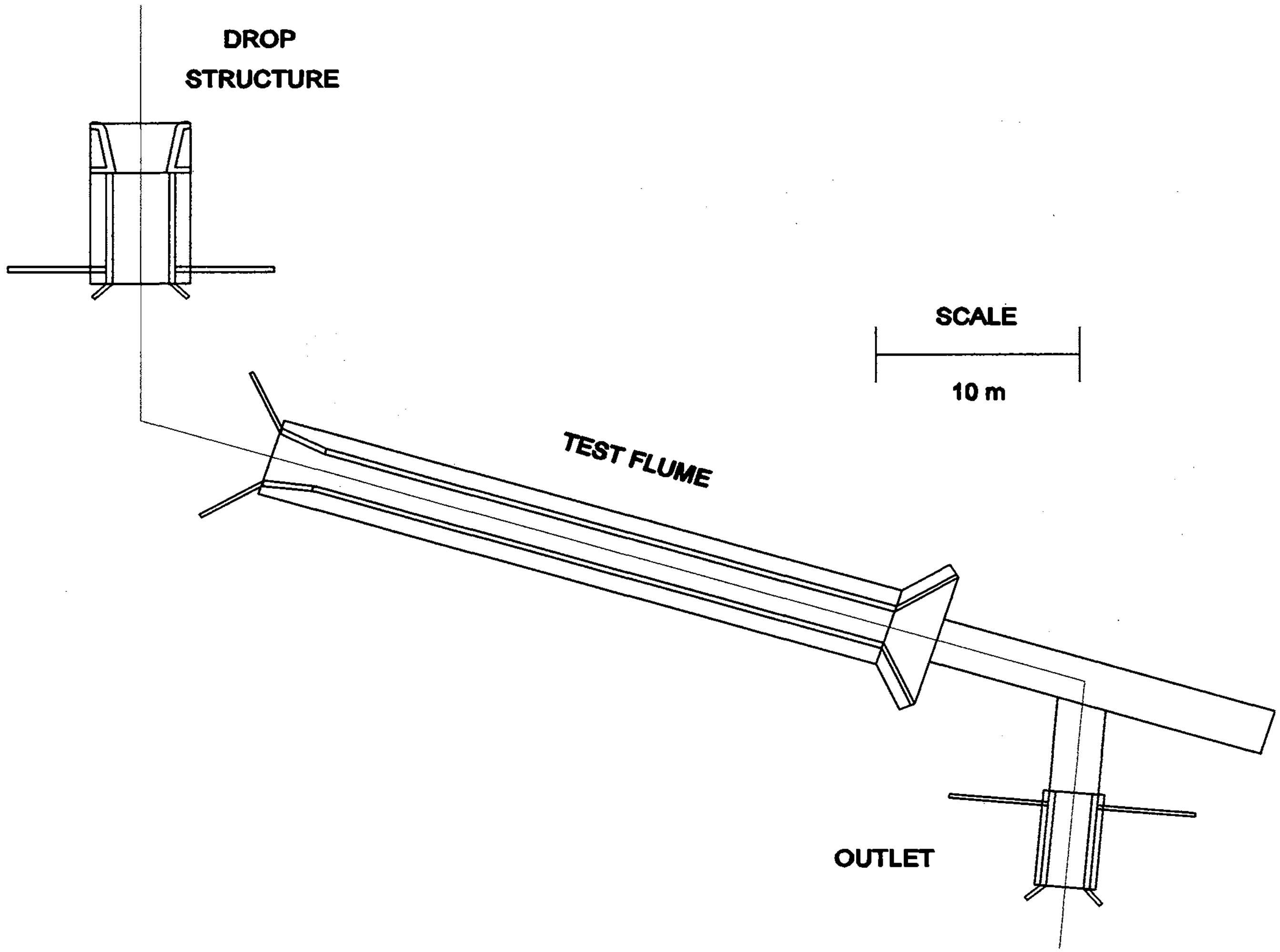

Figure 3.1. Large-scale headcut test facility

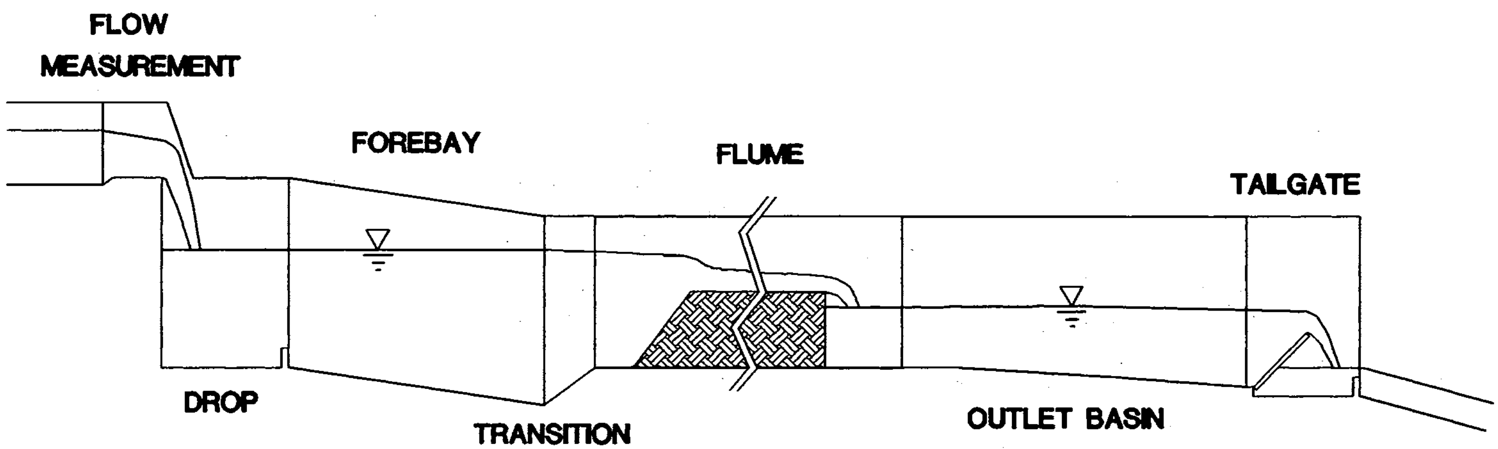

Figure 3.2. Test facility centerline profile

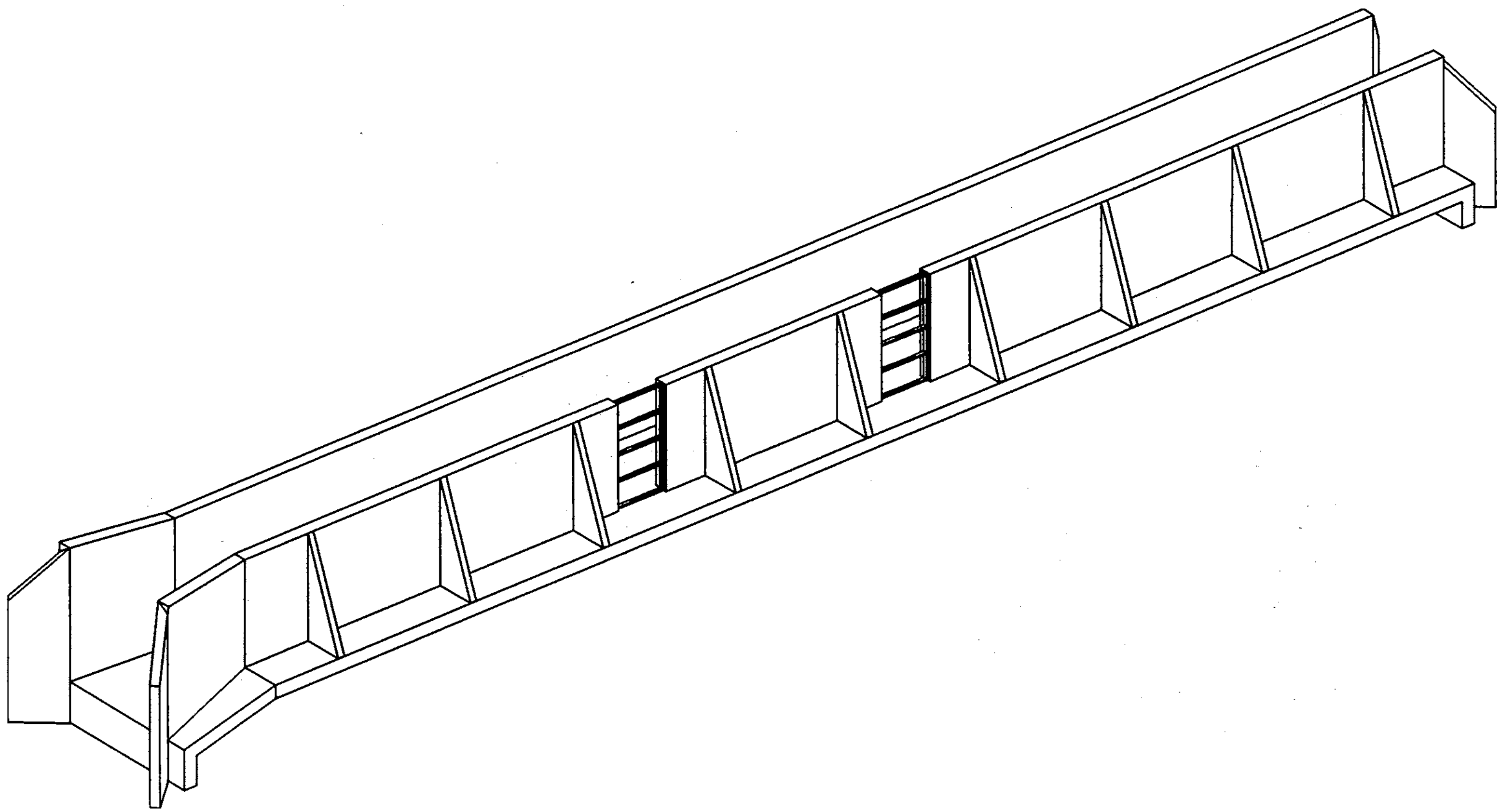

Figure 3.3. Headcut test flume

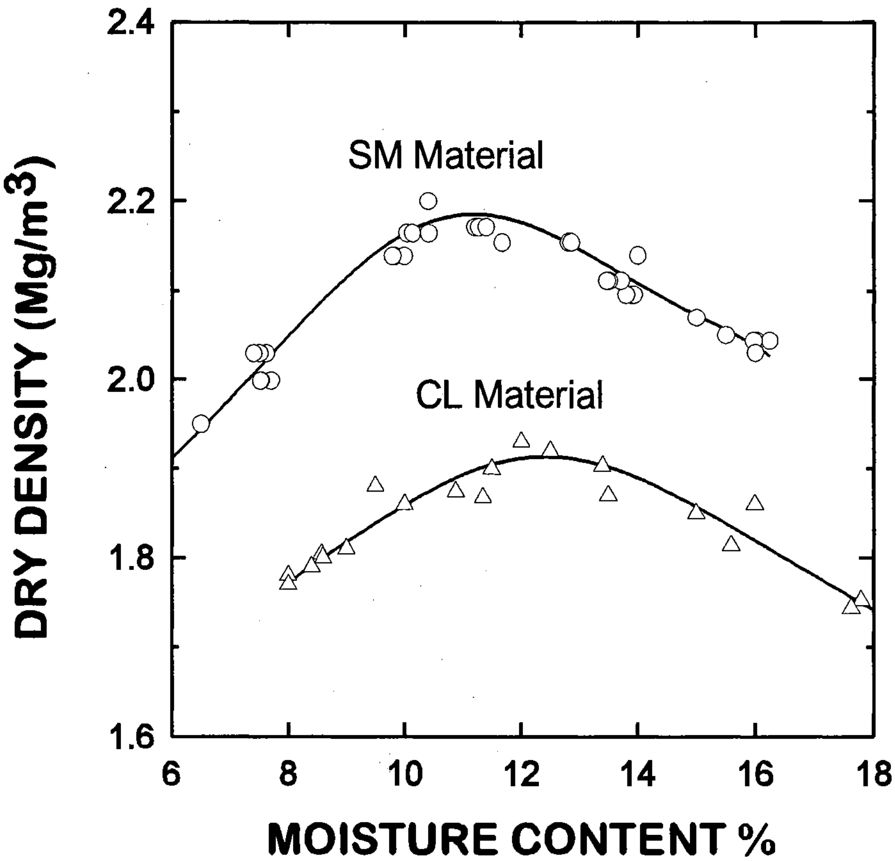

Figure 3.4. Standard Proctor test results

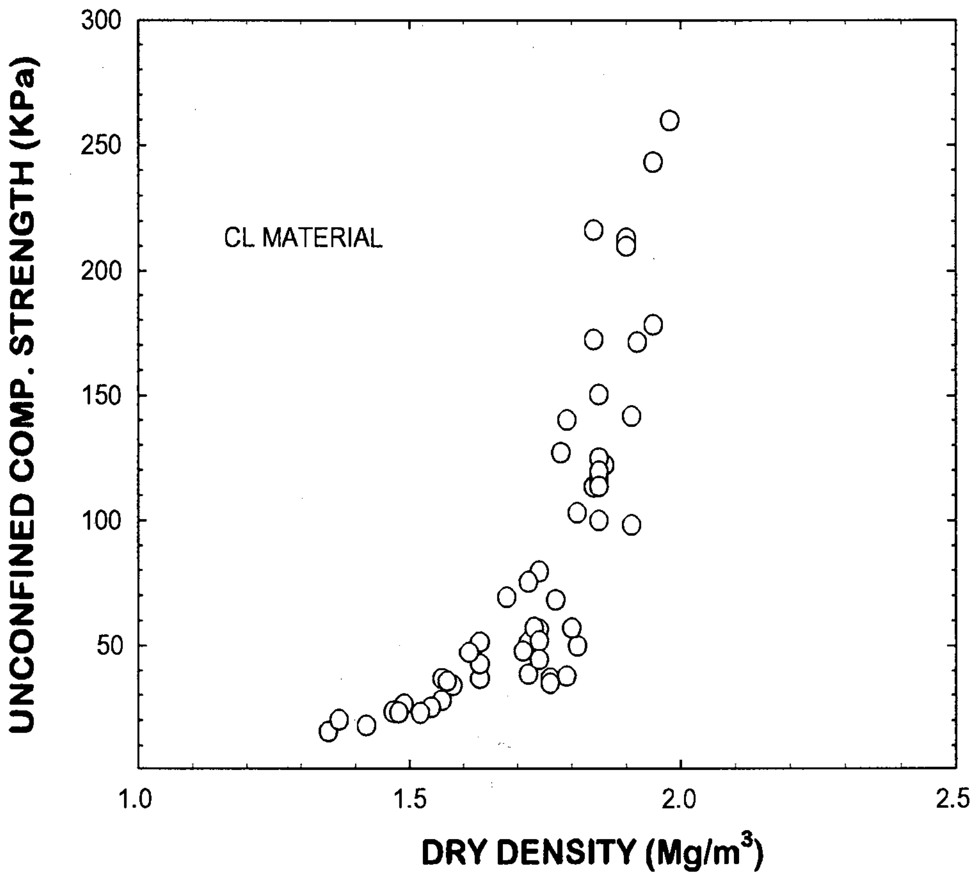

Figure 3.5. Strength versus dry density for the CL soil

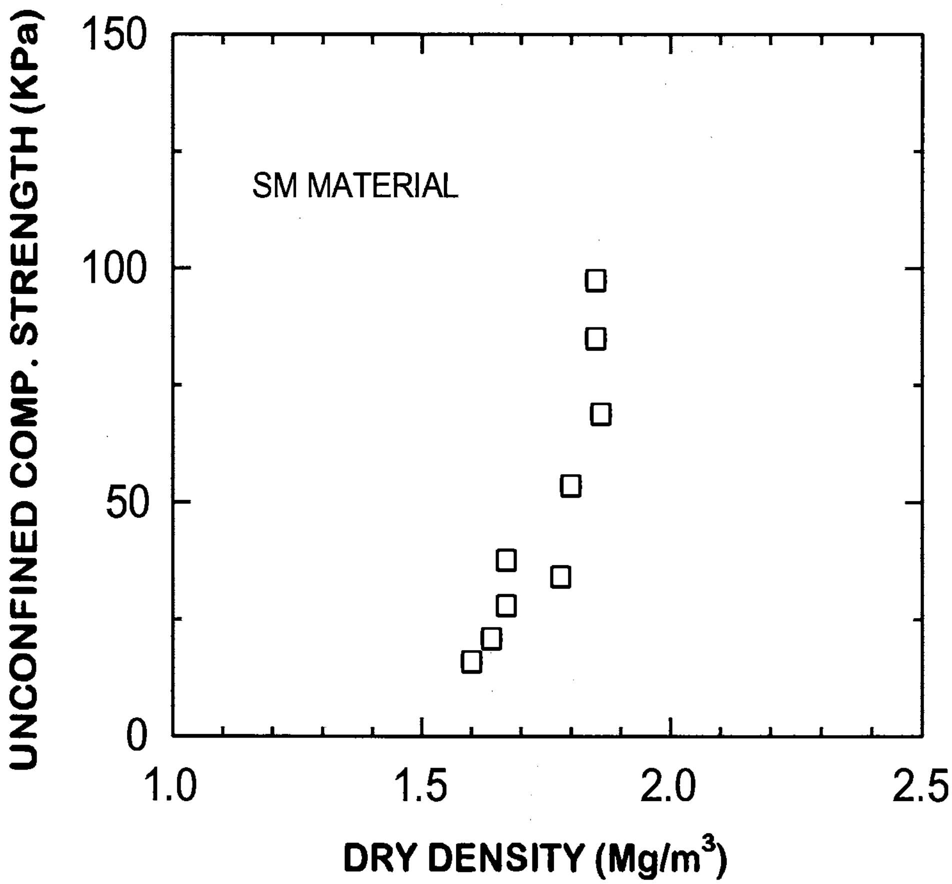

Figure 3.6. Strength versus dry density for the SM soil

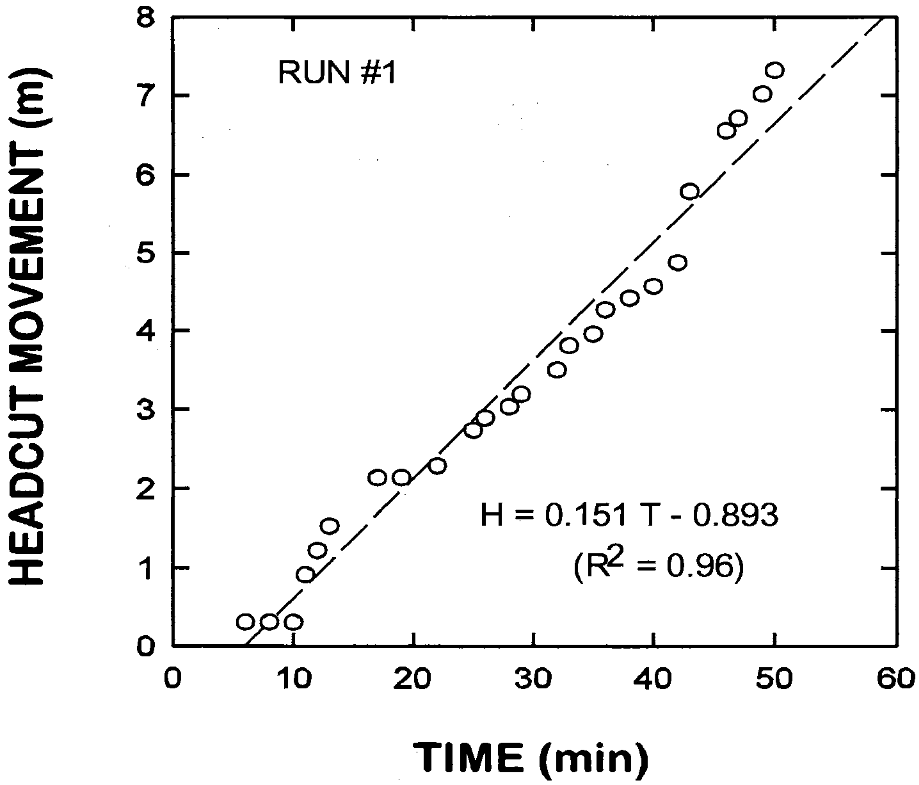

Figure 3.7. Headcut advance versus time for test 1

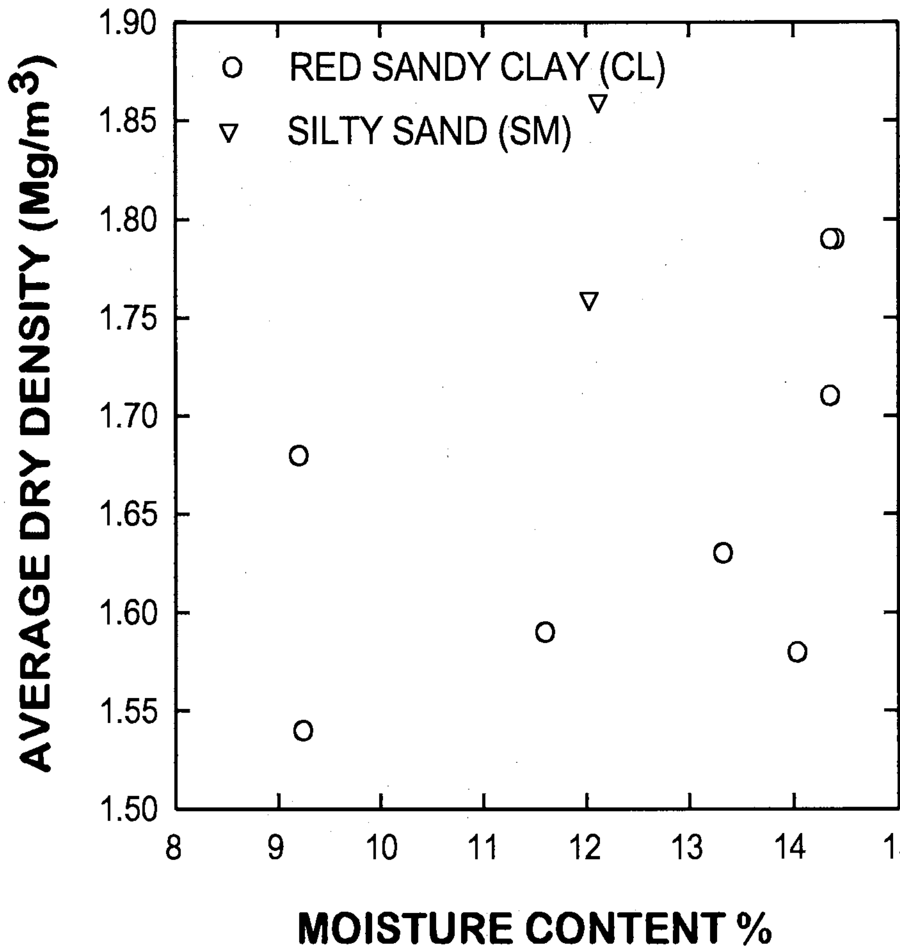

Figure 3.8. Average dry density versus average moisture content

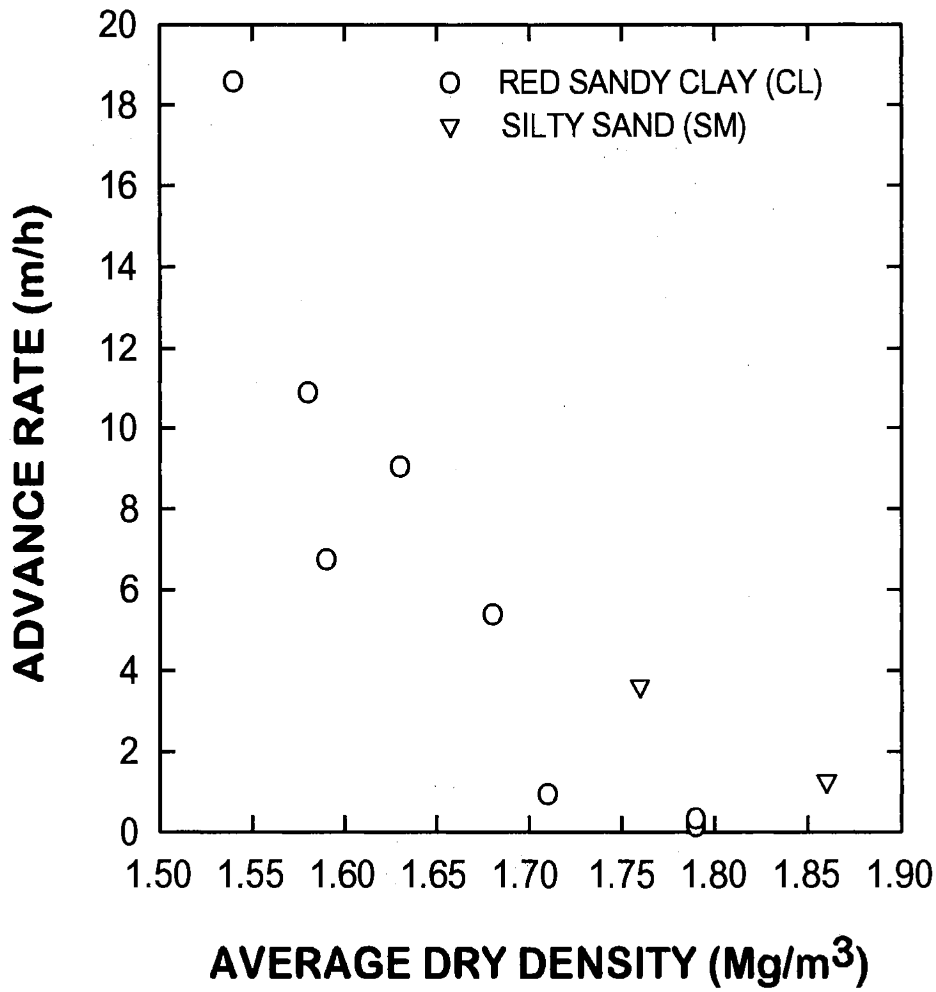

Figure 3.9. Advance rate versus average dry density

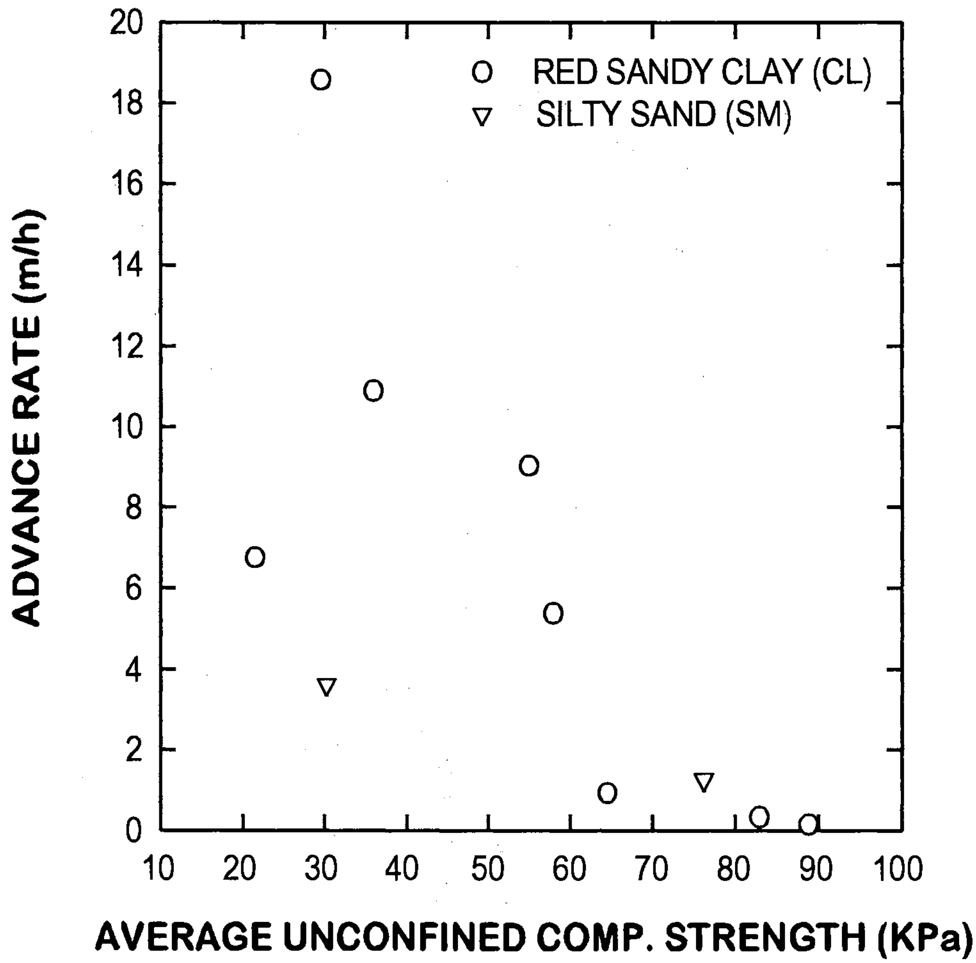

Figure 3.10. Advance rate versus average strength

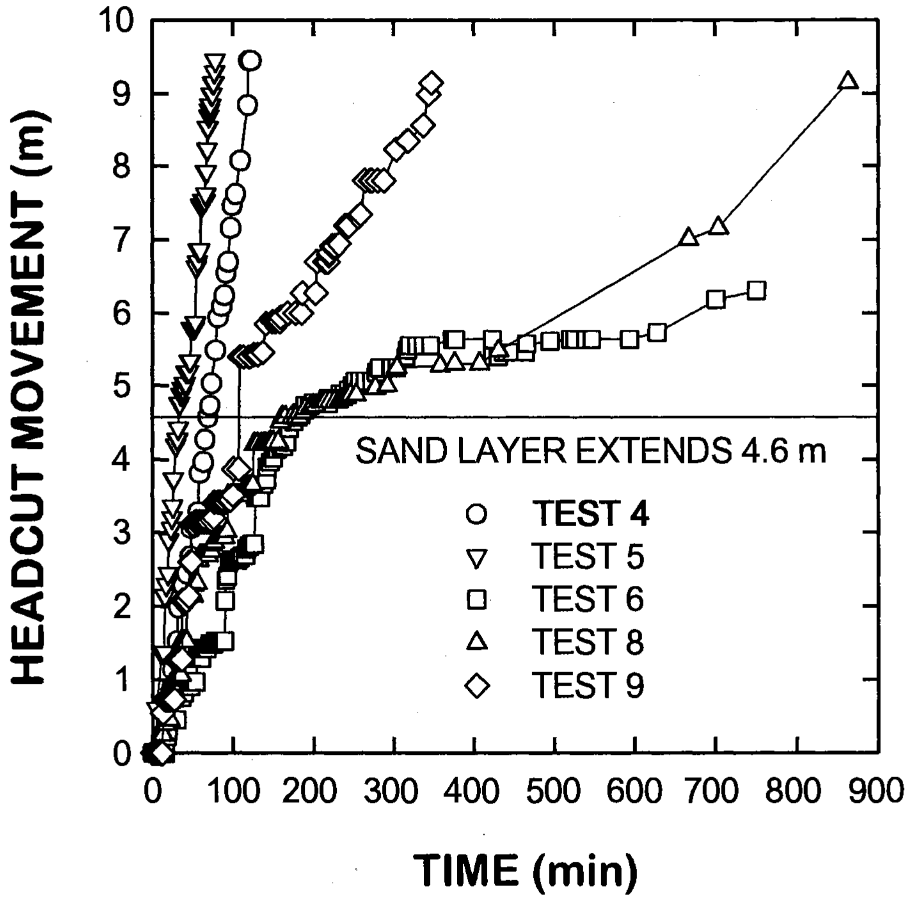

Figure 3.11. Headcut advance with and without a sand layer

CHAPTER 4

INFLUENCE OF A SAND LAYER ON HEADCUT ADVANCE

ABSTRACT

The presence of an erodible material layer in the soil profile has been observed to influence headcut movement in earth emergency spillways. Large-scale flume tests were conducted to examine headcut advance through a cohesive soil with and without a sand layer in the profile. The sand layer was observed to accelerate the erosion process by being readily removed by the flow, thus undercutting the overlying material. Once unsupported, the overlying material failed by mass wasting. As the erodibility of the overlying material increases, the influence of the sand layer diminishes.

INTRODUCTION

Headcut advance is of critical importance in assessing the risk an earth dam or spillway experiences while passing a flood flow. Spillway headcuts can cause significant damage or can, as a worst case, cause a breach of the structure. The threat to spillway integrity and thus to people and property downstream serves as the motivation for improving our understanding of headcut advance. Observations of field damage suggest that the presence of a relatively thin layer of more erodible material can have a major impact on headcut advance. The objective of this paper is to determine the influence of a sand layer on the headcut advance rate.

RELATED WORK

Related areas of study such as rill erosion, field gully erosion, embankment overtopping, and fuse plug design can benefit from an improved understanding of headcut erosion processes. Lumped parameter headcut erosion models developed by De Ploey (1989) and Temple (1992) provide a rapid estimate of headcut movement. These relatively simple mathematical models can be applied once the material-dependent erodibility coefficients are estimated. Stein and Julien (1993) determined that headcut erosion was related to sediment detachment just upstream and downstream of the headcut. If erosion upstream of the headcut dominates, then the overfall gradually decreases and approaches the eroding channel bed. If the downstream erosion dominates, then a headcut with a near vertical face migrates upstream with time. Robinson (1992) developed prediction equations for stress and pressure on the boundary of an overfall. Stress measurements were made in a fixed-bed overfall model at various combinations of discharge, overfall height, and backwater level. This stress model was combined with a mass wasting component to create a headcut advance model (Robinson and Hanson, 1992). This modeling effort identified needed research, and a large test flume was constructed in order to conduct this research. Examination of the influence of sand layers on headcut advance is a part of that ongoing investigation.

EXPERIMENTAL EQUIPMENT

Headcut advance tests were performed in a 1.8-m wide and 29-m long reinforced concrete test flume. The 2.4-m tall flume sidewalls were equipped with two viewing ports or windows to allow a side view of the headcutting activity. Flow was delivered to the test flume via an open channel through a modified Parshall flume. The flow then passed through a 3.0-m vertical drop structure that released flow into a forebay. The test flume entrance was constructed with a transition section and a vane flow straightener to insure uniform flow conditions from the forebay to the test flume. A rail-mounted carriage was installed on top of the test flume walls to allow rapid water surface and bed elevation measurement. Flow exited the test flume into an outlet control basin. This basin was equipped with a winch-operated overflow tailgate for backwater control. The basin also served as the primary sedimentation basin. The outlet basin could be supplied with water separately from the flume; therefore, a selected backwater level could be established before beginning a test flow.

EXPERIMENTAL PROCEDURE

The test flume was filled by placing soil in horizontal loose lift layers 15 cm thick. If necessary, water was added to achieve the desired soil moisture. A tiller was used to mix the soil layer and to reduce aggregate sizes. An 86-cm wide vibratory padfoot roller was used to compact each layer, and a hand-held pneumatic compactor was used to compact the soil against the flume walls. The compactive effort was varied by altering the number of compactor passes and using the vibratory head. A sand layer was placed at the bottom of the fill and extended horizontally under the downstream half of the test section. The sand layer was 30 cm deep for all but run 3, which used a 15-cm sand layer.

A skid loader was used to remove the downstream soil ramp that allowed compactor access to the top of the fill. Density and strength samples were taken with push tubes at regular depth intervals at the downstream end of the test section. A near vertical overfall was preformed at the downstream end of the test section. The surface of the fill was protected by all-weather carpet strips that were overlapped much like roofing shingles. This surface protection scheme minimized surface erosion.

The outlet basin was then filled to the desired tailwater, and the flow was delivered to the test flume. Headcut position was monitored with time. Water surface profiles and flow measurements were taken at regular intervals.

RESULTS AND DISCUSSION

A total of six tests were performed with sand layers underlying the downstream half of the fill. All tests used a red clay soil as the overlying material. This CL soil exhibited a liquid limit of 26 and a plasticity index of 15. The sand layer was composed of a non-plastic SP-SM material for runs 3, 4, and 5 and an SM material with a plasticity index of 3 for runs 6, 8, and 9. All six tests were conducted with an overfall height of 1.2 m, a flow rate of 1.55 m^3/s, and a backwater setting of 1.0 m as measured at the flume exit. The length of the test section was 9.1 m for all but run 3, which used a 12.2-m long section.

Table 4.1 provides a summary of test results. The average moisture content, average dry density, and average unconfined compressive strength are presented, as are the observed advance rates with and without the sand layer. The ranges of the moisture, density, and strength measurements are presented to illustrate the observed parameter variability. As might be expected, the advance rate decreased as the density and strength of the overlying material increased. The headcut movement data with and without the sand layer displayed a linear advance rate (Fig. 4.1). The correlation coefficient was 0.90 or larger for all runs, with only two runs less than 0.96. The linear advance suggests that the test fill was consistently prepared. Figure 4.1 also serves to illustrate how differently the sand layer can influence headcut advance. Runs 3, 4, and 5 were prepared with lower moisture contents and lower dry densities. The sand layer produced little change in the headcut advance rate for these runs. The overlying material exhibited such a high erodibility that the presence of the sand layer was not a factor. The overfall typically retreated with a more sloping face rather than a vertical face. Runs 6, 8, and 9 were prepared at high moisture contents and higher dry densities. The sand layer dramatically increased the headcut movement rates for these tests. Classical mass wasting failures were observed as the sand was removed from the base of the overfall, tension cracks formed, and large blocks of soil were removed. The headcut would move upstream with a near vertical face.

SUMMARY

The formation and movement of gully headcuts in earth emergency spillways can pose a serious threat to dams. Large-scale flume tests were performed to examine the influence of a sand layer on headcut advance rate. A test soil was carefully compacted in horizontal layers with a sand layer extending under the downstream half of the fill. This arrangement allowed examination of the headcut advance with and without the sand layer. All tests were conducted with a constant flow rate of 1.55 m^3/s, a backwater setting of 1.0 m, and a preformed overfall height of 1.2 m. A summary table of test results is provided.

Linear advance rates were observed for all tests, suggesting the fill was consistently placed. The advance rates were found to decrease as the average density and the average unconfined compressive strength of the test soil increased. The soil strength also increased as the soil density increased. When the overlying material was more erosion resistant, the sand layer dramatically increased the rate of headcut movement. Material was removed from the overfall base, tension cracks would form, and mass wasting would occur. As the erodibility of the overlying material increases, the influence of the sand layer diminishes.

REFERENCES

De Ploey, J. 1989. A model for headcut retreat in rills and gullies. CATENA Supplement 14, pp.81-86. Cremlingen, W. Germany.

Robinson, K. M. 1992. Predicting stress and pressure at an overfall. *Transactions of the ASAE* 35(2):561-569.

Robinson, K. M. and G. J. Hanson. 1992. A deterministic headcut advance model. ASAE Paper 922638, St. Joseph, MI.

Stein, O. R. and P. Y. Julien. 1993. Criterion delineating the mode of headcut migration. *ASCE Journal of Hydraulic Engineering*, Vol 119, No. 1, pp. 37-50.

Temple, D. M. 1992. Estimating flood damage to vegetated deep soil spillways. *Applied Engineering in Agriculture* 8(2):237-242.

Table 4.1. Summary of test results

	TEST#	3	4	5	6	8	9
MOISTURE CONTENT (%)	AVG	9.2	9.2	11.6	14.4	14.4	14.4
	MAX	10.7	10.3	14.7	15.9	16.4	16.6
	MIN	7.8	6.8	9.0	11.9	13.1	12.1
DRY DENSITY (g/cc)	AVG	1.54	1.68	1.59	1.79	1.79	1.71
	MAX	1.76	1.84	1.77	1.81	1.83	1.82
	MIN	1.35	1.56	1.44	1.76	1.75	1.55
UNCONF. COMP. STRENGTH (KPa)	AVG	29.5	57.9	21.4	88.8	82.9	64.5
	MAX	36.8	79.7	23.2	150.4	116.1	102.9
	MIN	25.3	42.6	18.1	47.7	57.2	38.6
ADVANCE RATE (m/min)	WITH SAND	0.293	0.078	0.152	0.028	0.028	0.037
	WITHOUT SAND	0.310	0.090	0.112	0.002	0.006	0.016

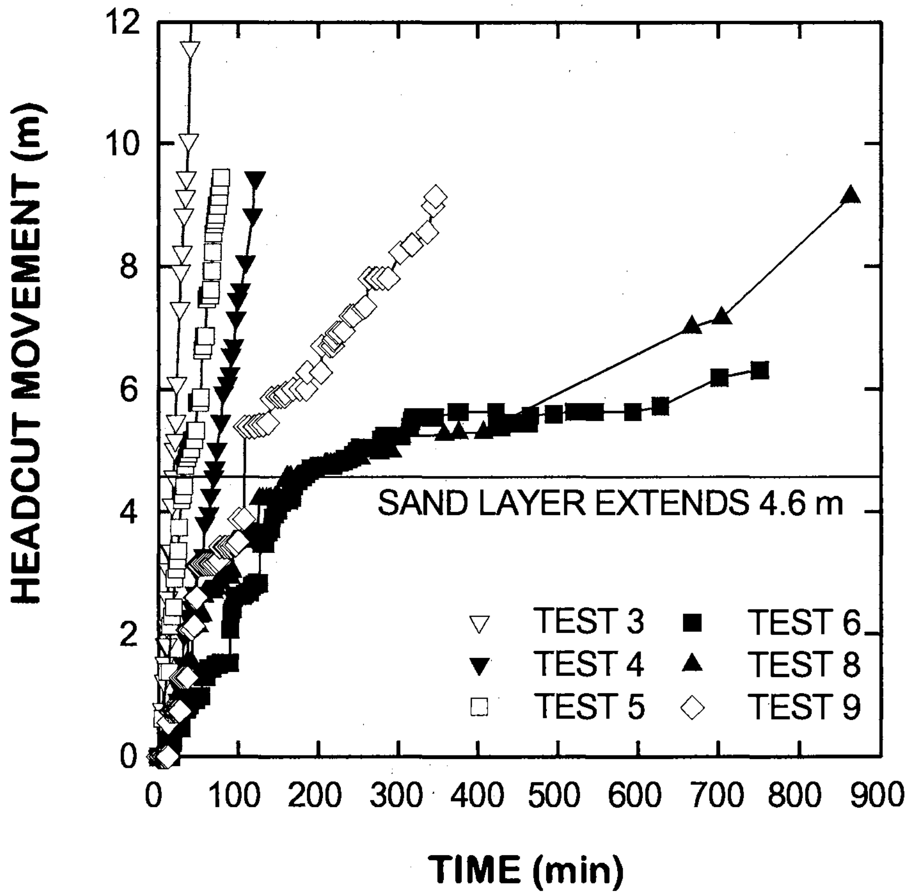

Figure 4.1. Headcut movement versus time

CHAPTER 5

GULLY HEADCUT ADVANCE

ABSTRACT

Gully headcut advance rates were examined in a cohesive soil with multiple overfall heights and discharges. Eleven tests were conducted in a 1.8-m wide and 29-m long flume at field scale. Preformed overfalls with average heights of 0.96, 1.25, and 1.55 m were tested to failure at average discharges of 0.75, 1.59, and 2.42 m^3/s. Soil from the same source was used for all tests. The observed headcut advance rates ranged from 0 to 1.6 m/h. All but one test displayed uniform headcut advance rates. The tests were performed while attempting to hold soil moisture and soil density constant and examining the influence of overfall height and discharge on headcut advance. The observed variation in placed soil conditions appeared to influence headcut advance as did the overfall height and discharge variations. Examination of a subset of the data suggests that the advance rate increases as the overfall height increases. The aeration status of the headcut and the dominant mode of failure are discussed.

INTRODUCTION

This ongoing research is being conducted to better understand the development and movement of gullies in earthen emergency spillways. This work has the potential of providing benefits in related areas such as field gully growth, rill erosion, dam overtopping, and fuseplug design. As the dominant form of spillway damage, gully headcut advance can threaten the integrity of a dam. A properly designed spillway with a well maintained and uniform vegetative cover helps reduce, but does not eliminate, the possibility of gully formation and movement. If a gully headcut advances through a spillway, a dam breach can occur. The rapid release of impounded water poses a threat to people and property downstream.

A simple sketch of an overfall is provided (fig. 5.1) to illustrate several terms used in this paper. The overfall height (H) or headcut is the vertical distance between the upper and lower floors. This height is the vertical drop the water must negotiate once reaching an abrupt change in elevation. The discharge (Q) or total flow rate may also be expressed as a unit discharge since spillways typically transmit wide shallow flows. The tailwater or backwater level (B_w) is the depth of flow downstream of the overfall. The relatively thin sheet of water flowing over the overfall is the nappe. An aerated overfall has an air pocket beneath the nappe that exists at atmospheric pressure. The nappe is non-aerated if the air pocket is completely filled with water or if the air pocket is at less than atmospheric pressure. The air pocket reduces in size as the discharge increases and/or when the backwater level is increased.

The objective of this study was to examine the influence of flow rate and overfall height on the rate of headcut advance. The large-scale tests were performed to develop hydraulic and soil forces near magnitudes commonly found in the field.

RELATED WORK

The hydraulics of the overfall has received substantial historical attention by such researchers as Rouse (1936), Moore (1943), and Rand (1955). Holland and Pickup (1967) examined how these hydraulic forces produce erosion at a headcut. In a small flume the headcut movement rates were generally observed to increase as the discharge rates increase. Substantial variation of the rate of movement was also observed. Stein and Julien (1993) developed a criterion that separates stepped headcuts from rotating headcuts. The stepped headcuts have a vertical face and are routinely observed in the field. Rotating headcuts alter their shape as they migrate. Typically, a rotating headcut changes from a near vertical to a sloping face. Previous tests conducted by the authors in 1993 examined the headcut advance rates for various soil conditions while holding the overfall height, discharge, and backwater level constant (Robinson and Hanson, 1995). This paper describes tests conducted in 1994 while attempting to hold the soil conditions constant and varying the overfall height and discharge rate. The data sets are referred to in this paper as 1993 and 1994 data.

EXPERIMENTAL EQUIPMENT

The headcut advance test facility is composed of three concrete structures connected by earthen dikes (fig. 5.2). A centerline profile of the test facility is also provided (fig. 5.3). Flow measurement is provided with a 2.4-m wide modified Parshall flume. Immediately downstream of this flume is a 2.7-m wide straight drop spillway (Donnelly and Blaisdell, 1965) with a 3.0-m vertical drop. An earth forebay connects the drop structure with the test flume. The drop structure and forebay provide subcritical flow to the test flume.

A 2.4-m long concrete transition section is located at the upstream end of the flume to provide uniform approach flow conditions. The 29-m long horizontal test flume is 1.8 m wide and has 2.4-m tall sidewalls. A rail-mounted carriage operates on top of the flume walls, and the flume wall also has two windows that allow a side view of the erosion process.

The flume exits into an earthen outlet basin where the majority of sediment is deposited after a test. An outlet structure, located at the downstream end of the outlet basin, is equipped with a 2.3-m wide overflow tailgate. This tailgate allows control of the flume tailwater setting. The outlet basin that exits into a collection channel is also connected to a supply canal so it can be filled to a desired backwater before beginning a test flow. A more detailed description of this test facility is provided in Robinson and Hanson (1995).

EXPERIMENTAL PROCEDURE

Soil Material and Sampling

The soil examined in this study exhibited a liquid limit of 26 and a plasticity index of 15. Using the Unified Classification System, this red sandy clay (CL) exhibited 25% clay, 40% silt, and 35% sand. This soil was selected primarily because large quantities with uniform soil properties could be obtained locally. Standard Proctor tests displayed a maximum dry density of 1.9 Mg/m^3 at an optimum moisture of 12%. Soil strength is an important parameter in headcut advance. Figure 5.4 suggests that a strong relationship exists between the density and strength for this soil. The 1993 strength and density data were intentionally varied over a wide range (Robinson and Hanson, 1995). In 1994 the soil strength and density were held as constant as possible.

Following placement of the soil in the flume and before testing, samples were taken from the downstream end of the placed soil. Density samples were taken with 76-mm diameter push tubes at 152-mm intervals in the profile. Unconfined compressive strength samples were taken at 305-mm intervals with 51-mm diameter push tubes.

Fill Preparation

The test flume was filled by placing soil in horizontal loose lift layers of 152 mm thickness. Typically, water was added to achieve the desired soil moisture. A 1.75-m wide PTO- operated tiller was used to mix the soil layer and to reduce aggregate sizes. Depending on the soil moisture conditions, the wetting and tilling process was repeated several times. A 0.9-m wide self-propelled vibratory padfoot roller was used to compact each soil layer. The fill was compacted with six passes of the padfoot roller, and the vibratory load was not used. A hand-held pneumatic compactor was used to compact the soil next to the concrete walls. The compacted soil surface was then scarified with a garden tiller to improve bonding with subsequent layers. These fill placement procedures were repeated until the desired fill depth was obtained. As the fill depth increased, a ramp was constructed at each end of the fill. This ramp allowed equipment access to the top of the fill. Before testing, the downstream ramp was removed with a skid-steer loader, and a near vertical overfall or headcut was prepared at the end of the test section. Typically, the fill section included approximately 1.2 m of additional horizontal length to allow for soil sampling at the downstream end of the test section. The total length of horizontal fill was 6.1 m, while the tested overfall heights were 0.96, 1.25, and 1.55 m. The overfall height varied somewhat since the layered fill did not exactly match the targeted fill height. While gully headcuts can exist in the field at heights much larger than 1.55 m, many gullies encounter an erosion resistant material that limits depth.

The desired mode of failure of the placed soil was by headcut advance. To minimize the potential influence of stress detachment erosion along the horizontal surface, a soil cement treatment was added to the fill surface. This surface treatment consisted of a 4% mixture (by weight) of Portland cement. The cement was mixed into the top 75 mm of the soil surface and then compacted. The soil cement treatment served to retard surface detachment without restricting the headcut erosion processes.

Testing

Each flume test was conducted following a routine sequence of events. Soil sampling was conducted, and the headcut was preformed. The tailgate was set to a low position, and the flow was introduced into the forebay. Once the forebay was filled and the flow reached the overfall, the headcut position was monitored with time. Water surface and bed profiles were taken periodically during the test, as were discharge measurements. Normally, the test continued until the horizontal fill section was completely breached.

RESULTS AND DISCUSSION

While additional tests were performed, this paper considers only the 11 tests that received six compactor passes and a 4% soil-cement surface treatment. The discharge, backwater, and overfall heights for each test are summarized in Table 5.1. The discharge is the average of all modified Parshall flow measurements, and the overfall height is the average depth of the horizontal fill. The backwater level or tailwater is the average flow depth measured near the flume exit. The lowest possible backwater setting was used for these tests. The backwater level increased as the flow rate increased (Table 5.1).

A plot of the average moisture content versus the average dry density for each test (fig. 5.5) displays the soil placement test conditions. The density varied between 1.73 and 1.80 Mg/m^3, while the moisture varied between 12.6 and 15.9%. All average moistures were above the optimum moisture content of 12% for this soil. The moistures and densities tested are compared with previous tests (fig. 5.6) to indicate the range of conditions examined for this soil. If the soil conditions were identical, all 1994 data would plot at the same point. The plot shows considerable scatter particularly in moisture content. Maintaining a uniform moisture content was difficult due to rainfall, differential drying, and moisture addition techniques on the soil stockpile. Previous work with this soil suggests that a strong relationship exists between moisture content and headcut advance. Therefore, all of the tests cannot be considered the same. For this soil, the advance rate decreases as the moisture content increases and the density increases. The moisture contents for tests 20 and 27 are much lower, and the moisture contents for tests 23 and 26 are much higher than the remaining tests (fig. 5.5). The density for tests 18, 20, 24, and 27 also are lower than the remaining runs.

Table 5.2 provides the average moisture content, average dry density, and the average unconfined compressive strength for each test. The maximum and minimum values are also shown to illustrate parameter variation. Table 5.2 also lists the advance rates.

The advance rate was determined as the slope of the headcut position versus time plot. A typical plot of headcut position versus time is shown for test 27 (fig. 5.7). This plot resembles a step function because the headcut moved as discrete mass wasting events. Typically, hydraulic stresses would undercut the overfall for a period of time until the headcut became unstable and failed. Failure debris would be quickly swept downstream and the undercutting process would begin again. A linear regression was performed on the advance data, and all runs except test 22 displayed a correlation coefficient (R) of 0.96 or greater. Test 22 exhibited an R of 0.87. That is, all tests but 22 displayed very uniform headcut movement with time. Minor fill contamination in test 22 is thought to have influenced the observed rate of movement. Overall, the uniform movement suggests that the fill was placed consistently.

The advance rate is plotted versus the overfall height for the three discharges (fig. 5.8). All 11 tests are plotted. While a direct relationship was expected, the data show no consistent trend. A plot of the advance rate versus the discharge for the three overfall heights (fig. 5.9) also displays no clear functional relationship. A best fit equation was intentionally omitted for these plots. The variability of the soil properties, particularly moisture, makes it difficult to compare results. About all that can be determined from figures 5.8 and 5.9 is that the advance rates generally varied from 0.5 to 1.5 m/h over the tested ranges. Test 26 is an exception, since this test was run for over 24 hours and no erosion was observed. Test 26 was prepared with consistently wet material that exhibited the least moisture content variability.

A typical test section contained over 15 m^3 of compacted fill. The soil exhibited variability in the placed soil moisture content that in turn introduced variability in the headcut advance rate. While moisture variation is undesirable, real world limitations on moisture control make it necessary to accept a range of moisture contents. Indeed, variability should be expected in the resisting soil forces and the attacking hydraulic forces. The 1994 advance rate data is also compared with the 1993 data (fig. 5.10). The variability of the 1994 advance rate data appears to be no greater than was observed in the 1993 data. The changes in overfall height and discharge appear to be overshadowed by the placed soil properties. Perhaps just as important is the observation that the overfall height and discharge did not have a strong influence on headcut advance for the range of heights and discharges examined.

A smaller subset of the data was examined to look for trends. Again examining figure 5.5, tests 16, 17, 19, 21, and 22 appear to exhibit similar densities, with moisture contents between 13.4 and 14.6%. Three of these five tests (16, 17, and 21) are at the same discharge but different overfall heights (fig. 5.11). This plot suggests that the advance rate increases as the overfall height increases. Three of these tests (19, 21, and 22) are also at the same overfall height but different discharges (fig. 5.12). This plot suggests that the advance rate is not greatly influenced by discharge over this range. Additional testing is needed to gain confidence in these relationships.

The aeration status can also have an influence on advance rate. Tests 18 and 27 were conducted at a high overfall and a low discharge. This combination was most likely to produce an aerated nappe, and these tests were observed to be aerated or slightly nonaerated. The remaining tests ranged from partially to completely nonaerated. Aeration is important since the nappe trajectory is influenced by this condition. A fully aerated nappe strikes the floor farther downstream than a nonaerated nappe and therefore transmits lower stresses to the base of the overfall (Robinson, 1992). A nonaerated nappe also tends to fluctuate more than an aerated nappe causing the peak stress to be expressed over a larger area.

The observed erosion processes also varied during the tests. Some tests, typically the lower moisture tests, failed with a sloping headcut indicative of stress detachment along the face of the headcut. These sloping headcuts tended to fail in small chunks, with the individual compacted layers very visible. The higher moisture content tests typically failed with a vertical face largely due to tension cracking and larger mass failure events. The soil behaved more as a homogeneous mass with less evidence of the placed soil layers.

SUMMARY

A large-scale flume was used to examine the advance rate of a gully headcut at three overfall heights and three discharges. Eleven tests were conducted on a red sandy clay soil. Measurements of soil moisture, dry density, unconfined compressive strength, and advance rate are tabulated, as are the tested overfall heights, backwater levels, and discharges. The individual tests produced very uniform headcut advance rates for all but one test. While the dry densities of the tests were reasonably similar, the average moisture contents ranged from 12.6 to 15.9%. This variability presented difficulty in comparing test results. Generally speaking, the tests exhibited an advance rate of 0.5 to 1.5 m/h. A subset of the data with less variability in density and moisture content indicated that the advance rate increased slightly as the overfall height increased at a constant discharge. This data subset also suggests that the advance rate is not greatly affected by discharge over the tested range. Comparisons with previously collected advance rate data suggest that the changes in overfall height and discharge were overshadowed by the soil properties.

High overfalls and low discharges were most likely to produce aerated nappes, while low overfalls and high discharges produced nonaerated nappes. The air pocket below the nappe became smaller as the overfall height decreased and as the discharge increased. The headcuts eroded with both sloping and vertical faces. The lower moisture content tests were more likely to erode with a sloping face. Typically the erosion occurred along placed soil layers with relatively small sized failure blocks. The higher moisture tests exhibited erosion

along a vertical face. Undercutting, tension cracking, and mass failure of relatively large blocks of soil were common.

REFERENCES

Donnelly, C. A. and F. W. Blaisdell. 1965. Straight drop spillway stilling basin. *J. Hydr. Div., ASCE* 91(HY 3):101-145.

Holland, W. N. and G. Pickup. 1967. Flume study of knickpoint development in stratified sediment. *Bull. Geological Soc. of Am.* 87:76-82.

Moore, W. L. 1943. Energy loss at the base of a free overfall. *ASCE Trans.* 108:1343-1360.

Rand, W. 1955. Flow geometry at straight drop spillways. *J. Hydr. Div., ASCE* 81, Paper No. 791.

Robinson, K. M. 1992. Predicting stress and pressure at an overfall. *Transactions of the ASAE* 35(2):561-569.

Robinson, K. M. and G. J. Hanson. 1995. Large-scale headcut erosion testing. *Transactions of the ASAE* 38(2):429-434.

Rouse, H. 1936. Discharge characteristics of the free overfall. *Civil Eng.* 6(4):257-260.

Stein, O. R. and P. Y. Julien. 1993. Criterion delineating the mode of headcut migration. *J. Hydr. Div., ASCE* 119(1):37-50.

Table 5.1. Test conditions

TEST #	DISCHARGE (m^3/s)	BACKWATER LEVEL (m)	OVERFALL HEIGHT (m)
16	1.65	0.26	0.93
17	1.63	0.24	1.58
18	0.78	0.12	1.58
19	0.72	0.15	1.24
20	0.75	0.14	0.91
21	1.60	0.22	1.23
22	2.40	0.28	1.28
23	2.42	0.30	1.01
24	2.43	0.28	1.24
26	1.49	0.22	1.01
27	0.77	0.15	1.48

Table 5.2. Experimental test results

TEST #	MOISTURE CONTENT (%)			DRY DENSITY (Mg/m^3)			UNCONFINED COMP. STRENGTH (kPa)			ADVANCE RATE (m/h)
	AVG	MAX	MIN	AVG	MAX	MIN	AVG	MAX	MIN	
16	13.7	14.3	12.4	1.79	1.84	1.62	56.7	69.5	43.7	0.94
17	14.4	15.2	12.9	1.79	1.84	1.72	68.6	81.2	53.7	1.34
18	13.5	14.9	12.1	1.76	1.84	1.69	71.2	104.4	58.1	0.42
19	13.4	15.0	12.1	1.80	1.85	1.73	71.3	85.6	55.4	1.48
20	12.6	15.5	10.8	1.75	1.79	1.68	48.8	52.2	45.7	1.58
21	13.7	15.1	12.1	1.80	1.85	1.73	86.1	96.1	62.5	1.28
22	14.6	17.8	12.2	1.78	1.82	1.70	63.1	71.7	49.7	1.27
23	15.9	17.7	14.0	1.78	1.81	1.75	75.5	89.0	65.4	0.85
24	13.4	15.1	11.5	1.73	1.80	1.59	44.6	57.7	27.4	1.50
26	15.2	16.4	14.5	1.79	1.83	1.75	63.3	79.0	54.7	0
27	12.8	16.6	8.8	1.73	1.82	1.63	57.8	73.2	43.1	0.83

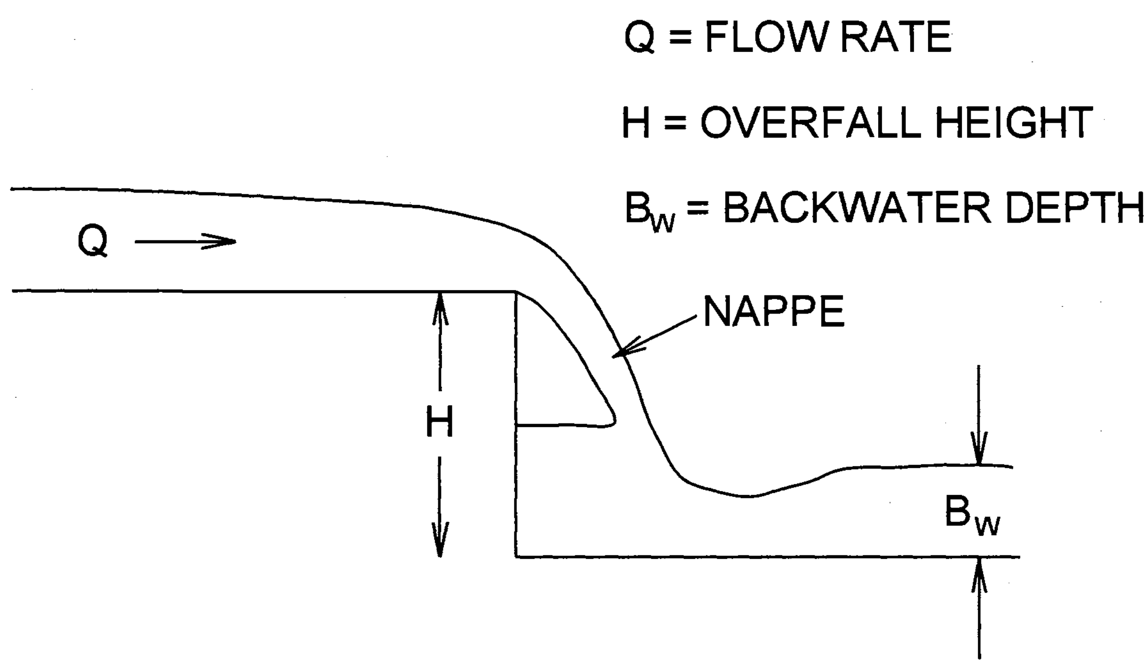

Figure 5.1. Overfall sketch

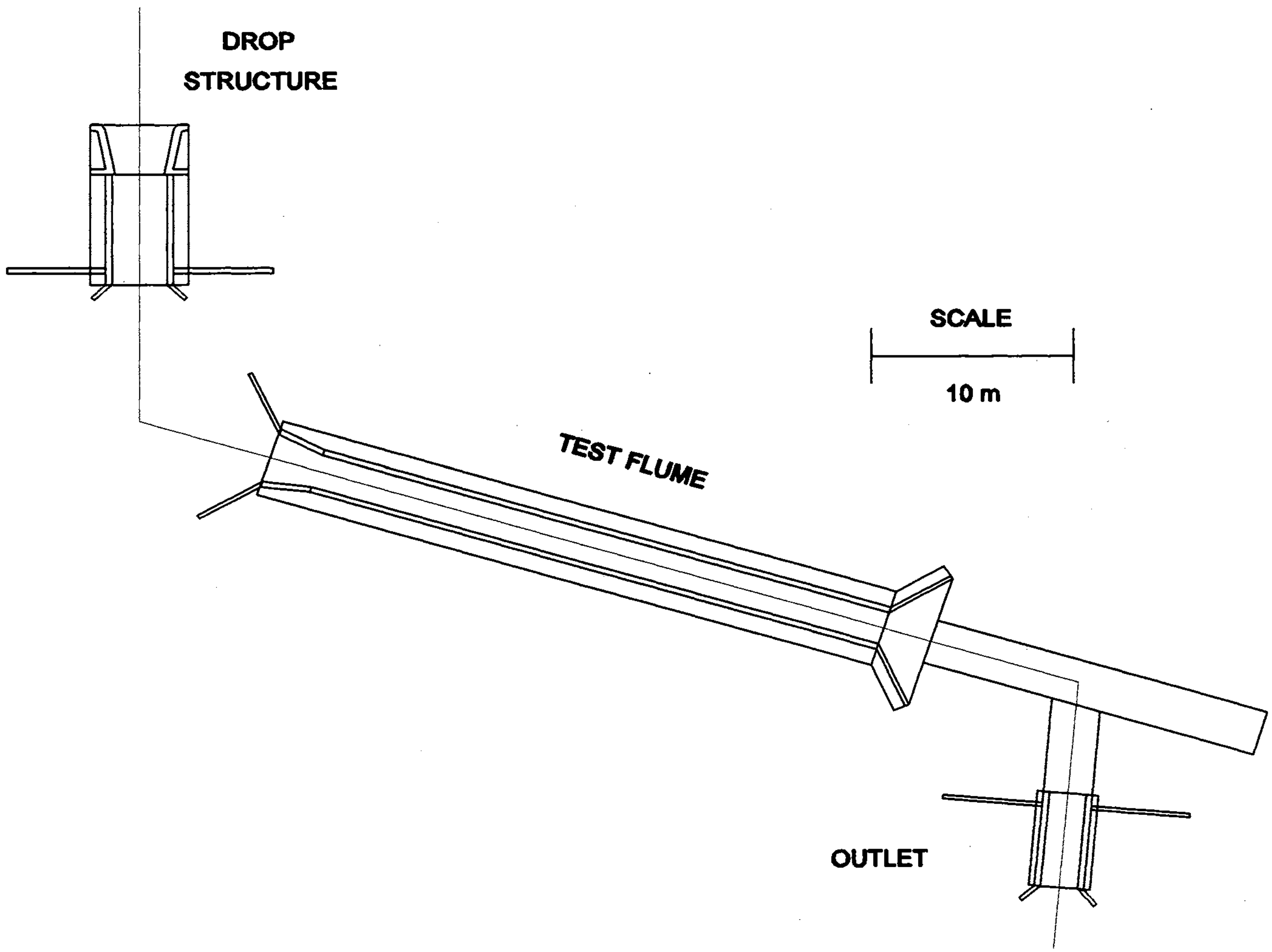

Figure 5.2. Large-scale headcut test facility

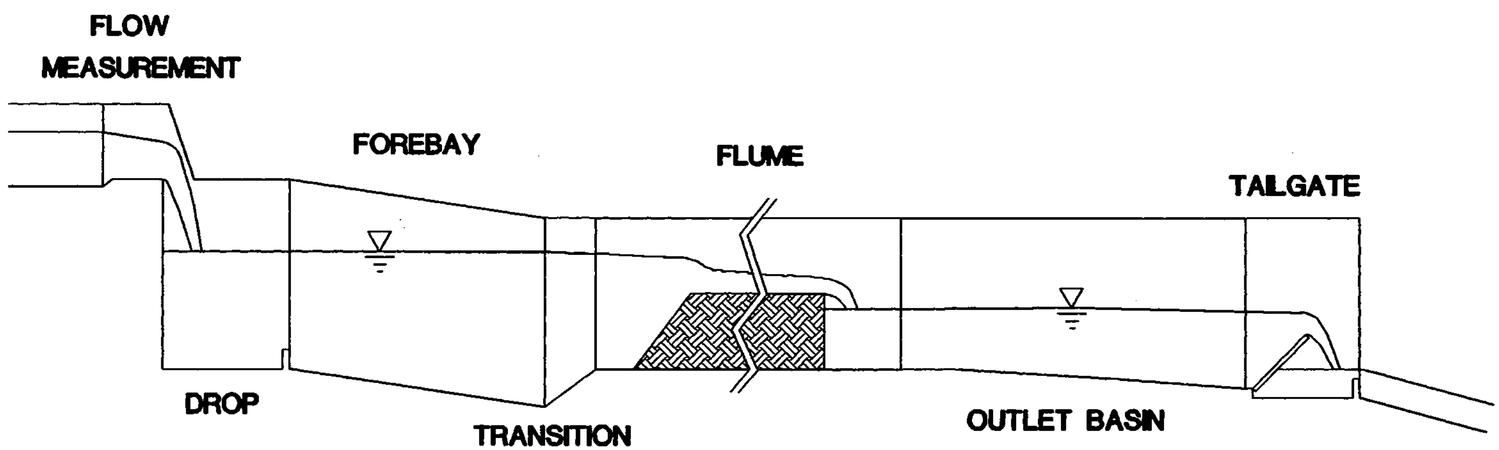

Figure 5.3. Test facility centerline profile

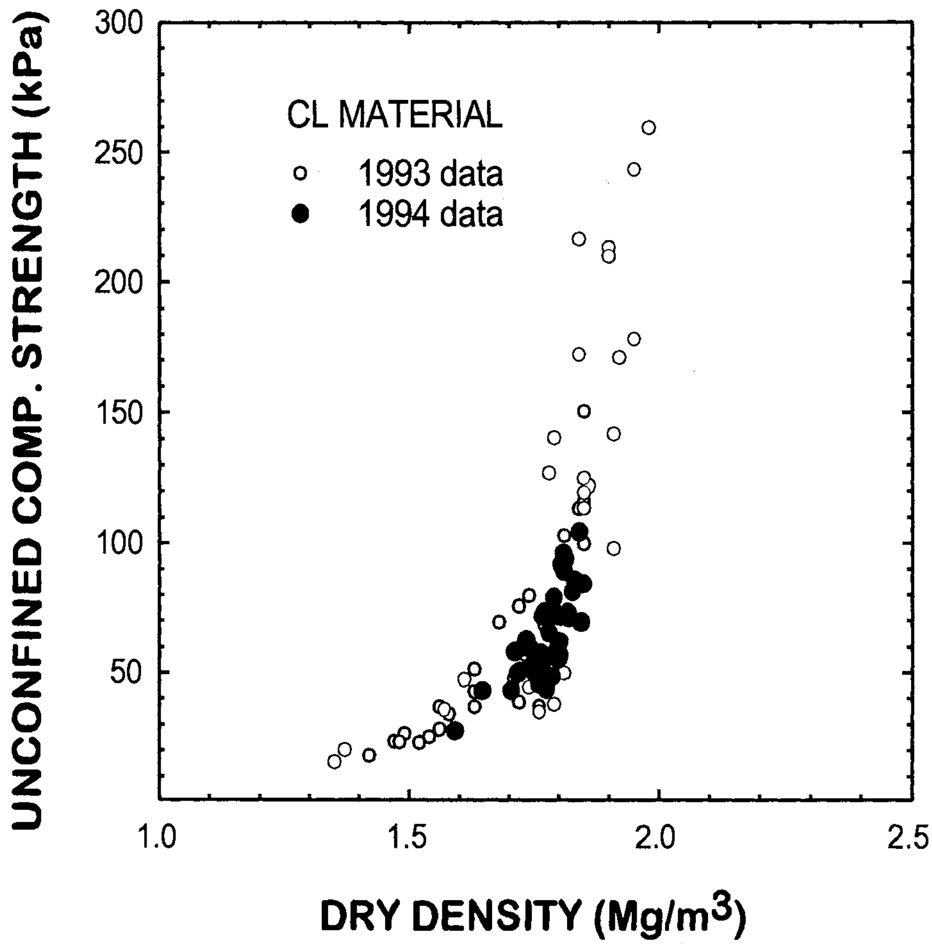

Figure 5.4. Strength versus dry density

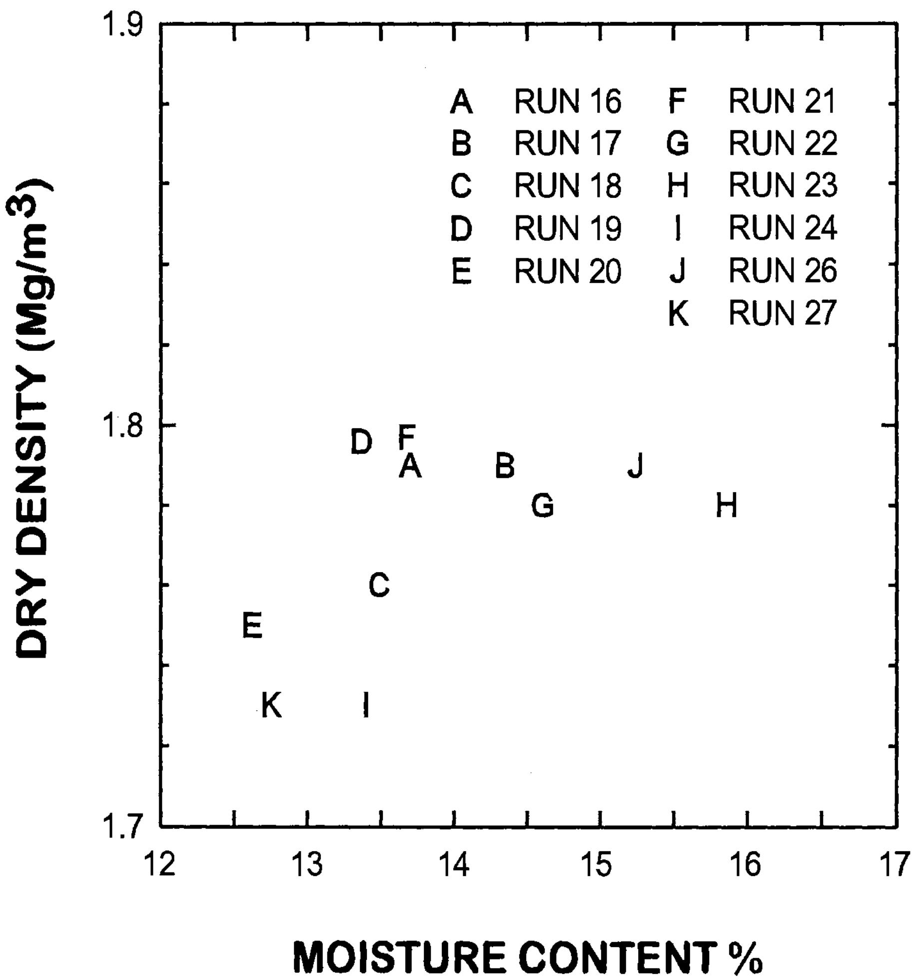

Figure 5.5. Dry density versus moisture content

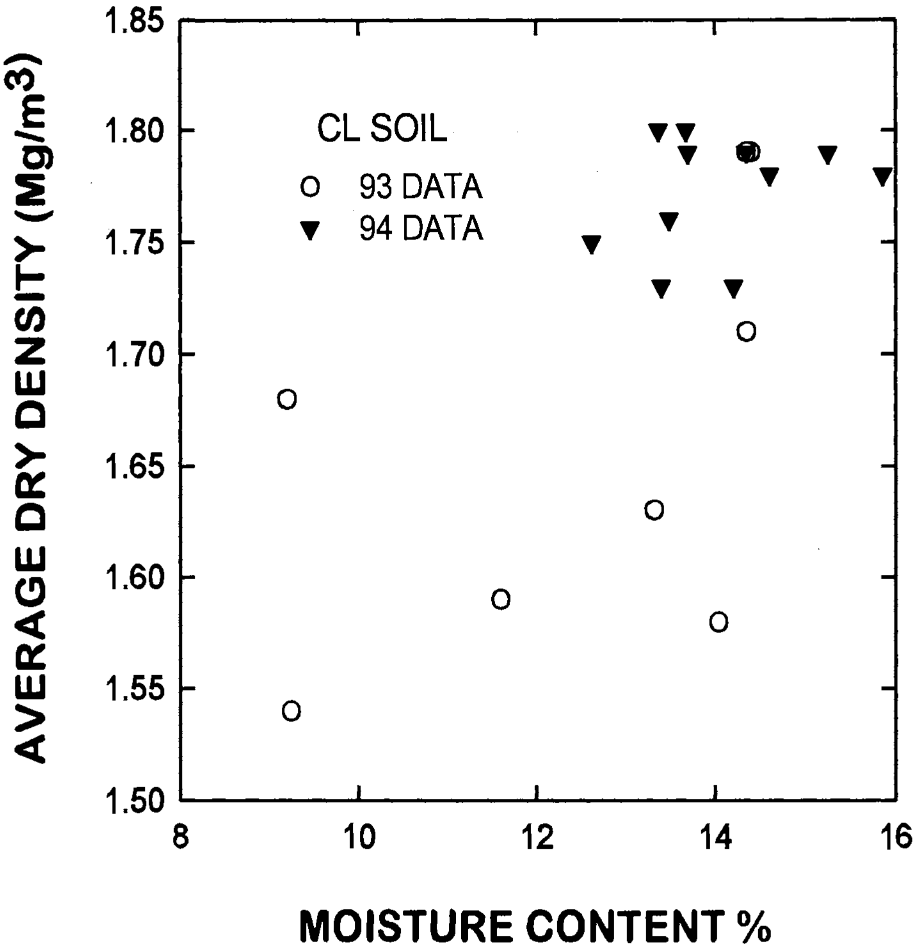

Figure 5.6. Dry density versus moisture for 1993 and 1994 data

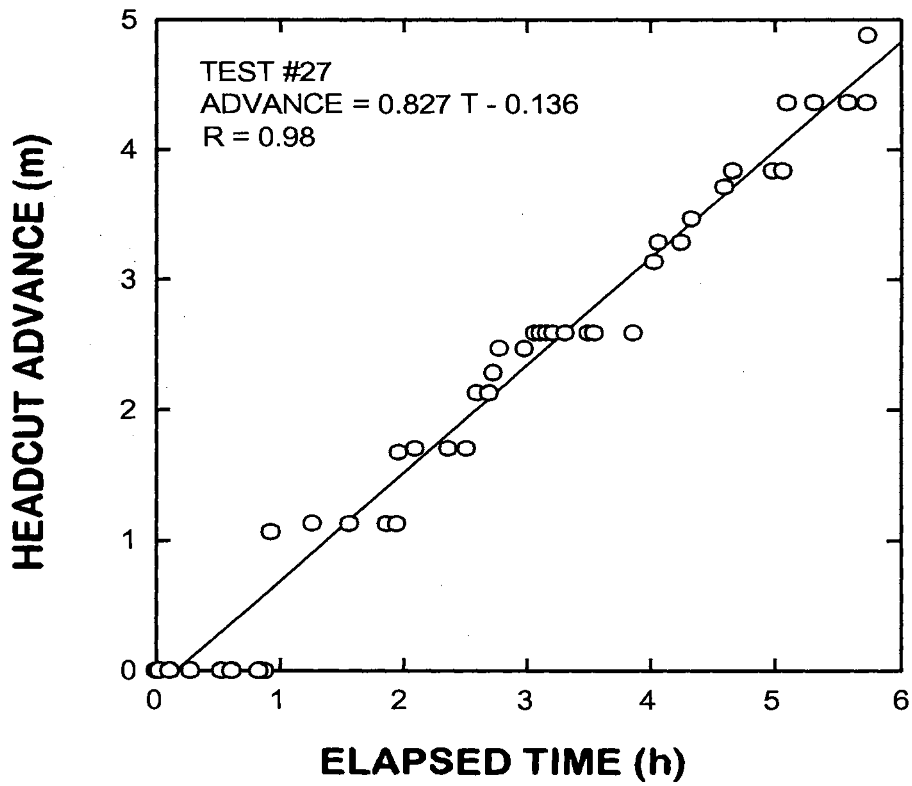

Figure 5.7. Headcut movement versus time for test 27

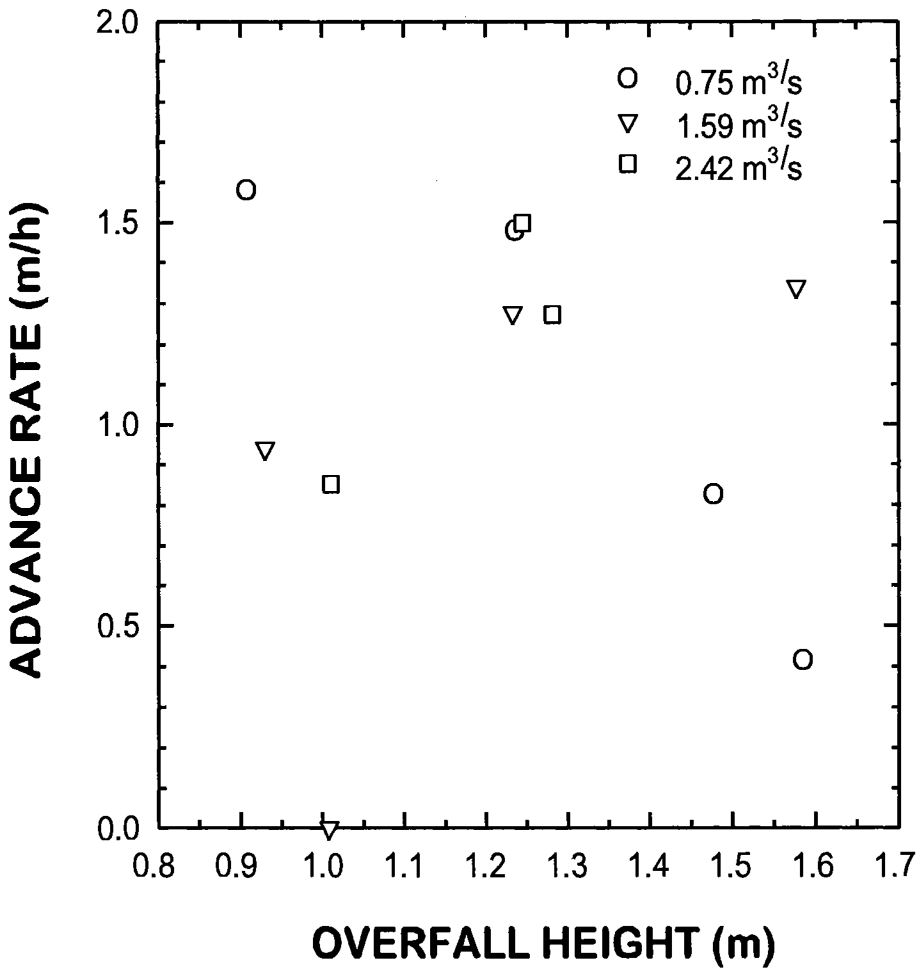

Figure 5.8. Advance rate versus overfall height for three discharges

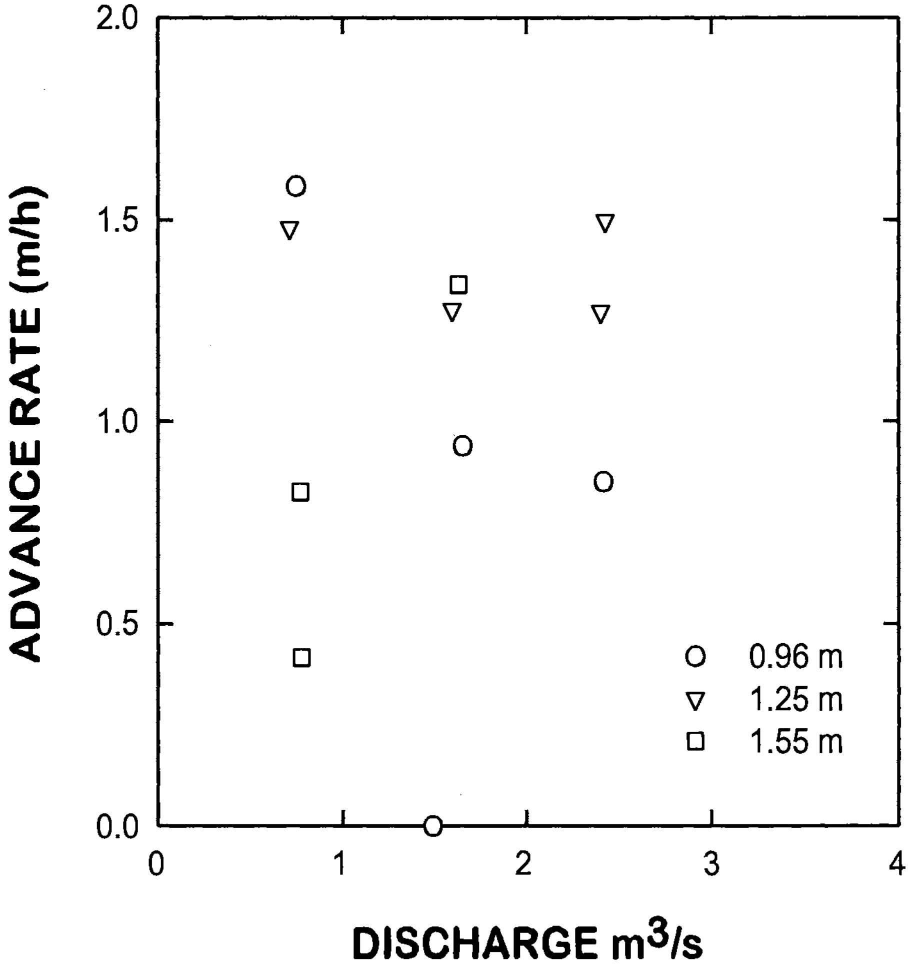

Figure 5.9. Advance rate versus discharge
for three overfall heights

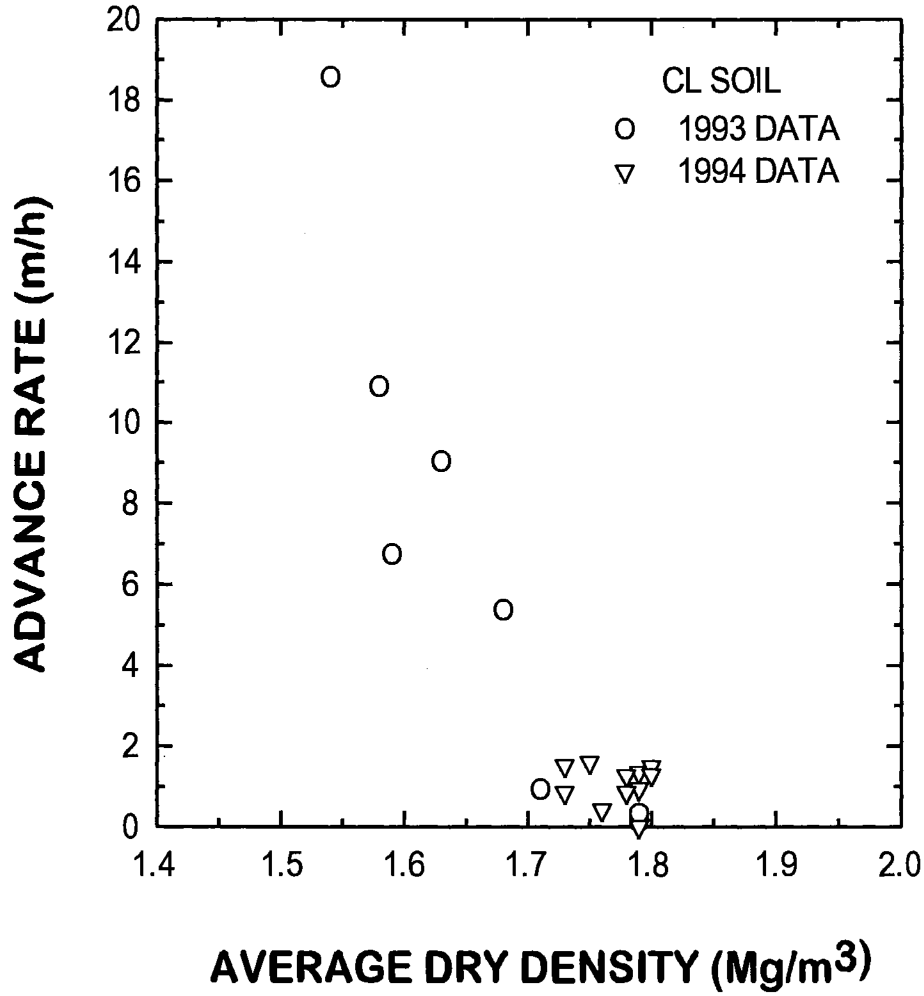

Figure 5.10. Advance rate versus dry density for 1993 and 1994 data

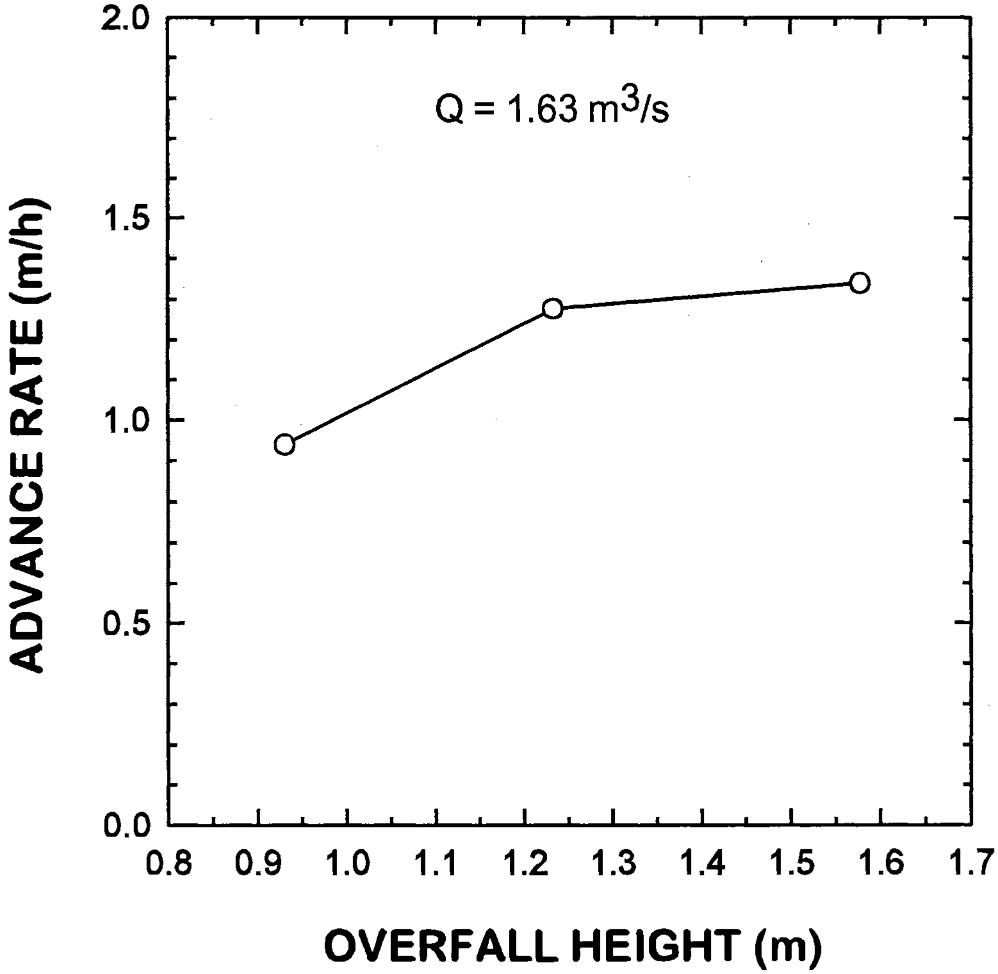

Figure 5.11. Advance rate versus overfall height for a data subset

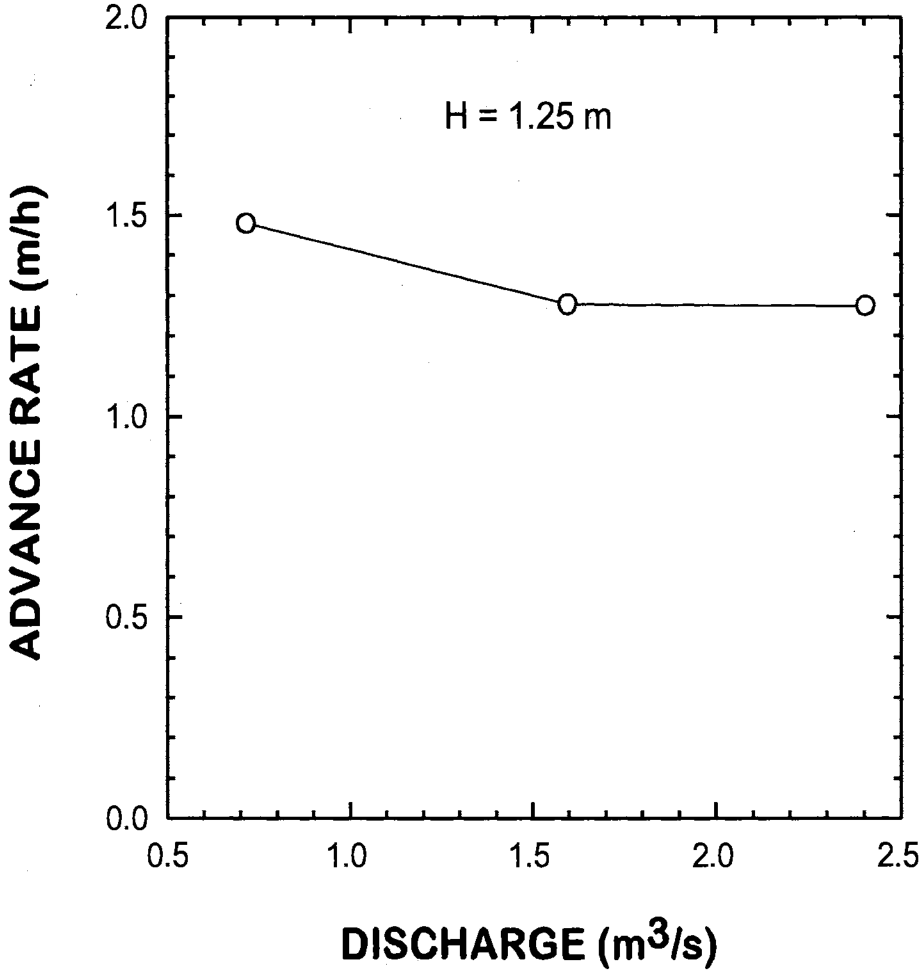

Figure 5.12. Advance rate versus discharge for a data subset

CHAPTER 6

INFLUENCE OF BACKWATER ON HEADCUT ADVANCE

ABSTRACT

A study was performed to examine the influence of backwater level downstream of an overfall on headcut advance. The discharge, overfall height, and soil type were held constant while varying tailwater level. The intermediate tailwater levels with a backwater to overfall height ratio of approximately 0.8 produced the largest headcut advance rates. The tailwater level downstream of the overfall was observed to vary the advance rate by a factor of 2.6 to 7.5 over the range of soil conditions tested.

INTRODUCTION

Headcut erosion research is being conducted to better describe and predict this poorly understood erosion process. Headcut advance predictions are of critical importance in assessing the risk an earthen dam or spillway encounters while passing a flood flow. Once a gully forms in an earthen spillway, the headcut moves upstream at a rate determined by the hydraulic attack and the soil resistance. The backwater or tailwater level below the overfall is one of many important parameters in this process. The objective of this study is to determine how backwater level influences the rate of headcut advance.

BACKGROUND

A spillway gully can experience many backwater levels during passage of a flood flow. These gullies normally form near the spillway exit where they can be exposed to high backwater levels caused by the base stream elevation at flood stage. As a gully headcut retreats up the spillway slope, the tailwater depth is largely affected by the gully geometry, gully bed slope, and discharge. If the gully enters the horizontal crest section of the spillway, the headcut can begin to submerge thereby experiencing much higher tailwater levels.

Numerous studies have been conducted examining the influence of tailwater on hydraulic structures such as the straight drop spillway (Donnelly and Blaisdell, 1965). These researchers found that the overfall nappe switched from a plunging to a floating or surface nappe when the tailwater depth exceeded the overfall height plus two-thirds of the approach flow critical depth. Many hydraulic structures are designed to operate at specific backwater conditions for optimum performance. While the scour below an overfall has been studied, little information exists relating tailwater level to the migration rate of a gully headcut.

The hydraulic shear stress and pressure forces transmitted to the boundary of a straight drop overfall were measured in time and space for a full range of plunging backwater levels (Robinson, 1989). The stress measured on the vertical wall or headcut face was observed to peak for intermediate backwater levels, and the location of this peak stress was always near the overfall base. This information was used to develop generalized prediction equations for the magnitude, location, and variance of the stress and pressure at an overfall (Robinson, 1992). A large-scale headcut erosion test facility was constructed, and the dominant headcut erosion parameters are under investigation (Robinson and Hanson, 1995). The tailwater investigation described herein is part of this ongoing project.

EXPERIMENTAL EQUIPMENT

The influence of different backwater levels on headcut advance was examined in a 1.8-m wide and 29-m long reinforced concrete flume. The 2.4-m tall flume sidewalls are equipped with two windows to allow a limited side view of the headcut erosion. Flow is delivered to the flume in an open channel, and the discharge is measured just upstream of the flume with a modified Parshall flume. The test flume entrance is equipped with a transition section and a vane flow straightener to insure uniform approach flow conditions. A rail-mounted bridge and point gage carriage is installed on top of the flume walls to allow rapid water surface and bed elevation measurement along the channel centerline. Flow exits the flume into a controlled outlet basin. This basin is equipped with a winch-operated overflow tailgate that allows the flume backwater level to be controlled. The outlet basin can be supplied with water separately from the flume; therefore, a selected backwater level could be established before beginning a test flow.

EXPERIMENTAL PROCEDURE

Soil was placed in the flume in 15-cm thick loose lift layers. If necessary, water was added to achieve a uniform soil moisture. A tractor mounted tiller was used to mix the soil layer and to reduce aggregate sizes once the material was placed in the flume. An 86-cm wide self-propelled sheepsfoot roller was used to compact each layer, and a pneumatic hand-held compactor was used to compact the soil against the flume walls. A soil cement treatment was applied to the fill surface to insure erosion occurred at the overfall rather than along the horizontal fill surface. A near vertical overfall was preformed at the downstream end of the fill, and soil samples were also extracted from the soil profile at the downstream end of the fill. A red sandy clay soil with a liquid limit of 26 and a plasticity index of 15 was used as the test material.

Each test fill was 12.2-m long, 1.8-m wide, and approximately 1.3-m high. Soil sampling consumed approximately 1.2 m of the fill. The remaining 11m of fill was tested by exposing each 2.75-m long section to a different backwater. That is, four backwater levels were tested as a headcut advanced through the 11-m long fill section. The backwater level was changed by adjusting the outlet structure tailgate. The backwater was adjusted during each test while maintaining a constant flow rate. A water surface and bed profile is provided to illustrate the four typical backwater conditions (Fig. 6.1). Some minor variation in discharge, overfall height, and backwater level was observed for each test. The backwater level was measured near the flume exit. Localized flow acceleration just below the overfall normally caused backwater to be less at this location. The discharge for all tests was approximately 1.6 m^3/s.

RESULTS AND DISCUSSION

A total of four tests were performed with four backwaters per test. This test schedule produced 16 headcut advance rate measurements for roughly four backwater conditions. While the overfall height, discharge, and backwater levels were similar for all tests, the soil conditions at the time of fill placement varied from test to test. Maintaining large quantities of soil with uniform bulk properties posed a logistical problem due to rainfall and differential drying of the stocklpiled soil. Tests 1 and 3 exhibited similar average moisture contents of 12.1% and average dry densities of 1.68 g/cc. Tests 2 and 4 displayed average moisture contents of 11.7% and 14.4% and average dry densities of 1.60 and 1.73 g/cc, respectively. The variation in soil moisture and density has been shown to have a dramatic impact on headcut advance (Robinson and Hanson, 1995). Previous work with this soil indicates that as the moisture content and density increase the headcut advance rate decreases. While tests 1 and 3 can be directly compared, test 2 and 4 should be recognized as representing much different soil conditions.

The headcut advance rate was determined for each segment of fill material by plotting the headcut advance versus time for each backwater condition. Data for test 3 is shown (Fig. 6.2) along with the advance rate for each backwater test. Vertical lines are drawn on the plot to separate the backwater segments. The coefficient of determination for each segment was 0.92 or greater. The headcut typically moved in a uniform manner between backwater changes. The headcut advance was comparatively low for the low tailwater, and the advance rate increased as the tailwater was raised to the second setting. Subsequent increases in tailwater caused the advance rate to decrease. The intermediate backwater levels caused the fastest advance rates. For test 3 the fastest advance rate was 2.7 times faster than the slowest advance rate. Of the sixteen tests, fourteen tests suggest that intermediate backwaters produce the largest advance rates. The two exceptions were the high backwater for test 2 and the low backwater for test 4. Both of these segments experienced a faster advance rate than expected. The high backwater for test 2 produced the fastest advance rate due to the premature failure of the soil cement surface. This condition was visually confirmed. The relatively rapid advance for the low backwater in test 4 is thought to be due to the presence of a substantially drier layer of material at the base of the overfall. The low backwater was apparently able to focus the flow energy in the reverse roller on the dryer layer and produce a rapid advance rate.

The observed headcut erosion correlates well with the boundary stresses previously measured (Robinson, 1989). For test 4 the peak stress on the vertical face of the overfall was estimated using the prediction relations developed by Robinson (1992) (Fig. 6.3). The maximum stress transferred to the overfall face occurs at a backwater to overfall height ratio of approximately 0.8. This peak B_W/H ratio was also observed in the earlier experimental stress measurements. Starting with a low backwater, the stress increases as the backwater increases until reaching the peak stress. The stress decreases dramatically as the backwater increases beyond this point. While the resolution of the measured headcut advance data is quite coarse, the peak advance rates were also observed near $B_W/H = 0.8$. A plot of the advance rate versus the backwater, nondimensionalized with the overfall height, illustrates how the bulk of the data provides the fastest headcut advance at intermediate backwater levels (Fig. 6.4). The two cases that performed differently are shown on the plot with an unfilled symbol. The reader should note that tests 1 and 3, with similar soil moisture and density, performed much the same. Test 2, the drier and less dense fill, provided the most rapid headcut advance, while test 4, the wetter and more dense fill, exhibited the lowest advance rates. Visual observations of the overfall erosion, particularly through the flume windows, are the basis for the following comments concerning flow circulation. The turbulence below the overfall is high for low backwater conditions, but the size of the flow circulation or reverse roller in contact with the overfall face is normally small. At intermediate backwater levels the reverse roller apparently reaches an optimum size, and the stress can more efficiently be transferred to the overfall face. At high backwater levels the nappe is deflected farther downstream, and the larger scale circulation produces less stress at the overfall. The reader is reminded that the headcut moves by discrete mass failure events. The stress detachment forces set up the mass failure by systematically removing material from the base of the overfall until the soil mass becomes unstable.

Disregarding the two tests previously discussed, the ratio of largest to smallest headcut advance rate for the same soil conditions varied from 2.6 to 7.5. That is, the backwater level was observed to increase the headcut advance by a factor of up to 7.5. This study suggests that the backwater level is an important parameter in the prediction of headcut advance.

SUMMARY

Tests were conducted in a large-scale flume to evaluate the influence of backwater level on the observed rate of headcut advance. The discharge, overfall height, and soil type were held constant and the backwater level was varied. Four tests generated 16 headcut advance measurements for which results are presented. The variation in soil moisture and soil density for each test is described. Low moisture and low density conditions produced the largest headcut advance rate, while high moisture and high density conditions produced the lowest advance rate. With two exceptions, the intermediate backwater levels produced the largest headcut advance rate for a given soil condition. While the resolution of the backwater measurements was coarse, the maximum headcut advance rate was observed for a backwater to overfall height ratio of approximately 0.8. The predicted stress on the vertical headcut face agrees well with the observed advance rates. The tailwater level downstream of an overfall was observed to vary the advance rate by a factor of 2.6 to 7.5 over the range of soil conditions tested. This study suggests that an accurate prediction of headcut advance must incorporate accurate backwater information.

REFERENCES

Donnelly, C. A. and F. W. Blaisdell. 1965. Straight drop spillway stilling basin. *J. of the Hydraulics Div., Proc. of the ASCE* 91(HY3):101-145.

Robinson, K. M. 1989. Hydraulic stresses on an overfall boundary. *Transactions of the ASAE* 32(4):1269-1274.

Robinson, K. M. 1992. Predicting stress and pressure at an overfall. *Transactions of the ASAE* 35(2):561-569.

Robinson, K. M. and G. J. Hanson. 1995. Large-scale headcut erosion testing. *Transactions of the ASAE* 38(2):429-434.

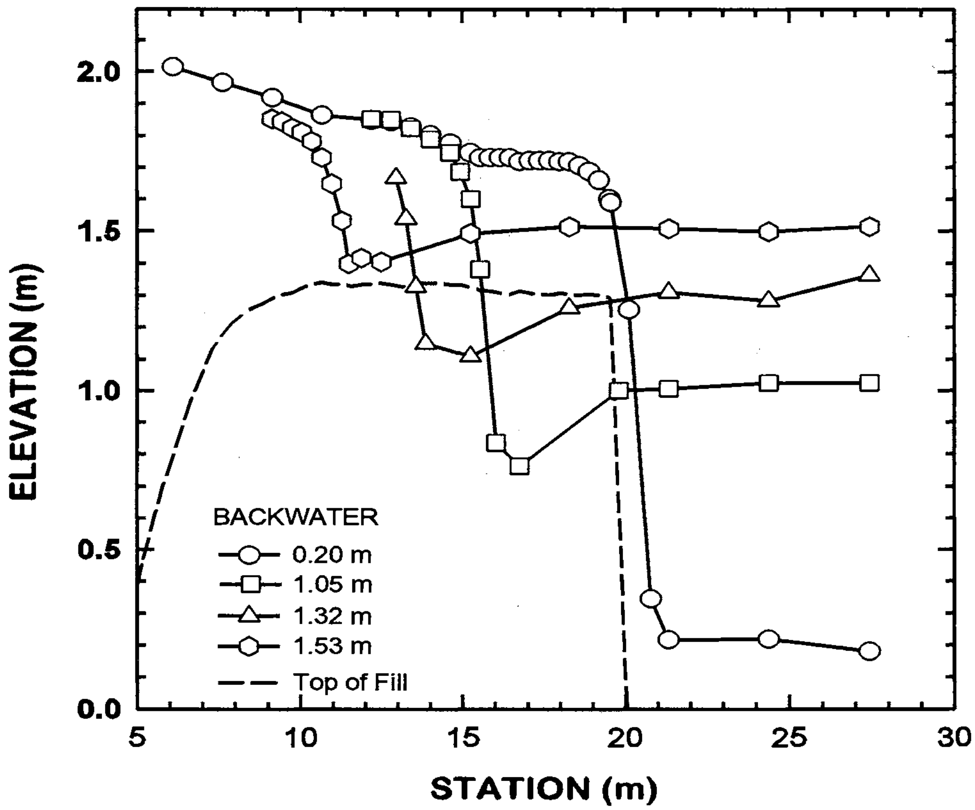

Figure 6.1. Typical backwater profiles for run 1

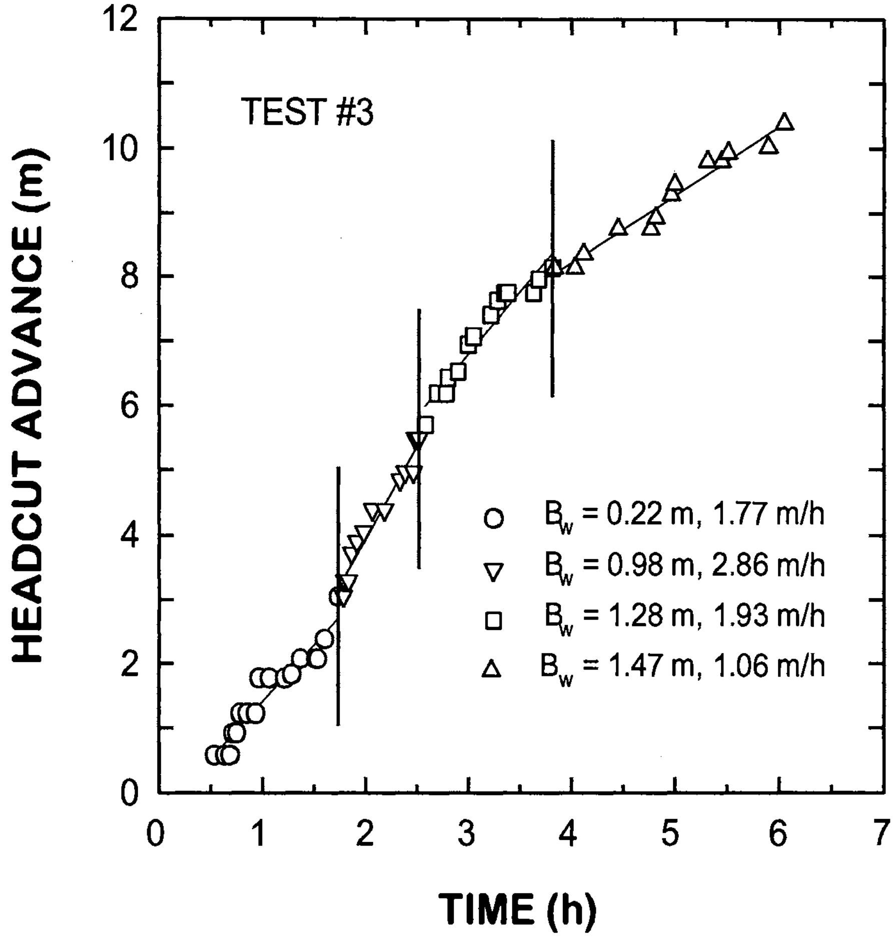

Figure 6.2. Headcut advance versus time

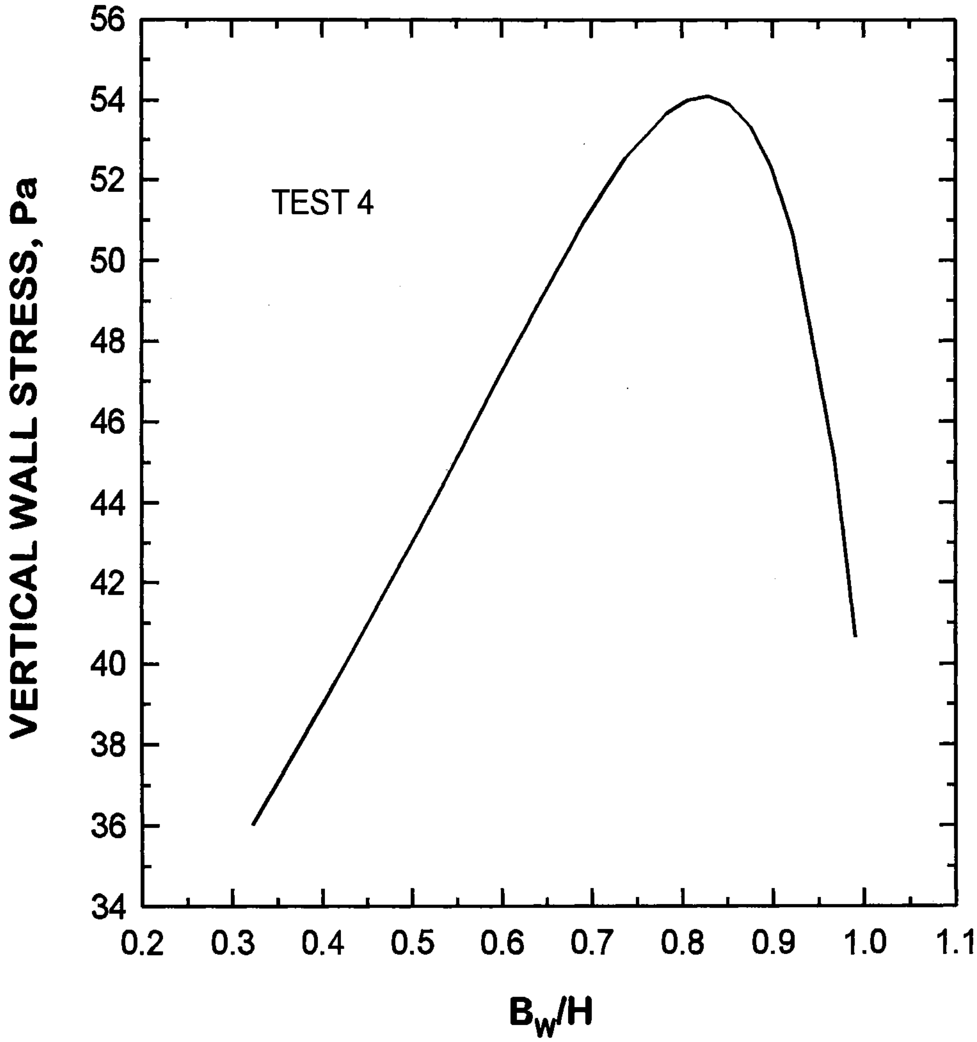

Figure 6.3. Wall stress versus backwater

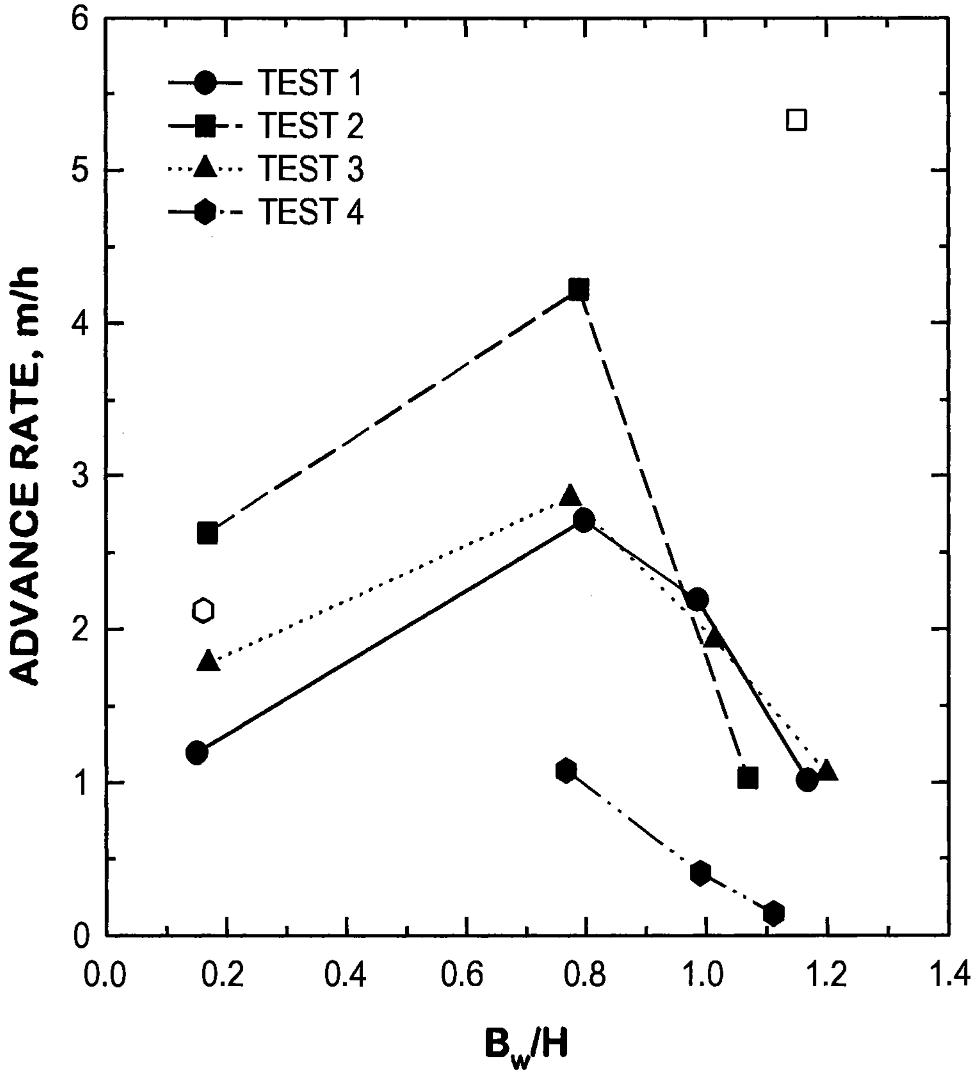

Figure 6.4. Advance rate versus backwater with two outliers shown

CHAPTER 7

SUMMARY AND RECOMMENDATIONS

SUMMARY

Earth auxiliary spillways are routinely used to transfer flood waters around a dam. While the vast majority of spillways perform as expected, some spillways encounter damage passing a flood flow. The formation and movement of a gully headcut is the dominant form of spillway damage. Headcut migration through a spillway can breach a dam and pose a substantial risk to people and property downstream. This research was conducted to better understand the development and movement of gullies in earth auxiliary spillways.

The hydraulic shear stress transmitted to the boundary of an overfall is a dominant force in the development and growth of gullies. While other failure processes contribute to headcut movement, particularly mass wasting due to headcut instability, the boundary stress is considered to be a trigger force that can strongly influence the erosion process. A fixed-bed overfall model was used to measure these stresses using hot-film anemometry. Prediction equations were developed to estimate the magnitude, location, and variance of shear stress and pressure forces acting on the overfall boundary. While these prediction equations represent the measured data well, they must be used cautiously if extrapolated outside the data base.

A large-scale headcut advance facility was constructed to examine the interaction of the attacking hydraulic forces and the resisting soil forces. The mechanics of headcut advance were examined at near field-scale to more accurately represent field conditions. A compacted cohesive fill material was placed in a test flume, and headcut advance rates were measured for a range of soil moistures and densities. The overfall height and flow rates were held constant. The advance rate was found to decrease as the average density and average unconfined compressive strength increased. The soil strength increased as the soil density increased.

Flume tests were also conducted to determine the influence of a sand layer on headcut advance. Each test was conducted with a sand layer extending under half the fill. This arrangement allowed comparison of headcut movement with and without the sand layer. When the material overlying the sand layer was more erosion resistant, the sand layer dramatically increased the rate of headcut movement. The sand material was eroded from the overfall base, tension cracks would form, and mass wasting would occur. As the erodibility of the overlying material increased, the influence of the sand layer diminished.

The influence of discharge and overfall height was also examined by attempting to hold the soil properties constant. The changes in overfall height and discharge were overshadowed by the placed soil properties. These tests suggest that the overfall height and discharge did not have a strong influence on headcut advance for the range of heights and discharges examined. A subset of the data does indicate that the advance rate increases slightly as the overfall height increases.

The erosion processes that occurred during the tests were also observed. Some tests, typically the lower moisture tests, failed with a sloping headcut indicative of stress detachment. These sloping headcuts tended to fail in small chunks, with the individual compacted layers very visible. The higher moisture content tests typically failed with a vertical face largely due to tension cracking and larger mass failure events. The soil behaved more as a homogeneous mass with less evidence of the placed soil layers.

Tests were also conducted to examine the influence of backwater level on the rate of headcut advance. The soil properties were held constant while changing the tailwater level downstream of the headcut. The intermediate backwater levels (backwater to overfall height ratios of approximately 0.8) produced the largest headcut advance rate for a given soil condition. The predicted shear stress on the headcut face correlates well with the observed advance rates.

Collectively, these studies provide additional insight into the complex headcut erosion process.

RECOMMENDATIONS

While the research described herein extends our understanding of headcut erosion, the topic is by no means fully understood. The recommendations for future research are:

1. The mass failure mechanisms contributing to headcut advance are not well understood. The location and depth of tension cracks plays an important role in the mass failure process. Additional

study is needed to determine the horizontal position of tension cracks relative to the overfall for different soil conditions. The contribution of existing soil joints or cracks is also poorly understood. The presence of soil cracks in the spillway is thought to accelerate the headcut advance rate by providing an existing failure plane and a path for water to enter the soil and hydraulically lubricate a failure surface. Tests are recommended to examine different soil crack distributions in a placed fill section.

2. The stress prediction equations presented herein were developed for relatively small overfall heights (0.25 to 0.76 m) and relatively low flow rates (0.028 to 0.113 m^3/s). The validity of these prediction equations for conditions other than those tested can be legitimately questioned. The measurement of stresses at or near field-scale is desired. Hot-film anemometry or Preston tube techniques could be used to collect stress measurements for near field conditions.

3. The large-scale overfall model tests were all conducted by preforming a near vertical overfall just in advance of testing. The flume floor acted as an inerodible boundary layer preventing additional deepening of the overfall. While erosion resistant layers are often found in the field, tests should be performed with soil material below the overfall. This arrangement would allow examination of the rate of deepening, the typical scour hole profile, and the contribution of bed scour to headcut instability. The

deepening could also be examined with a constant tailwater depth and a tailwater depth that increases as the scour increases.

4. Only two soils have been tested in the large-scale flume with the bulk of the tests conducted on one soil. Additional material types should be examined to identify material dependent behavior. More information is also needed about the soil erodibility coefficient. Accurate predictions of erodibility are necessary to produce good estimates of headcut advance.

5. The information contained in this dissertation could be used to develop a headcut advance model. This data base could also be used to calibrate an existing model. A predictive model, if accurate, would be of enormous value in determining the risk of spillway failure.

6. Headcuts were observed to erode with either a sloping face or a near vertical face. The sloping headcuts were observed to fail by stress detachment erosion processes, while the vertical headcuts failed by undercutting and mass failure processes. Additional study is needed to determine why a headcut transitions between a sloping and vertical face.

7. Measurement of the boundary stresses upstream of an overfall could provide additional information on the forces that produce a rotating headcut. A rotating headcut typically transitions from a near vertical to a sloping face. The distribution of stresses upstream of an overfall may well explain this behavior.

8. Subsurface seepage can have a major impact on headcut advance. Additional testing is needed to determine how and when subsurface seepage can influence spillway erosion. An improved understanding of seepage influences would be particularly useful in field gully settings.

APPENDICES

APPENDIX A

STRESS AND WATER SURFACE DATA

INTRODUCTION

A fixed-bed overfall model with multiple drop heights was used to collect boundary hydraulic shear stress data in time and space. Drop heights of 10, 20, and 30 in were examined at flow rates of 1, 2, 3, 3.2, and 4 ft^3/s. The 30-in wide model was instrumented with a flush mounted hot-film anemometry probe. A pipe loop was used to calibrate the hot-film probe before and after each model run. The stress was measured on the horizontal floor downstream of the overfall brink, as well as, on the vertical overfall wall. Each drop height and flow rate combination was examined at multiple backwater levels downstream of the brink.

The overfall data were collected under non-aerated conditions. That is, the air pocket underneath the nappe was not maintained at atmospheric pressure. This lack of aeration caused deflection of the nappe trajectory. Because the nappe impacted the bed closer to the overfall, the boundary stress also increased slightly. This flow condition was selected because it represents the worst case condition for stresses downstream of an overfall.

DESCRIPTION OF TERMS

The terms used in Tables A1 and A2 are described to clarify their meaning. The parameters presented in Table A1 are:

Year.	The year the data were collected.
Stress.	The time-averaged boundary shear stress (lb/ft^2)
Variance.	The shear stress variance ($(lb/ft^2)^2$)
Max. Stress.	The maximum shear stress observed in the sweep (lb/ft^2)
Min. Stress.	The minimum shear stress observed in the sweep (lb/ft^2)
Temp.	The time-averaged temperature in degrees F
Unit Wt.	The unit weight of the water (lb/ft^3)
Q.	The flow rate measured in the model (ft^3/s)
Bw.	The basin backwater level measured 8 ft downstream of the overfall (ft)
X.	The horizontal probe position measured as the distance downstream of the overfall (in)
Y.	The vertical probe position measured as the distance above the basin floor (in)
H.	The vertical overfall height (in)

The parameters presented in Table A2 are:

Station.	The horizontal tape station - station 10 is the location of the overfall (ft)
Elev.	The point gage reading - distance above the floor (ft)
Q.	The total model flow rate (ft^3/s)
Bw.	The backwater level measured 8 ft downstream of the overfall (ft)
Da.	The approach flow depth determined iteratively as the flow depth at a location 3.5 times that depth upstream of the overfall (ft)
F.	$V^2/(g\ D_a)$ This term is equal to the Froude number squared.
H.	The overfall height (in)
X.	The horizontal position downstream of the overfall (ft)
X/Da.	Nondimensional horizontal distance
Y.	The vertical distance above or below the overfall brink (ft)
Y/Da.	Nondimensional vertical distance

TABLE A1. Stress data

Year	Stress	Variance	Max. stress	Min. stress	Temp.	Unit Wt.	Q	Bw	X	Y	H
	lb/ft^2	(lb/ft^2)^2	lb/ft^2	lb/ft^2	F	lb/ft^3	ft^3/s	ft	in	in	in
87	1.17E-03	2E-07	3.55E-03	3.86E-04	77.9	62.23	1.001	2.75	6	0	30
87	5.74E-04	1E-07	2.11E-03	1.85E-04	79.5	62.22	0.997	2.75	12	0	30
87	3.63E-04	1E-07	1.71E-03	1.30E-04	77.5	62.24	0.997	2.75	18	0	30
87	4.27E-04	1E-07	2.39E-03	1.26E-04	75.1	62.26	0.995	2.75	24	0	30
87	5.61E-04	1E-07	2.00E-03	1.92E-04	74.6	62.26	0.999	2.75	36	0	30
87	1.20E-03	3E-07	5.43E-03	4.82E-04	74.9	62.26	0.997	2.75	0	18	30
87	2.96E-03	4.6E-06	2.17E-02	4.69E-04	77.9	62.23	1.001	2.5	6	0	30
87	9.99E-04	4E-07	9.35E-03	2.42E-04	79.6	62.22	1.001	2.5	12	0	30
87	7.30E-04	2E-07	4.34E-03	1.85E-04	77.5	62.24	0.997	2.5	18	0	30
87	9.05E-04	4E-07	5.65E-03	1.65E-04	75.1	62.26	0.997	2.5	24	0	30
87	1.21E-03	6E-07	9.78E-03	3.00E-04	74.6	62.26	0.999	2.5	36	0	30
87	2.99E-03	2.7E-06	1.26E-02	4.96E-04	74.9	62.26	0.997	2.5	0	18	30
87	1.06E-02	3.01E-05	5.31E-02	1.32E-03	77.9	62.23	1.001	2.25	6	0	30
87	7.38E-03	2.95E-05	4.94E-02	6.58E-04	79.6	62.22	1.001	2.25	12	0	30
87	9.08E-03	2.88E-05	4.67E-02	8.81E-04	77.4	62.24	0.999	2.25	18	0	30
87	1.07E-02	3.72E-05	6.35E-02	1.06E-03	75.1	62.26	0.999	2.25	24	0	30
87	7.94E-03	1.73E-05	3.94E-02	1.94E-03	74.6	62.26	0.999	2.25	36	0	30
87	7.60E-03	0.000013	2.89E-02	1.36E-03	74.9	62.26	0.997	2.25	0	18	30
87	8.67E-03	0.000012	3.42E-02	1.60E-03	78.0	62.23	0.999	2	6	0	30
87	7.00E-03	4.15E-05	7.15E-02	6.80E-04	79.7	62.22	1.001	2	12	0	30
87	7.19E-03	0.000028	6.90E-02	3.27E-04	77.4	62.24	1.001	2	18	0	30
87	8.35E-03	2.89E-05	5.68E-02	8.51E-04	75.1	62.26	0.997	2	24	0	30
87	3.22E-03	5.1E-06	2.33E-02	4.53E-04	74.7	62.26	0.999	2	36	0	30
87	5.66E-03	8.3E-06	3.11E-02	8.58E-04	74.9	62.26	0.995	2	0	18	30
87	4.75E-03	1.12E-05	4.37E-02	7.72E-04	78.0	62.23	0.997	1.75	6	0	30
87	8.00E-03	5.45E-05	1.01E-01	4.64E-04	79.7	62.21	1.001	1.75	12	0	30
87	6.45E-03	3.75E-05	6.46E-02	2.73E-04	77.3	62.24	0.999	1.75	18	0	30
87	6.35E-03	0.000028	4.89E-02	3.77E-04	75.1	62.26	0.999	1.75	24	0	30
87	1.61E-03	1.9E-06	1.57E-02	2.81E-04	74.7	62.26	0.999	1.75	36	0	30
87	1.01E-02	3.46E-05	3.47E-02	9.62E-04	74.9	62.26	0.995	1.75	0	18	30
87	8.04E-03	2.02E-05	5.16E-02	8.24E-04	78.0	62.23	0.997	1.5	6	0	30

TABLE A1. Stress data

Year	Stress	Variance	Max. stress	Min. stress	Temp.	Unit Wt.	Q	Bw	X	Y	H
	lb/ft^2	(lb/ft^2)^2	lb/ft^2	lb/ft^2	F	lb/ft^3	ft^3/s	ft	in	in	in
87	6.86E-03	5.93E-05	9.18E-02	4.99E-04	79.7	62.21	1.001	1.5	12	0	30
87	7.57E-03	6.58E-05	1.10E-01	3.84E-04	77.3	62.24	0.997	1.5	18	0	30
87	7.26E-03	3.79E-05	5.24E-02	3.78E-04	75.1	62.26	1.001	1.5	24	0	30
87	2.24E-03	2.7E-06	1.41E-02	5.13E-04	74.7	62.26	0.997	1.5	36	0	30
87	7.64E-03	0.000023	7.85E-02	1.39E-03	78.0	62.23	0.997	1.25	6	0	30
87	2.16E-02	0.000472	2.28E-01	1.20E-03	79.8	62.21	0.999	1.25	12	0	30
87	3.76E-02	0.00075	2.31E-01	1.52E-03	77.3	62.24	0.999	1.25	18	0	30
87	1.23E-02	9.99E-05	9.96E-02	5.29E-04	75.1	62.26	0.999	1.25	24	0	30
87	6.49E-03	1.16E-05	3.05E-02	8.23E-04	74.7	62.26	0.999	1.25	36	0	30
87	1.22E-02	8.45E-05	7.86E-02	1.11E-03	78.1	62.23	0.999	1	6	0	30
87	4.69E-02	0.001265	3.46E-01	2.04E-03	79.8	62.21	0.999	1	12	0	30
87	8.27E-02	0.002063	3.91E-01	1.40E-03	77.3	62.24	0.999	1	18	0	30
87	4.12E-02	0.000658	2.17E-01	1.78E-03	75.1	62.26	0.999	1	24	0	30
87	8.79E-03	3.97E-05	7.76E-02	5.94E-04	74.7	62.26	0.999	1	36	0	30
87	2.53E-02	0.000349	1.68E-01	1.17E-03	78.1	62.23	0.999	0.75	6	0	30
87	1.08E-01	0.003262	5.14E-01	8.16E-03	79.8	62.21	0.999	0.75	12	0	30
87	1.58E-01	0.005707	6.28E-01	1.29E-02	77.3	62.24	1.001	0.75	18	0	30
87	7.27E-02	0.001679	3.64E-01	3.04E-03	75.1	62.26	0.999	0.75	24	0	30
87	5.83E-03	3.04E-05	9.73E-02	5.84E-04	74.7	62.26	1.001	0.75	36	0	30
87	2.48E-02	0.000407	2.17E-01	1.51E-03	78.1	62.23	1.001	0.5	6	0	30
87	1.68E-01	0.006691	8.01E-01	1.18E-02	79.9	62.21	1.001	0.5	12	0	30
87	3.28E-01	0.020317	1.12E+00	1.82E-02	77.3	62.24	0.999	0.5	18	0	30
87	7.31E-02	0.002345	3.96E-01	2.15E-03	75.2	62.26	0.999	0.5	24	0	30
87	7.72E-03	5.85E-05	8.12E-02	6.30E-04	74.8	62.26	0.999	0.5	36	0	30
87	1.87E-02	0.000254	1.98E-01	1.03E-03	78.2	62.23	1.001	0.11	6	0	30
87	1.69E-01	0.009791	8.16E-01	6.75E-03	79.9	62.21	0.999	0.11	12	0	30
87	5.14E-01	0.020854	1.17E+00	4.83E-02	77.2	62.24	0.997	0.11	18	0	30
87	2.86E-01	0.007462	6.59E-01	4.83E-02	75.1	62.26	0.999	0.12	24	0	30
87	2.04E-01	0.006097	6.27E-01	2.62E-02	74.8	62.26	1.001	0.1	36	0	30
87	1.13E-03	2E-07	4.37E-03	2.95E-04	79.7	62.22	1.990	2.75	6	0	30
87	1.97E-03	1.5E-06	1.05E-02	3.47E-04	80.7	62.21	1.990	2.75	24	0	30

TABLE A1. Stress data											
Year	Stress	Variance	Max. stress	Min. stress	Temp.	Unit Wt.	Q	Bw	X	Y	H
	lb/ft^2	(lb/ft^2)^2	lb/ft^2	lb/ft^2	F	lb/ft^3	ft^3/s	ft	in	in	in
87	1.83E-03	1.2E-06	8.90E-03	3.82E-04	80.3	62.21	1.983	2.75	30	0	30
87	2.34E-03	2.3E-06	2.73E-02	3.43E-04	80.2	62.21	1.983	2.75	36	0	30
87	7.44E-03	1.85E-05	4.14E-02	8.16E-04	79.8	62.21	2.005	2.75	48	0	30
87	8.25E-04	2E-07	4.19E-03	2.30E-04	79.8	62.21	1.990	2.75	0	6	30
87	2.21E-03	1.6E-06	1.19E-02	5.01E-04	81.1	62.20	1.990	2.75	0	12	30
87	1.38E-03	6E-07	7.13E-03	2.71E-04	80.9	62.20	1.990	2.75	0	18	30
87	2.16E-03	2.1E-06	1.76E-02	2.56E-04	79.8	62.21	1.990	2.5	6	0	30
87	2.11E-03	2.2E-06	3.94E-02	3.59E-04	80.8	62.21	1.990	2.5	24	0	30
87	1.93E-03	1.9E-06	2.03E-02	2.99E-04	80.4	62.21	1.990	2.5	30	0	30
87	2.07E-03	2.4E-06	1.54E-02	3.38E-04	80.1	62.21	1.990	2.5	36	0	30
87	6.42E-03	2.15E-05	4.57E-02	8.17E-04	79.8	62.21	1.990	2.5	48	0	30
87	4.67E-03	3.1E-06	1.66E-02	1.19E-03	79.7	62.21	1.990	2.5	0	6	30
87	6.85E-03	1.37E-05	3.28E-02	1.16E-03	81.1	62.20	1.990	2.5	0	12	30
87	3.54E-03	0.000007	2.71E-02	5.98E-04	80.9	62.20	1.982	2.5	0	18	30
87	1.79E-02	9.25E-05	8.05E-02	1.64E-03	79.8	62.21	1.990	2.25	6	0	30
87	2.76E-02	0.000294	1.39E-01	1.52E-03	80.8	62.20	1.990	2.25	24	0	30
87	3.25E-02	0.000267	1.47E-01	1.59E-03	80.4	62.21	1.990	2.25	30	0	30
87	2.64E-02	0.000172	1.08E-01	2.90E-03	80.0	62.21	1.990	2.25	36	0	30
87	3.10E-02	0.000199	1.16E-01	2.34E-03	79.8	62.21	1.990	2.25	48	0	30
87	2.10E-02	0.00005	6.91E-02	3.49E-03	79.7	62.21	1.990	2.25	0	6	30
87	3.60E-02	0.000236	1.59E-01	3.72E-03	81.1	62.20	1.990	2.25	0	12	30
87	4.80E-03	9.4E-06	5.35E-02	6.91E-04	81.0	62.20	1.990	2.25	0	18	30
87	2.06E-02	0.000125	1.08E-01	2.00E-03	80.0	62.21	1.983	2	6	0	30
87	3.93E-02	0.000438	1.96E-01	3.59E-03	80.8	62.20	1.990	2	24	0	30
87	3.34E-02	0.000287	1.43E-01	2.86E-03	80.4	62.21	1.983	2	30	0	30
87	2.07E-02	0.000147	1.27E-01	9.51E-04	80.0	62.21	1.990	2	36	0	30
87	1.91E-02	0.000117	9.18E-02	1.69E-03	79.8	62.21	1.990	2	48	0	30
87	1.50E-02	4.22E-05	6.91E-02	2.10E-03	79.7	62.21	1.990	2	0	6	30
87	2.42E-02	0.000172	1.12E-01	2.28E-03	81.1	62.20	1.990	2	0	12	30
87	5.02E-03	1.18E-05	5.75E-02	7.97E-04	81.0	62.20	1.990	2	0	18	30
87	1.33E-02	4.95E-05	5.77E-02	1.70E-03	80.0	62.21	1.983	1.75	6	0	30

TABLE A1. Stress data											
Year	Stress	Variance	Max. stress	Min. stress	Temp.	Unit Wt.	Q	Bw	X	Y	H
	lb/ft^2	(lb/ft^2)^2	lb/ft^2	lb/ft^2	F	lb/ft^3	ft^3/s	ft	in	in	in
87	5.07E-02	0.00074	2.45E-01	2.24E-03	80.8	62.20	1.990	1.75	24	0	30
87	3.32E-02	0.000418	2.14E-01	1.09E-03	80.4	62.21	1.990	1.75	30	0	30
87	2.00E-02	0.000163	1.08E-01	1.06E-03	80.0	62.21	1.990	1.75	36	0	30
87	1.91E-02	0.00018	1.48E-01	1.11E-03	79.8	62.21	1.990	1.75	48	0	30
87	1.31E-02	3.92E-05	4.62E-02	1.27E-03	79.7	62.21	1.990	1.75	0	6	30
87	1.67E-02	0.0001	8.39E-02	1.47E-03	81.1	62.20	1.990	1.75	0	12	30
87	5.78E-03	8.2E-06	3.72E-02	6.72E-04	81.1	62.20	1.990	1.75	0	18	30
87	1.76E-02	0.000123	8.53E-02	1.25E-03	80.1	62.21	1.983	1.5	6	0	30
87	7.44E-02	0.001457	3.95E-01	3.58E-03	80.8	62.20	1.990	1.5	24	0	30
87	5.07E-02	0.000642	2.14E-01	4.25E-03	80.4	62.21	1.990	1.5	30	0	30
87	2.00E-02	0.000332	1.86E-01	7.36E-04	80.0	62.21	1.990	1.5	36	0	30
87	2.06E-02	0.0002	1.39E-01	1.78E-03	79.8	62.21	1.983	1.5	48	0	30
87	1.47E-02	0.000042	9.17E-02	1.61E-03	79.7	62.21	1.990	1.5	0	6	30
87	1.38E-02	8.84E-05	8.99E-02	9.87E-04	81.1	62.20	1.990	1.5	0	12	30
87	1.57E-02	8.77E-05	7.74E-02	2.02E-03	80.1	62.21	1.983	1.25	6	0	30
87	1.04E-01	0.003157	4.51E-01	3.47E-03	80.8	62.20	1.990	1.25	24	0	30
87	6.29E-02	0.001358	3.01E-01	2.11E-03	80.5	62.21	1.990	1.25	30	0	30
87	3.12E-02	0.000572	1.89E-01	1.31E-03	79.9	62.21	1.990	1.25	36	0	30
87	8.91E-03	4.42E-05	1.03E-01	1.33E-03	79.8	62.21	1.990	1.25	48	0	30
87	1.28E-02	4.18E-05	7.59E-02	1.36E-03	79.7	62.21	1.990	1.25	0	6	30
87	1.33E-02	5.29E-05	9.93E-02	2.65E-03	81.1	62.20	1.990	1.25	0	12	30
87	2.30E-02	0.000177	1.05E-01	1.52E-03	80.1	62.21	1.983	1	6	0	30
87	1.65E-01	0.006179	6.75E-01	1.09E-02	80.8	62.20	1.990	1	24	0	30
87	8.41E-02	0.002489	4.05E-01	2.21E-03	80.5	62.21	1.990	1	30	0	30
87	3.66E-02	0.000833	2.24E-01	1.42E-03	79.9	62.21	1.990	1	36	0	30
87	1.24E-02	5.47E-05	1.17E-01	1.70E-03	79.8	62.21	1.990	1	48	0	30
87	1.75E-02	0.000131	9.63E-02	1.12E-03	79.7	62.21	1.990	1	0	6	30
87	2.34E-02	0.000271	1.56E-01	1.62E-03	80.2	62.21	1.983	0.75	6	0	30
87	2.95E-01	0.016419	1.09E+00	2.30E-02	80.8	62.20	1.990	0.75	24	0	30
87	1.32E-01	0.005012	6.51E-01	5.32E-03	80.5	62.21	1.990	0.75	30	0	30
87	4.19E-02	0.001246	2.94E-01	1.76E-03	79.9	62.21	1.990	0.75	36	0	30

TABLE A1. Stress data											
Year	Stress	Variance	Max. stress	Min. stress	Temp.	Unit Wt.	Q	Bw	X	Y	H
	lb/ft^2	(lb/ft^2)^2	lb/ft^2	lb/ft^2	F	lb/ft^3	ft^3/s	ft	in	in	in
87	1.26E-02	6.52E-05	1.01E-01	1.29E-03	79.8	62.21	1.990	0.75	48	0	30
87	1.13E-02	9.55E-05	1.01E-01	8.69E-04	79.7	62.22	1.990	0.75	0	6	30
87	1.67E-02	0.000192	1.84E-01	1.18E-03	80.2	62.21	1.983	0.1	6	0	30
87	5.79E-01	0.024377	1.22E+00	4.53E-02	80.8	62.20	1.990	0.085	24	0	30
87	3.84E-01	0.009983	8.39E-01	1.27E-01	80.5	62.21	1.990	0.085	30	0	30
87	2.76E-01	0.005059	6.18E-01	8.39E-02	79.8	62.21	1.990	0.075	36	0	30
87	3.35E-01	0.006978	7.86E-01	9.49E-02	79.8	62.21	1.990	0.075	48	0	30
87	1.94E-03	2.5E-06	1.28E-02	1.36E-04	71.5	62.28	3.989	2.75	6	0	30
87	3.97E-03	1.13E-05	7.55E-02	4.20E-04	71.4	62.29	3.996	2.75	18	0	30
87	3.78E-03	5.6E-06	2.79E-02	5.12E-04	70.2	62.29	3.997	2.75	30	0	30
87	3.89E-03	7.5E-06	4.22E-02	5.66E-04	64.5	62.33	3.994	2.75	36	0	30
87	3.90E-03	7.8E-06	2.67E-02	4.19E-04	68.1	62.31	3.986	2.75	42	0	30
87	1.55E-02	9.46E-05	8.02E-02	1.41E-03	68.2	62.31	3.993	2.75	48	0	30
87	5.01E-03	0.000008	2.38E-02	9.09E-04	71.8	62.28	3.989	2.75	0	6	30
87	9.62E-03	1.63E-05	4.73E-02	2.05E-03	73.7	62.27	3.981	2.75	0	18	30
87	1.78E-03	1.7E-06	1.36E-02	2.02E-04	71.5	62.28	3.985	2.5	6	0	30
87	4.34E-03	1.09E-05	3.50E-02	4.55E-04	71.4	62.28	3.993	2.5	18	0	30
87	4.23E-03	7.3E-06	3.10E-02	6.04E-04	70.2	62.29	3.997	2.5	30	0	30
87	5.90E-03	1.88E-05	5.08E-02	6.15E-04	64.5	62.33	4.002	2.5	36	0	30
87	5.55E-03	1.19E-05	3.37E-02	4.91E-04	68.1	62.31	3.993	2.5	42	0	30
87	2.24E-02	0.000139	1.20E-01	2.46E-03	68.2	62.31	3.990	2.5	48	0	30
87	5.55E-03	9.2E-06	2.59E-02	8.79E-04	71.8	62.28	3.978	2.5	0	6	30
87	1.03E-02	4.03E-05	4.51E-02	1.12E-03	73.7	62.27	3.979	2.5	0	18	30
87	9.04E-03	3.07E-05	4.98E-02	5.28E-04	71.5	62.28	3.989	2.25	6	0	30
87	4.31E-02	0.000663	5.26E-01	3.71E-03	71.5	62.28	3.989	2.25	18	0	30
87	6.15E-02	0.001203	2.45E-01	3.10E-03	70.1	62.30	3.989	2.25	30	0	30
87	8.23E-02	0.00142	2.92E-01	7.40E-03	64.5	62.33	3.983	2.25	36	0	30
87	4.92E-02	0.000488	1.84E-01	6.89E-03	68.1	62.31	3.982	2.25	42	0	30
87	9.35E-02	0.001725	3.27E-01	6.45E-03	68.2	62.31	3.982	2.25	48	0	30
87	3.60E-02	0.000223	1.39E-01	4.89E-03	71.7	62.28	3.985	2.25	0	6	30
87	1.61E-02	0.000122	1.31E-01	1.09E-03	73.3	62.27	3.976	2.25	0	18	30

TABLE A1. Stress data

Year	Stress	Variance	Max. stress	Min. stress	Temp.	Unit Wt.	Q	Bw	X	Y	H
	lb/ft^2	(lb/ft^2)^2	lb/ft^2	lb/ft^2	F	lb/ft^3	ft^3/s	ft	in	in	in
87	1.71E-02	7.45E-05	8.92E-02	1.55E-03	71.5	62.28	3.985	2	6	0	30
87	4.13E-02	0.001097	3.61E-01	2.79E-03	71.5	62.28	3.989	2	18	0	30
87	1.07E-01	0.002419	4.34E-01	8.67E-03	70.0	62.30	3.993	2	30	0	30
87	1.02E-01	0.002082	3.96E-01	9.21E-03	64.5	62.33	3.994	2	36	0	30
87	5.58E-02	0.000702	2.05E-01	3.34E-03	68.1	62.31	3.986	2	42	0	30
87	9.63E-02	0.002267	3.90E-01	4.89E-03	68.2	62.31	3.982	2	48	0	30
87	4.42E-02	0.00024	1.52E-01	6.00E-03	71.7	62.28	3.985	2	0	6	30
87	1.00E-02	0.000051	8.56E-02	1.11E-03	73.5	62.27	3.981	2	0	18	30
87	1.67E-02	0.000079	8.35E-02	1.07E-03	71.5	62.28	3.989	1.75	6	0	30
87	5.83E-02	0.001902	4.65E-01	3.36E-03	71.5	62.28	3.985	1.75	18	0	30
87	1.43E-01	0.004403	6.44E-01	1.27E-02	70.0	62.30	3.989	1.75	30	0	30
87	1.22E-01	0.003198	4.65E-01	5.14E-03	64.6	62.33	3.987	1.75	36	0	30
87	6.51E-02	0.001028	2.92E-01	1.64E-03	68.0	62.31	3.993	1.75	42	0	30
87	1.04E-01	0.003321	4.09E-01	3.00E-03	68.3	62.31	3.971	1.75	48	0	30
87	4.30E-02	0.000267	1.66E-01	4.09E-03	71.8	62.28	3.985	1.75	0	6	30
87	1.03E-02	6.31E-05	9.67E-02	1.27E-03	73.8	62.27	3.985	1.75	0	18	30
87	1.36E-02	7.02E-05	8.50E-02	6.55E-04	71.5	62.28	3.989	1.5	6	0	30
87	9.72E-02	0.004226	5.55E-01	4.42E-03	71.5	62.28	3.982	1.5	18	0	30
87	1.84E-01	0.008113	1.12E+00	8.26E-03	70.0	62.30	3.997	1.5	30	0	30
87	1.45E-01	0.004791	5.68E-01	4.11E-03	64.6	62.33	3.987	1.5	36	0	30
87	7.19E-02	0.001593	3.44E-01	1.76E-03	68.0	62.31	3.997	1.5	42	0	30
87	1.06E-01	0.004133	5.63E-01	3.33E-03	68.3	62.31	3.986	1.5	48	0	30
87	4.18E-02	0.0003	1.52E-01	4.64E-03	71.8	62.28	3.978	1.5	0	6	30
87	1.15E-02	5.59E-05	5.85E-02	5.93E-04	71.5	62.28	3.989	1.25	6	0	30
87	1.58E-01	0.008125	8.62E-01	1.04E-02	71.5	62.28	3.982	1.25	18	0	30
87	2.40E-01	0.013399	9.29E-01	1.40E-02	70.0	62.30	3.997	1.25	30	0	30
87	1.81E-01	0.00795	6.65E-01	7.53E-03	64.6	62.33	3.987	1.25	36	0	30
87	8.34E-02	0.002134	3.73E-01	3.08E-03	68.0	62.31	3.997	1.25	42	0	30
87	1.21E-01	0.005329	5.05E-01	6.57E-03	68.3	62.31	3.979	1.25	48	0	30
87	3.39E-02	0.000277	1.93E-01	3.37E-03	71.8	62.28	3.980	1.25	0	6	30
87	8.25E-03	4.11E-05	6.52E-02	4.51E-04	71.5	62.28	3.987	1	6	0	30

TABLE A1. Stress data

Year	Stress	Variance	Max. stress	Min. stress	Temp.	Unit Wt.	Q	Bw	X	Y	H
	lb/ft^2	(lb/ft^2)^2	lb/ft^2	lb/ft^2	F	lb/ft^3	ft^3/s	ft	in	in	in
87	2.15E-01	0.01309	1.26E+00	1.19E-02	71.5	62.28	3.978	1	18	0	30
87	3.51E-01	0.023957	1.16E+00	1.51E-02	69.9	62.30	3.993	1	30	0	30
87	2.45E-01	0.014591	9.09E-01	8.15E-03	64.6	62.33	3.987	1	36	0	30
87	9.20E-02	0.003617	6.92E-01	3.37E-03	68.1	62.31	4.008	1	42	0	30
87	9.16E-02	0.005446	6.39E-01	3.20E-03	68.3	62.31	3.990	1	48	0	30
87	1.96E-02	0.000148	1.17E-01	2.53E-03	71.8	62.28	3.983	1	0	6	30
87	6.46E-03	2.94E-05	4.99E-02	3.51E-04	71.6	62.28	3.989	0.21	6	0	30
87	2.01E-01	0.011824	8.36E-01	1.09E-02	71.5	62.28	3.982	0.21	18	0	30
87	5.51E-01	0.021591	1.28E+00	7.03E-02	69.9	62.30	3.997	0.21	30	0	30
87	5.27E-01	0.016577	1.12E+00	1.73E-01	64.7	62.33	3.990	0.22	36	0	30
87	2.95E-01	0.004642	5.99E-01	1.11E-01	68.0	62.31	4.008	0.2	42	0	30
87	5.01E-01	0.012234	1.03E+00	1.99E-01	68.2	62.31	3.993	0.2	48	0	30
87	1.43E-02	7.02E-05	9.45E-02	2.40E-03	71.8	62.28	3.982	0.21	0	6	30
87	4.99E-03	8.8E-06	2.79E-02	5.80E-04	77.1	62.24	3.169	2.75	6	0	30
87	3.23E-03	5.1E-06	2.13E-02	3.99E-04	77.8	62.23	3.183	2.75	12	0	30
87	2.93E-03	0.000006	2.81E-02	2.89E-04	76.3	62.25	3.197	2.75	18	0	30
87	3.31E-03	4.6E-06	1.66E-02	6.00E-04	75.8	62.25	3.207	2.75	24	0	30
87	5.48E-03	0.000014	2.97E-02	8.02E-04	75.2	62.25	3.198	2.75	30	0	30
87	3.36E-03	5.4E-06	2.90E-02	6.32E-04	77.5	62.23	3.211	2.75	36	0	30
87	4.13E-03	1.01E-05	2.91E-02	3.36E-04	77.7	62.23	3.211	2.75	42	0	30
87	1.51E-03	1.8E-06	1.36E-02	7.19E-05	78.4	62.23	3.183	2.75	0	3	30
87	2.91E-03	3.6E-06	3.14E-02	5.23E-04	79.0	62.22	3.192	2.75	0	6	30
87	4.76E-03	0.000008	2.80E-02	6.27E-04	80.4	62.21	3.201	2.75	0	12	30
87	5.39E-03	2.13E-05	4.92E-02	4.00E-04	77.3	62.24	3.160	2.5	6	0	30
87	2.86E-03	5.3E-06	2.82E-02	3.93E-04	77.9	62.23	3.188	2.5	12	0	30
87	3.77E-03	8.3E-06	2.46E-02	3.56E-04	76.3	62.25	3.193	2.5	18	0	30
87	4.49E-03	7.2E-06	2.07E-02	5.94E-04	75.9	62.25	3.216	2.5	24	0	30
87	8.37E-03	4.47E-05	9.45E-02	8.40E-04	75.3	62.25	3.202	2.5	30	0	30
87	5.56E-03	1.53E-05	3.75E-02	5.76E-04	77.6	62.23	3.211	2.5	36	0	30
87	9.51E-03	4.08E-05	7.15E-02	5.03E-04	77.7	62.23	3.193	2.5	42	0	30
87	2.28E-03	5.1E-06	2.66E-02	9.94E-05	78.5	62.23	3.192	2.5	0	3	30

TABLE A1. Stress data											
Year	Stress	Variance	Max. stress	Min. stress	Temp.	Unit Wt.	Q	Bw	X	Y	H
	lb/ft^2	(lb/ft^2)^2	lb/ft^2	lb/ft^2	F	lb/ft^3	ft^3/s	ft	in	in	in
87	3.96E-03	0.000008	3.84E-02	2.66E-04	79.0	62.22	3.192	2.5	0	6	30
87	1.27E-02	2.53E-05	4.03E-02	2.68E-03	80.5	62.21	3.201	2.5	0	12	30
87	3.24E-02	0.000427	2.28E-01	1.42E-03	76.3	62.25	3.193	2.25	18	0	30
87	2.62E-02	0.000355	1.89E-01	1.95E-03	75.8	62.25	3.211	2.25	24	0	30
87	8.37E-02	0.00131	2.76E-01	8.21E-03	75.3	62.25	3.198	2.25	30	0	30
87	7.80E-02	0.001177	2.92E-01	4.73E-03	77.6	62.23	3.206	2.25	36	0	30
87	7.61E-02	0.001195	3.13E-01	2.88E-03	77.8	62.23	3.197	2.25	42	0	30
87	1.20E-02	7.86E-05	8.46E-02	4.11E-04	78.6	62.23	3.192	2.25	0	3	30
87	3.66E-02	0.00026	1.40E-01	2.13E-03	79.1	62.22	3.192	2.25	0	6	30
87	5.40E-02	0.000477	1.97E-01	7.25E-03	80.6	62.21	3.206	2.25	0	12	30
87	5.17E-02	0.000708	2.21E-01	3.28E-03	77.4	62.24	3.155	2	6	0	30
87	5.51E-02	0.000747	2.67E-01	5.75E-03	78.0	62.23	3.188	2	12	0	30
87	4.03E-02	0.001114	3.31E-01	1.28E-03	76.3	62.25	3.193	2	18	0	30
87	6.42E-02	0.000838	2.20E-01	4.50E-03	75.8	62.25	3.211	2	24	0	30
87	1.14E-01	0.001569	3.99E-01	2.05E-02	75.0	62.26	3.202	2	30	0	30
87	8.96E-02	0.001278	2.82E-01	6.04E-03	77.7	62.23	3.211	2	36	0	30
87	7.12E-02	0.001272	4.14E-01	5.55E-03	77.9	62.23	3.197	2	42	0	30
87	1.86E-02	0.000131	9.55E-02	5.54E-04	78.6	62.23	3.192	2	0	3	30
87	3.89E-02	0.000263	1.47E-01	5.14E-03	79.1	62.22	3.192	2	0	6	30
87	4.73E-02	0.000513	2.40E-01	3.93E-03	80.6	62.21	3.201	2	0	12	30
87	5.91E-02	0.00237	4.53E-01	2.12E-03	76.3	62.25	3.193	1.75	18	0	30
87	7.51E-02	0.001428	3.26E-01	6.01E-03	75.8	62.25	3.211	1.75	24	0	30
87	1.35E-01	0.003239	4.48E-01	7.46E-03	75.4	62.25	3.198	1.75	30	0	30
87	1.00E-01	0.001605	3.82E-01	1.24E-02	77.7	62.23	3.206	1.75	36	0	30
87	8.79E-02	0.001646	3.39E-01	6.13E-03	77.9	62.23	3.192	1.75	42	0	30
87	1.62E-02	0.000108	8.50E-02	4.16E-04	78.6	62.23	3.197	1.75	0	3	30
87	2.88E-02	0.000202	1.01E-01	1.05E-03	79.1	62.22	3.192	1.75	0	6	30
87	3.56E-02	0.000316	1.52E-01	3.04E-03	80.7	62.21	3.201	1.75	0	12	30
87	2.83E-02	0.000522	2.26E-01	1.67E-03	77.5	62.23	3.155	1.5	6	0	30
87	6.79E-02	0.001618	4.12E-01	3.75E-03	78.1	62.23	3.188	1.5	12	0	30
87	6.89E-02	0.003546	5.96E-01	2.53E-03	76.3	62.25	3.193	1.5	18	0	30

TABLE A1. Stress data

Year	Stress	Variance	Max. stress	Min. stress	Temp.	Unit Wt.	Q	Bw	X	Y	H
	lb/ft^2	(lb/ft^2)^2	lb/ft^2	lb/ft^2	F	lb/ft^3	ft^3/s	ft	in	in	in
87	9.60E-02	0.002544	4.25E-01	7.26E-03	75.8	62.25	3.211	1.5	24	0	30
87	1.73E-01	0.004906	6.19E-01	1.34E-02	75.4	62.25	3.202	1.5	30	0	30
87	1.27E-01	0.00261	4.36E-01	4.41E-03	77.7	62.23	3.206	1.5	36	0	30
87	8.74E-02	0.003329	5.92E-01	1.93E-03	78.0	62.23	3.188	1.5	42	0	30
87	1.62E-02	0.000131	1.09E-01	5.61E-04	78.6	62.22	3.192	1.5	0	3	30
87	2.97E-02	0.000253	1.17E-01	2.16E-03	79.1	62.22	3.192	1.5	0	6	30
87	2.93E-02	0.000289	2.19E-01	3.22E-03	80.7	62.21	3.201	1.5	0	12	30
87	1.05E-01	0.007182	1.05E+00	3.88E-03	76.3	62.25	3.193	1.25	18	0	30
87	1.47E-01	0.005416	5.89E-01	1.26E-02	75.9	62.25	3.216	1.25	24	0	30
87	2.36E-01	0.008303	7.40E-01	1.60E-02	75.4	62.25	3.202	1.25	30	0	30
87	1.56E-01	0.005038	5.36E-01	5.10E-03	77.8	62.23	3.206	1.25	36	0	30
87	1.14E-01	0.004365	4.63E-01	3.51E-03	78.0	62.23	3.192	1.25	42	0	30
87	1.54E-02	0.000124	1.28E-01	3.51E-04	78.7	62.22	3.192	1.25	0	3	30
87	3.16E-02	0.00031	1.55E-01	2.00E-03	79.2	62.22	3.197	1.25	0	6	30
87	1.96E-02	0.000162	1.39E-01	2.90E-03	80.8	62.20	3.201	1.25	0	12	30
87	3.25E-02	0.000595	2.63E-01	2.20E-03	77.6	62.23	3.151	1	6	0	30
87	9.90E-02	0.002709	5.06E-01	5.84E-03	78.2	62.23	3.192	1	12	0	30
87	1.70E-01	0.015149	1.21E+00	5.45E-03	76.3	62.25	3.193	1	18	0	30
87	2.15E-01	0.009758	8.68E-01	1.49E-02	75.9	62.25	3.211	1	24	0	30
87	3.46E-01	0.018145	1.12E+00	1.71E-02	75.4	62.25	3.202	1	30	0	30
87	2.14E-01	0.009338	8.46E-01	8.07E-03	77.8	62.23	3.206	1	36	0	30
87	1.35E-01	0.00699	6.77E-01	3.99E-03	78.0	62.23	3.188	1	42	0	30
87	1.06E-02	7.62E-05	1.12E-01	3.29E-04	78.7	62.22	3.192	1	0	3	30
87	1.69E-02	0.00015	1.46E-01	1.31E-03	79.2	62.22	3.188	1	0	6	30
87	3.09E-01	0.030375	1.57E+00	1.30E-02	76.3	62.25	3.197	0.75	18	0	30
87	3.34E-01	0.015255	1.02E+00	2.58E-02	75.9	62.25	3.207	0.75	24	0	30
87	5.52E-01	0.031636	1.29E+00	3.47E-02	75.4	62.25	3.202	0.75	30	0	30
87	3.17E-01	0.022908	9.68E-01	1.08E-02	77.8	62.23	3.211	0.75	36	0	30
87	1.68E-01	0.014019	8.67E-01	4.29E-03	78.0	62.23	3.192	0.75	42	0	30
87	8.11E-03	0.000033	6.44E-02	6.05E-04	78.7	62.22	3.192	0.75	0	3	30
87	1.14E-02	4.87E-05	9.91E-02	1.08E-03	79.2	62.22	3.192	0.75	0	6	30

TABLE A1. Stress data

Year	Stress	Variance	Max. stress	Min. stress	Temp.	Unit Wt.	Q	Bw	X	Y	H
	lb/ft^2	(lb/ft^2)^2	lb/ft^2	lb/ft^2	F	lb/ft^3	ft^3/s	ft	in	in	in
87	3.18E-02	0.000661	4.00E-01	1.41E-03	77.8	62.23	3.137	0.16	6	0	30
87	8.41E-02	0.002422	3.95E-01	4.92E-03	78.3	62.23	3.192	0.17	12	0	30
87	2.82E-01	0.029533	1.68E+00	1.08E-02	76.2	62.25	3.197	0.17	18	0	30
87	3.48E-01	0.016277	1.30E+00	2.94E-02	75.9	62.25	3.207	0.165	24	0	30
87	6.63E-01	0.024453	1.25E+00	2.00E-01	75.5	62.25	3.202	0.165	30	0	30
87	5.59E-01	0.013879	1.15E+00	2.09E-01	77.9	62.23	3.206	0.16	36	0	30
87	5.29E-01	0.013465	1.05E+00	1.92E-01	78.1	62.23	3.197	0.16	42	0	30
87	7.53E-03	2.49E-05	7.68E-02	5.33E-04	78.8	62.22	3.192	0.16	0	3	30
87	1.17E-02	4.47E-05	8.06E-02	1.70E-03	79.3	62.22	3.192	0.16	0	6	30
88	7.71E-04	1E-07	2.05E-03	4.11E-04	79.8	62.21	0.993	1.25	3	0	10
88	1.62E-03	3E-07	4.74E-03	5.07E-04	79.9	62.21	0.993	1.25	6	0	10
88	2.45E-03	6E-07	5.28E-03	8.01E-04	79.9	62.21	0.997	1.25	9	0	10
88	1.46E-03	4E-07	4.84E-03	6.63E-04	79.9	62.21	0.993	1.25	12	0	10
88	1.41E-03	5E-07	4.79E-03	5.05E-04	79.9	62.21	0.993	1.25	15	0	10
88	1.34E-03	2E-07	4.55E-03	4.79E-04	79.9	62.21	0.993	1.25	18	0	10
88	1.94E-03	4E-07	4.51E-03	6.77E-04	79.9	62.21	0.997	1.25	21	0	10
88	1.82E-03	5E-07	5.43E-03	7.20E-04	80.0	62.21	0.997	1.25	24	0	10
88	1.98E-03	5E-07	9.75E-03	7.24E-04	80.0	62.21	0.993	1.25	27	0	10
88	1.72E-03	8E-07	8.36E-03	5.62E-04	80.1	62.21	0.997	1.25	30	0	10
88	2.97E-03	1.2E-06	1.11E-02	1.49E-03	80.1	62.21	0.989	1.25	33	0	10
88	2.42E-03	8E-07	6.25E-03	6.95E-04	80.1	62.21	0.993	1.25	36	0	10
88	2.07E-03	6E-07	7.42E-03	6.00E-04	80.1	62.21	0.993	1.25	39	0	10
88	1.97E-03	5E-07	6.23E-03	7.15E-04	80.2	62.21	0.989	1.25	42	0	10
88	1.62E-03	5E-07	4.87E-03	5.86E-04	80.2	62.21	0.989	1.25	45	0	10
88	1.87E-03	5E-07	5.18E-03	7.34E-04	80.2	62.21	0.993	1.25	48	0	10
88	1.62E-03	1.3E-06	5.29E-03	3.37E-04	79.9	62.21	1.001	1.25	0	3	10
88	2.04E-03	9E-07	8.18E-03	5.62E-04	79.8	62.21	0.993	1	3	0	10
88	2.04E-03	8E-07	7.91E-03	6.14E-04	79.8	62.21	0.997	1	6	0	10
88	2.82E-03	1.5E-06	9.35E-03	5.76E-04	79.9	62.21	0.997	1	9	0	10
88	2.12E-03	1.5E-06	1.17E-02	5.35E-04	79.9	62.21	0.993	1	12	0	10
88	1.82E-03	9E-07	9.19E-03	4.99E-04	79.9	62.21	0.993	1	15	0	10

TABLE A1. Stress data

Year	Stress	Variance	Max. stress	Min. stress	Temp.	Unit Wt.	Q	Bw	X	Y	H
	lb/ft^2	(lb/ft^2)^2	lb/ft^2	lb/ft^2	F	lb/ft^3	ft^3/s	ft	in	in	in
88	2.52E-03	2.1E-06	1.40E-02	6.75E-04	79.9	62.21	0.993	1	18	0	10
88	3.59E-03	4.2E-06	1.57E-02	7.07E-04	80.0	62.21	0.997	1	21	0	10
88	4.06E-03	0.000004	1.89E-02	7.94E-04	80.0	62.21	0.997	1	24	0	10
88	4.28E-03	4.9E-06	2.40E-02	8.61E-04	80.0	62.21	0.993	1	27	0	10
88	5.01E-03	6.1E-06	2.23E-02	9.15E-04	80.1	62.21	0.997	1	30	0	10
88	7.68E-03	1.35E-05	3.72E-02	1.05E-03	80.1	62.21	0.989	1	33	0	10
88	7.29E-03	1.49E-05	3.51E-02	1.35E-03	80.1	62.21	0.989	1	36	0	10
88	6.46E-03	7.6E-06	2.64E-02	1.57E-03	80.1	62.21	0.989	1	39	0	10
88	6.81E-03	1.12E-05	4.72E-02	1.34E-03	80.1	62.21	0.993	1	42	0	10
88	6.76E-03	7.5E-06	2.71E-02	2.01E-03	80.1	62.21	0.989	1	45	0	10
88	6.01E-03	1.14E-05	3.58E-02	8.40E-04	80.2	62.21	0.993	1	48	0	10
88	2.25E-03	1.1E-06	9.33E-03	5.89E-04	79.9	62.21	0.997	1	0	3	10
88	4.94E-02	0.000757	2.40E-01	3.57E-03	79.8	62.21	0.993	0.75	3	0	10
88	7.43E-02	0.001438	4.36E-01	8.22E-03	79.9	62.21	0.993	0.75	6	0	10
88	6.05E-02	0.001207	5.17E-01	4.35E-03	79.9	62.21	0.997	0.75	9	0	10
88	5.93E-02	0.000519	2.38E-01	1.16E-02	79.9	62.21	0.993	0.75	12	0	10
88	5.42E-02	0.000383	2.29E-01	1.34E-02	79.9	62.21	0.993	0.75	15	0	10
88	3.70E-02	0.000234	1.24E-01	4.76E-03	79.9	62.21	0.993	0.75	18	0	10
88	4.18E-02	0.000314	1.34E-01	6.33E-03	79.9	62.21	0.997	0.75	21	0	10
88	2.61E-02	0.000182	1.28E-01	1.86E-03	80.0	62.21	0.997	0.75	24	0	10
88	2.11E-02	0.000147	1.12E-01	2.75E-03	80.0	62.21	0.993	0.75	27	0	10
88	1.47E-02	0.000098	1.01E-01	1.67E-03	80.1	62.21	0.997	0.75	30	0	10
88	1.13E-02	8.56E-05	1.34E-01	1.50E-03	80.1	62.21	0.989	0.75	33	0	10
88	1.20E-02	9.43E-05	1.40E-01	2.06E-03	80.1	62.21	0.993	0.75	36	0	10
88	8.44E-03	3.44E-05	7.20E-02	1.28E-03	80.1	62.21	0.993	0.75	39	0	10
88	2.41E-03	3.7E-06	2.90E-02	5.87E-04	80.1	62.21	0.993	0.75	42	0	10
88	4.43E-03	1.15E-05	3.40E-02	8.33E-04	80.1	62.21	0.993	0.75	45	0	10
88	4.42E-03	6.8E-06	2.05E-02	1.02E-03	80.2	62.21	0.993	0.75	48	0	10
88	2.23E-02	0.000257	1.95E-01	2.11E-03	80.0	62.21	1.001	0.75	0	3	10
88	1.02E-01	0.001631	3.45E-01	1.53E-02	79.8	62.21	0.993	0.5	3	0	10
88	1.23E-01	0.006157	7.95E-01	8.83E-03	79.9	62.21	0.997	0.5	6	0	10

TABLE A1. Stress data											
Year	Stress	Variance	Max. stress	Min. stress	Temp.	Unit Wt.	Q	Bw	X	Y	H
	lb/ft^2	(lb/ft^2)^2	lb/ft^2	lb/ft^2	F	lb/ft^3	ft^3/s	ft	in	in	in
88	1.41E-01	0.002778	5.03E-01	2.70E-02	79.9	62.21	0.993	0.5	9	0	10
88	1.09E-01	0.001615	3.84E-01	1.93E-02	79.9	62.21	0.993	0.5	12	0	10
88	7.95E-02	0.001187	3.39E-01	6.99E-03	79.9	62.21	0.997	0.5	15	0	10
88	5.02E-02	0.000645	2.17E-01	4.06E-03	79.9	62.21	0.993	0.5	18	0	10
88	3.22E-02	0.000402	1.85E-01	2.65E-03	80.0	62.21	0.997	0.5	21	0	10
88	1.95E-02	0.0002	1.21E-01	1.54E-03	80.0	62.21	0.997	0.5	24	0	10
88	1.46E-02	0.00017	1.46E-01	1.30E-03	80.0	62.21	0.993	0.5	27	0	10
88	1.11E-02	7.56E-05	1.04E-01	1.27E-03	80.1	62.21	0.997	0.5	30	0	10
88	7.42E-03	4.36E-05	8.18E-02	9.45E-04	80.1	62.21	0.993	0.5	33	0	10
88	7.22E-03	5.29E-05	6.53E-02	8.80E-04	80.1	62.21	0.993	0.5	36	0	10
88	7.34E-03	3.83E-05	8.25E-02	1.03E-03	80.1	62.21	0.993	0.5	39	0	10
88	5.82E-03	2.61E-05	8.57E-02	8.38E-04	80.1	62.21	0.993	0.5	42	0	10
88	5.21E-03	7.8E-06	3.45E-02	8.33E-04	80.1	62.21	0.993	0.5	45	0	10
88	4.69E-03	9.3E-06	3.87E-02	1.01E-03	80.2	62.21	0.993	0.5	48	0	10
88	4.04E-02	0.000449	2.71E-01	8.35E-03	80.0	62.21	0.997	0.5	0	3	10
88	7.54E-02	0.001131	3.36E-01	1.04E-02	79.8	62.21	0.997	0.07	3	0	10
88	2.43E-01	0.018607	1.25E+00	2.56E-02	79.9	62.21	0.997	0.07	6	0	10
88	2.36E-01	0.008567	8.12E-01	6.05E-02	79.9	62.21	0.997	0.07	9	0	10
88	2.28E-01	0.004308	6.73E-01	6.46E-02	79.9	62.21	0.993	0.07	12	0	10
88	1.97E-01	0.003409	5.50E-01	5.67E-02	79.9	62.21	0.993	0.07	15	0	10
88	1.53E-01	0.002229	4.34E-01	2.26E-02	79.9	62.21	0.993	0.07	18	0	10
88	1.54E-01	0.001998	4.12E-01	3.97E-02	80.0	62.21	0.997	0.07	21	0	10
88	1.32E-01	0.00156	4.73E-01	4.16E-02	80.0	62.21	0.997	0.07	24	0	10
88	1.32E-01	0.001443	3.67E-01	4.21E-02	80.1	62.21	0.997	0.07	27	0	10
88	1.30E-01	0.001487	3.82E-01	4.09E-02	80.1	62.21	0.997	0.07	30	0	10
88	1.72E-01	0.002522	4.89E-01	5.27E-02	80.1	62.21	0.989	0.07	33	0	10
88	1.66E-01	0.002093	4.49E-01	5.79E-02	80.1	62.21	0.993	0.07	36	0	10
88	1.42E-01	0.001638	3.92E-01	3.68E-02	80.1	62.21	0.993	0.07	39	0	10
88	1.38E-01	0.001446	3.75E-01	5.16E-02	80.1	62.21	0.989	0.07	42	0	10
88	1.18E-01	0.001148	3.00E-01	3.37E-02	80.1	62.21	0.989	0.07	45	0	10
88	1.22E-01	0.001274	3.62E-01	4.13E-02	80.2	62.21	0.993	0.07	48	0	10

TABLE A1. Stress data

Year	Stress	Variance	Max. stress	Min. stress	Temp.	Unit Wt.	Q	Bw	X	Y	H
	lb/ft^2	(lb/ft^2)^2	lb/ft^2	lb/ft^2	F	lb/ft^3	ft^3/s	ft	in	in	in
88	1.56E-02	0.000223	2.39E-01	1.38E-03	80.0	62.21	0.997	0.07	0	3	10
88	1.65E-03	6E-07	7.79E-03	6.31E-04	79.4	62.22	2.003	1.25	3	0	10
88	2.54E-03	2.2E-06	1.23E-02	6.68E-04	79.5	62.22	2.007	1.25	6	0	10
88	3.30E-03	1.7E-06	9.25E-03	1.05E-03	79.5	62.22	2.005	1.25	9	0	10
88	3.31E-03	3.9E-06	1.57E-02	7.74E-04	79.7	62.22	2.005	1.25	12	0	10
88	3.31E-03	2.5E-06	1.17E-02	9.30E-04	79.8	62.21	2.005	1.25	15	0	10
88	6.15E-03	1.07E-05	3.99E-02	1.12E-03	79.6	62.22	1.998	1.25	18	0	10
88	7.56E-03	1.16E-05	3.13E-02	1.56E-03	79.6	62.22	1.999	1.25	21	0	10
88	7.53E-03	1.03E-05	3.16E-02	2.21E-03	79.6	62.22	2.005	1.25	24	0	10
88	6.71E-03	1.88E-05	9.38E-02	1.16E-03	79.5	62.22	1.999	1.25	27	0	10
88	5.73E-03	7.4E-06	2.13E-02	1.56E-03	79.6	62.22	2.001	1.25	30	0	10
88	5.52E-03	6.1E-06	2.47E-02	1.26E-03	79.6	62.22	1.999	1.25	33	0	10
88	5.59E-03	6.2E-06	2.39E-02	9.89E-04	79.6	62.22	1.999	1.25	36	0	10
88	5.16E-03	6.4E-06	3.36E-02	1.29E-03	79.6	62.22	1.999	1.25	39	0	10
88	5.74E-03	0.00001	6.28E-02	1.29E-03	79.7	62.21	2.001	1.25	42	0	10
88	4.61E-03	7.7E-06	2.86E-02	8.71E-04	79.8	62.21	1.999	1.25	45	0	10
88	4.83E-03	7.4E-06	2.49E-02	1.00E-03	79.8	62.21	1.999	1.25	48	0	10
88	3.43E-03	1.6E-06	1.04E-02	6.32E-04	80.0	62.21	1.995	1.25	0	3	10
88	4.78E-03	8.4E-06	2.70E-02	1.02E-03	79.4	62.22	2.009	1	3	0	10
88	4.26E-03	8.2E-06	2.55E-02	5.98E-04	79.5	62.22	2.005	1	6	0	10
88	4.98E-03	6.1E-06	2.98E-02	8.54E-04	79.5	62.22	2.007	1	9	0	10
88	5.01E-03	8.6E-06	4.03E-02	1.14E-03	79.7	62.22	2.005	1	12	0	10
88	4.73E-03	1.04E-05	4.21E-02	9.36E-04	79.8	62.21	2.003	1	15	0	10
88	9.37E-03	4.43E-05	7.55E-02	1.60E-03	79.6	62.22	1.999	1	18	0	10
88	1.75E-02	0.000123	1.48E-01	2.45E-03	79.6	62.22	1.999	1	21	0	10
88	1.77E-02	0.000132	1.50E-01	2.45E-03	79.6	62.22	2.001	1	24	0	10
88	2.20E-02	0.000129	1.05E-01	2.51E-03	79.6	62.22	1.999	1	27	0	10
88	2.01E-02	0.00012	1.32E-01	3.25E-03	79.6	62.22	2.001	1	30	0	10
88	1.66E-02	9.37E-05	1.58E-01	1.94E-03	79.6	62.22	2.001	1	33	0	10
88	1.66E-02	0.000085	1.05E-01	2.13E-03	79.6	62.22	1.998	1	36	0	10
88	1.65E-02	0.000102	1.10E-01	2.60E-03	79.6	62.22	1.999	1	39	0	10

TABLE A1. Stress data											
Year	Stress	Variance	Max. stress	Min. stress	Temp.	Unit Wt.	Q	Bw	X	Y	H
	lb/ft^2	(lb/ft^2)^2	lb/ft^2	lb/ft^2	F	lb/ft^3	ft^3/s	ft	in	in	in
88	1.52E-02	7.69E-05	1.00E-01	1.98E-03	79.7	62.21	2.001	1	42	0	10
88	1.31E-02	5.48E-05	1.01E-01	2.05E-03	79.8	62.21	1.999	1	45	0	10
88	1.53E-02	8.75E-05	8.85E-02	1.98E-03	79.8	62.21	2.005	1	48	0	10
88	3.98E-03	9.5E-06	3.52E-02	6.13E-04	80.0	62.21	2.003	1	0	3	10
88	5.93E-02	0.001271	3.33E-01	5.96E-03	79.4	62.22	2.003	0.75	3	0	10
88	1.03E-01	0.001893	3.88E-01	9.19E-03	79.5	62.22	2.001	0.75	6	0	10
88	8.86E-02	0.00383	7.48E-01	7.79E-03	79.5	62.22	2.005	0.75	9	0	10
88	1.35E-01	0.003159	7.03E-01	2.19E-02	79.7	62.22	2.005	0.75	12	0	10
88	1.34E-01	0.002841	4.78E-01	2.52E-02	79.8	62.21	2.005	0.75	15	0	10
88	1.84E-01	0.00491	8.18E-01	4.04E-02	79.6	62.22	2.001	0.75	18	0	10
88	1.62E-01	0.004005	6.91E-01	2.57E-02	79.6	62.22	2.001	0.75	21	0	10
88	1.14E-01	0.002479	5.22E-01	1.37E-02	79.6	62.22	2.005	0.75	24	0	10
88	9.24E-02	0.001905	4.04E-01	7.38E-03	79.6	62.22	2.001	0.75	27	0	10
88	7.65E-02	0.001337	3.92E-01	5.75E-03	79.6	62.22	2.001	0.75	30	0	10
88	6.06E-02	0.001136	3.42E-01	4.82E-03	79.6	62.22	1.999	0.75	33	0	10
88	5.21E-02	0.000983	3.20E-01	3.36E-03	79.6	62.22	1.999	0.75	36	0	10
88	3.17E-02	0.000512	2.42E-01	3.15E-03	79.7	62.22	1.999	0.75	39	0	10
88	3.27E-02	0.000484	2.27E-01	3.44E-03	79.8	62.21	2.001	0.75	42	0	10
88	2.23E-02	0.000221	1.55E-01	1.74E-03	79.8	62.21	2.001	0.75	45	0	10
88	1.77E-02	0.000215	1.40E-01	1.63E-03	79.8	62.21	2.005	0.75	48	0	10
88	4.37E-02	0.000774	3.08E-01	2.88E-03	80.0	62.21	2.001	0.75	0	3	10
88	8.88E-02	0.001586	4.47E-01	1.46E-02	79.4	62.22	2.003	0.5	3	0	10
88	1.62E-01	0.006297	9.80E-01	1.75E-02	79.5	62.22	2.000	0.5	6	0	10
88	2.18E-01	0.006943	7.12E-01	2.51E-02	79.5	62.22	2.007	0.5	9	0	10
88	2.47E-01	0.010589	1.01E+00	3.30E-02	79.7	62.21	2.001	0.5	12	0	10
88	1.86E-01	0.007005	9.50E-01	1.69E-02	79.8	62.21	2.003	0.5	15	0	10
88	2.01E-01	0.010451	1.39E+00	1.52E-02	79.6	62.22	2.003	0.5	18	0	10
88	1.38E-01	0.00723	8.75E-01	9.91E-03	79.6	62.22	2.001	0.5	21	0	10
88	8.37E-02	0.002859	5.77E-01	6.29E-03	79.6	62.22	1.999	0.5	24	0	10
88	6.00E-02	0.00161	4.88E-01	5.40E-03	79.6	62.22	2.001	0.5	27	0	10
88	4.61E-02	0.000959	2.84E-01	4.86E-03	79.6	62.22	1.999	0.5	30	0	10

TABLE A1. Stress data											
Year	Stress	Variance	Max. stress	Min. stress	Temp.	Unit Wt.	Q	Bw	X	Y	H
	lb/ft^2	(lb/ft^2)^2	lb/ft^2	lb/ft^2	F	lb/ft^3	ft^3/s	ft	in	in	in
88	3.35E-02	0.000582	3.32E-01	2.89E-03	79.6	62.22	1.999	0.5	33	0	10
88	2.34E-02	0.000214	1.52E-01	2.64E-03	79.6	62.22	2.001	0.5	36	0	10
88	2.34E-02	0.000199	1.42E-01	3.04E-03	79.7	62.22	1.999	0.5	39	0	10
88	2.30E-02	0.000191	1.35E-01	2.69E-03	79.7	62.21	2.001	0.5	42	0	10
88	2.15E-02	0.000197	1.38E-01	2.56E-03	79.8	62.21	2.003	0.5	45	0	10
88	1.71E-02	8.79E-05	9.20E-02	3.09E-03	79.8	62.21	2.003	0.5	48	0	10
88	4.82E-02	0.000669	3.13E-01	4.53E-03	80.1	62.21	2.005	0.5	0	3	10
88	8.68E-02	0.001384	4.87E-01	1.37E-02	79.4	62.22	2.005	0.11	3	0	10
88	1.60E-01	0.006005	1.02E+00	1.95E-02	79.5	62.22	2.005	0.11	6	0	10
88	2.36E-01	0.007864	1.14E+00	1.94E-02	79.5	62.22	2.003	0.11	9	0	10
88	2.83E-01	0.010924	1.31E+00	6.50E-02	79.7	62.21	2.007	0.11	12	0	10
88	2.69E-01	0.006342	8.41E-01	8.85E-02	79.8	62.21	2.007	0.11	15	0	10
88	3.65E-01	0.011574	1.04E+00	1.00E-01	79.6	62.22	2.001	0.11	18	0	10
88	3.47E-01	0.010683	9.54E-01	8.54E-02	79.6	62.22	1.999	0.11	21	0	10
88	2.84E-01	0.006926	9.42E-01	6.80E-02	79.6	62.22	1.999	0.11	24	0	10
88	2.61E-01	0.005649	6.57E-01	8.29E-02	79.6	62.22	2.001	0.11	27	0	10
88	2.58E-01	0.005507	8.26E-01	9.85E-02	79.6	62.22	1.999	0.11	30	0	10
88	2.41E-01	0.004472	6.39E-01	8.92E-02	79.6	62.22	2.001	0.11	33	0	10
88	2.25E-01	0.003909	5.76E-01	6.98E-02	79.6	62.22	2.003	0.11	36	0	10
88	2.11E-01	0.00354	5.39E-01	6.83E-02	79.6	62.22	2.001	0.11	39	0	10
88	2.09E-01	0.003428	6.20E-01	7.28E-02	79.7	62.21	2.001	0.11	42	0	10
88	2.00E-01	0.003201	6.52E-01	7.48E-02	79.8	62.21	2.001	0.11	45	0	10
88	1.94E-01	0.002919	5.34E-01	5.84E-02	79.8	62.21	2.001	0.11	48	0	10
88	3.84E-02	0.000431	2.09E-01	5.73E-03	80.1	62.21	2.007	0.11	0	3	10
88	2.92E-03	2.3E-06	1.42E-02	9.09E-04	78.7	62.22	2.987	1.25	3	0	10
88	3.66E-03	2.6E-06	2.28E-02	1.01E-03	78.8	62.22	2.982	1.25	6	0	10
88	5.80E-03	5.4E-06	2.68E-02	1.24E-03	78.9	62.22	2.987	1.25	9	0	10
88	4.59E-03	4.1E-06	1.91E-02	1.21E-03	79.0	62.22	2.987	1.25	12	0	10
88	5.76E-03	8.8E-06	3.04E-02	1.47E-03	78.6	62.23	2.992	1.25	15	0	10
88	7.45E-03	2.68E-05	4.37E-02	1.10E-03	78.6	62.22	2.992	1.25	18	0	10
88	7.99E-03	2.38E-05	5.58E-02	1.92E-03	78.7	62.22	2.987	1.25	21	0	10

TABLE A1. Stress data											
Year	Stress	Variance	Max. stress	Min. stress	Temp.	Unit Wt.	Q	Bw	X	Y	H
	lb/ft^2	(lb/ft^2)^2	lb/ft^2	lb/ft^2	F	lb/ft^3	ft^3/s	ft	in	in	in
88	9.51E-03	3.16E-05	4.06E-02	1.63E-03	78.7	62.22	2.992	1.25	24	0	10
88	1.07E-02	5.08E-05	1.02E-01	1.69E-03	78.8	62.22	2.987	1.25	27	0	10
88	1.22E-02	6.17E-05	1.13E-01	2.24E-03	78.8	62.22	2.987	1.25	30	0	10
88	1.28E-02	4.46E-05	8.39E-02	2.41E-03	78.9	62.22	2.992	1.25	33	0	10
88	1.70E-02	0.000152	1.16E-01	2.60E-03	79.0	62.22	2.992	1.25	36	0	10
88	6.75E-03	2.17E-05	9.95E-02	1.07E-03	79.2	62.22	2.987	1.25	39	0	10
88	5.72E-03	1.26E-05	3.94E-02	1.00E-03	79.2	62.22	2.992	1.25	42	0	10
88	6.71E-03	3.03E-05	8.09E-02	1.10E-03	79.3	62.22	2.992	1.25	45	0	10
88	8.06E-03	2.63E-05	6.41E-02	1.23E-03	79.3	62.22	2.997	1.25	48	0	10
88	3.46E-03	4.2E-06	1.56E-02	4.29E-04	80.2	62.21	2.982	1.25	0	3	10
88	8.20E-03	0.000032	1.00E-01	1.57E-03	78.7	62.22	2.987	1	3	0	10
88	6.25E-03	1.19E-05	2.71E-02	1.58E-03	78.8	62.22	2.987	1	6	0	10
88	1.14E-02	4.95E-05	7.92E-02	1.77E-03	78.9	62.22	2.992	1	9	0	10
88	9.89E-03	4.25E-05	6.26E-02	1.43E-03	79.0	62.22	2.987	1	12	0	10
88	1.76E-02	0.000175	1.51E-01	2.60E-03	78.6	62.23	2.992	1	15	0	10
88	2.91E-02	0.000381	2.23E-01	2.36E-03	78.6	62.22	2.987	1	18	0	10
88	3.08E-02	0.000458	4.05E-01	4.61E-03	78.7	62.22	2.987	1	21	0	10
88	3.65E-02	0.000346	2.33E-01	5.23E-03	78.7	62.22	2.997	1	24	0	10
88	3.72E-02	0.000425	1.93E-01	3.57E-03	78.8	62.22	2.987	1	27	0	10
88	3.89E-02	0.00032	1.91E-01	7.36E-03	78.9	62.22	2.987	1	30	0	10
88	4.12E-02	0.000402	2.55E-01	5.07E-03	78.9	62.22	2.997	1	33	0	10
88	2.89E-02	0.000407	2.76E-01	3.43E-03	79.0	62.22	2.992	1	36	0	10
88	1.30E-02	8.59E-05	1.07E-01	1.84E-03	79.2	62.22	2.992	1	39	0	10
88	7.38E-03	2.99E-05	6.64E-02	1.27E-03	79.3	62.22	2.992	1	42	0	10
88	1.23E-02	0.000104	1.34E-01	1.53E-03	79.3	62.22	2.992	1	45	0	10
88	1.05E-02	7.81E-05	1.36E-01	1.28E-03	79.3	62.22	2.997	1	48	0	10
88	4.97E-03	1.58E-05	3.29E-02	3.74E-04	80.2	62.21	2.982	1	0	3	10
88	4.05E-02	0.000573	2.01E-01	6.04E-03	78.7	62.22	2.987	0.75	3	0	10
88	8.97E-02	0.001292	3.59E-01	1.47E-02	78.8	62.22	2.997	0.75	6	0	10
88	1.17E-01	0.003335	5.69E-01	1.57E-02	78.9	62.22	2.992	0.75	9	0	10
88	1.20E-01	0.002247	4.34E-01	1.71E-02	79.0	62.22	2.992	0.75	12	0	10

TABLE A1. Stress data											
Year	Stress	Variance	Max. stress	Min. stress	Temp.	Unit Wt.	Q	Bw	X	Y	H
	lb/ft^2	(lb/ft^2)^2	lb/ft^2	lb/ft^2	F	lb/ft^3	ft^3/s	ft	in	in	in
88	2.87E-01	0.012322	1.14E+00	5.11E-02	78.6	62.23	2.992	0.75	15	0	10
88	2.77E-01	0.011577	9.16E-01	2.45E-02	78.7	62.22	2.987	0.75	18	0	10
88	2.15E-01	0.006875	8.08E-01	3.26E-02	78.7	62.22	2.992	0.75	21	0	10
88	1.94E-01	0.006088	7.93E-01	2.54E-02	78.7	62.22	2.987	0.75	24	0	10
88	1.71E-01	0.005297	6.79E-01	1.21E-02	78.8	62.22	2.992	0.75	27	0	10
88	1.43E-01	0.004047	5.36E-01	1.81E-02	78.8	62.22	2.987	0.75	30	0	10
88	1.30E-01	0.003518	6.44E-01	1.11E-02	78.9	62.22	2.997	0.75	33	0	10
88	1.12E-01	0.003131	4.21E-01	1.12E-02	79.0	62.22	2.997	0.75	36	0	10
88	5.28E-02	0.000886	3.45E-01	3.45E-03	79.2	62.22	2.987	0.75	39	0	10
88	4.55E-02	0.000713	2.26E-01	2.95E-03	79.3	62.22	2.992	0.75	42	0	10
88	3.72E-02	0.000506	2.48E-01	2.32E-03	79.3	62.22	2.992	0.75	45	0	10
88	3.19E-02	0.000427	1.64E-01	2.65E-03	79.3	62.22	2.997	0.75	48	0	10
88	6.20E-02	0.002033	5.03E-01	3.38E-03	80.2	62.21	2.982	0.75	0	3	10
88	4.55E-02	0.000806	2.81E-01	5.84E-03	78.8	62.22	2.992	0.15	3	0	10
88	1.20E-01	0.002898	7.44E-01	1.89E-02	78.8	62.22	2.987	0.15	6	0	10
88	1.22E-01	0.005806	9.52E-01	1.44E-02	78.9	62.22	2.982	0.15	9	0	10
88	1.85E-01	0.003736	5.93E-01	4.59E-02	79.0	62.22	2.992	0.15	12	0	10
88	4.51E-01	0.019381	1.43E+00	1.22E-01	78.6	62.23	2.992	0.15	15	0	10
88	4.15E-01	0.013428	1.05E+00	1.27E-01	78.6	62.22	2.997	0.15	18	0	10
88	3.46E-01	0.008945	7.79E-01	1.33E-01	78.7	62.22	2.992	0.15	21	0	10
88	3.40E-01	0.008406	9.53E-01	1.19E-01	78.7	62.22	2.987	0.15	24	0	10
88	3.20E-01	0.007629	8.22E-01	1.23E-01	78.8	62.22	2.997	0.15	27	0	10
88	3.16E-01	0.007488	7.33E-01	1.17E-01	78.9	62.22	2.982	0.15	30	0	10
88	3.14E-01	0.00718	8.24E-01	1.03E-01	78.9	62.22	2.992	0.155	33	0	10
88	3.12E-01	0.007255	7.81E-01	1.07E-01	79.0	62.22	3.002	0.15	36	0	10
88	1.76E-01	0.002483	4.84E-01	6.44E-02	79.2	62.22	2.992	0.15	39	0	10
88	1.73E-01	0.002382	4.20E-01	6.20E-02	79.3	62.22	2.992	0.15	42	0	10
88	1.70E-01	0.002405	4.85E-01	4.99E-02	79.3	62.22	2.997	0.15	45	0	10
88	1.69E-01	0.002303	3.99E-01	5.55E-02	79.3	62.22	2.987	0.15	48	0	10
88	8.40E-02	0.002439	5.12E-01	8.93E-03	80.2	62.21	2.987	0.15	0	3	10
88	7.87E-03	2.54E-05	5.87E-02	1.55E-03	78.1	62.23	3.965	1.25	3	0	10

TABLE A1. Stress data											
Year	Stress	Variance	Max. stress	Min. stress	Temp.	Unit Wt.	Q	Bw	X	Y	H
	lb/ft^2	(lb/ft^2)^2	lb/ft^2	lb/ft^2	F	lb/ft^3	ft^3/s	ft	in	in	in
88	5.50E-03	8.1E-06	3.46E-02	1.40E-03	78.5	62.23	3.984	1.25	6	0	10
88	6.22E-03	9.7E-06	3.36E-02	1.59E-03	78.4	62.23	3.988	1.25	9	0	10
88	7.81E-03	2.48E-05	7.31E-02	1.62E-03	78.5	62.23	3.991	1.25	12	0	10
88	7.89E-03	2.58E-05	9.79E-02	1.68E-03	78.5	62.23	3.984	1.25	15	0	10
88	8.92E-03	0.000033	6.19E-02	1.68E-03	78.5	62.23	3.984	1.25	18	0	10
88	1.19E-02	5.25E-05	9.78E-02	2.07E-03	78.5	62.23	3.980	1.25	21	0	10
88	1.44E-02	8.14E-05	8.57E-02	1.80E-03	78.5	62.23	3.980	1.25	24	0	10
88	1.80E-02	0.000143	1.98E-01	2.46E-03	78.6	62.22	3.980	1.25	27	0	10
88	2.17E-02	0.000163	1.65E-01	2.81E-03	78.7	62.22	3.980	1.25	30	0	10
88	1.72E-02	0.000122	1.10E-01	2.86E-03	78.2	62.23	3.984	1.25	33	0	10
88	2.06E-02	0.000115	2.09E-01	3.15E-03	78.3	62.23	3.984	1.25	36	0	10
88	1.62E-02	8.94E-05	1.14E-01	2.32E-03	78.4	62.23	3.980	1.25	39	0	10
88	1.85E-02	0.000127	1.55E-01	1.96E-03	78.4	62.23	3.980	1.25	42	0	10
88	1.75E-02	9.21E-05	9.28E-02	2.77E-03	78.5	62.23	3.980	1.25	45	0	10
88	1.67E-02	0.000118	1.11E-01	2.21E-03	78.6	62.23	3.980	1.25	48	0	10
88	8.14E-03	2.95E-05	1.55E-01	1.15E-03	80.2	62.21	3.987	1.25	0	3	10
88	1.61E-02	0.000139	1.33E-01	2.15E-03	78.4	62.23	3.976	1	3	0	10
88	4.71E-02	0.000549	2.27E-01	4.12E-03	78.5	62.23	3.988	1	6	0	10
88	6.33E-02	0.000819	2.39E-01	7.58E-03	78.4	62.23	3.991	1	9	0	10
88	1.01E-01	0.001873	4.53E-01	1.39E-02	78.4	62.23	3.995	1	12	0	10
88	7.27E-02	0.002516	4.79E-01	8.17E-03	78.4	62.23	3.976	1	15	0	10
88	1.07E-01	0.002116	4.56E-01	1.04E-02	78.4	62.23	3.976	1	18	0	10
88	1.26E-01	0.002202	4.75E-01	3.16E-02	78.4	62.23	3.984	1	21	0	10
88	1.36E-01	0.002456	4.36E-01	2.53E-02	78.5	62.23	3.980	1	24	0	10
88	1.49E-01	0.002779	4.77E-01	3.91E-02	78.6	62.22	3.984	1	27	0	10
88	1.45E-01	0.003074	4.53E-01	2.33E-02	78.7	62.22	3.980	1	30	0	10
88	1.09E-01	0.001642	3.62E-01	1.56E-02	78.2	62.23	3.980	1	33	0	10
88	1.02E-01	0.001389	3.34E-01	1.59E-02	78.3	62.23	3.988	1	36	0	10
88	7.81E-02	0.000955	3.35E-01	1.56E-02	78.4	62.23	3.984	1	39	0	10
88	7.61E-02	0.001008	2.69E-01	8.46E-03	78.4	62.23	3.980	1	42	0	10
88	6.99E-02	0.000789	2.90E-01	1.05E-02	78.5	62.23	3.988	1	45	0	10

TABLE A1. Stress data											
Year	Stress	Variance	Max. stress	Min. stress	Temp.	Unit Wt.	Q	Bw	X	Y	H
	lb/ft^2	(lb/ft^2)^2	lb/ft^2	lb/ft^2	F	lb/ft^3	ft^3/s	ft	in	in	in
88	7.38E-02	0.000875	2.27E-01	9.97E-03	78.6	62.23	3.984	1	48	0	10
88	2.31E-02	0.000481	2.61E-01	1.61E-03	80.2	62.21	3.987	1	0	3	10
88	5.97E-02	0.001113	6.39E-01	6.16E-03	78.4	62.23	3.984	0.75	3	0	10
88	1.12E-01	0.002165	4.16E-01	1.84E-02	78.4	62.23	3.984	0.75	6	0	10
88	1.41E-01	0.004674	6.52E-01	2.02E-02	78.4	62.23	3.991	0.75	9	0	10
88	1.63E-01	0.005017	1.05E+00	2.07E-02	78.4	62.23	3.984	0.75	12	0	10
88	2.41E-01	0.006379	8.29E-01	6.09E-02	78.4	62.23	3.984	0.75	15	0	10
88	2.49E-01	0.00618	6.30E-01	2.07E-02	78.4	62.23	3.984	0.75	18	0	10
88	2.19E-01	0.007926	8.15E-01	1.07E-02	78.5	62.23	3.976	0.75	21	0	10
88	1.55E-01	0.004551	6.57E-01	1.27E-02	77.6	62.23	3.984	0.75	24	0	10
88	1.78E-01	0.007686	7.56E-01	1.10E-02	78.6	62.22	3.984	0.75	27	0	10
88	1.44E-01	0.006033	6.74E-01	9.20E-03	78.7	62.22	3.980	0.75	30	0	10
88	9.88E-02	0.002737	5.81E-01	6.49E-03	78.2	62.23	3.984	0.75	33	0	10
88	8.10E-02	0.002092	3.41E-01	7.15E-03	78.3	62.23	3.980	0.75	36	0	10
88	6.22E-02	0.001239	2.82E-01	6.36E-03	78.4	62.23	3.984	0.75	39	0	10
88	5.23E-02	0.001092	2.55E-01	4.36E-03	78.4	62.23	3.988	0.75	42	0	10
88	4.32E-02	0.000778	2.52E-01	4.02E-03	78.5	62.23	3.980	0.75	45	0	10
88	4.81E-02	0.000739	2.57E-01	5.01E-03	78.6	62.23	3.980	0.75	48	0	10
88	5.21E-02	0.001659	7.97E-01	4.73E-03	80.3	62.21	3.987	0.75	0	3	10
88	5.27E-02	0.000847	2.75E-01	4.53E-03	78.3	62.23	3.988	0.21	3	0	10
88	1.11E-01	0.002166	4.02E-01	1.24E-02	78.5	62.23	3.988	0.21	6	0	10
88	1.49E-01	0.005576	1.23E+00	1.75E-02	78.5	62.23	3.995	0.215	9	0	10
88	2.01E-01	0.006036	1.25E+00	3.02E-02	78.5	62.23	3.984	0.21	12	0	10
88	2.70E-01	0.007932	9.23E-01	9.23E-02	78.4	62.23	3.980	0.21	15	0	10
88	3.08E-01	0.006643	7.90E-01	8.86E-02	78.5	62.23	3.984	0.21	18	0	10
88	2.87E-01	0.005452	6.83E-01	1.05E-01	78.5	62.23	3.980	0.215	21	0	10
88	2.92E-01	0.005657	7.51E-01	1.27E-01	78.5	62.23	3.976	0.21	24	0	10
88	3.07E-01	0.006129	7.76E-01	1.22E-01	78.7	62.22	3.980	0.21	27	0	10
88	2.90E-01	0.005632	6.81E-01	9.14E-02	78.7	62.22	3.984	0.21	30	0	10
88	2.27E-01	0.00322	5.39E-01	9.01E-02	78.3	62.23	3.984	0.21	33	0	10
88	2.19E-01	0.002958	5.18E-01	9.07E-02	78.3	62.23	3.991	0.21	36	0	10

TABLE A1. Stress data											
Year	Stress	Variance	Max. stress	Min. stress	Temp.	Unit Wt.	Q	Bw	X	Y	H
	lb/ft^2	(lb/ft^2)^2	lb/ft^2	lb/ft^2	F	lb/ft^3	ft^3/s	ft	in	in	in
88	1.86E-01	0.002208	4.06E-01	7.43E-02	78.4	62.23	3.980	0.21	39	0	10
88	1.98E-01	0.002604	5.36E-01	7.77E-02	78.4	62.23	3.984	0.21	42	0	10
88	1.93E-01	0.002487	4.80E-01	7.57E-02	78.5	62.23	3.984	0.21	45	0	10
88	2.04E-01	0.002601	4.85E-01	7.52E-02	78.6	62.23	3.980	0.215	48	0	10
88	2.27E-03	8E-07	5.09E-03	9.94E-04	79.1	62.22	1.001	2	3	0	20
88	2.30E-03	9E-07	6.28E-03	8.46E-04	79.2	62.22	1.005	2	6	0	20
88	2.88E-03	6E-07	4.88E-03	1.17E-03	79.2	62.22	1.005	2	9	0	20
88	1.80E-03	2E-07	3.59E-03	8.47E-04	79.3	62.22	1.001	2	12	0	20
88	1.40E-03	2E-07	3.05E-03	6.00E-04	78.2	62.23	0.997	2	15	0	20
88	1.55E-03	4E-07	4.69E-03	5.06E-04	78.1	62.23	1.001	2	18	0	20
88	1.10E-03	1E-07	2.14E-03	5.08E-04	78.0	62.23	0.997	2	21	0	20
88	1.05E-03	1E-07	2.38E-03	4.79E-04	78.0	62.23	1.001	2	24	0	20
88	1.96E-03	4E-07	5.18E-03	8.29E-04	77.6	62.23	1.001	2	27	0	20
88	1.79E-03	5E-07	4.58E-03	6.95E-04	77.6	62.23	1.001	2	30	0	20
88	2.28E-03	9E-07	6.83E-03	9.34E-04	77.5	62.23	1.005	2	33	0	20
88	1.83E-03	7E-07	5.26E-03	5.75E-04	77.5	62.23	1.005	2	36	0	20
88	7.99E-03	2.2E-06	1.42E-02	4.26E-03	78.9	62.22	0.993	2	0	3	20
88	3.48E-03	8E-07	6.70E-03	2.41E-03	79.1	62.22	0.993	2	0	6	20
88	6.32E-03	1.2E-06	1.13E-02	3.77E-03	79.1	62.22	0.993	2	0	9	20
88	4.11E-03	7E-07	6.48E-03	2.21E-03	79.1	62.22	0.997	2	0	12	20
88	5.75E-03	1.44E-05	2.60E-02	9.67E-04	79.2	62.22	1.005	1.75	3	0	20
88	3.73E-03	1.7E-06	1.35E-02	1.10E-03	79.2	62.22	1.005	1.75	6	0	20
88	4.97E-03	4.1E-06	1.84E-02	1.38E-03	79.2	62.22	1.001	1.75	9	0	20
88	3.96E-03	3.3E-06	1.58E-02	9.42E-04	79.3	62.22	1.001	1.75	12	0	20
88	3.11E-03	2.5E-06	1.20E-02	1.02E-03	78.2	62.23	0.997	1.75	15	0	20
88	2.75E-03	2.3E-06	1.39E-02	7.60E-04	78.1	62.23	1.001	1.75	18	0	20
88	2.64E-03	1.8E-06	8.74E-03	6.30E-04	78.1	62.23	0.997	1.75	21	0	20
88	2.06E-03	1.5E-06	1.65E-02	5.93E-04	78.0	62.23	1.001	1.75	24	0	20
88	3.64E-03	0.000003	1.56E-02	1.10E-03	77.6	62.23	1.001	1.75	27	0	20
88	3.77E-03	4.7E-06	2.08E-02	7.21E-04	77.6	62.23	1.005	1.75	30	0	20
88	5.22E-03	0.000005	2.49E-02	1.48E-03	77.5	62.23	1.005	1.75	33	0	20

TABLE A1. Stress data

Year	Stress	Variance	Max. stress	Min. stress	Temp.	Unit Wt.	Q	Bw	X	Y	H
	lb/ft^2	(lb/ft^2)^2	lb/ft^2	lb/ft^2	F	lb/ft^3	ft^3/s	ft	in	in	in
88	3.67E-03	2.7E-06	1.39E-02	1.14E-03	77.5	62.24	1.005	1.75	36	0	20
88	1.65E-02	0.000015	3.07E-02	6.46E-03	78.9	62.22	0.993	1.75	0	3	20
88	1.02E-02	1.44E-05	3.17E-02	3.52E-03	79.0	62.22	0.997	1.75	0	6	20
88	1.35E-02	2.66E-05	4.40E-02	5.04E-03	79.1	62.22	0.993	1.75	0	9	20
88	6.96E-03	4.8E-06	2.01E-02	3.83E-03	79.1	62.22	0.993	1.75	0	12	20
88	1.67E-02	0.000209	1.25E-01	1.67E-03	79.2	62.22	1.001	1.5	3	0	20
88	4.01E-02	0.00036	1.87E-01	4.56E-03	79.2	62.22	1.001	1.5	6	0	20
88	3.06E-02	0.000383	2.27E-01	3.85E-03	79.2	62.22	1.001	1.5	9	0	20
88	3.12E-02	0.000369	2.21E-01	3.05E-03	79.3	62.22	1.001	1.5	12	0	20
88	3.82E-02	0.000364	2.00E-01	3.86E-03	78.2	62.23	0.997	1.5	15	0	20
88	3.56E-02	0.000217	1.40E-01	4.22E-03	78.2	62.23	1.001	1.5	18	0	20
88	3.00E-02	0.00016	1.40E-01	6.33E-03	78.1	62.23	0.997	1.5	21	0	20
88	2.48E-02	0.000127	1.19E-01	3.31E-03	78.0	62.23	1.001	1.5	24	0	20
88	3.37E-02	0.000199	1.33E-01	6.16E-03	77.6	62.23	1.001	1.5	27	0	20
88	3.37E-02	0.000222	1.52E-01	4.33E-03	77.6	62.23	1.005	1.5	30	0	20
88	2.41E-02	0.000122	1.04E-01	2.40E-03	77.5	62.23	1.005	1.5	33	0	20
88	2.17E-02	0.000111	1.01E-01	2.44E-03	77.5	62.23	1.005	1.5	36	0	20
88	6.11E-02	0.000365	1.50E-01	1.21E-02	79.0	62.22	0.997	1.5	0	3	20
88	5.86E-02	0.000371	1.74E-01	1.23E-02	79.1	62.22	0.997	1.5	0	6	20
88	4.38E-02	0.000299	1.42E-01	8.25E-03	79.1	62.22	0.993	1.5	0	9	20
88	1.64E-02	6.74E-05	8.25E-02	4.56E-03	79.1	62.22	0.997	1.5	0	12	20
88	2.30E-02	0.000276	1.56E-01	1.85E-03	79.2	62.22	1.001	1.25	3	0	20
88	3.77E-02	0.000511	3.04E-01	4.35E-03	79.2	62.22	1.001	1.25	6	0	20
88	4.10E-02	0.000706	2.32E-01	4.24E-03	79.2	62.22	1.001	1.25	9	0	20
88	3.73E-02	0.000457	1.95E-01	3.83E-03	79.3	62.22	1.001	1.25	12	0	20
88	2.49E-02	0.000334	2.58E-01	2.73E-03	78.1	62.23	1.001	1.25	15	0	20
88	3.12E-02	0.000304	1.86E-01	3.59E-03	78.2	62.23	1.001	1.25	18	0	20
88	1.24E-02	9.12E-05	9.82E-02	9.45E-04	78.1	62.23	0.997	1.25	21	0	20
88	2.55E-02	0.000252	1.33E-01	2.64E-03	78.0	62.23	1.001	1.25	24	0	20
88	2.25E-02	0.000236	1.29E-01	2.26E-03	77.6	62.23	1.005	1.25	27	0	20
88	1.24E-02	8.41E-05	9.26E-02	1.97E-03	77.6	62.23	1.005	1.25	30	0	20

TABLE A1. Stress data											
Year	Stress	Variance	Max. stress	Min. stress	Temp.	Unit Wt.	Q	Bw	X	Y	H
	lb/ft^2	(lb/ft^2)^2	lb/ft^2	lb/ft^2	F	lb/ft^3	ft^3/s	ft	in	in	in
88	1.57E-02	0.000147	1.59E-01	1.95E-03	77.6	62.23	1.005	1.25	33	0	20
88	1.11E-02	5.47E-05	7.05E-02	1.49E-03	77.5	62.24	1.005	1.25	36	0	20
88	5.64E-02	0.000885	2.16E-01	7.43E-03	79.0	62.22	0.997	1.25	0	3	20
88	4.61E-02	0.000421	2.31E-01	6.55E-03	79.0	62.22	0.993	1.25	0	6	20
88	3.22E-02	0.000386	2.31E-01	6.18E-03	79.0	62.22	0.993	1.25	0	9	20
88	1.78E-02	0.000126	1.37E-01	4.52E-03	79.1	62.22	0.993	1.25	0	12	20
88	1.58E-02	0.000168	1.50E-01	1.94E-03	79.2	62.22	1.005	1	3	0	20
88	3.49E-02	0.000853	3.69E-01	3.64E-03	79.2	62.22	0.997	1	6	0	20
88	5.30E-02	0.001016	3.02E-01	4.97E-03	79.2	62.22	1.005	1	9	0	20
88	4.71E-02	0.000587	2.18E-01	3.76E-03	79.3	62.22	1.001	1	12	0	20
88	2.82E-02	0.000285	1.61E-01	3.82E-03	78.2	62.23	0.997	1	15	0	20
88	1.81E-02	0.000171	1.05E-01	2.05E-03	78.1	62.23	1.001	1	18	0	20
88	1.02E-02	5.95E-05	1.72E-01	1.35E-03	78.1	62.23	1.001	1	21	0	20
88	8.64E-03	5.65E-05	6.91E-02	1.09E-03	78.0	62.23	1.001	1	24	0	20
88	9.61E-03	5.15E-05	1.48E-01	1.25E-03	77.6	62.23	1.005	1	27	0	20
88	5.10E-03	1.55E-05	4.78E-02	1.20E-03	77.6	62.23	1.005	1	30	0	20
88	5.21E-03	0.000019	5.07E-02	1.01E-03	77.5	62.23	1.005	1	33	0	20
88	6.20E-03	1.58E-05	3.93E-02	1.29E-03	77.5	62.24	1.005	1	36	0	20
88	2.88E-02	0.000206	1.11E-01	8.35E-03	79.0	62.22	0.997	1	0	3	20
88	1.43E-02	5.27E-05	1.76E-01	5.59E-03	79.1	62.22	0.993	1	0	6	20
88	1.98E-02	0.000152	2.63E-01	5.71E-03	79.0	62.22	0.993	1	0	9	20
88	5.55E-02	0.000752	2.78E-01	5.20E-03	79.2	62.22	1.005	0.75	3	0	20
88	9.43E-02	0.002319	5.53E-01	1.05E-02	79.2	62.22	1.001	0.75	6	0	20
88	1.16E-01	0.005212	6.78E-01	1.01E-02	79.2	62.22	1.001	0.75	9	0	20
88	1.07E-01	0.002162	6.24E-01	1.67E-02	79.3	62.22	1.001	0.75	12	0	20
88	1.01E-01	0.001964	4.90E-01	1.18E-02	78.1	62.23	0.997	0.75	15	0	20
88	6.67E-02	0.001214	3.46E-01	5.68E-03	78.1	62.23	1.001	0.75	18	0	20
88	3.80E-02	0.000403	1.86E-01	4.13E-03	78.1	62.23	1.001	0.75	21	0	20
88	1.82E-02	0.000191	1.27E-01	1.65E-03	78.0	62.23	1.001	0.75	24	0	20
88	2.13E-02	0.000394	1.83E-01	1.28E-03	77.6	62.23	1.005	0.75	27	0	20
88	1.31E-02	0.000175	1.97E-01	1.85E-03	77.6	62.23	1.005	0.75	30	0	20

TABLE A1. Stress data

Year	Stress	Variance	Max. stress	Min. stress	Temp.	Unit Wt.	Q	Bw	X	Y	H
	lb/ft^2	(lb/ft^2)^2	lb/ft^2	lb/ft^2	F	lb/ft^3	ft^3/s	ft	in	in	in
88	5.07E-03	1.69E-05	6.03E-02	1.20E-03	77.5	62.23	1.005	0.75	33	0	20
88	4.03E-03	9.1E-06	3.25E-02	7.79E-04	77.5	62.23	1.005	0.75	36	0	20
88	7.55E-02	0.000849	2.25E-01	1.37E-02	79.0	62.22	0.997	0.75	0	3	20
88	3.46E-02	0.000398	2.45E-01	7.09E-03	79.1	62.22	0.993	0.75	0	6	20
88	3.77E-02	0.000684	2.30E-01	4.41E-03	79.2	62.22	0.997	0.5	3	0	20
88	1.36E-01	0.003863	5.12E-01	1.57E-02	79.2	62.22	1.001	0.5	6	0	20
88	2.49E-01	0.023548	1.76E+00	2.24E-02	79.2	62.22	1.001	0.5	9	0	20
88	2.24E-01	0.010301	1.03E+00	2.91E-02	79.3	62.22	1.001	0.5	12	0	20
88	1.76E-01	0.005828	7.29E-01	1.64E-02	78.1	62.23	0.997	0.5	15	0	20
88	1.01E-01	0.002378	4.80E-01	6.32E-03	78.2	62.23	1.001	0.5	18	0	20
88	5.15E-02	0.001085	3.12E-01	4.19E-03	78.1	62.23	1.001	0.5	21	0	20
88	2.59E-02	0.000336	1.92E-01	3.05E-03	78.0	62.23	1.001	0.5	24	0	20
88	2.68E-02	0.000421	2.07E-01	2.55E-03	77.6	62.23	1.001	0.5	27	0	20
88	8.59E-03	8.73E-05	1.23E-01	1.47E-03	77.6	62.23	1.005	0.5	30	0	20
88	7.95E-03	9.75E-05	1.09E-01	9.11E-04	77.5	62.23	1.005	0.5	33	0	20
88	7.31E-03	3.09E-05	7.08E-02	1.28E-03	77.5	62.23	1.005	0.5	36	0	20
88	6.13E-02	0.000842	2.52E-01	1.12E-02	79.0	62.22	0.997	0.5	0	3	20
88	2.02E-02	0.000241	1.77E-01	2.85E-03	79.2	62.22	1.001	0.15	3	0	20
88	1.18E-01	0.003597	6.88E-01	1.20E-02	79.2	62.22	1.001	0.15	6	0	20
88	4.12E-01	0.053227	1.95E+00	3.51E-02	79.3	62.22	1.001	0.15	9	0	20
88	3.77E-01	0.022015	1.49E+00	4.20E-02	79.3	62.22	1.001	0.15	12	0	20
88	3.88E-01	0.018302	1.04E+00	4.78E-02	78.1	62.23	1.001	0.075	15	0	20
88	2.63E-01	0.007593	7.99E-01	5.24E-02	78.1	62.23	1.001	0.075	18	0	20
88	1.90E-01	0.004218	5.76E-01	3.68E-02	78.0	62.23	0.997	0.075	21	0	20
88	1.73E-01	0.003467	5.99E-01	3.63E-02	78.0	62.23	1.001	0.075	24	0	20
88	2.10E-01	0.004807	6.35E-01	5.18E-02	77.6	62.23	1.001	0.075	27	0	20
88	2.16E-01	0.004589	6.58E-01	5.46E-02	77.5	62.23	1.005	0.075	30	0	20
88	1.77E-01	0.00292	5.50E-01	5.29E-02	77.5	62.24	1.005	0.075	36	0	20
88	4.31E-02	0.000621	2.80E-01	9.11E-03	79.0	62.22	0.997	0.075	0	3	20
88	3.22E-03	3.4E-06	1.58E-02	5.35E-04	77.0	62.24	2.002	2	3	0	20
88	2.00E-03	8E-07	5.88E-03	5.39E-04	77.1	62.24	2.002	2	6	0	20

TABLE A1. Stress data

Year	Stress	Variance	Max. stress	Min. stress	Temp.	Unit Wt.	Q	Bw	X	Y	H
	lb/ft^2	(lb/ft^2)^2	lb/ft^2	lb/ft^2	F	lb/ft^3	ft^3/s	ft	in	in	in
88	4.44E-03	3.3E-06	1.49E-02	9.92E-04	77.3	62.24	1.998	2	9	0	20
88	2.81E-03	2.4E-06	1.42E-02	7.22E-04	77.5	62.24	2.004	2	12	0	20
88	3.39E-03	2.5E-06	1.66E-02	8.79E-04	77.6	62.23	2.006	2	15	0	20
88	2.86E-03	2.4E-06	1.19E-02	8.03E-04	77.7	62.23	2.000	2	18	0	20
88	3.51E-03	3.3E-06	2.56E-02	9.68E-04	77.8	62.23	2.006	2	21	0	20
88	2.92E-03	2.5E-06	1.72E-02	7.74E-04	77.9	62.23	2.002	2	24	0	20
88	3.37E-03	3.1E-06	1.79E-02	6.54E-04	77.9	62.23	2.002	2	27	0	20
88	2.42E-03	1.4E-06	9.40E-03	5.53E-04	78.0	62.23	2.000	2	30	0	20
88	3.22E-03	3.4E-06	1.95E-02	8.93E-04	78.0	62.23	1.998	2	33	0	20
88	3.06E-03	2.3E-06	1.27E-02	7.95E-04	78.1	62.23	2.002	2	36	0	20
88	1.86E-03	1.7E-06	9.72E-03	3.71E-04	77.1	62.24	2.000	2	39	0	20
88	3.01E-03	2.5E-06	1.35E-02	5.85E-04	77.3	62.24	2.004	2	42	0	20
88	4.00E-03	4.1E-06	2.07E-02	7.37E-04	77.4	62.24	2.000	2	45	0	20
88	3.93E-03	3.9E-06	1.75E-02	7.69E-04	77.5	62.24	2.002	2	48	0	20
88	1.33E-02	2.19E-05	3.06E-02	5.34E-03	77.6	62.23	2.004	2	0	3	20
88	9.29E-03	1.37E-05	2.57E-02	3.61E-03	77.7	62.23	2.002	2	0	6	20
88	8.70E-03	8.5E-06	2.15E-02	2.88E-03	78.0	62.23	2.000	2	0	9	20
88	8.53E-03	0.00001	3.48E-02	2.43E-03	78.2	62.23	2.000	2	0	12	20
88	6.77E-03	1.54E-05	4.84E-02	1.07E-03	77.0	62.24	2.002	1.75	3	0	20
88	4.23E-03	6.7E-06	2.06E-02	7.40E-04	77.1	62.24	2.002	1.75	6	0	20
88	4.83E-03	0.000006	4.54E-02	9.40E-04	77.3	62.24	2.002	1.75	9	0	20
88	3.89E-03	6.1E-06	1.92E-02	7.27E-04	77.5	62.24	2.002	1.75	12	0	20
88	2.95E-03	3.8E-06	2.34E-02	5.64E-04	77.6	62.23	1.994	1.75	15	0	20
88	3.79E-03	5.5E-06	4.02E-02	1.01E-03	77.7	62.23	2.002	1.75	18	0	20
88	5.40E-03	7.6E-06	2.77E-02	1.26E-03	77.8	62.23	2.004	1.75	21	0	20
88	5.34E-03	1.26E-05	4.05E-02	9.99E-04	77.9	62.23	2.002	1.75	24	0	20
88	3.65E-03	5.4E-06	5.36E-02	6.75E-04	77.9	62.23	2.004	1.75	27	0	20
88	3.33E-03	3.8E-06	2.82E-02	8.51E-04	77.9	62.23	2.000	1.75	30	0	20
88	4.98E-03	1.07E-05	3.42E-02	1.08E-03	78.0	62.23	1.998	1.75	33	0	20
88	4.94E-03	7.2E-06	2.58E-02	9.74E-04	78.1	62.23	2.000	1.75	36	0	20
88	4.06E-03	6.1E-06	1.81E-02	4.64E-04	77.1	62.24	1.996	1.75	39	0	20

TABLE A1. Stress data

Year	Stress	Variance	Max. stress	Min. stress	Temp.	Unit Wt.	Q	Bw	X	Y	H
	lb/ft^2	(lb/ft^2)^2	lb/ft^2	lb/ft^2	F	lb/ft^3	ft^3/s	ft	in	in	in
88	5.22E-03	1.39E-05	3.63E-02	8.32E-04	77.3	62.24	2.006	1.75	42	0	20
88	7.01E-03	1.15E-05	3.03E-02	1.45E-03	77.4	62.24	2.006	1.75	45	0	20
88	6.95E-03	1.37E-05	4.70E-02	9.70E-04	77.4	62.24	2.004	1.75	48	0	20
88	2.69E-02	0.000184	8.32E-02	6.29E-03	77.6	62.23	2.004	1.75	0	3	20
88	1.65E-02	5.92E-05	8.88E-02	5.33E-03	77.7	62.23	2.004	1.75	0	6	20
88	1.36E-02	2.29E-05	3.85E-02	4.21E-03	78.1	62.23	1.998	1.75	0	9	20
88	8.83E-03	9.4E-06	2.69E-02	3.72E-03	78.2	62.23	2.000	1.75	0	12	20
88	6.41E-02	0.001327	4.08E-01	4.51E-03	77.0	62.24	2.002	1.5	3	0	20
88	7.24E-02	0.001387	4.18E-01	7.95E-03	77.1	62.24	2.004	1.5	6	0	20
88	8.05E-02	0.001539	4.31E-01	5.42E-03	77.3	62.24	2.002	1.5	9	0	20
88	6.94E-02	0.001814	4.61E-01	6.06E-03	77.5	62.24	2.002	1.5	12	0	20
88	8.59E-02	0.001899	3.91E-01	7.57E-03	77.6	62.23	1.992	1.5	15	0	20
88	9.29E-02	0.001618	3.54E-01	1.34E-02	77.7	62.23	2.000	1.5	18	0	20
88	8.56E-02	0.00172	3.82E-01	4.64E-03	77.8	62.23	2.006	1.5	21	0	20
88	7.45E-02	0.001066	2.60E-01	5.16E-03	77.9	62.23	2.002	1.5	24	0	20
88	5.65E-02	0.000696	2.24E-01	3.66E-03	77.9	62.23	2.004	1.5	27	0	20
88	5.62E-02	0.000848	2.18E-01	2.22E-03	77.9	62.23	1.998	1.5	30	0	20
88	3.61E-02	0.000343	2.03E-01	4.29E-03	78.0	62.23	1.998	1.5	33	0	20
88	3.23E-02	0.000318	1.63E-01	3.50E-03	78.1	62.23	2.000	1.5	36	0	20
88	1.84E-02	0.000131	1.09E-01	1.57E-03	77.1	62.24	1.998	1.5	39	0	20
88	1.78E-02	0.000125	9.73E-02	1.15E-03	77.3	62.24	2.002	1.5	42	0	20
88	2.11E-02	0.000162	1.20E-01	1.69E-03	77.4	62.24	2.002	1.5	45	0	20
88	1.48E-02	8.03E-05	9.27E-02	1.43E-03	77.5	62.24	2.002	1.5	48	0	20
88	7.89E-02	0.000755	2.50E-01	9.75E-03	77.6	62.23	2.002	1.5	0	3	20
88	7.68E-02	0.000815	2.94E-01	1.55E-02	77.8	62.23	2.002	1.5	0	6	20
88	5.27E-02	0.000566	2.46E-01	8.36E-03	78.1	62.23	1.998	1.5	0	9	20
88	3.13E-02	0.000223	1.34E-01	6.83E-03	78.2	62.23	2.002	1.5	0	12	20
88	7.23E-02	0.002029	4.81E-01	5.32E-03	77.0	62.24	2.002	1.25	3	0	20
88	1.15E-01	0.002422	5.82E-01	1.98E-02	77.1	62.24	2.002	1.25	6	0	20
88	1.02E-01	0.003872	6.28E-01	1.04E-02	77.3	62.24	2.002	1.25	9	0	20
88	1.18E-01	0.003936	6.06E-01	7.56E-03	77.5	62.24	2.002	1.25	12	0	20

TABLE A1. Stress data											
Year	Stress	Variance	Max. stress	Min. stress	Temp.	Unit Wt.	Q	Bw	X	Y	H
	lb/ft^2	(lb/ft^2)^2	lb/ft^2	lb/ft^2	F	lb/ft^3	ft^3/s	ft	in	in	in
88	1.38E-01	0.003115	5.28E-01	2.75E-02	77.6	62.23	1.992	1.25	15	0	20
88	1.25E-01	0.002474	4.85E-01	1.75E-02	77.7	62.23	2.000	1.25	18	0	20
88	1.14E-01	0.002047	4.02E-01	1.29E-02	77.8	62.23	2.004	1.25	21	0	20
88	9.90E-02	0.00131	3.05E-01	1.08E-02	77.9	62.23	2.004	1.25	24	0	20
88	7.83E-02	0.001008	2.71E-01	1.61E-02	77.9	62.23	2.004	1.25	27	0	20
88	6.46E-02	0.000762	2.27E-01	7.30E-03	77.9	62.23	2.000	1.25	30	0	20
88	5.37E-02	0.000578	2.24E-01	3.12E-03	78.0	62.23	1.998	1.25	33	0	20
88	4.77E-02	0.000465	2.20E-01	7.03E-03	78.1	62.23	2.000	1.25	36	0	20
88	3.29E-02	0.000288	1.86E-01	3.46E-03	77.2	62.24	2.002	1.25	39	0	20
88	3.60E-02	0.000386	1.85E-01	2.67E-03	77.3	62.24	2.002	1.25	42	0	20
88	3.17E-02	0.000415	1.81E-01	2.92E-03	77.4	62.24	2.002	1.25	45	0	20
88	2.01E-02	0.000176	1.37E-01	1.65E-03	77.5	62.24	2.006	1.25	48	0	20
88	1.12E-01	0.000846	3.45E-01	2.89E-02	77.6	62.23	2.004	1.25	0	3	20
88	1.03E-01	0.001069	3.47E-01	2.72E-02	77.8	62.23	2.002	1.25	0	6	20
88	4.71E-02	0.000527	2.94E-01	9.64E-03	78.1	62.23	2.000	1.25	0	9	20
88	2.91E-02	0.000284	2.17E-01	7.16E-03	78.2	62.23	2.002	1.25	0	12	20
88	8.86E-02	0.002822	4.50E-01	6.69E-03	77.0	62.24	2.002	1	3	0	20
88	1.43E-01	0.004253	9.12E-01	1.32E-02	77.1	62.24	2.002	1	6	0	20
88	1.27E-01	0.007748	8.06E-01	1.01E-02	77.4	62.24	2.004	1	9	0	20
88	1.84E-01	0.008924	8.89E-01	1.88E-02	77.5	62.23	2.000	1	12	0	20
88	1.95E-01	0.007258	9.84E-01	1.46E-02	77.6	62.23	1.996	1	15	0	20
88	1.51E-01	0.00419	5.19E-01	1.90E-02	77.7	62.23	2.002	1	18	0	20
88	1.32E-01	0.003566	4.63E-01	8.72E-03	77.8	62.23	2.002	1	21	0	20
88	1.05E-01	0.002428	4.24E-01	8.23E-03	77.9	62.23	2.006	1	24	0	20
88	7.58E-02	0.001707	3.37E-01	6.47E-03	77.9	62.23	2.004	1	27	0	20
88	6.05E-02	0.001523	3.22E-01	4.93E-03	78.0	62.23	2.000	1	30	0	20
88	4.26E-02	0.000807	4.11E-01	3.62E-03	78.0	62.23	1.996	1	33	0	20
88	2.69E-02	0.000418	1.89E-01	1.79E-03	78.1	62.23	2.000	1	36	0	20
88	1.83E-02	0.000302	1.97E-01	1.41E-03	77.2	62.24	2.002	1	39	0	20
88	9.39E-03	8.11E-05	1.22E-01	7.72E-04	77.3	62.24	2.002	1	42	0	20
88	9.17E-03	9.42E-05	1.17E-01	9.92E-04	77.4	62.24	2.002	1	45	0	20

TABLE A1. Stress data

Year	Stress	Variance	Max. stress	Min. stress	Temp.	Unit Wt.	Q	Bw	X	Y	H
	lb/ft^2	(lb/ft^2)^2	lb/ft^2	lb/ft^2	F	lb/ft^3	ft^3/s	ft	in	in	in
88	9.21E-03	6.94E-05	1.15E-01	1.18E-03	77.4	62.24	2.006	1	48	0	20
88	1.09E-01	0.001008	3.09E-01	2.15E-02	77.6	62.23	2.006	1	0	3	20
88	8.44E-02	0.000875	2.77E-01	2.17E-02	77.8	62.23	2.002	1	0	6	20
88	3.27E-02	0.00031	1.81E-01	7.58E-03	78.1	62.23	1.998	1	0	9	20
88	2.83E-02	0.000209	1.83E-01	5.33E-03	78.2	62.23	2.000	1	0	12	20
88	6.53E-02	0.001556	3.98E-01	6.74E-03	77.0	62.24	2.002	0.75	3	0	20
88	1.48E-01	0.004341	5.70E-01	1.33E-02	77.2	62.24	2.002	0.75	6	0	20
88	2.56E-01	0.019028	1.43E+00	2.21E-02	77.4	62.24	2.002	0.75	9	0	20
88	2.95E-01	0.027306	2.05E+00	1.43E-02	77.5	62.24	2.000	0.75	12	0	20
88	3.21E-01	0.017601	1.37E+00	6.01E-02	77.6	62.23	2.000	0.75	15	0	20
88	2.64E-01	0.010787	1.18E+00	4.12E-02	77.7	62.23	2.002	0.75	18	0	20
88	2.16E-01	0.007081	7.14E-01	2.50E-02	77.8	62.23	2.004	0.75	21	0	20
88	1.55E-01	0.004303	5.99E-01	9.41E-03	77.9	62.23	2.002	0.75	24	0	20
88	1.07E-01	0.002909	4.75E-01	7.83E-03	77.9	62.23	2.004	0.75	27	0	20
88	7.99E-02	0.001752	3.93E-01	6.68E-03	78.0	62.23	2.000	0.75	30	0	20
88	6.16E-02	0.001297	3.29E-01	3.53E-03	78.0	62.23	2.000	0.75	33	0	20
88	4.80E-02	0.001028	3.20E-01	2.12E-03	78.1	62.23	2.004	0.75	36	0	20
88	2.67E-02	0.000396	2.17E-01	2.19E-03	77.2	62.24	2.002	0.75	39	0	20
88	1.92E-02	0.000258	2.22E-01	1.84E-03	77.3	62.24	2.002	0.75	42	0	20
88	1.84E-02	0.000215	2.33E-01	1.28E-03	77.4	62.24	2.002	0.75	45	0	20
88	1.17E-02	0.000107	1.30E-01	1.02E-03	77.4	62.24	2.002	0.75	48	0	20
88	9.97E-02	0.001086	3.65E-01	1.63E-02	77.7	62.23	2.006	0.75	0	3	20
88	4.83E-02	0.000659	2.44E-01	8.95E-03	77.8	62.23	2.002	0.75	0	6	20
88	4.65E-02	0.001279	3.74E-01	3.86E-03	77.0	62.24	2.002	0.125	3	0	20
88	1.04E-01	0.003411	7.37E-01	7.81E-03	77.2	62.24	2.002	0.115	6	0	20
88	2.85E-01	0.022736	1.88E+00	2.17E-02	77.4	62.24	2.000	0.12	9	0	20
88	4.27E-01	0.071468	2.86E+00	2.42E-02	77.5	62.23	2.002	0.12	12	0	20
88	5.61E-01	0.062606	2.36E+00	1.05E-01	77.6	62.23	2.000	0.125	15	0	20
88	5.10E-01	0.027768	1.56E+00	1.05E-01	77.7	62.23	2.000	0.125	18	0	20
88	4.54E-01	0.019322	1.26E+00	1.15E-01	77.8	62.23	2.002	0.125	21	0	20
88	3.54E-01	0.012196	9.61E-01	1.04E-01	78.0	62.23	2.004	0.125	24	0	20

TABLE A1. Stress data

Year	Stress	Variance	Max. stress	Min. stress	Temp.	Unit Wt.	Q	Bw	X	Y	H
	lb/ft^2	(lb/ft^2)^2	lb/ft^2	lb/ft^2	F	lb/ft^3	ft^3/s	ft	in	in	in
88	2.94E-01	0.00803	8.16E-01	8.08E-02	77.9	62.23	2.002	0.12	27	0	20
88	2.61E-01	0.006884	8.38E-01	6.73E-02	78.0	62.23	2.000	0.12	30	0	20
88	2.28E-01	0.004923	6.66E-01	3.26E-02	78.0	62.23	2.000	0.12	33	0	20
88	2.39E-01	0.005028	6.67E-01	6.94E-02	78.1	62.23	2.004	0.12	36	0	20
88	1.95E-01	0.003445	5.43E-01	4.42E-02	77.2	62.24	2.002	0.12	39	0	20
88	2.01E-01	0.00365	5.35E-01	6.11E-02	77.3	62.24	2.002	0.12	42	0	20
88	2.03E-01	0.003555	5.95E-01	6.58E-02	77.4	62.24	2.002	0.12	45	0	20
88	1.96E-01	0.003234	5.67E-01	6.28E-02	77.5	62.23	2.002	0.125	48	0	20
88	4.08E-02	0.000561	2.22E-01	8.28E-03	77.7	62.23	2.002	0.12	0	3	20
88	7.60E-03	2.79E-05	4.38E-02	1.05E-03	75.8	62.25	3.002	2	3	0	20
88	3.64E-03	4.8E-06	3.08E-02	6.60E-04	75.0	62.26	2.988	2	6	0	20
88	1.04E-02	3.89E-05	7.39E-02	1.24E-03	76.2	62.25	2.983	2	9	0	20
88	5.82E-03	1.54E-05	2.84E-02	1.15E-03	76.4	62.24	2.983	2	12	0	20
88	3.55E-03	0.000008	2.10E-02	5.68E-04	76.9	62.24	2.988	2	15	0	20
88	4.39E-03	8.6E-06	4.52E-02	6.97E-04	77.0	62.24	2.988	2	18	0	20
88	4.33E-03	5.8E-06	1.93E-02	5.84E-04	77.1	62.24	2.988	2	21	0	20
88	6.33E-03	1.11E-05	3.22E-02	1.11E-03	77.2	62.24	2.988	2	24	0	20
88	4.91E-03	8.2E-06	3.42E-02	9.77E-04	77.3	62.24	2.992	2	27	0	20
88	7.02E-03	1.33E-05	4.46E-02	1.22E-03	77.4	62.24	2.978	2	30	0	20
88	7.08E-03	1.44E-05	3.17E-02	9.21E-04	77.5	62.24	2.987	2	33	0	20
88	7.33E-03	2.08E-05	6.20E-02	1.16E-03	77.6	62.23	2.987	2	36	0	20
88	1.36E-02	6.36E-05	8.14E-02	1.36E-03	75.9	62.25	2.988	1.75	3	0	20
88	4.72E-03	1.35E-05	3.37E-02	6.63E-04	76.0	62.25	2.985	1.75	6	0	20
88	1.27E-02	3.71E-05	6.38E-02	1.63E-03	76.2	62.25	2.983	1.75	9	0	20
88	8.87E-03	3.35E-05	5.00E-02	1.33E-03	76.4	62.24	2.978	1.75	12	0	20
88	6.38E-03	2.02E-05	6.61E-02	6.84E-04	76.9	62.24	2.988	1.75	15	0	20
88	7.61E-03	2.89E-05	1.20E-01	7.08E-04	77.0	62.24	2.988	1.75	18	0	20
88	7.06E-03	2.25E-05	7.23E-02	8.77E-04	77.1	62.24	2.988	1.75	21	0	20
88	9.31E-03	2.51E-05	5.26E-02	1.40E-03	77.1	62.24	2.983	1.75	24	0	20
88	8.62E-03	3.65E-05	8.54E-02	1.10E-03	77.3	62.24	2.992	1.75	27	0	20
88	1.27E-02	3.76E-05	5.68E-02	1.54E-03	77.4	62.24	2.978	1.75	30	0	20

TABLE A1. Stress data											
Year	Stress	Variance	Max. stress	Min. stress	Temp.	Unit Wt.	Q	Bw	X	Y	H
	lb/ft^2	(lb/ft^2)^2	lb/ft^2	lb/ft^2	F	lb/ft^3	ft^3/s	ft	in	in	in
88	1.45E-02	5.07E-05	6.86E-02	1.77E-03	77.5	62.23	2.997	1.75	33	0	20
88	1.31E-02	4.77E-05	6.42E-02	2.26E-03	77.6	62.23	2.982	1.75	36	0	20
88	8.10E-02	0.002501	4.82E-01	5.64E-03	75.9	62.25	2.988	1.5	3	0	20
88	1.15E-01	0.003204	5.79E-01	8.47E-03	76.0	62.25	2.988	1.5	6	0	20
88	1.31E-01	0.005083	9.32E-01	8.91E-03	76.2	62.25	2.983	1.5	9	0	20
88	1.13E-01	0.006961	9.20E-01	6.49E-03	76.4	62.24	2.988	1.5	12	0	20
88	9.15E-02	0.004137	5.18E-01	5.88E-03	76.9	62.24	2.983	1.5	15	0	20
88	1.29E-01	0.003696	5.88E-01	7.61E-03	77.0	62.24	2.983	1.5	18	0	20
88	1.32E-01	0.003099	5.56E-01	2.62E-02	77.0	62.24	2.988	1.5	21	0	20
88	1.28E-01	0.002821	4.33E-01	1.13E-02	77.1	62.24	2.983	1.5	24	0	20
88	1.38E-01	0.002946	4.60E-01	2.20E-02	77.4	62.24	2.990	1.5	27	0	20
88	1.18E-01	0.002299	4.76E-01	1.73E-02	77.4	62.24	2.987	1.5	30	0	20
88	1.05E-01	0.001822	4.57E-01	1.37E-02	77.5	62.23	2.992	1.5	33	0	20
88	1.05E-01	0.002215	5.52E-01	3.04E-03	77.6	62.23	2.982	1.5	36	0	20
88	1.12E-01	0.003897	7.14E-01	8.15E-03	75.9	62.25	2.983	1.25	3	0	20
88	1.88E-01	0.005964	7.68E-01	2.29E-02	76.0	62.25	2.988	1.25	6	0	20
88	1.70E-01	0.010465	1.12E+00	1.38E-02	76.3	62.25	2.988	1.25	9	0	20
88	2.07E-01	0.01555	1.59E+00	1.40E-02	76.4	62.24	2.983	1.25	12	0	20
88	2.20E-01	0.009199	8.46E-01	2.57E-02	76.9	62.24	2.983	1.25	15	0	20
88	2.09E-01	0.006517	7.27E-01	3.79E-02	77.0	62.24	2.988	1.25	18	0	20
88	1.87E-01	0.004884	6.58E-01	4.34E-02	77.1	62.24	2.992	1.25	21	0	20
88	1.79E-01	0.004012	7.84E-01	4.42E-02	77.1	62.24	2.983	1.25	24	0	20
88	1.76E-01	0.003409	5.68E-01	4.54E-02	77.3	62.24	2.990	1.25	27	0	20
88	1.59E-01	0.002806	6.50E-01	2.71E-02	77.4	62.24	2.987	1.25	30	0	20
88	1.46E-01	0.002557	4.47E-01	2.81E-02	77.5	62.23	2.983	1.25	33	0	20
88	1.39E-01	0.002457	6.12E-01	3.35E-02	77.6	62.23	2.992	1.25	36	0	20
88	1.03E-01	0.003988	7.07E-01	9.96E-03	75.9	62.25	2.985	1	3	0	20
88	2.15E-01	0.008652	8.19E-01	3.15E-02	76.1	62.25	2.988	1	6	0	20
88	2.63E-01	0.016996	1.25E+00	2.53E-02	76.3	62.25	2.988	1	9	0	20
88	2.57E-01	0.033274	2.04E+00	1.29E-02	76.4	62.24	2.988	1	12	0	20
88	3.19E-01	0.019372	1.33E+00	4.33E-02	77.0	62.24	2.983	1	15	0	20

TABLE A1. Stress data											
Year	Stress	Variance	Max. stress	Min. stress	Temp.	Unit Wt.	Q	Bw	X	Y	H
	lb/ft^2	(lb/ft^2)^2	lb/ft^2	lb/ft^2	F	lb/ft^3	ft^3/s	ft	in	in	in
88	3.00E-01	0.014692	1.14E+00	5.49E-02	77.0	62.24	2.988	1	18	0	20
88	2.70E-01	0.011009	1.07E+00	4.94E-02	77.1	62.24	2.988	1	21	0	20
88	2.43E-01	0.008826	1.01E+00	2.67E-02	77.2	62.24	2.985	1	24	0	20
88	2.36E-01	0.008201	7.88E-01	2.14E-02	77.3	62.24	2.987	1	27	0	20
88	1.97E-01	0.006362	7.04E-01	1.61E-02	77.4	62.24	2.978	1	30	0	20
88	1.55E-01	0.005378	6.43E-01	1.11E-02	77.5	62.23	2.987	1	33	0	20
88	1.36E-01	0.00543	5.70E-01	9.45E-03	77.7	62.23	2.992	1	36	0	20
88	1.53E-02	0.000155	1.87E-01	1.21E-03	72.5	62.28	2.983	0.165	3	0	20
88	1.36E-01	0.004752	8.26E-01	1.38E-02	76.1	62.25	2.988	0.175	6	0	20
88	2.05E-01	0.010236	1.34E+00	1.42E-02	76.3	62.25	2.978	0.175	9	0	20
88	4.33E-01	0.056377	2.50E+00	2.53E-02	76.4	62.24	2.985	0.16	12	0	20
88	5.20E-01	0.056839	2.16E+00	5.64E-02	76.9	62.24	2.988	0.17	15	0	20
88	5.50E-01	0.046954	2.21E+00	1.33E-01	77.0	62.24	2.983	0.16	18	0	20
88	5.47E-01	0.028007	1.52E+00	1.40E-01	77.1	62.24	2.988	0.165	21	0	20
88	5.18E-01	0.021734	1.39E+00	1.80E-01	77.1	62.24	2.992	0.16	24	0	20
88	5.20E-01	0.017069	1.24E+00	2.06E-01	77.3	62.24	2.990	0.16	27	0	20
88	4.77E-01	0.014815	1.08E+00	1.74E-01	77.5	62.24	2.987	0.16	30	0	20
88	4.44E-01	0.013631	1.13E+00	1.44E-01	77.6	62.23	2.985	0.16	33	0	20
88	4.31E-01	0.012587	1.11E+00	1.57E-01	77.7	62.23	2.997	0.16	36	0	20
88	6.80E-03	2.87E-05	7.08E-02	9.35E-04	74.0	62.26	3.985	2	15	0	20
88	5.71E-03	2.76E-05	7.40E-02	9.38E-04	74.2	62.26	3.974	2	18	0	20
88	6.15E-03	1.47E-05	3.91E-02	9.58E-04	74.3	62.26	3.985	2	21	0	20
88	6.12E-03	2.03E-05	5.21E-02	1.03E-03	74.5	62.26	3.985	2	24	0	20
88	4.82E-03	1.94E-05	7.87E-02	3.87E-04	72.7	62.28	3.989	2	0	3	20
88	9.61E-03	0.000089	8.66E-02	5.43E-04	72.6	62.28	3.985	2	0	6	20
88	5.16E-03	0.000013	3.06E-02	4.47E-04	72.5	62.28	3.985	2	0	9	20
88	4.02E-03	1.39E-05	5.09E-02	3.13E-04	72.3	62.28	3.992	2	0	12	20
88	1.05E-02	6.28E-05	9.67E-02	1.16E-03	74.0	62.26	3.983	1.75	15	0	20
88	3.72E-03	1.74E-05	4.40E-02	4.40E-04	74.2	62.26	3.974	1.75	18	0	20
88	1.16E-02	6.42E-05	8.38E-02	9.42E-04	74.3	62.26	3.985	1.75	21	0	20
88	1.57E-02	9.55E-05	7.28E-02	1.73E-03	74.5	62.26	3.985	1.75	24	0	20

TABLE A1. Stress data											
Year	Stress	Variance	Max. stress	Min. stress	Temp.	Unit Wt.	Q	Bw	X	Y	H
	lb/ft^2	(lb/ft^2)^2	lb/ft^2	lb/ft^2	F	lb/ft^3	ft^3/s	ft	in	in	in
88	1.19E-02	0.000226	1.58E-01	5.16E-04	72.7	62.28	3.981	1.75	0	3	20
88	6.04E-03	3.75E-05	8.40E-02	4.08E-04	72.6	62.28	3.985	1.75	0	6	20
88	1.57E-03	2.2E-06	1.49E-02	2.26E-04	72.5	62.28	3.985	1.75	0	9	20
88	4.60E-03	1.08E-05	2.46E-02	3.67E-04	72.3	62.28	3.992	1.75	0	12	20
88	1.15E-01	0.007523	8.69E-01	6.23E-03	74.0	62.26	3.974	1.5	15	0	20
88	1.74E-01	0.008406	7.91E-01	1.02E-02	74.2	62.26	3.983	1.5	18	0	20
88	2.19E-01	0.008866	8.87E-01	1.48E-02	74.3	62.26	3.981	1.5	21	0	20
88	2.27E-01	0.008398	9.40E-01	3.42E-02	74.5	62.26	3.981	1.5	24	0	20
88	8.80E-02	0.003177	5.87E-01	5.76E-03	72.7	62.28	3.985	1.5	0	3	20
88	7.47E-02	0.002207	4.44E-01	3.51E-03	72.6	62.28	3.985	1.5	0	6	20
88	4.29E-02	0.000933	3.31E-01	1.57E-03	72.5	62.28	3.981	1.5	0	9	20
88	3.08E-02	0.000526	2.07E-01	1.58E-03	72.3	62.28	3.989	1.5	0	12	20
88	2.92E-01	0.019303	1.48E+00	3.01E-02	74.0	62.26	3.985	1.25	15	0	20
88	3.14E-01	0.016898	1.30E+00	3.10E-02	74.2	62.26	3.981	1.25	18	0	20
88	3.10E-01	0.016177	1.87E+00	3.19E-02	74.3	62.26	3.985	1.25	21	0	20
88	2.86E-01	0.012095	1.02E+00	4.69E-02	74.5	62.26	3.981	1.25	24	0	20
88	2.07E-01	0.010561	9.15E-01	1.85E-02	72.7	62.28	3.985	1.25	0	3	20
88	1.59E-01	0.007281	9.64E-01	4.79E-03	72.6	62.28	3.981	1.25	0	6	20
88	8.69E-02	0.003653	5.44E-01	3.13E-03	72.5	62.28	3.985	1.25	0	9	20
88	3.39E-02	0.001226	6.78E-01	1.93E-03	72.4	62.28	3.992	1.25	0	12	20
88	2.98E-01	0.03304	1.73E+00	1.49E-02	74.0	62.26	3.974	1	15	0	20
88	4.38E-01	0.033459	1.66E+00	5.69E-02	74.2	62.26	3.987	1	18	0	20
88	4.74E-01	0.035201	1.96E+00	3.31E-02	74.3	62.26	3.966	1	21	0	20
88	4.42E-01	0.029622	1.65E+00	5.86E-02	74.5	62.26	3.985	1	24	0	20
88	1.41E-01	0.006597	8.56E-01	6.97E-03	72.7	62.28	3.989	1	0	3	20
88	1.06E-01	0.003435	5.51E-01	8.46E-03	72.6	62.28	3.989	1	0	6	20
88	2.83E-02	0.000588	2.78E-01	1.59E-03	72.5	62.28	3.985	1	0	9	20
88	1.89E-02	0.000359	3.26E-01	9.31E-04	72.4	62.28	3.989	1	0	12	20
88	3.38E-01	0.060016	3.36E+00	1.92E-02	74.0	62.26	3.977	0.22	15	0	20
88	5.59E-01	0.052552	2.59E+00	7.36E-02	74.2	62.26	3.977	0.21	18	0	20
88	6.72E-01	0.054715	1.99E+00	1.65E-01	74.4	62.26	3.985	0.23	21	0	20

TABLE A1. Stress data											
Year	Stress	Variance	Max. stress	Min. stress	Temp.	Unit Wt.	Q	Bw	X	Y	H
	lb/ft^2	(lb/ft^2)^2	lb/ft^2	lb/ft^2	F	lb/ft^3	ft^3/s	ft	in	in	in
88	6.86E-01	0.035685	1.73E+00	2.61E-01	74.5	62.26	3.981	0.22	24	0	20
88	8.04E-02	0.003252	5.37E-01	3.26E-03	72.7	62.28	3.989	0.22	0	3	20
88	3.25E-02	0.000898	3.34E-01	1.62E-03	72.6	62.28	3.985	0.225	0	6	20
88	2.20E-02	0.000633	6.18E-01	8.95E-04	72.5	62.28	3.985	0.22	0	9	20
88	2.94E-03	3.9E-06	3.65E-02	4.83E-04	70.4	62.29	3.993	2.75	15	0	30
88	4.67E-03	1.68E-05	6.72E-02	3.93E-04	70.7	62.29	3.996	2.75	18	0	30
88	4.97E-03	1.41E-05	2.96E-02	3.96E-04	70.9	62.29	3.985	2.75	21	0	30
88	6.29E-03	1.89E-05	4.56E-02	7.73E-04	69.6	62.30	3.967	2.75	36	0	30
88	8.51E-03	0.000028	5.68E-02	8.55E-04	69.9	62.30	3.989	2.75	39	0	30
88	6.71E-03	2.93E-05	4.43E-02	7.61E-04	70.1	62.30	3.993	2.75	42	0	30
88	1.03E-02	5.83E-05	9.61E-02	6.85E-04	70.3	62.29	3.989	2.75	45	0	30
88	5.84E-03	4.16E-05	1.06E-01	2.86E-04	72.7	62.28	3.989	2.75	0	3	30
88	5.23E-03	2.63E-05	5.13E-02	6.17E-04	72.5	62.28	3.985	2.75	0	6	30
88	5.59E-03	0.000039	6.89E-02	3.93E-04	72.4	62.28	3.985	2.75	0	9	30
88	5.91E-03	2.63E-05	6.54E-02	3.66E-04	72.3	62.28	3.985	2.75	0	12	30
88	3.37E-03	2.21E-05	5.60E-02	2.36E-04	72.1	62.28	3.989	2.75	0	15	30
88	4.16E-03	1.88E-05	3.93E-02	3.08E-04	71.9	62.28	3.985	2.75	0	18	30
88	3.21E-03	1.84E-05	7.36E-02	2.34E-04	71.7	62.28	3.982	2.75	0	21	30
88	6.22E-03	3.01E-05	5.31E-02	3.98E-04	70.4	62.29	3.989	2.5	15	0	30
88	6.73E-03	2.22E-05	6.24E-02	6.32E-04	70.7	62.29	3.985	2.5	18	0	30
88	7.06E-03	0.000031	6.66E-02	5.21E-04	70.9	62.29	3.985	2.5	21	0	30
88	8.57E-03	6.46E-05	8.63E-02	6.91E-04	69.6	62.30	3.993	2.5	36	0	30
88	1.12E-02	6.08E-05	9.03E-02	1.25E-03	69.9	62.30	3.989	2.5	39	0	30
88	1.09E-02	7.36E-05	1.72E-01	7.57E-04	70.1	62.30	3.993	2.5	42	0	30
88	1.31E-02	8.57E-05	9.70E-02	9.06E-04	70.3	62.29	3.986	2.5	45	0	30
88	8.73E-03	9.55E-05	1.04E-01	4.03E-04	72.7	62.28	3.989	2.5	0	3	30
88	6.66E-03	6.35E-05	9.93E-02	3.58E-04	72.5	62.28	3.985	2.5	0	6	30
88	5.92E-03	3.38E-05	7.55E-02	5.18E-04	72.4	62.28	3.989	2.5	0	9	30
88	6.62E-03	5.14E-05	1.11E-01	3.10E-04	72.3	62.28	3.985	2.5	0	12	30
88	5.30E-03	2.45E-05	5.21E-02	5.63E-04	72.1	62.28	3.985	2.5	0	15	30
88	4.58E-03	0.000027	7.07E-02	3.09E-04	71.9	62.28	3.978	2.5	0	18	30

TABLE A1. Stress data											
Year	Stress	Variance	Max. stress	Min. stress	Temp.	Unit Wt.	Q	Bw	X	Y	H
	lb/ft^2	(lb/ft^2)^2	lb/ft^2	lb/ft^2	F	lb/ft^3	ft^3/s	ft	in	in	in
88	4.21E-03	1.89E-05	5.35E-02	4.23E-04	71.8	62.28	3.978	2.5	0	21	30
88	8.35E-02	0.002052	5.14E-01	5.95E-03	70.5	62.29	3.993	2.25	15	0	30
88	6.06E-02	0.001569	6.47E-01	4.50E-03	70.7	62.29	3.982	2.25	18	0	30
88	4.98E-02	0.001693	5.89E-01	1.66E-03	71.0	62.29	3.985	2.25	21	0	30
88	1.12E-01	0.0029	4.31E-01	1.07E-02	69.6	62.30	3.993	2.25	36	0	30
88	1.03E-01	0.002241	4.29E-01	1.52E-02	69.9	62.30	3.982	2.25	39	0	30
88	9.31E-02	0.00177	4.31E-01	1.15E-02	70.1	62.29	3.982	2.25	42	0	30
88	8.14E-02	0.001463	3.92E-01	5.94E-03	70.3	62.29	3.989	2.25	45	0	30
88	3.28E-02	0.000712	2.56E-01	1.67E-03	72.7	62.28	3.989	2.25	0	3	30
88	6.75E-02	0.00111	3.91E-01	7.45E-03	72.6	62.28	3.985	2.25	0	6	30
88	6.82E-02	0.0012	3.07E-01	7.37E-03	72.4	62.28	3.989	2.25	0	9	30
88	5.42E-02	0.000763	2.88E-01	2.22E-03	72.3	62.28	3.992	2.25	0	12	30
88	3.43E-02	0.0005	2.81E-01	1.38E-03	72.1	62.28	3.981	2.25	0	15	30
88	1.58E-02	0.000194	1.88E-01	7.95E-04	72.0	62.28	3.978	2.25	0	18	30
88	7.48E-03	0.000093	2.17E-01	4.77E-04	71.8	62.28	3.985	2.25	0	21	30
88	1.09E-01	0.005856	1.12E+00	4.38E-03	70.5	62.29	3.989	2	15	0	30
88	6.47E-02	0.003457	7.28E-01	3.28E-03	70.7	62.29	3.985	2	18	0	30
88	9.21E-02	0.003431	9.03E-01	5.67E-03	71.0	62.29	3.985	2	21	0	30
88	1.36E-01	0.003899	6.25E-01	6.82E-03	69.6	62.30	3.982	2	36	0	30
88	1.20E-01	0.002895	5.86E-01	6.57E-03	69.9	62.30	3.989	2	39	0	30
88	1.06E-01	0.00282	6.01E-01	9.45E-03	70.1	62.29	3.978	2	42	0	30
88	9.01E-02	0.001946	4.03E-01	5.85E-03	70.3	62.29	3.993	2	45	0	30
88	7.24E-02	0.002223	5.49E-01	5.71E-03	72.7	62.27	3.992	2	0	3	30
88	9.09E-02	0.001474	3.87E-01	1.41E-02	72.6	62.28	3.985	2	0	6	30
88	7.87E-02	0.001151	3.42E-01	1.12E-02	72.4	62.28	3.985	2	0	9	30
88	5.21E-02	0.000794	3.11E-01	1.22E-03	72.3	62.28	3.974	2	0	12	30
88	2.30E-02	0.000417	2.55E-01	1.43E-03	72.1	62.28	3.989	2	0	15	30
88	1.20E-02	0.000142	1.68E-01	9.02E-04	72.0	62.28	3.978	2	0	18	30
88	3.96E-03	0.000018	5.93E-02	3.15E-04	71.8	62.28	3.978	2	0	21	30
88	1.37E-01	0.007386	1.28E+00	1.03E-02	70.5	62.29	3.989	1.75	15	0	30
88	9.84E-02	0.007305	1.20E+00	3.07E-03	70.8	62.29	3.989	1.75	18	0	30

TABLE A1. Stress data

Year	Stress	Variance	Max. stress	Min. stress	Temp.	Unit Wt.	Q	Bw	X	Y	H
	lb/ft^2	(lb/ft^2)^2	lb/ft^2	lb/ft^2	F	lb/ft^3	ft^3/s	ft	in	in	in
88	1.04E-01	0.005474	7.89E-01	5.13E-03	71.0	62.29	3.985	1.75	21	0	30
88	1.76E-01	0.005997	8.43E-01	1.57E-02	69.6	62.30	3.971	1.75	36	0	30
88	1.52E-01	0.004707	5.82E-01	1.82E-02	69.9	62.30	3.989	1.75	39	0	30
88	1.34E-01	0.004093	5.87E-01	1.02E-02	70.1	62.29	3.997	1.75	42	0	30
88	1.07E-01	0.003288	4.90E-01	3.08E-03	70.3	62.29	3.989	1.75	45	0	30
88	6.01E-02	0.001885	7.33E-01	3.44E-03	72.7	62.28	3.992	1.75	0	3	30
88	8.86E-02	0.001711	4.47E-01	4.05E-03	72.6	62.28	3.989	1.75	0	6	30
88	7.74E-02	0.001218	3.90E-01	9.96E-03	72.5	62.28	3.989	1.75	0	9	30
88	5.17E-02	0.000845	3.83E-01	4.03E-03	72.3	62.28	3.989	1.75	0	12	30
88	2.20E-02	0.000366	3.39E-01	8.94E-04	72.2	62.28	3.985	1.75	0	15	30
88	1.06E-02	0.000142	1.62E-01	4.66E-04	72.0	62.28	3.985	1.75	0	18	30
88	7.36E-03	4.62E-05	7.60E-02	4.55E-04	71.8	62.28	3.978	1.75	0	21	30
88	1.93E-01	0.011299	2.04E+00	1.34E-02	70.5	62.29	3.989	1.5	15	0	30
88	1.47E-01	0.011699	1.11E+00	6.05E-03	70.8	62.29	3.985	1.5	18	0	30
88	1.36E-01	0.011221	1.38E+00	6.51E-03	71.0	62.29	3.985	1.5	21	0	30
88	1.93E-01	0.007631	8.11E-01	1.18E-02	69.7	62.30	4.000	1.5	36	0	30
88	1.68E-01	0.006512	7.76E-01	8.50E-03	69.9	62.30	3.989	1.5	39	0	30
88	1.46E-01	0.005696	6.76E-01	4.89E-03	70.1	62.29	3.986	1.5	42	0	30
88	1.18E-01	0.004568	6.63E-01	4.76E-03	70.4	62.29	3.986	1.5	45	0	30
88	5.96E-02	0.002169	5.28E-01	3.00E-03	72.8	62.27	3.992	1.5	0	3	30
88	8.79E-02	0.001975	7.29E-01	4.71E-03	72.6	62.28	3.992	1.5	0	6	30
88	7.20E-02	0.001528	3.32E-01	2.96E-03	72.5	62.28	3.989	1.5	0	9	30
88	4.88E-02	0.000913	2.97E-01	2.20E-03	72.3	62.28	3.992	1.5	0	12	30
88	1.85E-02	0.000305	3.40E-01	1.15E-03	72.2	62.28	3.992	1.5	0	15	30
88	2.22E-02	0.000383	4.27E-01	6.74E-04	72.0	62.28	3.985	1.5	0	18	30
88	2.25E-01	0.014473	1.68E+00	1.20E-02	70.5	62.29	3.993	1.25	15	0	30
88	2.24E-01	0.018747	1.45E+00	8.33E-03	70.8	62.29	3.985	1.25	18	0	30
88	1.99E-01	0.02449	1.69E+00	7.64E-03	71.0	62.29	3.989	1.25	21	0	30
88	2.51E-01	0.014414	1.02E+00	1.57E-02	69.6	62.30	3.989	1.25	36	0	30
88	2.00E-01	0.009615	1.08E+00	1.21E-02	69.9	62.30	3.993	1.25	39	0	30
88	1.51E-01	0.007054	9.81E-01	4.40E-03	70.1	62.29	3.997	1.25	42	0	30

TABLE A1. Stress data

Year	Stress	Variance	Max. stress	Min. stress	Temp.	Unit Wt.	Q	Bw	X	Y	H
	lb/ft^2	(lb/ft^2)^2	lb/ft^2	lb/ft^2	F	lb/ft^3	ft^3/s	ft	in	in	in
88	1.26E-01	0.005829	5.87E-01	4.20E-03	70.3	62.29	3.989	1.25	45	0	30
88	5.83E-02	0.002616	7.67E-01	2.33E-03	72.8	62.27	3.992	1.25	0	3	30
88	7.91E-02	0.002401	5.08E-01	3.52E-03	72.6	62.28	3.989	1.25	0	6	30
88	5.93E-02	0.001383	4.16E-01	2.08E-03	72.5	62.28	3.985	1.25	0	9	30
88	2.38E-02	0.000415	2.40E-01	1.53E-03	72.4	62.28	3.989	1.25	0	12	30
88	2.03E-01	0.011937	1.12E+00	9.78E-03	70.5	62.29	3.989	1	15	0	30
88	2.66E-01	0.020269	1.66E+00	2.85E-02	70.8	62.29	3.985	1	18	0	30
88	2.97E-01	0.041354	2.84E+00	1.02E-02	71.1	62.29	3.985	1	21	0	30
88	3.15E-01	0.02572	1.70E+00	1.26E-02	69.7	62.30	3.989	1	36	0	30
88	2.41E-01	0.017495	1.23E+00	8.29E-03	69.9	62.30	3.986	1	39	0	30
88	1.82E-01	0.011562	9.40E-01	4.99E-03	70.2	62.29	3.989	1	42	0	30
88	1.32E-01	0.008325	7.63E-01	3.48E-03	70.4	62.29	3.989	1	45	0	30
88	4.25E-02	0.001967	6.37E-01	1.60E-03	72.8	62.27	3.992	1	0	3	30
88	4.92E-02	0.0019	4.98E-01	2.36E-03	72.6	62.28	3.989	1	0	6	30
88	2.97E-02	0.000786	3.83E-01	1.42E-03	72.5	62.28	3.989	1	0	9	30
88	2.63E-01	0.020634	1.58E+00	1.88E-02	70.8	62.29	3.985	0.22	18	0	30
88	3.61E-01	0.057995	2.79E+00	1.68E-02	71.1	62.29	3.989	0.215	21	0	30
88	6.24E-01	0.03231	1.76E+00	1.73E-01	69.7	62.30	3.989	0.215	36	0	30
88	5.37E-01	0.021848	1.55E+00	2.11E-01	70.0	62.30	3.986	0.22	39	0	30
88	5.09E-01	0.019562	1.53E+00	1.91E-01	70.2	62.29	3.986	0.22	42	0	30
88	4.65E-01	0.016759	1.31E+00	1.60E-01	70.4	62.29	3.993	0.21	45	0	30
88	3.14E-02	0.001157	4.92E-01	1.57E-03	72.8	62.27	3.992	0.215	0	3	30
88	3.73E-02	0.001095	4.05E-01	1.92E-03	72.6	62.28	3.989	0.225	0	6	30
89	4.47E-03	6.4E-06	1.93E-02	8.80E-04	52.1	62.39	1.999	1.75	3	0	20
89	2.02E-03	1.7E-06	1.14E-02	5.58E-04	52.2	62.39	1.997	1.75	6	0	20
89	3.67E-03	2.5E-06	2.37E-02	8.24E-04	52.4	62.39	2.001	1.75	9	0	20
89	4.02E-03	4.1E-06	1.85E-02	8.89E-04	52.5	62.39	1.999	1.75	12	0	20
89	3.15E-03	3.9E-06	2.23E-02	6.17E-04	52.4	62.39	1.997	1.75	15	0	20
89	3.16E-03	3.2E-06	1.43E-02	6.59E-04	52.6	62.39	1.997	1.75	18	0	20
89	5.75E-03	6.1E-06	2.38E-02	1.11E-03	52.7	62.39	1.993	1.75	21	0	20
89	3.58E-03	0.000005	3.65E-02	7.85E-04	53.0	62.39	2.005	1.75	24	0	20

TABLE A1. Stress data											
Year	Stress	Variance	Max. stress	Min. stress	Temp.	Unit Wt.	Q	Bw	X	Y	H
	lb/ft^2	(lb/ft^2)^2	lb/ft^2	lb/ft^2	F	lb/ft^3	ft^3/s	ft	in	in	in
89	9.97E-03	2.58E-05	8.19E-02	2.74E-03	53.2	62.39	2.003	1.75	0	3	20
89	2.77E-03	8E-07	1.06E-02	1.26E-03	52.9	62.39	2.007	1.75	0	6	20
89	2.68E-03	1.7E-06	1.09E-02	8.50E-04	52.7	62.39	2.003	1.75	0	9	20
89	8.98E-04	1.00E-08	1.73E-03	4.56E-04	52.6	62.39	2.003	1.75	0	12	20
89	1.41E-02	0.000126	2.41E-01	1.46E-03	52.1	62.39	1.999	1.5	3	0	20
89	1.81E-02	0.00016	2.05E-01	1.85E-03	52.2	62.39	1.999	1.5	6	0	20
89	3.39E-02	0.000401	1.98E-01	2.43E-03	52.4	62.39	1.995	1.5	9	0	20
89	3.94E-02	0.000485	2.01E-01	3.68E-03	52.5	62.39	1.997	1.5	12	0	20
89	3.34E-02	0.000579	2.66E-01	3.25E-03	52.4	62.39	1.997	1.5	15	0	20
89	3.51E-02	0.000701	2.40E-01	2.21E-03	52.6	62.39	1.991	1.5	18	0	20
89	4.74E-02	0.000787	2.68E-01	3.92E-03	52.8	62.39	1.991	1.5	21	0	20
89	4.98E-02	0.000744	2.76E-01	3.96E-03	53.0	62.39	2.003	1.5	24	0	20
89	4.99E-02	0.000365	1.82E-01	1.00E-02	53.2	62.39	2.005	1.5	0	3	20
89	3.54E-02	0.000303	2.04E-01	2.64E-03	52.9	62.39	2.005	1.5	0	6	20
89	2.59E-02	0.000259	1.85E-01	2.74E-03	52.8	62.39	2.005	1.5	0	9	20
89	1.80E-02	0.000117	1.12E-01	2.07E-03	52.6	62.39	1.999	1.5	0	12	20
89	2.05E-02	0.00015	1.17E-01	2.84E-03	52.1	62.39	1.999	1.25	3	0	20
89	5.52E-02	0.000881	3.06E-01	7.03E-03	52.2	62.39	1.999	1.25	6	0	20
89	5.91E-02	0.001291	3.78E-01	3.56E-03	52.4	62.39	1.999	1.25	9	0	20
89	4.84E-02	0.001249	4.04E-01	3.88E-03	52.5	62.39	1.997	1.25	12	0	20
89	9.28E-02	0.002235	4.15E-01	7.41E-03	52.4	62.39	1.999	1.25	15	0	20
89	8.98E-02	0.001533	3.44E-01	1.25E-02	52.6	62.39	1.991	1.25	18	0	20
89	7.80E-02	0.001249	2.97E-01	9.30E-03	52.8	62.39	1.995	1.25	21	0	20
89	6.86E-02	0.001038	2.66E-01	7.40E-03	53.0	62.39	2.005	1.25	24	0	20
89	3.81E-02	0.000266	1.38E-01	7.06E-03	53.2	62.39	2.001	1.25	0	3	20
89	3.15E-02	0.000243	2.33E-01	3.55E-03	52.9	62.39	2.003	1.25	0	6	20
89	1.56E-02	0.00012	1.90E-01	1.56E-03	52.8	62.39	2.005	1.25	0	9	20
89	8.61E-03	4.65E-05	1.07E-01	1.39E-03	52.6	62.39	1.999	1.25	0	12	20
89	2.60E-02	0.000238	2.19E-01	2.92E-03	52.1	62.39	1.997	1	3	0	20
89	7.19E-02	0.000982	2.89E-01	6.72E-03	52.3	62.39	1.997	1	6	0	20
89	9.27E-02	0.002289	4.74E-01	1.03E-02	52.4	62.39	1.999	1	9	0	20

TABLE A1. Stress data

Year	Stress	Variance	Max. stress	Min. stress	Temp.	Unit Wt.	Q	Bw	X	Y	H
	lb/ft^2	(lb/ft^2)^2	lb/ft^2	lb/ft^2	F	lb/ft^3	ft^3/s	ft	in	in	in
89	6.86E-02	0.002867	6.15E-01	4.60E-03	52.5	62.39	1.995	1	12	0	20
89	1.58E-01	0.006598	8.05E-01	1.29E-02	52.4	62.39	1.999	1	15	0	20
89	1.48E-01	0.004259	6.13E-01	1.96E-02	52.7	62.39	1.993	1	18	0	20
89	1.17E-01	0.003048	4.11E-01	7.81E-03	52.8	62.39	1.991	1	21	0	20
89	9.59E-02	0.002503	5.03E-01	4.70E-03	53.0	62.39	2.005	1	24	0	20
89	4.34E-02	0.000355	1.88E-01	6.46E-03	53.2	62.39	2.001	1	0	3	20
89	2.73E-02	0.0004	2.75E-01	2.11E-03	52.9	62.39	2.003	1	0	6	20
89	2.12E-02	0.000303	1.53E-01	1.84E-03	52.8	62.39	2.003	1	0	9	20
89	2.23E-02	0.000244	2.10E-01	2.46E-03	52.1	62.39	1.999	0.75	3	0	20
89	5.87E-02	0.000885	3.56E-01	2.90E-03	52.3	62.39	1.997	0.75	6	0	20
89	1.14E-01	0.003806	5.60E-01	8.61E-03	52.5	62.39	2.003	0.75	9	0	20
89	1.43E-01	0.009951	1.15E+00	1.15E-02	52.5	62.39	1.999	0.75	12	0	20
89	2.42E-01	0.01897	1.26E+00	1.71E-02	52.4	62.39	1.997	0.75	15	0	20
89	2.65E-01	0.014101	1.14E+00	3.47E-02	52.7	62.39	1.993	0.75	18	0	20
89	1.79E-01	0.006745	8.70E-01	1.56E-02	52.8	62.39	1.995	0.75	21	0	20
89	1.37E-01	0.004861	5.68E-01	4.43E-03	53.0	62.39	2.005	0.75	24	0	20
89	4.13E-02	0.000495	2.36E-01	3.83E-03	53.3	62.39	2.001	0.75	0	3	20
89	2.40E-02	0.00036	2.36E-01	1.86E-03	52.9	62.39	2.003	0.75	0	6	20
89	1.52E-02	0.000129	1.32E-01	1.58E-03	52.2	62.39	1.999	0.1	3	0	20
89	3.01E-02	0.000604	2.61E-01	2.89E-03	52.3	62.39	1.999	0.1	6	0	20
89	8.28E-02	0.002522	4.25E-01	5.84E-03	52.5	62.39	1.997	0.09	9	0	20
89	2.44E-01	0.023027	1.75E+00	1.45E-02	52.5	62.39	1.999	0.095	12	0	20
89	4.25E-01	0.040668	2.14E+00	2.38E-02	52.5	62.39	1.999	0.095	15	0	20
89	5.24E-01	0.03341	1.56E+00	1.33E-01	52.7	62.39	1.991	0.095	18	0	20
89	4.19E-01	0.016777	1.11E+00	1.08E-01	52.8	62.39	1.991	0.09	21	0	20
89	3.48E-01	0.011279	1.02E+00	9.09E-02	53.1	62.39	2.003	0.095	24	0	20
89	1.43E-02	0.00013	1.19E-01	1.13E-03	53.3	62.39	2.001	0.095	0	3	20
89	1.69E-02	0.000175	1.48E-01	1.50E-03	51.9	62.39	3.986	1.75	3	0	20
89	4.47E-03	7.4E-06	3.22E-02	9.91E-04	52.0	62.39	3.972	1.75	6	0	20
89	7.31E-03	1.98E-05	3.23E-02	1.01E-03	52.1	62.39	3.979	1.75	9	0	20
89	5.56E-03	1.21E-05	2.64E-02	1.02E-03	52.1	62.39	3.972	1.75	12	0	20

TABLE A1. Stress data

Year	Stress	Variance	Max. stress	Min. stress	Temp.	Unit Wt.	Q	Bw	X	Y	H
	lb/ft^2	(lb/ft^2)^2	lb/ft^2	lb/ft^2	F	lb/ft^3	ft^3/s	ft	in	in	in
89	5.41E-03	1.12E-05	3.26E-02	9.13E-04	52.2	62.39	3.972	1.75	15	0	20
89	6.87E-03	1.43E-05	3.78E-02	1.16E-03	52.3	62.39	3.983	1.75	18	0	20
89	6.77E-03	2.11E-05	5.61E-02	1.21E-03	50.9	62.40	3.983	1.75	21	0	20
89	1.26E-02	0.000108	2.26E-01	1.18E-03	51.1	62.40	3.983	1.75	24	0	20
89	1.31E-02	8.04E-05	9.22E-02	1.13E-03	51.2	62.40	3.983	1.75	27	0	20
89	1.45E-02	7.25E-05	9.67E-02	1.73E-03	51.3	62.40	3.979	1.75	30	0	20
89	1.94E-02	0.000123	1.82E-01	2.34E-03	51.5	62.40	3.994	1.75	33	0	20
89	1.97E-02	0.000138	1.57E-01	1.74E-03	51.7	62.39	3.983	1.75	36	0	20
89	7.01E-03	2.38E-05	4.14E-02	9.12E-04	52.8	62.39	3.983	1.75	0	3	20
89	7.61E-03	1.92E-05	3.72E-02	1.73E-03	52.6	62.39	3.983	1.75	0	6	20
89	6.78E-03	2.11E-05	5.20E-02	1.11E-03	52.5	62.39	3.983	1.75	0	9	20
89	6.18E-03	2.76E-05	4.77E-02	7.11E-04	52.4	62.39	3.983	1.75	0	12	20
89	5.54E-02	0.00126	2.91E-01	4.47E-03	51.9	62.39	3.990	1.5	3	0	20
89	5.40E-02	0.000702	2.45E-01	4.72E-03	52.0	62.39	3.979	1.5	6	0	20
89	6.57E-02	0.001234	3.90E-01	4.60E-03	52.1	62.39	3.979	1.5	9	0	20
89	6.66E-02	0.001434	3.55E-01	4.03E-03	52.1	62.39	3.975	1.5	12	0	20
89	4.56E-02	0.001081	3.86E-01	4.32E-03	52.2	62.39	3.972	1.5	15	0	20
89	5.25E-02	0.001235	3.09E-01	2.37E-03	52.3	62.39	3.983	1.5	18	0	20
89	1.58E-01	0.006054	7.11E-01	1.27E-02	51.0	62.40	3.979	1.5	21	0	20
89	1.86E-01	0.007211	7.59E-01	1.43E-02	51.1	62.40	3.979	1.5	24	0	20
89	1.96E-01	0.006533	7.38E-01	2.66E-02	51.2	62.40	3.983	1.5	27	0	20
89	1.71E-01	0.004983	7.51E-01	2.41E-02	51.3	62.40	3.983	1.5	30	0	20
89	1.71E-01	0.004965	6.45E-01	1.64E-02	51.6	62.40	3.979	1.5	33	0	20
89	1.77E-01	0.006257	7.00E-01	1.84E-02	51.7	62.39	3.983	1.5	36	0	20
89	6.56E-02	0.000926	2.94E-01	6.97E-03	52.8	62.39	3.983	1.5	0	3	20
89	5.65E-02	0.000985	3.19E-01	3.48E-03	52.6	62.39	3.979	1.5	0	6	20
89	4.12E-02	0.000717	2.37E-01	2.17E-03	52.5	62.39	3.983	1.5	0	9	20
89	2.41E-02	0.000255	1.35E-01	1.91E-03	52.4	62.39	3.983	1.5	0	12	20
89	7.80E-02	0.002286	5.04E-01	5.72E-03	51.9	62.39	3.986	1.25	3	0	20
89	8.78E-02	0.001493	3.71E-01	8.60E-03	52.0	62.39	3.983	1.25	6	0	20
89	9.93E-02	0.002265	4.33E-01	1.27E-02	52.1	62.39	3.983	1.25	9	0	20

TABLE A1. Stress data											
Year	Stress	Variance	Max. stress	Min. stress	Temp.	Unit Wt.	Q	Bw	X	Y	H
	lb/ft^2	(lb/ft^2)^2	lb/ft^2	lb/ft^2	F	lb/ft^3	ft^3/s	ft	in	in	in
89	6.68E-02	0.00222	4.92E-01	4.95E-03	52.1	62.39	3.979	1.25	12	0	20
89	9.81E-02	0.003347	5.03E-01	8.33E-03	52.2	62.39	3.972	1.25	15	0	20
89	1.34E-01	0.003173	5.04E-01	1.12E-02	52.3	62.39	3.983	1.25	18	0	20
89	2.79E-01	0.014726	8.71E-01	3.14E-02	51.0	62.40	3.979	1.25	21	0	20
89	2.64E-01	0.012185	1.07E+00	1.99E-02	51.1	62.40	3.983	1.25	24	0	20
89	2.34E-01	0.009764	1.02E+00	1.80E-02	51.3	62.40	3.979	1.25	27	0	20
89	1.99E-01	0.007331	8.21E-01	1.17E-02	51.4	62.40	3.983	1.25	30	0	20
89	1.72E-01	0.006761	7.11E-01	8.54E-03	51.6	62.40	3.968	1.25	33	0	20
89	1.61E-01	0.007603	1.01E+00	7.27E-03	51.8	62.39	3.983	1.25	36	0	20
89	8.81E-02	0.001528	3.64E-01	6.48E-03	52.9	62.39	3.983	1.25	0	3	20
89	7.33E-02	0.001263	3.15E-01	8.62E-03	52.6	62.39	3.979	1.25	0	6	20
89	4.44E-02	0.000784	2.62E-01	2.42E-03	52.5	62.39	3.983	1.25	0	9	20
89	1.54E-02	0.000159	1.66E-01	1.75E-03	52.4	62.39	3.986	1.25	0	12	20
89	4.24E-02	0.000899	3.58E-01	4.04E-03	51.9	62.39	3.986	1	3	0	20
89	5.95E-02	0.000908	2.95E-01	6.50E-03	52.0	62.39	3.979	1	6	0	20
89	9.77E-02	0.002262	5.71E-01	9.16E-03	52.1	62.39	3.983	1	9	0	20
89	1.34E-01	0.004283	9.53E-01	1.34E-02	52.1	62.39	3.975	1	12	0	20
89	1.14E-01	0.005213	8.75E-01	9.81E-03	52.3	62.39	3.972	1	15	0	20
89	1.33E-01	0.005303	6.38E-01	8.06E-03	52.4	62.39	3.983	1	18	0	20
89	3.77E-01	0.026283	1.61E+00	3.54E-02	51.0	62.40	3.979	1	21	0	20
89	3.91E-01	0.02981	1.23E+00	2.18E-02	51.2	62.40	3.979	1	24	0	20
89	3.36E-01	0.023448	1.54E+00	1.45E-02	51.3	62.40	3.979	1	27	0	20
89	2.68E-01	0.01757	1.06E+00	1.59E-02	51.4	62.40	3.983	1	30	0	20
89	2.10E-01	0.013935	1.01E+00	9.68E-03	51.6	62.39	3.979	1	33	0	20
89	1.97E-01	0.01408	1.02E+00	6.01E-03	51.8	62.39	3.983	1	36	0	20
89	5.61E-02	0.001113	3.39E-01	6.02E-03	52.9	62.39	3.983	1	0	3	20
89	5.53E-02	0.001005	3.02E-01	3.61E-03	52.7	62.39	3.979	1	0	6	20
89	2.53E-02	0.000379	1.85E-01	2.34E-03	52.5	62.39	3.979	1	0	9	20
89	3.30E-02	0.000597	6.06E-01	4.09E-03	51.9	62.39	3.986	0.175	3	0	20
89	3.98E-02	0.000665	2.34E-01	3.88E-03	52.1	62.39	3.983	0.175	6	0	20
89	6.94E-02	0.001405	3.50E-01	6.89E-03	52.2	62.39	3.983	0.175	9	0	20

TABLE A1. Stress data											
Year	Stress	Variance	Max. stress	Min. stress	Temp.	Unit Wt.	Q	Bw	X	Y	H
	lb/ft^2	(lb/ft^2)^2	lb/ft^2	lb/ft^2	F	lb/ft^3	ft^3/s	ft	in	in	in
89	1.13E-01	0.003269	4.87E-01	8.80E-03	52.2	62.39	3.979	0.175	12	0	20
89	1.71E-01	0.007998	8.32E-01	1.20E-02	52.3	62.39	3.968	0.175	15	0	20
89	1.21E-01	0.006008	8.54E-01	1.00E-02	52.4	62.39	3.983	0.175	18	0	20
89	5.14E-01	0.032059	1.60E+00	6.26E-02	51.0	62.40	3.983	0.175	21	0	20
89	6.10E-01	0.033409	1.68E+00	1.13E-01	51.2	62.40	3.979	0.175	24	0	20
89	5.97E-01	0.02599	1.38E+00	1.73E-01	51.3	62.40	3.983	0.175	27	0	20
89	5.42E-01	0.021534	1.50E+00	1.95E-01	51.4	62.40	3.979	0.175	30	0	20
89	5.41E-01	0.020068	1.27E+00	1.63E-01	51.6	62.39	3.983	0.175	33	0	20
89	5.69E-01	0.023229	1.56E+00	1.61E-01	51.8	62.39	3.983	0.175	36	0	20
89	3.02E-02	0.000572	2.65E-01	2.04E-03	52.9	62.39	3.986	0.175	0	3	20
89	2.46E-02	0.000364	2.01E-01	2.55E-03	52.7	62.39	3.983	0.175	0	6	20

TABLE A2. Water surface profile data										
Station	Elev.	Q	Bw	Da	F	H	X	X/Da	Y	Y/Da
ft	ft	ft^3/s	ft	ft		in	ft		ft	
10	0.935	0.991	0.07	0.128	1.62	10	0	0.000	0.102	0.794
10.25	0.777	0.991	0.07	0.128	1.62	10	0.25	1.953	-0.056	-0.440
10.5	0.188	0.991	0.07	0.128	1.62	10	0.5	3.906	-0.645	-5.042
10	0.933	1.003	0.5	0.127	1.69	10	0	0.000	0.100	0.785
10.25	0.746	1.003	0.5	0.127	1.69	10	0.25	1.969	-0.087	-0.688
10	0.935	1.004	0.75	0.129	1.63	10	0	0.000	0.102	0.788
10.25	0.76	1.004	0.75	0.129	1.63	10	0.25	1.938	-0.073	-0.568
10	0.991	1.996	0.11	0.196	1.83	10	0	0.000	0.158	0.804
10.25	0.862	1.996	0.11	0.196	1.83	10	0.25	1.276	0.029	0.146
10.5	0.463	1.996	0.11	0.196	1.83	10	0.5	2.551	-0.370	-1.889
10	0.991	1.998	0.5	0.199	1.74	10	0	0.000	0.158	0.792
10.25	0.87	1.998	0.5	0.199	1.74	10	0.25	1.256	0.037	0.184
10.5	0.438	1.998	0.5	0.199	1.74	10	0.5	2.513	-0.395	-1.987
10	0.99	2.006	0.75	0.2	1.74	10	0	0.000	0.157	0.783
10.25	0.865	2.006	0.75	0.2	1.74	10	0.25	1.250	0.032	0.158
10	1.039	2.992	0.15	0.251	1.96	10	0	0.000	0.206	0.819
10.25	0.916	2.992	0.15	0.251	1.96	10	0.25	0.996	0.083	0.329
10.5	0.607	2.992	0.15	0.251	1.96	10	0.5	1.992	-0.226	-0.902
10.75	0.214	2.992	0.15	0.251	1.96	10	0.75	2.988	-0.619	-2.467
10	1.042	2.992	0.75	0.252	1.93	10	0	0.000	0.209	0.828
10.25	0.931	2.992	0.75	0.252	1.93	10	0.25	0.992	0.098	0.388
10.5	0.703	2.992	0.75	0.252	1.93	10	0.5	1.984	-0.130	-0.517
10	1.076	3.98	0.21	0.306	1.92	10	0	0.000	0.243	0.793
10.25	0.981	3.98	0.21	0.306	1.92	10	0.25	0.817	0.148	0.483
10.5	0.779	3.98	0.21	0.306	1.92	10	0.5	1.634	-0.054	-0.178
10.75	0.46	3.98	0.21	0.306	1.92	10	0.75	2.451	-0.373	-1.220
10	1.077	2.978	0.75	0.31	1.84	10	0	0.000	0.244	0.786
10.25	0.981	2.978	0.75	0.31	1.84	10	0.25	0.806	0.148	0.476
10.5	0.778	2.978	0.75	0.31	1.84	10	0.5	1.613	-0.055	-0.178
10.75	0.487	2.978	0.75	0.31	1.84	10	0.75	2.419	-0.346	-1.117
10	1.777	0.991	0.07	0.155	0.91	20	0	0.000	0.110	0.712

TABLE A2. Water surface profile data										
Station	Elev.	Q	Bw	Da	F	H	X	X/Da	Y	Y/Da
ft	ft	ft^3/s	ft	ft		in	ft		ft	
10.25	1.622	0.991	0.07	0.155	0.91	20	0.25	1.613	-0.045	-0.288
10.5	1.214	0.991	0.07	0.155	0.91	20	0.5	3.226	-0.453	-2.920
10.75	0.16	0.991	0.07	0.155	0.91	20	0.75	4.839	-1.507	-9.720
10	1.778	1.001	0.5	0.147	1.09	20	0	0.000	0.111	0.757
10.25	1.625	1.001	0.5	0.147	1.09	20	0.25	1.701	-0.042	-0.283
10.5	1.217	1.001	0.5	0.147	1.09	20	0.5	3.401	-0.450	-3.059
10	1.776	0.997	0.75	0.152	0.99	20	0	0.000	0.109	0.719
10.25	1.617	0.997	0.75	0.152	0.99	20	0.25	1.645	-0.050	-0.327
10.5	1.008	0.997	0.75	0.152	0.99	20	0.5	3.289	-0.659	-4.333
10	1.778	1.001	1	0.152	0.99	20	0	0.000	0.111	0.732
10.25	1.604	1.001	1	0.152	0.99	20	0.25	1.645	-0.063	-0.412
10	1.777	0.999	1.25	0.151	1.01	20	0	0.000	0.110	0.731
10.25	1.588	0.999	1.25	0.151	1.01	20	0.25	1.656	-0.079	-0.521
10	1.776	1.001	1.5	0.148	1.07	20	0	0.000	0.109	0.739
10.25	1.623	1.001	1.5	0.148	1.07	20	0.25	1.689	-0.044	-0.295
10	1.844	2.008	0.125	0.225	1.23	20	0	0.000	0.177	0.788
10.25	1.726	2.008	0.125	0.225	1.23	20	0.25	1.111	0.059	0.264
10.5	1.453	2.008	0.125	0.225	1.23	20	0.5	2.222	-0.214	-0.950
10.75	0.977	2.008	0.125	0.225	1.23	20	0.75	3.333	-0.690	-3.065
11	0.18	2.008	0.125	0.225	1.23	20	1	4.444	-1.487	-6.607
10	1.838	2.002	0.75	0.225	1.22	20	0	0.000	0.171	0.761
10.25	1.725	2.002	0.75	0.225	1.22	20	0.25	1.111	0.058	0.259
10.5	1.422	2.002	0.75	0.225	1.22	20	0.5	2.222	-0.245	-1.087
10.75	0.769	2.002	0.75	0.225	1.22	20	0.75	3.333	-0.898	-3.990
10	1.836	2.003	1	0.229	1.16	20	0	0.000	0.169	0.739
10.25	1.71	2.003	1	0.229	1.16	20	0.25	1.092	0.043	0.189
10.5	1.344	2.003	1	0.229	1.16	20	0.5	2.183	-0.323	-1.409
10	1.835	2	1.25	0.234	1.08	20	0	0.000	0.168	0.719
10.25	1.692	2	1.25	0.234	1.08	20	0.25	1.068	0.025	0.108
10.5	1.243	2	1.25	0.234	1.08	20	0.5	2.137	-0.424	-1.811
10	1.83	2.006	1.5	0.227	1.19	20	0	0.000	0.163	0.720

TABLE A2. Water surface profile data

Station	Elev.	Q	Bw	Da	F	H	X	X/Da	Y	Y/Da
ft	ft	ft^3/s	ft	ft		in	ft		ft	
10.25	1.669	2.006	1.5	0.227	1.19	20	0.25	1.101	0.002	0.010
10	1.886	2.995	0.17	0.292	1.24	20	0	0.000	0.219	0.751
10.25	1.781	2.995	0.17	0.292	1.24	20	0.25	0.856	0.114	0.392
10.5	1.558	2.995	0.17	0.292	1.24	20	0.5	1.712	-0.109	-0.372
10.75	1.123	2.995	0.17	0.292	1.24	20	0.75	2.568	-0.544	-1.862
11	0.435	2.995	0.17	0.292	1.24	20	1	3.425	-1.232	-4.218
10	1.89	3	1	0.293	1.23	20	0	0.000	0.223	0.762
10.25	1.78	3	1	0.293	1.23	20	0.25	0.853	0.113	0.387
10.5	1.502	3	1	0.293	1.23	20	0.5	1.706	-0.165	-0.562
10.75	0.941	3	1	0.293	1.23	20	0.75	2.560	-0.726	-2.477
10	1.879	2.997	1.25	0.294	1.22	20	0	0.000	0.212	0.722
10.25	1.756	2.997	1.25	0.294	1.22	20	0.25	0.850	0.089	0.304
10.5	1.406	2.997	1.25	0.294	1.22	20	0.5	1.701	-0.261	-0.887
10	1.883	3	1.5	0.297	1.18	20	0	0.000	0.216	0.728
10.25	1.753	3	1.5	0.297	1.18	20	0.25	0.842	0.086	0.291
10.5	1.46	3	1.5	0.297	1.18	20	0.5	1.684	-0.207	-0.696
10	1.939	3.966	0.225	0.345	1.32	20	0	0.000	0.272	0.789
10.25	1.847	3.966	0.225	0.345	1.32	20	0.25	0.725	0.180	0.523
10.5	1.662	3.966	0.225	0.345	1.32	20	0.5	1.449	-0.005	-0.014
10.75	1.368	3.966	0.225	0.345	1.32	20	0.75	2.174	-0.299	-0.866
11	0.884	3.966	0.225	0.345	1.32	20	1	2.899	-0.783	-2.269
11.25	0.335	3.966	0.225	0.345	1.32	20	1.25	3.623	-1.332	-3.860
10	1.942	3.979	1	0.348	1.29	20	0	0.000	0.275	0.791
10.25	1.847	3.979	1	0.348	1.29	20	0.25	0.718	0.180	0.518
10.5	1.62	3.979	1	0.348	1.29	20	0.5	1.437	-0.047	-0.134
10.75	1.236	3.979	1	0.348	1.29	20	0.75	2.155	-0.431	-1.238
10	1.927	3.979	1.25	0.345	1.33	20	0	0.000	0.260	0.755
10.25	1.795	3.979	1.25	0.345	1.33	20	0.25	0.725	0.128	0.372
10.5	1.503	3.979	1.25	0.345	1.33	20	0.5	1.449	-0.164	-0.474
10.75	1.053	3.979	1.25	0.345	1.33	20	0.75	2.174	-0.614	-1.779
10	1.926	3.982	1.5	0.346	1.32	20	0	0.000	0.259	0.750

TABLE A2. Water surface profile data										
Station	Elev.	Q	Bw	Da	F	H	X	X/Da	Y	Y/Da
ft	ft	ft^3/s	ft	ft		in	ft		ft	
10.25	1.804	3.982	1.5	0.346	1.32	20	0.25	0.723	0.137	0.397
10.5	1.585	3.982	1.5	0.346	1.32	20	0.5	1.445	-0.082	-0.236
10	2.604	0.997	0.06	0.121	1.95	30	0	0.000	0.104	0.860
10.25	2.479	0.997	0.06	0.121	1.95	30	0.25	2.066	-0.021	-0.174
10.5	2.189	0.997	0.06	0.121	1.95	30	0.5	4.132	-0.311	-2.570
10.75	1.723	0.997	0.06	0.121	1.95	30	0.75	6.198	-0.777	-6.421
11	1.058	0.997	0.06	0.121	1.95	30	1	8.264	-1.442	-11.917
11.25	0.056	0.997	0.06	0.121	1.95	30	1.25	10.331	-2.444	-20.198
10	2.602	1.004	0.07	0.127	1.68	30	0	0.000	0.102	0.803
10.25	2.481	1.004	0.07	0.127	1.68	30	0.25	1.969	-0.019	-0.150
10.5	2.178	1.004	0.07	0.127	1.68	30	0.5	3.937	-0.322	-2.535
10.75	1.669	1.004	0.07	0.127	1.68	30	0.75	5.906	-0.831	-6.543
11	0.943	1.004	0.07	0.127	1.68	30	1	7.874	-1.557	-12.260
10	2.601	0.997	0.5	0.119	2.02	30	0	0.000	0.101	0.849
10	2.603	1.002	0.5	0.126	1.71	30	0	0.000	0.103	0.817
10.25	2.483	0.997	0.5	0.119	2.02	30	0.25	2.101	-0.017	-0.143
10.25	2.475	1.002	0.5	0.126	1.71	30	0.25	1.984	-0.025	-0.198
10.5	2.178	1.002	0.5	0.126	1.71	30	0.5	3.968	-0.322	-2.556
10.5	2.192	0.997	0.5	0.119	2.02	30	0.5	4.202	-0.308	-2.588
10.75	1.721	0.997	0.5	0.119	2.02	30	0.75	6.303	-0.779	-6.546
10.75	1.666	1.002	0.5	0.126	1.71	30	0.75	5.952	-0.834	-6.619
11	0.9	1.002	0.5	0.126	1.71	30	1	7.937	-1.600	-12.698
11	1.036	0.997	0.5	0.119	2.02	30	1	8.403	-1.464	-12.303
10	2.602	1.006	0.625	0.125	1.78	30	0	0.000	0.102	0.816
10.25	2.472	1.006	0.625	0.125	1.78	30	0.25	2.000	-0.028	-0.224
10.5	2.177	1.006	0.625	0.125	1.78	30	0.5	4.000	-0.323	-2.584
10.75	1.656	1.006	0.625	0.125	1.78	30	0.75	6.000	-0.844	-6.752
11	0.895	1.006	0.625	0.125	1.78	30	1	8.000	-1.605	-12.840
10	2.603	1.002	0.75	0.126	1.74	30	0	0.000	0.103	0.817
10	2.601	0.997	0.75	0.12	1.98	30	0	0.000	0.101	0.842
10.25	2.47	1.002	0.75	0.126	1.74	30	0.25	1.984	-0.030	-0.238

TABLE A2. Water surface profile data										
Station	Elev.	Q	Bw	Da	F	H	X	X/Da	Y	Y/Da
ft	ft	ft^3/s	ft	ft		in	ft		ft	
10.25	2.475	0.997	0.75	0.12	1.98	30	0.25	2.083	-0.025	-0.208
10.5	2.182	0.997	0.75	0.12	1.98	30	0.5	4.167	-0.318	-2.650
10.5	2.173	1.002	0.75	0.126	1.74	30	0.5	3.968	-0.327	-2.595
10.75	1.626	1.002	0.75	0.126	1.74	30	0.75	5.952	-0.874	-6.937
10.75	1.696	0.997	0.75	0.12	1.98	30	0.75	6.250	-0.804	-6.700
11	0.868	1.002	0.75	0.126	1.74	30	1	7.937	-1.632	-12.952
11	0.943	0.997	0.75	0.12	1.98	30	1	8.333	-1.557	-12.975
10	2.6	1.004	0.875	0.127	1.68	30	0	0.000	0.100	0.787
10.25	2.474	1.004	0.875	0.127	1.68	30	0.25	1.969	-0.026	-0.205
10.5	2.161	1.004	0.875	0.127	1.68	30	0.5	3.937	-0.339	-2.669
10.75	1.64	1.004	0.875	0.127	1.68	30	0.75	5.906	-0.860	-6.772
10	2.6	0.997	1	0.12	1.97	30	0	0.000	0.100	0.833
10	2.603	1.002	1	0.127	1.67	30	0	0.000	0.103	0.811
10.25	2.475	0.997	1	0.12	1.97	30	0.25	2.083	-0.025	-0.208
10.25	2.478	1.002	1	0.127	1.67	30	0.25	1.969	-0.022	-0.173
10.5	2.155	1.002	1	0.127	1.67	30	0.5	3.937	-0.345	-2.717
10.5	2.169	0.997	1	0.12	1.97	30	0.5	4.167	-0.331	-2.758
10.75	1.656	0.997	1	0.12	1.97	30	0.75	6.250	-0.844	-7.033
10.75	1.621	1.002	1	0.127	1.67	30	0.75	5.906	-0.879	-6.921
11	1.013	0.997	1	0.12	1.97	30	1	8.333	-1.487	-12.392
10	2.601	1.002	1.125	0.126	1.73	30	0	0.000	0.101	0.802
10.25	2.472	1.002	1.125	0.126	1.73	30	0.25	1.984	-0.028	-0.222
10.5	2.154	1.002	1.125	0.126	1.73	30	0.5	3.968	-0.346	-2.746
10.75	1.628	1.002	1.125	0.126	1.73	30	0.75	5.952	-0.872	-6.921
10	2.602	0.997	1.25	0.116	2.20	30	0	0.000	0.102	0.879
10	2.6	1.004	1.25	0.125	1.79	30	0	0.000	0.100	0.800
10.25	2.472	1.004	1.25	0.125	1.79	30	0.25	2.000	-0.028	-0.224
10.25	2.474	0.997	1.25	0.116	2.20	30	0.25	2.155	-0.026	-0.224
10.5	2.152	1.004	1.25	0.125	1.79	30	0.5	4.000	-0.348	-2.784
10.5	2.163	0.997	1.25	0.116	2.20	30	0.5	4.310	-0.337	-2.905
10.75	1.556	1.004	1.25	0.125	1.79	30	0.75	6.000	-0.944	-7.552

TABLE A2. Water surface profile data										
Station	Elev.	Q	Bw	Da	F	H	X	X/Da	Y	Y/Da
ft	ft	ft^3/s	ft	ft		in	ft		ft	
10.75	1.59	0.997	1.25	0.116	2.20	30	0.75	6.466	-0.910	-7.845
10	2.602	1.004	1.375	0.126	1.74	30	0	0.000	0.102	0.810
10.25	2.475	1.004	1.375	0.126	1.74	30	0.25	1.984	-0.025	-0.198
10.5	2.141	1.004	1.375	0.126	1.74	30	0.5	3.968	-0.359	-2.849
10	2.601	1.008	1.5	0.125	1.80	30	0	0.000	0.101	0.808
10	2.601	0.997	1.5	0.119	2.04	30	0	0.000	0.101	0.849
10.25	2.473	1.008	1.5	0.125	1.80	30	0.25	2.000	-0.027	-0.216
10.25	2.471	0.997	1.5	0.119	2.04	30	0.25	2.101	-0.029	-0.244
10.5	2.141	0.997	1.5	0.119	2.04	30	0.5	4.202	-0.359	-3.017
10.5	2.138	1.008	1.5	0.125	1.80	30	0.5	4.000	-0.362	-2.896
10.75	1.499	1.008	1.5	0.125	1.80	30	0.75	6.000	-1.001	-8.008
10.75	1.531	0.997	1.5	0.119	2.04	30	0.75	6.303	-0.969	-8.143
10	2.602	1.005	1.625	0.126	1.71	30	0	0.000	0.102	0.810
10.25	2.465	1.005	1.625	0.126	1.71	30	0.25	1.984	-0.035	-0.278
10.5	2.125	1.005	1.625	0.126	1.71	30	0.5	3.968	-0.375	-2.976
10	2.599	1.007	1.75	0.124	1.82	30	0	0.000	0.099	0.798
10	2.603	0.997	1.75	0.119	2.02	30	0	0.000	0.103	0.866
10.25	2.465	0.997	1.75	0.119	2.02	30	0.25	2.101	-0.035	-0.294
10.25	2.458	1.007	1.75	0.124	1.82	30	0.25	2.016	-0.042	-0.339
10.5	2.077	1.007	1.75	0.124	1.82	30	0.5	4.032	-0.423	-3.411
10.5	2.115	0.997	1.75	0.119	2.02	30	0.5	4.202	-0.385	-3.235
10	2.6	1.009	1.875	0.127	1.70	30	0	0.000	0.100	0.787
10.25	2.463	1.009	1.875	0.127	1.70	30	0.25	1.969	-0.037	-0.291
10.5	2.08	1.009	1.875	0.127	1.70	30	0.5	3.937	-0.420	-3.307
10	2.601	0.997	2	0.119	2.05	30	0	0.000	0.101	0.849
10	2.599	1.009	2	0.123	1.87	30	0	0.000	0.099	0.805
10.25	2.461	0.997	2	0.119	2.05	30	0.25	2.101	-0.039	-0.328
10.25	2.446	1.009	2	0.123	1.87	30	0.25	2.033	-0.054	-0.439
10.5	2.065	0.997	2	0.119	2.05	30	0.5	4.202	-0.435	-3.655
10.5	2.039	1.009	2	0.123	1.87	30	0.5	4.065	-0.461	-3.748
10	2.6	1.005	2.125	0.127	1.71	30	0	0.000	0.100	0.787

TABLE A2. Water surface profile data										
Station	Elev.	Q	Bw	Da	F	H	X	X/Da	Y	Y/Da
ft	ft	ft^3/s	ft	ft		in	ft		ft	
10.25	2.456	1.005	2.125	0.127	1.71	30	0.25	1.969	-0.044	-0.346
10	2.599	0.997	2.25	0.119	2.02	30	0	0.000	0.099	0.832
10	2.597	1.005	2.25	0.124	1.83	30	0	0.000	0.097	0.782
10.25	2.429	0.997	2.25	0.119	2.02	30	0.25	2.101	-0.071	-0.597
10.25	2.427	1.005	2.25	0.124	1.83	30	0.25	2.016	-0.073	-0.589
10	2.663	1.99	0.075	0.196	1.83	30	0	0.000	0.163	0.832
10.25	2.561	1.99	0.075	0.196	1.83	30	0.25	1.276	0.061	0.311
10.5	2.356	1.99	0.075	0.196	1.83	30	0.5	2.551	-0.144	-0.735
10.75	1.999	1.99	0.075	0.196	1.83	30	0.75	3.827	-0.501	-2.556
11	1.505	1.99	0.075	0.196	1.83	30	1	5.102	-0.995	-5.077
11.25	0.895	1.99	0.075	0.196	1.83	30	1.25	6.378	-1.605	-8.189
11.5	0.166	1.99	0.075	0.196	1.83	30	1.5	7.653	-2.334	-11.908
10	2.663	2	0.11	0.19	2.04	30	0	0.000	0.163	0.858
10.25	2.577	2	0.11	0.19	2.04	30	0.25	1.316	0.077	0.405
10.5	2.368	2	0.11	0.19	2.04	30	0.5	2.632	-0.132	-0.695
10.75	2.047	2	0.11	0.19	2.04	30	0.75	3.947	-0.453	-2.384
11	1.588	2	0.11	0.19	2.04	30	1	5.263	-0.912	-4.800
11.25	0.907	2	0.11	0.19	2.04	30	1.25	6.579	-1.593	-8.384
11.5	0.195	2	0.11	0.19	2.04	30	1.5	7.895	-2.305	-12.132
10	2.67	2	0.625	0.194	1.88	30	0	0.000	0.170	0.876
10.25	2.577	2	0.625	0.194	1.88	30	0.25	1.289	0.077	0.397
10.5	2.377	2	0.625	0.194	1.88	30	0.5	2.577	-0.123	-0.634
10.75	2.041	2	0.625	0.194	1.88	30	0.75	3.866	-0.459	-2.366
11	1.598	2	0.625	0.194	1.88	30	1	5.155	-0.902	-4.649
11.25	0.938	2	0.625	0.194	1.88	30	1.25	6.443	-1.562	-8.052
10	2.663	2.001	0.75	0.193	1.92	30	0	0.000	0.163	0.845
10	2.663	1.99	0.75	0.193	1.91	30	0	0.000	0.163	0.845
10.25	2.571	2.001	0.75	0.193	1.92	30	0.25	1.295	0.071	0.368
10.25	2.56	1.99	0.75	0.193	1.91	30	0.25	1.295	0.060	0.311
10.5	2.372	2.001	0.75	0.193	1.92	30	0.5	2.591	-0.128	-0.663
10.5	2.342	1.99	0.75	0.193	1.91	30	0.5	2.591	-0.158	-0.819

TABLE A2. Water surface profile data

Station	Elev.	Q	Bw	Da	F	H	X	X/Da	Y	Y/Da
ft	ft	ft^3/s	ft	ft		in	ft		ft	
10.75	1.989	1.99	0.75	0.193	1.91	30	0.75	3.886	-0.511	-2.648
10.75	2.042	2.001	0.75	0.193	1.92	30	0.75	3.886	-0.458	-2.373
11	1.587	2.001	0.75	0.193	1.92	30	1	5.181	-0.913	-4.731
11	1.519	1.99	0.75	0.193	1.91	30	1	5.181	-0.981	-5.083
11.25	0.877	2.001	0.75	0.193	1.92	30	1.25	6.477	-1.623	-8.409
11.25	0.805	1.99	0.75	0.193	1.91	30	1.25	6.477	-1.695	-8.782
10	2.67	1.998	0.875	0.195	1.86	30	0	0.000	0.170	0.872
10.25	2.578	1.998	0.875	0.195	1.86	30	0.25	1.282	0.078	0.400
10.5	2.374	1.998	0.875	0.195	1.86	30	0.5	2.564	-0.126	-0.646
10.75	2.041	1.998	0.875	0.195	1.86	30	0.75	3.846	-0.459	-2.354
11	1.595	1.998	0.875	0.195	1.86	30	1	5.128	-0.905	-4.641
11.25	0.957	1.998	0.875	0.195	1.86	30	1.25	6.410	-1.543	-7.913
10	2.665	1.999	1	0.195	1.86	30	0	0.000	0.165	0.846
10	2.662	1.998	1	0.197	1.81	30	0	0.000	0.162	0.822
10.25	2.573	1.999	1	0.195	1.86	30	0.25	1.282	0.073	0.374
10.25	2.563	1.998	1	0.197	1.81	30	0.25	1.269	0.063	0.320
10.5	2.343	1.998	1	0.197	1.81	30	0.5	2.538	-0.157	-0.797
10.5	2.378	1.999	1	0.195	1.86	30	0.5	2.564	-0.122	-0.626
10.75	2.043	1.999	1	0.195	1.86	30	0.75	3.846	-0.457	-2.344
10.75	1.991	1.998	1	0.197	1.81	30	0.75	3.807	-0.509	-2.584
11	1.535	1.999	1	0.195	1.86	30	1	5.128	-0.965	-4.949
11	1.448	1.998	1	0.197	1.81	30	1	5.076	-1.052	-5.340
11.25	0.851	1.999	1	0.195	1.86	30	1.25	6.410	-1.649	-8.456
11.25	0.889	1.998	1	0.197	1.81	30	1.25	6.345	-1.611	-8.178
10	2.672	2.001	1.125	0.199	1.76	30	0	0.000	0.172	0.864
10.25	2.578	2.001	1.125	0.199	1.76	30	0.25	1.256	0.078	0.392
10.5	2.367	2.001	1.125	0.199	1.76	30	0.5	2.513	-0.133	-0.668
10.75	2.014	2.001	1.125	0.199	1.76	30	0.75	3.769	-0.486	-2.442
11	1.511	2.001	1.125	0.199	1.76	30	1	5.025	-0.989	-4.970
10	2.664	1.999	1.25	0.192	1.94	30	0	0.000	0.164	0.854
10	2.663	1.99	1.25	0.196	1.83	30	0	0.000	0.163	0.832

TABLE A2. Water surface profile data										
Station	Elev.	Q	Bw	Da	F	H	X	X/Da	Y	Y/Da
ft	ft	ft^3/s	ft	ft		in	ft		ft	
10.25	2.56	1.99	1.25	0.196	1.83	30	0.25	1.276	0.060	0.306
10.25	2.57	1.999	1.25	0.192	1.94	30	0.25	1.302	0.070	0.365
10.5	2.362	1.999	1.25	0.192	1.94	30	0.5	2.604	-0.138	-0.719
10.5	2.342	1.99	1.25	0.196	1.83	30	0.5	2.551	-0.158	-0.806
10.75	1.965	1.99	1.25	0.196	1.83	30	0.75	3.827	-0.535	-2.730
10.75	2.015	1.999	1.25	0.192	1.94	30	0.75	3.906	-0.485	-2.526
11	1.486	1.999	1.25	0.192	1.94	30	1	5.208	-1.014	-5.281
11	1.385	1.99	1.25	0.196	1.83	30	1	5.102	-1.115	-5.689
10	2.667	2.001	1.375	0.1944	1.89	30	0	0.000	0.167	0.859
10.25	2.568	2.001	1.375	0.1944	1.89	30	0.25	1.286	0.068	0.350
10.5	2.357	2.001	1.375	0.1944	1.89	30	0.5	2.572	-0.143	-0.736
10.75	1.973	2.001	1.375	0.1944	1.89	30	0.75	3.858	-0.527	-2.711
11	1.446	2.001	1.375	0.1944	1.89	30	1	5.144	-1.054	-5.422
10	2.665	1.998	1.5	0.192	1.94	30	0	0.000	0.165	0.859
10	2.661	1.992	1.5	0.197	1.79	30	0	0.000	0.161	0.817
10.25	2.565	1.998	1.5	0.192	1.94	30	0.25	1.302	0.065	0.339
10.25	2.556	1.992	1.5	0.197	1.79	30	0.25	1.269	0.056	0.284
10.5	2.349	1.998	1.5	0.192	1.94	30	0.5	2.604	-0.151	-0.786
10.5	2.326	1.992	1.5	0.197	1.79	30	0.5	2.538	-0.174	-0.883
10.75	1.979	1.998	1.5	0.192	1.94	30	0.75	3.906	-0.521	-2.714
10.75	1.878	1.992	1.5	0.197	1.79	30	0.75	3.807	-0.622	-3.157
11	1.434	1.998	1.5	0.192	1.94	30	1	5.208	-1.066	-5.552
10	2.668	1.998	1.625	0.195	1.85	30	0	0.000	0.168	0.862
10.25	2.57	1.998	1.625	0.195	1.85	30	0.25	1.282	0.070	0.359
10.5	2.341	1.998	1.625	0.195	1.85	30	0.5	2.564	-0.159	-0.815
10.75	1.911	1.998	1.625	0.195	1.85	30	0.75	3.846	-0.589	-3.021
10	2.664	2.001	1.75	0.192	1.95	30	0	0.000	0.164	0.854
10	2.662	1.99	1.75	0.195	1.84	30	0	0.000	0.162	0.831
10.25	2.564	2.001	1.75	0.192	1.95	30	0.25	1.302	0.064	0.333
10.25	2.584	1.99	1.75	0.195	1.84	30	0.25	1.282	0.084	0.431
10.5	2.329	2.001	1.75	0.192	1.95	30	0.5	2.604	-0.171	-0.891

TABLE A2. Water surface profile data										
Station	Elev.	Q	Bw	Da	F	H	X	X/Da	Y	Y/Da
ft	ft	ft^3/s	ft	ft		in	ft		ft	
10.5	2.298	1.99	1.75	0.195	1.84	30	0.5	2.564	-0.202	-1.036
10.75	1.815	1.99	1.75	0.195	1.84	30	0.75	3.846	-0.685	-3.513
10.75	1.895	2.001	1.75	0.192	1.95	30	0.75	3.906	-0.605	-3.151
10	2.662	2.003	1.875	0.193	1.92	30	0	0.000	0.162	0.839
10.25	2.552	2.003	1.875	0.193	1.92	30	0.25	1.295	0.052	0.269
10.5	2.31	2.003	1.875	0.193	1.92	30	0.5	2.591	-0.190	-0.984
10	2.66	1.992	2	0.195	1.84	30	0	0.000	0.160	0.821
10	2.66	2.001	2	0.193	1.92	30	0	0.000	0.160	0.829
10.25	2.544	1.992	2	0.195	1.84	30	0.25	1.282	0.044	0.226
10.25	2.549	2.001	2	0.193	1.92	30	0.25	1.295	0.049	0.254
10.5	2.223	1.992	2	0.195	1.84	30	0.5	2.564	-0.277	-1.421
10.5	2.277	2.001	2	0.193	1.92	30	0.5	2.591	-0.223	-1.155
10	2.657	2.001	2.125	0.191	1.98	30	0	0.000	0.157	0.822
10.25	2.541	2.001	2.125	0.191	1.98	30	0.25	1.309	0.041	0.215
10.5	2.235	2.001	2.125	0.191	1.98	30	0.5	2.618	-0.265	-1.387
10	2.662	2.002	2.25	0.194	1.90	30	0	0.000	0.162	0.835
10	2.66	1.99	2.25	0.195	1.84	30	0	0.000	0.160	0.821
10.25	2.546	1.99	2.25	0.195	1.84	30	0.25	1.282	0.046	0.236
10.25	2.53	2.002	2.25	0.194	1.90	30	0.25	1.289	0.030	0.155
10.5	2.297	1.99	2.25	0.195	1.84	30	0.5	2.564	-0.203	-1.041
10.5	2.212	2.002	2.25	0.194	1.90	30	0.5	2.577	-0.288	-1.485
10	2.718	2.995	0.125	0.269	1.58	30	0	0.000	0.218	0.810
10.25	2.631	2.995	0.125	0.269	1.58	30	0.25	0.929	0.131	0.487
10.5	2.463	2.995	0.125	0.269	1.58	30	0.5	1.859	-0.037	-0.138
10.75	2.191	2.995	0.125	0.269	1.58	30	0.75	2.788	-0.309	-1.149
11	1.836	2.995	0.125	0.269	1.58	30	1	3.717	-0.664	-2.468
11.25	1.284	2.995	0.125	0.269	1.58	30	1.25	4.647	-1.216	-4.520
11.5	0.646	2.995	0.125	0.269	1.58	30	1.5	5.576	-1.854	-6.892
10	2.717	3	0.75	0.272	1.53	30	0	0.000	0.217	0.798
10.25	2.631	3	0.75	0.272	1.53	30	0.25	0.919	0.131	0.482
10.5	2.465	3	0.75	0.272	1.53	30	0.5	1.838	-0.035	-0.129

TABLE A2. Water surface profile data										
Station	Elev.	Q	Bw	Da	F	H	X	X/Da	Y	Y/Da
ft	ft	ft^3/s	ft	ft		in	ft		ft	
10.75	2.183	3	0.75	0.272	1.53	30	0.75	2.757	-0.317	-1.165
11	1.823	3	0.75	0.272	1.53	30	1	3.676	-0.677	-2.489
11.25	1.292	3	0.75	0.272	1.53	30	1.25	4.596	-1.208	-4.441
11.5	0.688	3	0.75	0.272	1.53	30	1.5	5.515	-1.812	-6.662
10	2.717	2.995	0.875	0.277	1.45	30	0	0.000	0.217	0.783
10.25	2.63	2.995	0.875	0.277	1.45	30	0.25	0.903	0.130	0.469
10.5	2.463	2.995	0.875	0.277	1.45	30	0.5	1.805	-0.037	-0.134
10.75	2.174	2.995	0.875	0.277	1.45	30	0.75	2.708	-0.326	-1.177
11	1.82	2.995	0.875	0.277	1.45	30	1	3.610	-0.680	-2.455
11.25	1.264	2.995	0.875	0.277	1.45	30	1.25	4.513	-1.236	-4.462
10	2.716	3	1	0.273	1.53	30	0	0.000	0.216	0.791
10.25	2.626	3	1	0.273	1.53	30	0.25	0.916	0.126	0.462
10.5	2.458	3	1	0.273	1.53	30	0.5	1.832	-0.042	-0.154
10.75	2.181	3	1	0.273	1.53	30	0.75	2.747	-0.319	-1.168
11	1.797	3	1	0.273	1.53	30	1	3.663	-0.703	-2.575
11.25	1.201	3	1	0.273	1.53	30	1.25	4.579	-1.299	-4.758
10	2.719	3.003	1.125	0.271	1.54	30	0	0.000	0.219	0.808
10.25	2.627	3.003	1.125	0.271	1.54	30	0.25	0.923	0.127	0.469
10.5	2.457	3.003	1.125	0.271	1.54	30	0.5	1.845	-0.043	-0.159
10.75	2.16	3.003	1.125	0.271	1.54	30	0.75	2.768	-0.340	-1.255
11	1.786	3.003	1.125	0.271	1.54	30	1	3.690	-0.714	-2.635
11.25	1.234	3.003	1.125	0.271	1.54	30	1.25	4.613	-1.266	-4.672
10	2.717	3	1.25	0.276	1.47	30	0	0.000	0.217	0.786
10.25	2.629	3	1.25	0.276	1.47	30	0.25	0.906	0.129	0.467
10.5	2.453	3	1.25	0.276	1.47	30	0.5	1.812	-0.047	-0.170
10.75	2.162	3	1.25	0.276	1.47	30	0.75	2.717	-0.338	-1.225
11	1.734	3	1.25	0.276	1.47	30	1	3.623	-0.766	-2.775
10	2.716	3	1.375	0.275	1.48	30	0	0.000	0.216	0.785
10.25	2.627	3	1.375	0.275	1.48	30	0.25	0.909	0.127	0.462
10.5	2.448	3	1.375	0.275	1.48	30	0.5	1.818	-0.052	-0.189
10.75	2.146	3	1.375	0.275	1.48	30	0.75	2.727	-0.354	-1.287

TABLE A2. Water surface profile data

Station	Elev.	Q	Bw	Da	F	H	X	X/Da	Y	Y/Da
ft	ft	ft^3/s	ft	ft		in	ft		ft	
11	1.705	3	1.375	0.275	1.48	30	1	3.636	-0.795	-2.891
10	2.714	3.003	1.5	0.275	1.48	30	0	0.000	0.214	0.778
10.25	2.624	3.003	1.5	0.275	1.48	30	0.25	0.909	0.124	0.451
10.5	2.435	3.003	1.5	0.275	1.48	30	0.5	1.818	-0.065	-0.236
10.75	2.102	3.003	1.5	0.275	1.48	30	0.75	2.727	-0.398	-1.447
11	1.648	3.003	1.5	0.275	1.48	30	1	3.636	-0.852	-3.098
10	2.714	3.005	1.625	0.276	1.47	30	0	0.000	0.214	0.775
10.25	2.623	3.005	1.625	0.276	1.47	30	0.25	0.906	0.123	0.446
10.5	2.429	3.005	1.625	0.276	1.47	30	0.5	1.812	-0.071	-0.257
10.75	2.079	3.005	1.625	0.276	1.47	30	0.75	2.717	-0.421	-1.525
10	2.717	2.995	1.75	0.276	1.46	30	0	0.000	0.217	0.786
10.25	2.616	2.995	1.75	0.276	1.46	30	0.25	0.906	0.116	0.420
10.5	2.411	2.995	1.75	0.276	1.46	30	0.5	1.812	-0.089	-0.322
10.75	2.03	2.995	1.75	0.276	1.46	30	0.75	2.717	-0.470	-1.703
10	2.713	2.995	1.875	0.276	1.46	30	0	0.000	0.213	0.772
10.25	2.61	2.995	1.875	0.276	1.46	30	0.25	0.906	0.110	0.399
10.5	2.389	2.995	1.875	0.276	1.46	30	0.5	1.812	-0.111	-0.402
10.75	1.947	2.995	1.875	0.276	1.46	30	0.75	2.717	-0.553	-2.004
10	2.714	3.01	2	0.278	1.45	30	0	0.000	0.214	0.770
10.25	2.603	3.01	2	0.278	1.45	30	0.25	0.899	0.103	0.371
10.5	2.355	3.01	2	0.278	1.45	30	0.5	1.799	-0.145	-0.522
10	2.71	3.005	2.125	0.273	1.52	30	0	0.000	0.210	0.769
10.25	2.596	3.005	2.125	0.273	1.52	30	0.25	0.916	0.096	0.352
10.5	2.291	3.005	2.125	0.273	1.52	30	0.5	1.832	-0.209	-0.766
10	2.707	3.005	2.25	0.273	1.52	30	0	0.000	0.207	0.758
10.25	2.582	3.005	2.25	0.273	1.52	30	0.25	0.916	0.082	0.300
10.5	2.313	3.005	2.25	0.273	1.52	30	0.5	1.832	-0.187	-0.685
10	2.705	3.192	0.16	0.255	2.13	30	0	0.000	0.205	0.804
10.25	2.626	3.192	0.16	0.255	2.13	30	0.25	0.980	0.126	0.494
10.5	2.47	3.192	0.16	0.255	2.13	30	0.5	1.961	-0.030	-0.118
10.75	2.221	3.192	0.16	0.255	2.13	30	0.75	2.941	-0.279	-1.094

TABLE A2. Water surface profile data										
Station	Elev.	Q	Bw	Da	F	H	X	X/Da	Y	Y/Da
ft	ft	ft^3/s	ft	ft		in	ft		ft	
11	1.895	3.192	0.16	0.255	2.13	30	1	3.922	-0.605	-2.373
11.25	1.426	3.192	0.16	0.255	2.13	30	1.25	4.902	-1.074	-4.212
11.5	0.875	3.192	0.16	0.255	2.13	30	1.5	5.882	-1.625	-6.373
11.75	0.296	3.192	0.16	0.255	2.13	30	1.75	6.863	-2.204	-8.643
10	2.705	3.192	0.75	0.254	2.15	30	0	0.000	0.205	0.807
10.25	2.624	3.192	0.75	0.254	2.15	30	0.25	0.984	0.124	0.488
10.5	2.463	3.192	0.75	0.254	2.15	30	0.5	1.969	-0.037	-0.146
10.75	2.221	3.192	0.75	0.254	2.15	30	0.75	2.953	-0.279	-1.098
11	1.885	3.192	0.75	0.254	2.15	30	1	3.937	-0.615	-2.421
11.25	1.451	3.192	0.75	0.254	2.15	30	1.25	4.921	-1.049	-4.130
11.5	0.877	3.192	0.75	0.254	2.15	30	1.5	5.906	-1.623	-6.390
11.75	0.293	3.192	0.75	0.254	2.15	30	1.75	6.890	-2.207	-8.689
10	2.707	3.192	1	0.254	2.15	30	0	0.000	0.207	0.815
10.25	2.627	3.192	1	0.254	2.15	30	0.25	0.984	0.127	0.500
10.5	2.459	3.192	1	0.254	2.15	30	0.5	1.969	-0.041	-0.161
10.75	2.208	3.192	1	0.254	2.15	30	0.75	2.953	-0.292	-1.150
11	1.866	3.192	1	0.254	2.15	30	1	3.937	-0.634	-2.496
11.25	1.41	3.192	1	0.254	2.15	30	1.25	4.921	-1.090	-4.291
11.5	0.831	3.192	1	0.254	2.15	30	1.5	5.906	-1.669	-6.571
10	2.704	3.19	1.25	0.254	2.16	30	0	0.000	0.204	0.803
10.25	2.623	3.19	1.25	0.254	2.16	30	0.25	0.984	0.123	0.484
10.5	2.457	3.19	1.25	0.254	2.16	30	0.5	1.969	-0.043	-0.169
10.75	2.183	3.19	1.25	0.254	2.16	30	0.75	2.953	-0.317	-1.248
11	1.791	3.19	1.25	0.254	2.16	30	1	3.937	-0.709	-2.791
11.25	1.189	3.19	1.25	0.254	2.16	30	1.25	4.921	-1.311	-5.161
10	2.702	3.188	1.5	0.255	2.11	30	0	0.000	0.202	0.792
10.25	2.616	3.188	1.5	0.255	2.11	30	0.25	0.980	0.116	0.455
10.5	2.439	3.188	1.5	0.255	2.11	30	0.5	1.961	-0.061	-0.239
10.75	2.135	3.188	1.5	0.255	2.11	30	0.75	2.941	-0.365	-1.431
11	1.633	3.188	1.5	0.255	2.11	30	1	3.922	-0.867	-3.400
10	2.704	3.188	1.75	0.255	2.13	30	0	0.000	0.204	0.800

TABLE A2. Water surface profile data										
Station	Elev.	Q	Bw	Da	F	H	X	X/Da	Y	Y/Da
ft	ft	ft^3/s	ft	ft		in	ft		ft	
10.25	2.612	3.188	1.75	0.255	2.13	30	0.25	0.980	0.112	0.439
10.5	2.417	3.188	1.75	0.255	2.13	30	0.5	1.961	-0.083	-0.325
10.75	2.037	3.188	1.75	0.255	2.13	30	0.75	2.941	-0.463	-1.816
11	1.592	3.188	1.75	0.255	2.13	30	1	3.922	-0.908	-3.561
10	2.702	3.196	2	0.256	2.10	30	0	0.000	0.202	0.789
10.25	2.602	3.196	2	0.256	2.10	30	0.25	0.977	0.102	0.398
10.5	2.343	3.196	2	0.256	2.10	30	0.5	1.953	-0.157	-0.613
10.75	1.889	3.196	2	0.256	2.10	30	0.75	2.930	-0.611	-2.387
10	2.703	3.19	2.25	0.26	2.00	30	0	0.000	0.203	0.781
10.25	2.592	3.19	2.25	0.26	2.00	30	0.25	0.962	0.092	0.354
10.5	2.344	3.19	2.25	0.26	2.00	30	0.5	1.923	-0.156	-0.600
10	2.773	4.004	0.155	0.334	1.48	30	0	0.000	0.273	0.817
10.25	2.695	4.004	0.155	0.334	1.48	30	0.25	0.749	0.195	0.584
10.5	2.539	4.004	0.155	0.334	1.48	30	0.5	1.497	0.039	0.117
10.75	2.321	4.004	0.155	0.334	1.48	30	0.75	2.246	-0.179	-0.536
11	2.013	4.004	0.155	0.334	1.48	30	1	2.994	-0.487	-1.458
11.25	1.607	4.004	0.155	0.334	1.48	30	1.25	3.743	-0.893	-2.674
10	2.784	3.985	0.2	0.333	1.49	30	0	0.000	0.284	0.853
10.25	2.704	3.985	0.2	0.333	1.49	30	0.25	0.751	0.204	0.613
10.5	2.543	3.985	0.2	0.333	1.49	30	0.5	1.502	0.043	0.129
10.75	2.322	3.985	0.2	0.333	1.49	30	0.75	2.252	-0.178	-0.535
11	2.011	3.985	0.2	0.333	1.49	30	1	3.003	-0.489	-1.468
11.25	1.612	3.985	0.2	0.333	1.49	30	1.25	3.754	-0.888	-2.667
11.5	1.131	3.985	0.2	0.333	1.49	30	1.5	4.505	-1.369	-4.111
11.75	0.544	3.985	0.2	0.333	1.49	30	1.75	5.255	-1.956	-5.874
10	2.778	4.003	0.875	0.334	1.47	30	0	0.000	0.278	0.832
10.25	2.692	4.003	0.875	0.334	1.47	30	0.25	0.749	0.192	0.575
10.5	2.545	4.003	0.875	0.334	1.47	30	0.5	1.497	0.045	0.135
10.75	2.317	4.003	0.875	0.334	1.47	30	0.75	2.246	-0.183	-0.548
11	2.003	4.003	0.875	0.334	1.47	30	1	2.994	-0.497	-1.488
11.25	1.611	4.003	0.875	0.334	1.47	30	1.25	3.743	-0.889	-2.662

TABLE A2. Water surface profile data

Station	Elev.	Q	Bw	Da	F	H	X	X/Da	Y	Y/Da
ft	ft	ft^3/s	ft	ft		in	ft		ft	
10	2.779	3.983	1	0.33	1.52	30	0	0.000	0.279	0.845
10	2.774	4.003	1	0.334	1.47	30	0	0.000	0.274	0.820
10.25	2.696	3.983	1	0.33	1.52	30	0.25	0.758	0.196	0.594
10.25	2.692	4.003	1	0.334	1.47	30	0.25	0.749	0.192	0.575
10.5	2.545	3.983	1	0.33	1.52	30	0.5	1.515	0.045	0.136
10.5	2.543	4.003	1	0.334	1.47	30	0.5	1.497	0.043	0.129
10.75	2.335	4.003	1	0.334	1.47	30	0.75	2.246	-0.165	-0.494
10.75	2.313	3.983	1	0.33	1.52	30	0.75	2.273	-0.187	-0.567
11	2.005	4.003	1	0.334	1.47	30	1	2.994	-0.495	-1.482
11	1.986	3.983	1	0.33	1.52	30	1	3.030	-0.514	-1.558
11.25	1.588	3.983	1	0.33	1.52	30	1.25	3.788	-0.912	-2.764
11.25	1.619	4.003	1	0.334	1.47	30	1.25	3.743	-0.881	-2.638
11.5	1.062	3.983	1	0.33	1.52	30	1.5	4.545	-1.438	-4.358
10	2.782	4.002	1.125	0.338	1.43	30	0	0.000	0.282	0.834
10.25	2.687	4.002	1.125	0.338	1.43	30	0.25	0.740	0.187	0.553
10.5	2.543	4.002	1.125	0.338	1.43	30	0.5	1.479	0.043	0.127
10.75	2.308	4.002	1.125	0.338	1.43	30	0.75	2.219	-0.192	-0.568
11	1.981	4.002	1.125	0.338	1.43	30	1	2.959	-0.519	-1.536
11.25	1.535	4.002	1.125	0.338	1.43	30	1.25	3.698	-0.965	-2.855
10	2.773	3.983	1.25	0.329	1.54	30	0	0.000	0.273	0.830
10	2.77	4.001	1.25	0.332	1.50	30	0	0.000	0.270	0.813
10.25	2.688	3.983	1.25	0.329	1.54	30	0.25	0.760	0.188	0.571
10.25	2.686	4.001	1.25	0.332	1.50	30	0.25	0.753	0.186	0.560
10.5	2.529	4.001	1.25	0.332	1.50	30	0.5	1.506	0.029	0.087
10.5	2.537	3.983	1.25	0.329	1.54	30	0.5	1.520	0.037	0.112
10.75	2.299	4.001	1.25	0.332	1.50	30	0.75	2.259	-0.201	-0.605
10.75	2.297	3.983	1.25	0.329	1.54	30	0.75	2.280	-0.203	-0.617
11	1.963	3.983	1.25	0.329	1.54	30	1	3.040	-0.537	-1.632
11	1.958	4.001	1.25	0.332	1.50	30	1	3.012	-0.542	-1.633
11.25	1.508	4.001	1.25	0.332	1.50	30	1.25	3.765	-0.992	-2.988
11.25	1.513	3.983	1.25	0.329	1.54	30	1.25	3.799	-0.987	-3.000

TABLE A2. Water surface profile data

Station	Elev.	Q	Bw	Da	F	H	X	X/Da	Y	Y/Da
ft	ft	ft^3/s	ft	ft		in	ft		ft	
11.5	1.029	3.983	1.25	0.329	1.54	30	1.5	4.559	-1.471	-4.471
10	2.77	3.998	1.375	0.324	1.62	30	0	0.000	0.270	0.833
10.25	2.683	3.998	1.375	0.324	1.62	30	0.25	0.772	0.183	0.565
10.5	2.518	3.998	1.375	0.324	1.62	30	0.5	1.543	0.018	0.056
10.75	2.251	3.998	1.375	0.324	1.62	30	0.75	2.315	-0.249	-0.769
11	1.927	3.998	1.375	0.324	1.62	30	1	3.086	-0.573	-1.769
11.25	1.413	3.998	1.375	0.324	1.62	30	1.25	3.858	-1.087	-3.355
10	2.77	4.002	1.5	0.334	1.48	30	0	0.000	0.270	0.808
10	2.776	3.997	1.5	0.326	1.59	30	0	0.000	0.276	0.847
10.25	2.692	3.997	1.5	0.326	1.59	30	0.25	0.767	0.192	0.589
10.25	2.683	4.002	1.5	0.334	1.48	30	0.25	0.749	0.183	0.548
10.5	2.525	4.002	1.5	0.334	1.48	30	0.5	1.497	0.025	0.075
10.5	2.517	3.997	1.5	0.326	1.59	30	0.5	1.534	0.017	0.052
10.75	2.271	3.997	1.5	0.326	1.59	30	0.75	2.301	-0.229	-0.702
10.75	2.258	4.002	1.5	0.334	1.48	30	0.75	2.246	-0.242	-0.725
11	1.882	4.002	1.5	0.334	1.48	30	1	2.994	-0.618	-1.850
11	1.875	3.997	1.5	0.326	1.59	30	1	3.067	-0.625	-1.917
11.25	1.414	3.997	1.5	0.326	1.59	30	1.25	3.834	-1.086	-3.331
11.25	1.426	4.002	1.5	0.334	1.48	30	1.25	3.743	-1.074	-3.216
10	2.77	4	1.625	0.333	1.49	30	0	0.000	0.270	0.811
10.25	2.676	4	1.625	0.333	1.49	30	0.25	0.751	0.176	0.529
10.5	2.516	4	1.625	0.333	1.49	30	0.5	1.502	0.016	0.048
10.75	2.244	4	1.625	0.333	1.49	30	0.75	2.252	-0.256	-0.769
11	1.825	4	1.625	0.333	1.49	30	1	3.003	-0.675	-2.027
10	2.772	4.003	1.75	0.332	1.51	30	0	0.000	0.272	0.819
10	2.764	3.994	1.75	0.33	1.52	30	0	0.000	0.264	0.800
10.25	2.682	4.003	1.75	0.332	1.51	30	0.25	0.753	0.182	0.548
10.25	2.67	3.994	1.75	0.33	1.52	30	0.25	0.758	0.170	0.515
10.5	2.498	4.003	1.75	0.332	1.51	30	0.5	1.506	-0.002	-0.006
10.5	2.474	3.994	1.75	0.33	1.52	30	0.5	1.515	-0.026	-0.079
10.75	2.159	3.994	1.75	0.33	1.52	30	0.75	2.273	-0.341	-1.033

TABLE A2. Water surface profile data										
Station	Elev.	Q	Bw	Da	F	H	X	X/Da	Y	Y/Da
ft	ft	ft^3/s	ft	ft		in	ft		ft	
10.75	2.189	4.003	1.75	0.332	1.51	30	0.75	2.259	-0.311	-0.937
11	1.775	4.003	1.75	0.332	1.51	30	1	3.012	-0.725	-2.184
10	2.767	3.998	1.875	0.332	1.49	30	0	0.000	0.267	0.804
10.25	2.669	3.998	1.875	0.332	1.49	30	0.25	0.753	0.169	0.509
10.5	2.468	3.998	1.875	0.332	1.49	30	0.5	1.506	-0.032	-0.096
10.75	2.097	3.998	1.875	0.332	1.49	30	0.75	2.259	-0.403	-1.214
10	2.76	3.998	2	0.33	1.53	30	0	0.000	0.260	0.788
10	2.772	3.997	2	0.331	1.52	30	0	0.000	0.272	0.822
10.25	2.657	3.998	2	0.33	1.53	30	0.25	0.758	0.157	0.476
10.25	2.663	3.997	2	0.331	1.52	30	0.25	0.755	0.163	0.492
10.5	2.444	3.997	2	0.331	1.52	30	0.5	1.511	-0.056	-0.169
10.5	2.427	3.998	2	0.33	1.53	30	0.5	1.515	-0.073	-0.221
10.75	2.025	3.998	2	0.33	1.53	30	0.75	2.273	-0.475	-1.439
10.75	2.098	3.997	2	0.331	1.52	30	0.75	2.266	-0.402	-1.215
10	2.739	3.996	2.125	0.327	1.57	30	0	0.000	0.239	0.731
10.25	2.643	3.996	2.125	0.327	1.57	30	0.25	0.765	0.143	0.437
10.5	2.366	3.996	2.125	0.327	1.57	30	0.5	1.529	-0.134	-0.410
10	2.764	4.001	2.25	0.328	1.57	30	0	0.000	0.264	0.805
10	2.759	4	2.25	0.3333	1.48	30	0	0.000	0.259	0.777
10.25	2.652	4.001	2.25	0.328	1.57	30	0.25	0.762	0.152	0.463
10.25	2.638	4	2.25	0.3333	1.48	30	0.25	0.750	0.138	0.414
10.5	2.429	4.001	2.25	0.328	1.57	30	0.5	1.524	-0.071	-0.216
10.5	2.401	4	2.25	0.3333	1.48	30	0.5	1.500	-0.099	-0.297
10.75	2.17	4.001	2.25	0.328	1.57	30	0.75	2.287	-0.330	-1.006

APPENDIX B

HEADCUT ADVANCE DATA

INTRODUCTION

Summary tables present the test data for each experiment conducted in the large-scale flume. The data were collected over a three year period in a six-ft wide and 96-ft long flume constructed with 8-ft high sidewalls. A rail mounted point gage carriage operated on top of the flume walls to allow measurement of the bed and water surface profiles. The water was delivered to the flume in a supply canal, and flow measurements were made just upstream of the flume with a modified Parshall flume. The compacted cohesive fill material was placed and compacted in horizontal layers. A vibratory padfoot roller and a hand-held pneumatic compactor were used to compact the soil. Soil samples were extracted from the downstream end of the test fill just prior to preforming the headcut and conducting the test. An outlet control structure provided backwater control.

DESCRIPTION OF TERMS

The following parameters are presented in each table:

Test #. A unique test identification number

Moisture Content %. The average moisture content of all the soil samples extracted from the fill in advance of testing.

Dry Density, g/cc. The average dry density of all the 3 inch tube samples extracted from the fill in advance of testing.

Adv. Rate, ft/min. The linear advance rate determined as the slope of the headcut position versus time plot.

Adv. Rate, ft/hr. This is the same advance rate as above expressed in different units.

Fill Length, ft. The total horizontal length of the compacted fill section for this test.

Eroded Length, ft. The length of the fill section that was used to determine the advance rate for this test.

Total Comp. Passes. The total number of passes of the sheepsfoot roller over the test fill.

Passes with Vib. The number of passes using the vibratory load of the sheepsfoot roller.

Avg. Qu, psi. The average unconfined compressive strength of the two inch samples extracted from the test fill in advance of testing.

Avg. Q, cfs. The average of all discharges measured during this test.

Avg. H, ft. The average overfall height for the test.

Avg. Bw, ft. The average backwater level downstream of the overfall.

Bulk Density, g/cc. The average bulk density of the soil samples.

Void Ratio, e. The void ratio determined from the following equation:

$$e = \frac{G_s \gamma_w}{\gamma_d} - 1$$

where: G_s = The specific gravity of the soil assumed equal to 2.67

γ_w = Unit weight of the water

γ_d = Dry unit weight of the soil

Degree Sat, %. The degree of saturation of the placed soil material as determined from the following equation:

$$\%Sat = \frac{w\, G_s}{e}$$

where: w = the average moisture content

G_s = The specific gravity of the soil assumed equal to 2.67

e = The void ratio of the soil

TABLE B1. Headcut advance data for the red sandy clay (CL) soil															
Test #	Moisture Content %	Dry Density g/cc	Adv. Rate ft/min	Adv. Rate ft/hr	Fill Length ft	Eroded Length ft	Total Comp. Passes	Passes with Vib.	Avg Qu psi	Avg Q cfs	Avg H ft	Avg Bw ft	Bulk Density g/cc	Void Ratio e	Degree Sat. %
1	13.3	1.63	0.495	29.7	24.0	24.0	1	0	7.96	54.6	4.11	0.89	1.85	0.64	55.7
2	14.0	1.58	0.596	35.7	24.0	24.0	1	0	5.21	54.5	4.16	0.85	1.80	0.69	54.3
3	9.2	1.54	1.016	61.0	20.0	20.0	2	0	4.16	55.6	4.25	3.48*	1.68	0.73	33.6
4	9.2	1.68	0.294	17.6	15.0	15.0	3	2	8.39	54.1	3.99	3.30*	1.83	0.59	41.7
5	11.6	1.59	0.369	22.1	15.0	15.0	2	0	3.11	55.7	4.12	3.40*	1.77	0.68	45.6
6	14.4	1.79	0.008	0.5	15.0	7.6	3	2	12.88	55.6	4.11	3.30*	2.05	0.49	78.2
8	14.2	1.79	0.018	1.1	15.0	15.0	2	1	12.03	55.2	4.04	3.31*	2.04	0.49	77.3
9	14.4	1.71	0.051	3.1	15.0	15.0	6	0	9.15	54.9	4.21	3.44*	1.96	0.56	68.3
11	15.9	1.78	0.006	0.4	12.0	2.0	2	1	5.85	56.5	3.80	2.93*	2.06	0.50	85.1
12	14.9	1.79	0.050	3.0	20.0	18.0	6	0	9.25	55.9	4.96	0.77	2.06	0.49	81.0
13	12.4	1.84	0.081	4.9	10.0	3.6	4	3	16.85	57.7	3.96	3.42	2.07	0.45	73.3
14	10.5	1.62	0.145	8.7	16.0	16.0	5	0	8.76	88.1	3.97	1.12	1.79	0.65	43.4
15	14.8	1.81	0.007	0.4	16.0	8.5	2	1	15.51	88.1	3.24	1.08	2.08	0.48	83.2
16	13.7	1.78	0.051	3.1	16.0	16.0	6	0	8.21	57.8	3.07	0.86	2.02	0.50	73.1
17	14.2	1.80	0.073	4.4	16.0	16.0	6	0	9.95	57.4	5.19	0.75	2.06	0.48	78.7
18	13.5	1.75	0.023	1.4	16.0	14.5	6	0	10.32	27.0	4.87	0.40	1.99	0.53	68.7
19	13.4	1.78	0.081	4.9	16.0	16.0	6	0	10.34	25.3	4.08	0.48	2.02	0.50	71.6
20	12.9	1.75	0.087	5.2	16.0	15.7	6	0	7.08	26.1	3.00	0.46	1.98	0.53	65.5
21	13.7	1.80	0.070	4.2	16.0	15.8	6	0	12.49	56.0	4.05	0.71	2.05	0.48	75.4
22	14.6	1.77	0.070	4.2	16.0	15.4	6	0	9.16	85.2	4.21	0.94	2.03	0.51	76.4
23	16.0	1.77	0.047	2.8	16.0	15.6	6	0	10.96	85.4	3.31	1.00	2.05	0.51	83.9
24	13.6	1.75	0.082	4.9	16.0	15.5	6	0	6.46	84.7	4.09	0.94	1.99	0.53	68.8
25	16.0	1.77	0.004	0.3	16.0	2.7	6	0	10.31	55.2	3.31	0.66	2.05	0.51	84.1
26	15.3	1.80	0.000	0.0	16.0	0.0	6	0	9.18	52.7	3.33	0.73	2.08	0.48	84.6
27	12.7	1.71	0.045	2.7	16.0	16.0	6	0	8.38	27.2	4.87	0.38	1.93	0.56	60.3
28	17.3	1.70	0.054	3.3	16.0	15.9	2	0	5.97	56.0	3.83	3.42	1.99	0.57	81.1
29	15.4	1.75	0.001	0.1	36.0	1.2	6	0	9.06	55.1	4.17	0.68	2.02	0.53	78.2
	* - Indicates that the backwater was determined from the staff gage at the flume exit														

TABLE B2. Headcut advance data for the silty sand (SC) soil

Test #	Moisture Content %	Dry Density g/cc	Adv. Rate ft/min	Adv. Rate ft/hr	Fill Length ft	Eroded Length ft	Total Comp. Passes	Passes with Vib.	Avg Qu psi	Avg Q cfs	Avg H ft	Avg Bw ft	Bulk Density g/cc	Void Ratio e	Degree Sat. %
7	12.1	1.86	0.069	4.1	20	9.4	3	2	11.06	56.2	3.91	3.35*	2.09	0.44	74.3
10	12.0	1.76	0.198	11.9	24	23.1	2	0	4.38	54.4	3.90	3.34*	1.97	0.52	62.1

* - Indicates that the backwater was determined from the staff gage at the flume exit

TABLE B3. Headcut advance data for CL soil with an underlying sand layer

Test #	Moisture Content %	Dry Density g/cc	Adv. Rate ft/min	Adv. Rate ft/hr	Fill Length ft	Eroded Length ft	Total Comp. Passes	Passes with Vib.	Avg Qu psi	Avg Q cfs	Avg H ft	Avg Bw ft	Bulk Density g/cc	Void Ratio e	Degree Sat. %
3S	9.2	1.54	0.962	57.7	20	20	2	0	4.16	55.7	4.33	3.41*	1.68	0.73	33.6
4S	9.2	1.68	0.255	15.3	15	15	3	2	8.39	54.0	4.05	3.30*	1.83	0.59	41.7
5S	11.6	1.59	0.498	29.9	15	15	2	0	3.11	55.7	4.20	3.40*	1.77	0.68	45.6
6S	14.4	1.79	0.091	5.5	15	15	3	2	12.88	55.4	4.08	3.30*	2.05	0.49	78.2
8S	14.2	1.79	0.091	5.5	15	15	2	1	12.03	55.8	4.08	3.38*	2.04	0.49	77.3
9S	14.4	1.71	0.123	7.4	15	15	6	0	9.15	54.3	4.23	3.28*	1.96	0.56	68.3
11S	15.9	1.78	0.198	11.9	12	12	2	1	5.85	55.7	3.77	2.91*	2.06	0.50	85.1

* - Indicates that the backwater was determined from the staff gage at the flume exit

TABLE B4. Headcut advance data for different backwater levels

Test #	Moisture Content %	Dry Density g/cc	Adv. Rate ft/min	Adv. Rate ft/hr	Fill Length ft	Eroded Length ft	Total Comp. Passes	Passes with Vib.	Avg Qu psi	Avg Q cfs	Avg H ft	Avg Bw ft	Bulk Density g/cc	Void Ratio e	Degree Sat. %
30A	12.2	1.67	0.065	3.9	36.0	10.0	6	0	6.94	57.1	4.27	0.64	1.87	0.60	54.6
30B	12.2	1.67	0.148	8.9		8.3			6.94	57.4	4.34	3.46	1.87	0.60	54.6
30C	12.2	1.67	0.120	7.2		8.4			6.94	57.6	4.38	4.32	1.87	0.60	54.6
30D	12.2	1.67	0.056	3.3		8.4			6.94	57.7	4.30	5.02	1.87	0.60	54.6
31A	11.7	1.60	0.231	13.8	36.0	12.0	6	0	5.68	55.6	4.23	3.34	1.79	0.67	46.6
31B	11.7	1.60	0.144	8.6		7.5			5.68	55.5	4.21	0.71	1.79	0.67	46.6
31C*	11.7	1.60	0.292	17.5		8.5			5.68	55.6	4.14	4.78	1.79	0.67	46.6
31D	11.7	1.60	0.056	3.4		8.0			5.68	55.7	4.07	4.37	1.79	0.67	46.6
35A	12.0	1.68	0.097	5.8	36.0	10.0	6	0	5.72	54.9	4.17	0.71	1.88	0.59	54.4
35B	12.0	1.68	0.156	9.4		8.0			5.72	54.9	4.17	3.23	1.88	0.59	54.4
35C	12.0	1.68	0.105	6.3		8.7			5.72	54.9	4.15	4.21	1.88	0.59	54.4
35D	12.0	1.68	0.058	3.5		7.4			5.72	54.9	4.02	4.82	1.88	0.59	54.4
36A	14.4	1.73	0.059	3.5	36.0	9.6	2	0	5.70	55.9	4.30	3.30	1.98	0.54	70.6
36B*	14.4	1.73	0.116	7.0		8.2			5.70	55.7	4.35	0.70	1.98	0.54	70.6
36C	14.4	1.73	0.008	0.5		3.4			5.70	56.0	4.40	4.89	1.98	0.54	70.6
36D	14.4	1.73	0.022	1.3		10.0			5.70	56.0	4.31	4.27	1.98	0.54	70.6

* - These tests are believed to be influenced by other factors. See Chapter 6.

VITA

Kerry Mark Robinson

Candidate for the Degree of

Doctor of Philosophy

Thesis: GULLY EROSION AND HEADCUT ADVANCE

Major Field: Biosystems Engineering

Biographical:

Personal Data: Born in Altus, Oklahoma, on October 19, 1953, the son of Robert Calvin and Betty Jean Robinson.

Education: Graduated from Gould High School, Gould, Oklahoma in May 1971; attended Cameron University in Lawton, Oklahoma from September 1971 to May 1972; received Bachelor of Science and Master of Science degrees in Agricultural Engineering from Oklahoma State University, Stillwater, Oklahoma in December 1975 and May 1981, respectively; received Doctor of Philosophy degree in Biosystems Engineering from Oklahoma State University in May 1996.

Experience: Civil Engineer, U. S. Army, Fort Sill, Oklahoma (February 1976 to December 1979); Graduate Research Assistant, Agricultural Engineering, Oklahoma State University (January 1980 to March 1981); Consulting Engineer, C. H. Guernsey and Co., Oklahoma City, Oklahoma (April 1981 to March 1983); Research Hydraulic Engineer, U. S. Department of Agriculture, Agricultural Research Service, Stillwater, Oklahoma (March 1983 to present).

Professional Memberships: American Society of Agricultural Engineers, American Society of Civil Engineers, Association of State Dam Safety Officials, International Erosion Control Association, Tau Beta Pi, Phi Kappa Phi, Alpha Epsilon, Sigma Xi.